2809586056

REFERENCE ONLY

UNIVERSITY OF LONDON THESIS

Degree PhD Year 2007 Name of Author MASCARENHAS, Monica Sousa Dias

COPYRIGHT

This is a thesis accepted for a Higher Degree of the University of London. It is an unpublished typescript and the copyright is held by the author. All persons consulting this thesis must read and abide by the Copyright Declaration below.

COPYRIGHT DECLARATION

I recognise that the copyright of the above-described thesis rests with the author and that no quotation from it or information derived from it may be published without the prior written consent of the author.

LOANS

Theses may not be lent to individuals, but the Senate House Library may lend a copy to approved libraries within the United Kingdom, for consultation solely on the premises of those libraries. Application should be made to: Inter-Library Loans, Senate House Library, Senate House, Malet Street, London WC1E 7HU.

REPRODUCTION

University of London theses may not be reproduced without explicit written permission from the Senate House Library. Enquiries should be addressed to the Theses Section of the Library. Regulations concerning reproduction vary according to the date of acceptance of the thesis and are listed below as guidelines.

A. Before 1962. Permission granted only upon the prior written consent of the author. (The Senate House Library will provide addresses where possible).

B. 1962-1974. In many cases the author has agreed to permit copying upon completion of a Copyright Declaration.

C. 1975-1988. Most theses may be copied upon completion of a Copyright Declaration.

D. 1989 onwards. Most theses may be copied.

This thesis comes within category D.

☐ This copy has been deposited in the Library of UCL

☐ This copy has been deposited in the Senate House Library, Senate House, Malet Street, London WC1E 7HU.

ROLE OF HFE AND HEPCIDIN IN THE HOMEOSTASIS OF BODY IRON LEVELS

Thesis submitted by
Monica Sousa Dias Mascarenhas

For the Degree of
Doctor of Philosophy in Biochemistry

University of London
University College London

Department of Biochemistry and Molecular Biology
Royal Free & UCL Medical School
Rowland Hill Street
London NW3 2PF

UMI Number: U592118

All rights reserved

INFORMATION TO ALL USERS
The quality of this reproduction is dependent upon the quality of the copy submitted.

In the unlikely event that the author did not send a complete manuscript
and there are missing pages, these will be noted. Also, if material had to be removed,
a note will indicate the deletion.

UMI U592118
Published by ProQuest LLC 2013. Copyright in the Dissertation held by the Author.
Microform Edition © ProQuest LLC.
All rights reserved. This work is protected against
unauthorized copying under Title 17, United States Code.

ProQuest LLC
789 East Eisenhower Parkway
P.O. Box 1346
Ann Arbor, MI 48106-1346

Abstract

Recent studies have suggested that hepatic iron stores and the response to anaemia and inflammation are dependent on the mouse strains used and their Hfe status. Hepcidin and iron transporters such as DMT1 and Ireg1 are regulator molecules important in the pathology and physiology of iron metabolism. The aim of these studies was to produce Hfe KO mice on a strain known to have higher basal hepatic iron levels and study iron homeostasis in relation to variable dietary iron and inflammation in these mice. The regulation of hepcidin was investigated in Huh7 cells exposed to various stimuli such as iron, inflammation and hypoxia. In addition, Huh7 cells were exposed to conditioned medium obtained from HH1 patient's macrophages. Results obtained from these studies are described and discussed in this thesis.

In brief, it was found that the disruption of the Hfe gene causes a preferential accumulation of iron in the caudate lobe of the mouse liver. Contrary to previous findings, iron loaded diet does not have an effect on hepcidin expression in wt SWR mice while in Hfe KO SWR mice it significantly upregulates hepcidin expression. Furthermore, the upregulation of hepcidin by turpentine oil-induced inflammation in SWR mice is Hfe-dependent. Hepcidin expression is down regulated by hypoxia and anaemia and conditioned medium from patients with HH1 macrophages have no effect on hepcidin expression levels.

In conclusion, the results show that SWR Hfe KO mice is not an accurate model for the study of HH1, the studies described here, however, contribute to the understanding of how hepatocytes respond to iron status, hypoxia and inflammation and the relevance of the Hfe gene in the regulation of hepcidin expression levels as well as hepatic DMT1 and Ireg1 expression levels.

Dedicated to,

Mã

ACKNOWLEDGEMENTS

The work reported in this thesis was carried out in the Department of Biochemistry and Molecular Biology at the Royal Free and University College School of Medicine, London, UK. I am grateful to the MRC Iron Metabolism Interdisciplinary Research Group without which this work could not have been performed.

First and foremost, I would like to thank my supervisor Professor S. Kaila S. Srai for his enthusiasm, interest and invaluable advice during the course of my thesis.

I would like to thank fellow members of the Department of Biochemistry specifically, Nita Solanky and Sara Balesaria for their support, motivation and friendship. I should also like to thank Dr. Edward Debnam for being my mentor and giving advice during the writing of this thesis, Prof. Paul Dhillon for teaching me histology and Dr. Roozina Rafique who made a substantial contribution to this work by providing me with the Huh7 cell line. My sincere thanks are also extended to various members of King's College London. In particular, I thank Prof. Robert Simpson for the critical review of this work and Dr. Adrian Bomford for helping me understand the clinical aspects of haemochromatosis disease. I would also like to thank Dr. Paul Sharp, Dr. Abas Laftah and to Dr. Robert Evans for his generosity and efficiency in providing the apotransferrin and holotransferrin required for this thesis.

I would also like to thank my family and friends for their patience and invaluable support over the past four years. Especial thanks in this respect to Maria Macedo and Meera Thayalan for sharing this venture and giving me encouragement.

Last but by no means least, my thanks go to Ben for his encouragement, patience and invaluable support throughout these last fours years.

COLLABORATIONS

Chapter 4: Hepatoma cell line, Huh7 provided by Dr Roozina Rafique[1]

Huh7 cells treated with FAC and DFO provided by Dr Roozina Rafique[1]

Apotransferrin and Holotransferrin provided by Dr Robert W. Evans[2]

Blood samples from HH1 patients provided by Dr Adrian Bomford[3]

Chapter 5: Caco-2 cells exposed to cytokines provided by Dr Paul A. Sharp[4]

Hepatoma cell line, Huh7 provided by Dr Roozina Rafique[1]

Chapter 6: Duodenum and liver samples, haematological parameters of rats exposed to long term hypoxia provided by Dr Edward S. Debnam[5]

Hepatoma cell line, Huh7 provided by Dr Roozina Rafique[1]

Liver biopsies from Thalassemia patients provided by Dr. Farrah Shah[6]

[1] Department of Haematology, University College London Medical School, London, UK.

[2] Metalloprotein Research Group, Randall Division of Cell and Molecular Biophysics, King's College London, London, UK.

[3] Institute of Liver Studies, King's College Hospital, Denmark Hill, London, UK.

[4] Nutritional Sciences Division, King's College London, Franklin-Wilkins Building, London, UK.

[5] Department of Physiology, Royal Free and University College Medical School, Royal Free Campus, London, UK.

[6] Department of Haematology, Whittington Hospital NHS Trust, London, UK.

CONTENTS

LIST OF FIGURES

LIST OF TABLES

ABBREVIATIONS

ACD	Anaemia of chronic disease
Actin	β- Actin
AI	Anaemia of inflammation
AD	Autosomal dominant
AR	Autosomal Recessive
ApoTF	Apotransferrin
BMP	Bone morphogenetic protein
β2m	β 2-microglobulin
β2m	β 2-microglobulin knockout
CCl_4	Carbon tetrachloride
Cp	Caeruloplasmin
Dcytb	Duodenal cytochrome b
dL	Decilitre
DMT1	Divalent metal transporter 1
DMT1 (+ire)	Divalent metal transporter 1 with an iron responsive element
DMT1 (-ire)	Divalent metal transporter 1 without an iron responsive element
EPO	Erythropoietin
Fe	Iron
Fe^{2+}	Ferrous iron
Fe^{3+}	Ferric iron
Ferritin L-chain	Ferritin light chain
Ferritin H-chain	Ferritin heavy chain
g	Grams
GAPDH	Glyceraldehyde 3-phosphate dehydrogenase
HAMP or hepcidin	Hepcidin gene
Hepcidin	Hepcidin protein
Hb	Haemoglobin
Hfe KO	Hfe knockout
HJV	Hemojuvelin
HH	Hereditary Haemochromatosis
HH1 of HFE1	Hereditary Haemochromatosis type 1 or Hfe related HH
HH2	Hereditary Haemochromatosis type 2 or juvenile HH
HH3	Hereditary Haemochromatosis type 3 or TfR2 related HH
HH4	Hereditary Haemochromatosis type 4 or Ferroportin disease
HHCS	Hereditary hyperferritinemia-cataract syndrome
HIC	Hepatic iron concentration
HIF	Hypoxia inducible factor
HII	Hepatic iron index
HLA	Human leukocyte antigen
HO	Haem oxygenase
HoloTF	Holotransferrin

Hp	Hephaestin
HPRT	hypoxanthine phosphoribosyl transferase-encoding
hrs	Hours
H_2O_2	Hydrogen peroxide
IL-1	Interleukin 1
IL-6	Interleukin 6
Ire	Iron responsive element
Ireg1	Iron regulated transporter 1
IRP	Iron response protein
I.V.	Intravenous
kDa	kilo Dalton
Kg	Kilogram
KO	Knockout
LEAP-1	Liver expressed antimicrobial peptide 1
LPS	Lipopolysaccharide
M	Men
mg	Micrograms
MHC	Major histocompatibility
mL	Millilitre
Mr	Molecular mass
MRI	Magnetic Resonance Imaging
mRNA	Messenger ribonucleic acid
ng	Nanograms
NO	Nitric oxide
NRAMP	natural resistance-associated macrophage protein
NTBI	Non-transferrin bound iron
RBC	Red blood count
RE	Reticuloendothelial
RGM	Repulsive guidance molecule
RNA	Ribonucleic acid
SEM	Standard error of the mean
sTfR1	Soluble transferrin receptor 1
SWR	Swiss-Webster
TF	Transferrin
TfR	Transferrin receptor
TfR1	Transferrin receptor 1
TfR2	Transferrin receptor 2
TGF-β	Transforming growth factor beta
TI	Thalassemia intermedia
TM	Thalassemia major
TNF-α	Tumour necrosis factor- α
$Trf^{hpx/hpx}$	Hypotransferrinemic mice
UTR	Untranslated region of a mRNA transcript

µg	Microgram
µmol	Micromole
W	Women
wt	Wild type
3′	3 prime terminal
5′	5 prime terminal

Chapter 1
Background

1.1 Iron metabolism

The word "iron" comes from the Anglo-Saxon word "*iren*" and the symbol Fe comes from the Latin word "*ferrum*" meaning "*iron*". Possibly the word iron is derived from earlier words meaning "holy metal" because it was used to make the swords used in the Crusades.

Iron has been used by physicians to treat several conditions throughout history. According to Nicholas Monarde, a 16th century physician in Seville, the uses of iron as a medicine included treatment of disorders such as Tuberculosis, Fevers, Acne and Weakness. In 1713, Lemery and Geoffroy demonstrated the presence of iron in the blood, but only two centuries later the metabolism of iron in the body began to be understood. In 1925, Fontes and Trivolle (Fontes and Thivolle 1925) documented the existence of non haemoglobulin iron in serum and suggested that there was a circulating form of iron. Over the next two decades, the transport protein, transferrin, was identified and the fact that iron dissociated from it at low pH was established. In a classic 1937 article, Widdowson and McCance (Widdowson and McCance 1937) summarised the experimental findings showing that the main site of absorption was the upper intestine or duodenum and that very small amounts of iron were absorbed from the entire intestinal tract. Though how the mucosal iron absorption is regulated was not then understood.

In the first part of the 20th century, the study of Whipple on haemoglobin regeneration by means of liver and other foods in anemia due to blood loss in dogs (Whipple and Robscheit-Robbins 1925a;Whipple and Robscheit-Robbins 1925b) demonstrated the role of food in the enhancement of blood formation. This finding led Minot and Murphy (Minot 1934;Minot and Murphy 1926) to develop the first effective and life-saving therapy for pernicious anaemia thus winning the 1934 Nobel Prize for Medicine and Physiology. Once radioactive iron (radioiron) was available it was easier to assess how the mucosal regulation of iron absorption occurs. In 1963, Conrad and Crosby noted that radioiron appeared to enter mucosal cells but the cells were sloughed off with the iron they absorbed when the body iron

needs were low (Conrad, Jr. and Crosby 1963). This suggested that the regulation of iron absorption occurred at the level of transfer from the mucosal cell to the blood. This concept is still widely held today, but the mechanisms by which the transfer is regulated are still being studied and therefore not fully understood.

It is known that iron is recycled continually by the breakdown of dying red cells in macrophages and release of iron to serum transferrin (about 20-30mg/day). Iron is lost from the body by processes such as sloughing of skin, and menstruation (about 1-2mg/day of Iron) (Demaeyer 1980). Apart from these small losses, there is no physiological iron excretion system in mammals to regulate body iron levels and therefore the primary mechanism by which the total body iron level is controlled is through the regulation of iron uptake from the diet (Cavell and Widdowson 1964).

It is, therefore, necessary to fully understand the mechanisms of the systematic homeostasis, which requires the coordination of iron absorption, transport, storage, recycling and utilisation throughout the body, in order to prevent iron deficiency diseases such as anaemia and iron overload diseases such as hereditary Haemochromatosis (HH).

1.2 Iron circulation in the body

Iron is an essential element for cellular growth and development as it is essential for many fundamental biochemical reactions such as DNA synthesis, transport of oxygen and electrons and cellular respiration. Under most physiological conditions the Fe atom exists in its oxidized ferric state. If not appropriately shielded, iron (Fe) can readily participate in one-electron transfer reactions that can lead to the production of extremely toxic free radicals. Fe^{2+} (via the Fenton reaction) and Fe^{3+} (via the Haber-Weiss reaction) can generate toxic oxygen radicals in the presence of oxygen derivatives (H_2O_2, O_2) (Imlay and Linn 1988) (Halliwell 1994;Stadtman and Wittenberger 1985). To prevent "free" iron from reaching toxic levels, higher organisms have developed Fe-binding proteins known as the transferrins (Tfs)

(Richardson and Ponka 1997;Sahlstedt et al. 2002). After absorption, ferric iron binds to transferrin in the serum and is carried to the bone marrow to be used for erythropoiesis. Here the iron binds transferrin receptors in red cell precursors and is internalised by endocytocytosis. The transferrin cycle will be discussed in section 1.2.1.1.

A well-balanced diet must contain sufficient iron to meet the body requirements. About 1-2 mg of dietary iron is absorbed each day, and this is sufficient to balance the daily losses (Cook et al. 1973), and maintain a relatively constant amount of body iron throughout life. Adults have normally around 2-4 g of total body iron. About 2 g of this total is found in red blood cells as haeme in haemoglobin, and 1 g occurs as storage iron (haemosiderin or ferritin), with the remainder in muscle myoglobin and in tissue enzymes that require iron. The main site of iron storage is the liver (Fig. 1.1).

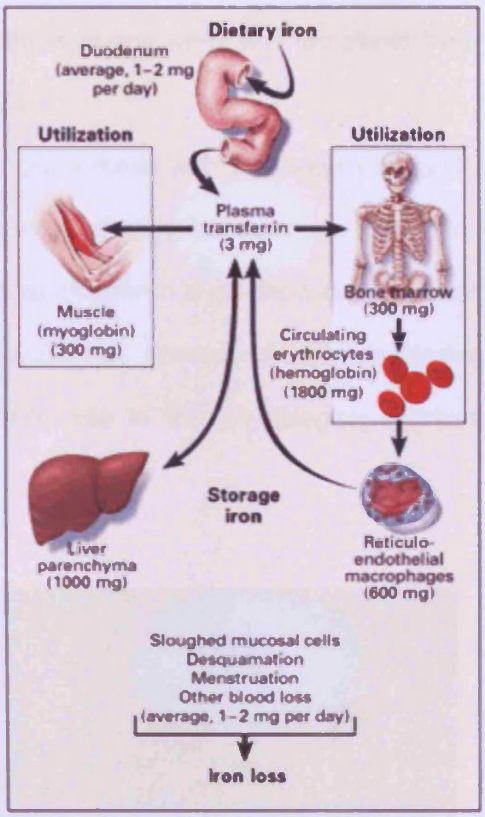

Figure 1.1 Iron circulation in the human body.

Dietary iron gets absorbed into the plasma at the proximal duodenum. In the erythroid marrow, iron gets incorporated into haemoglobin of the red blood cells which are then released into circulation. Senescent red blood cells are taken up by macrophages that then recycle the iron into circulation. Surplus iron is stored in the liver (Finch et al. 1950;Wessling-Resnick 2006). Figure adapted from (Andrews 1999).

1.2.1 Transferrin

Transferrin (Serum TF) is a protein from the Transferrin family which also includes lactoferrin, and ovotransferrin. Serum TF functions to transport iron between sites of absorption, storage, and use while ovotransferrin from egg white and lactoferrin from milk and other secretions have bacteriostatic functions.

Human TF is a monomeric glycoprotein with a molecular mass (Mr) of 80 kDa. It consists of two homologous domains, each of which contains one high-affinity Fe^{3+}-binding site (Bailey et al. 1988). Affinity of iron to transferrin is pH-dependent; in plasma (approximately pH 7.4), transferrin binds iron very strongly, whereas virtually no binding occurs at pH ≤4.5. This property plays an important role in the physiological mechanism of iron release from transferrin.

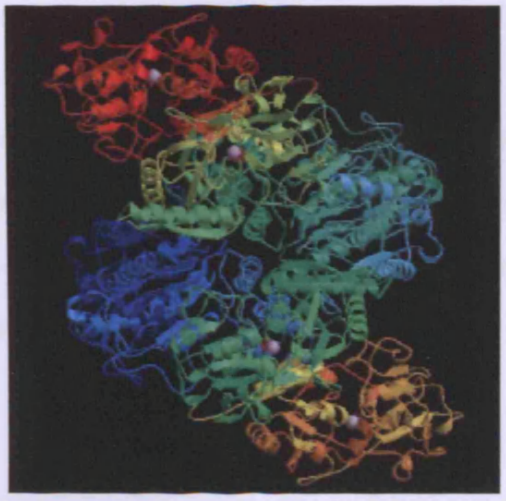

Figure 1.2 Ribbon representation of the transferrin receptor-transferrin (TFR-TF) complex

Iron circulates in the blood bound to transferrin. Transferrin binds two atoms of Fe^{3+} with high affinity. Taken from http://crystal.harvard.edu/structures.php) on 25/02/2007.

Transferrin binds two atoms of Fe^{3+} with high affinity, but only when concomitant binding of carbonate or bicarbonate occurs. Binding and release of iron by transferrin are accompanied by dramatic conformational changes in the protein. In the absence of iron, the two domains involved in the binding are widely separated and assume an "open" configuration. On the other hand, insertion of iron brings the two domains of the binding cleft close toward the metal, and transferrin assumes a "closed" conformational state.

Transferrin is normally about one-third saturated with iron, with approximately 10% present as diferric transferrin. In healthy adults, the total plasma iron pool (approximately 3 mg) remains remarkably constant despite being turned over more than 10-fold every day and is virtually unaffected by iron in stores (ferritin and haemosiderin) that can vary from 350 to 900 mg in females and males, respectively. There seems to be a control mechanism that guarantees that the rate of iron release from stores perfectly matches the one with which the iron is taken up by tissues, but the nature of this regulation is still unknown.

In vertebrates, the major protein involved in iron uptake of TF-bound iron into cells is the plasma membrane transferrin receptor (TFR). There are two molecules of TFR, TFR1 and TFR2; both receptors deliver iron to the cells and bind diferric transferrin in a pH dependent manner (Richardson and Ponka 1997).

1.2.1.1 Transferrin receptor 1 (TFR1) and TFR1 mediated iron uptake

Apart from mature red blood cells, all cells have TFR1 on their surface, with its highest numbers being in the erythron, placenta and liver. The TFR is a disulphide-linked homodimeric type II transmembrane protein, which has two identical subunits each of them having a binding site for TF. Following the binding of the two proteins (TF-TFR) (Fig. 1.2), the complex (TF-Fe^{3+}-TFR1), is internalised through clathrin-coated pits into specialised endosomes (Killisch et al. 1992). Upon maturation and loss of the clathrin coat, the decreased of pH leads to a protonation of the Fe-binding sites of TF and the release of Fe (Fig. 1.4). Fe

is then released into the cytosol through DMT1, which is selective for ferrous iron, Fe^{2+} (Fleming et al. 1998;Gruenheid et al. 1999). As TF carries ferric iron (Fe^{3+}), iron must be reduced in the TF cycle endosome. The erythroid reductase that carries out this activity has recently been identified as STEAP3, the epithelial antigen of the prostate 3 (Ohgami et al. 2005).

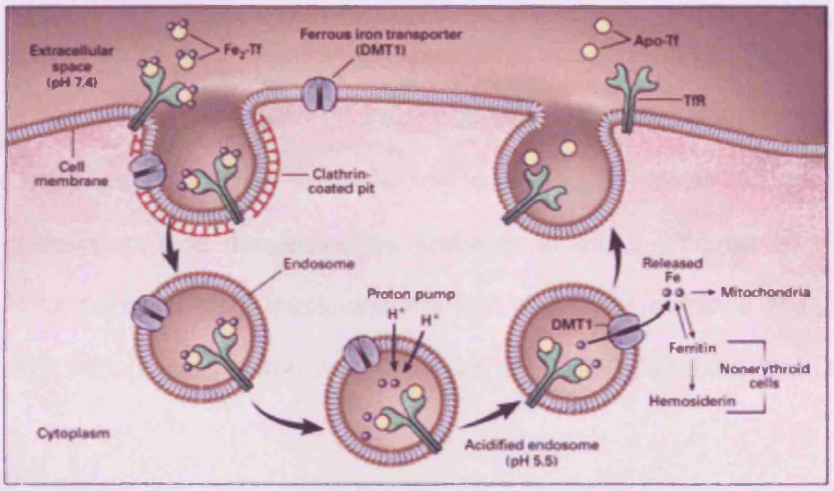

Figure 1.3 Transferrin Cycle

Following the binding of (TF-TFR) - Fe^{3+}, on the surface of erythroid precursors, the complex is internalised through clathrin-coated pits into specialised endosomes. Upon maturation and loss of the clathrin coat, a proton pump decreases pH leading to conformational changes in proteins that result in the release of Fe. Iron is then reduced by the newly described erythroid reductase STEAP3 before DMT1 moves iron across the endosomal membrane, to enter the cytoplasm. Once in the cytosol iron is either stored or utilised by the cell. Following the release of the iron, the transferrin-TFR1 complex is recycled to the cell surface, where each can be used for further cycles of iron binding and iron uptake (Andrews 1999).

Once in the cytosol iron is either stored or utilised by the cell. Following the release of the iron, the Transferrin-TFR1 complex is then recruited through exocytic vesicles back to the cell surface (van Weert et al. 1995). At physiological pH apotransferrin (iron-free TF) dissociates from the receptor and returns to the circulation where it is reutilised in further cycles (Richardson and Ponka 1997;Salter-Cid et al. 1999;Dautry-Varsat et al. 1983).

1.2.1.2 TFR2

A second human transferrin receptor gene, TFR2 has been cloned (Kawabata et al. 1999). TFR2 has significant sequence homology with the classical transferrin receptor (TFR1), and also mediates the cellular uptake of transferrin-bound iron. Although both TFR1 and TFR2 are capable of transporting transferrin-bound iron into the cell, their properties differ in several critical ways. TFR2 has a lower affinity for diferric transferrin than does TFR1 (Kawabata et al. 1999;West, Jr. et al. 2000). While TFR1 is expressed in almost all cells, TFR2 is expressed at much higher levels in liver compared with other tissues (Fleming et al. 2000;Kawabata et al. 2001). The receptors also differ in their response to changes in cellular iron status. The TFR1 transcript contains multiple iron-responsive elements in the 3'-untranslated region (UTR) while the TFR2 does not have these elements and thus TFR2 message and TFR2 protein levels vary little with changes in iron status (Fleming et al. 2000;Kawabata et al. 2000).

Recent data suggests that TFR2 senses the body iron status by sensing the concentration of diferric transferrin also called holotransferrin or iron-saturated transferrin (Aisen 2004;Camaschella 2005;Johnson and Enns 2004;Robb and Wessling-Resnick 2004;Scheiber-Mojdehkar et al. 2003). In hepatocyte-derived cell lines and animal models, increasing concentrations of holotransferrin but not apotransferrin increases TFR2 protein levels (Johnson and Enns 2004;Robb and Wessling-Resnick 2004). It has also been recently reported that the cytoplasmic domain of TfR2 is essential for its stabilization by diferric TF (Chen and Enns 2007).

Mutations in the TfR2 gene have been found to responsible for HFE4 (Girelli et al. 2002;Roetto et al. 2001), whereas functional loss of TfR1 (TfR1 KO mice) produces an embryonic lethal phenotype (Levy et al. 1999a). This indicates that the roles for TFR1 and TFR2 in iron homeostasis are not redundant.

1.3 Dietary Iron uptake

1.3.1 Structure of the duodenum

The proximal portion of the small intestine, starting at the lower end of the stomach and extending to the jejunum is called the duodenum. The name *duodenum* comes from the latin *duodenum digitorum*, twelve fingers' breadths due to its length (Duthie 1964;Johnson et al. 1983;Wheby et al. 1964). The lumen surface of the duodenum is covered by millions of small projections called villi which extend about 1 mm into the lumen (Fig. 1.4).

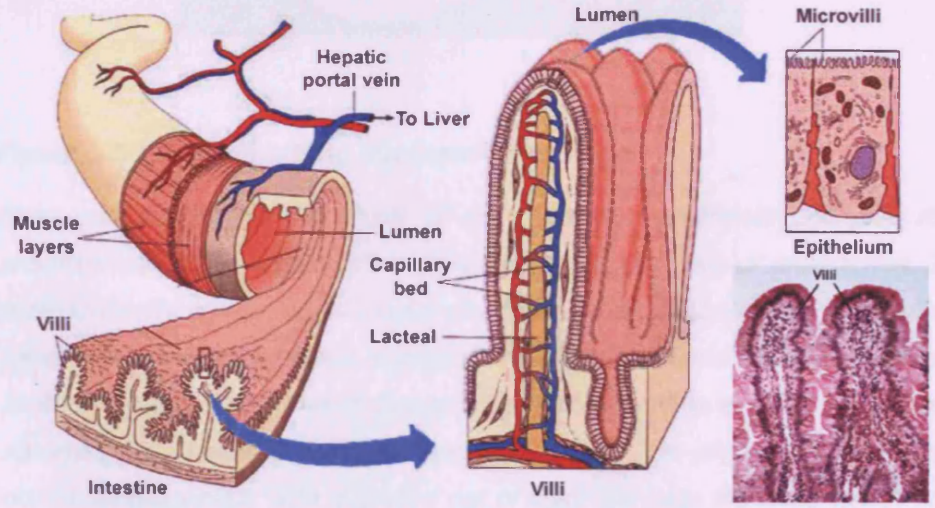

Figure 1.4 Structure and physiology of the duodenum

The lumen surface of the duodenum is covered by millions of small projections called villi which extend about 1 mm into the lumen.

Villi are covered predominantly with mature enterocytes, along with occasional mucus-secreting goblet cells. Intestinal mucosal mature enterocytes lining the villi close to the gastroduodenal junction are responsible for all the dietary iron absorption. The precursor cells differ from mature enterocytes in their expression of proteins. While mature enterocytes are

specialized for absorption and transport of iron, its precursor acts only as a sensor of body iron needs.

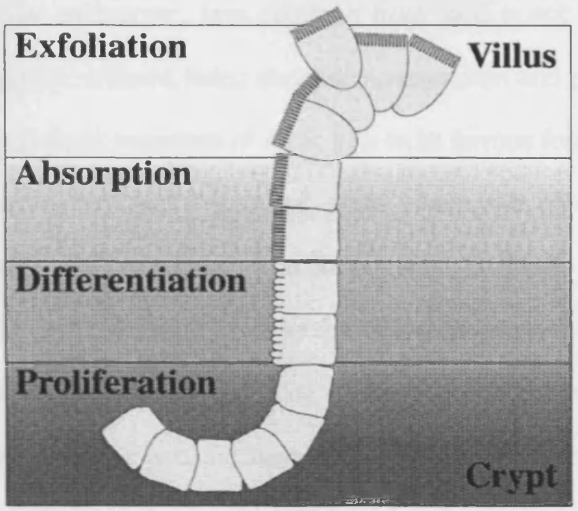

Figure 1.5 Life Cycle of the duodenal enterocytes

Stem cells present in the crypts of the duodenum proliferate and give rise to precursor cells that further differentiate into absorptive cells or enterocytes. These enterocytes are highly specialised for absorption of micronutrients from the intestinal lumen. Their apical membrane is structured with microvilli and contains enzymes that facilitate transport of nutrients through the epithelial cell layer. The majority of iron absorption is facilitated by these specialised cells. The process of differentiation occurs simultaneously with migration out of crypt and onto the villus. Zones of cells in similar stages are evident when the crypt/villus junction is viewed in cross section. After the cells have migrated to the villar tip, they are exfoliated and excreted (Roy and Enns 2000).

Enterocytes originate from undifferentiated cells in the crypts of Lieberkuhn (Ito and Terao 1994). From here they migrate apically along the villi and are finally lost by exfoliation and apoptosis (Fig. 1.5). By the time cells reach the mid-villus they have become mature (Morgan and Oates 2002;Roy and Enns 2000).

1.3.2 Duodenum iron uptake

To reach the plasma, iron must pass from the gut lumen through the apical and basolateral membranes of the mature enterocyte. Iron obtained from food is not bound to transferrin, instead, the low pH of gastric effluent helps dissolve ingested iron and provides a proton-rich milieu. This facilitates enzymatic reduction of ferric iron to its ferrous form.

Dietary iron compounds can be divided into two types, haem and non-haem. Haem iron is absorbed more efficiently than non-haem iron in humans (Bothwell and Charlton 1979). Consequently, haem iron may contribute more to the absorbed iron even though it represents a lesser fraction of ingested iron. The absorption of haem and non-haem iron differs in the initial uptake step. Haem iron enters mucosal cells through the brush border membrane probably by endocytosis or via HCP1, as the intact iron-protoporphyrin complex, and within the cells the iron is released by the action of the microsomal enzyme, haem oxygenase. From then on the iron enters the same intracellular pool as newly absorbed non-haem iron and therefore will be affected by the same factors (Morgan and Oates 2002).

Regulation of iron uptake into the body occurs at both the apical and basolateral membranes of the intestinal epithelium. The apical membrane of the differentiated (mature) enterocyte, which faces the intestinal lumen, is specialized for transport of haem and ferrous iron into the cell. Three pathways have been reported for this transport process: haem-iron uptake pathway involving HCP1, iron uptake pathway involving DMT1 and iron uptake involving mucin and mobilferrin. The most extensively characterized uptake pathway is via the divalent metal transporter, DMT1 (previously named Nramp2 and DCT1) which will be described in section 1.3.3.

Iron can also be absorbed by the haem-iron uptake pathway which involves the recently described iron-regulated intestinal haem transporter, HCP1 (Shayeghi et al. 2005). In this pathway, haem binds to the brush-border membrane of duodenal enterocytes, intact molecules are translocated across the membrane by HCP1 and in the cytoplasm haem is contained in membrane-bound vesicles (Conrad et al. 1966;Weintraub et al. 1965;Wheby 1970;Wyllie and Kaufman 1982). Haem is then degraded by haem oxygenase (HO) to yield

ferrous iron (Raffin et al. 1974), which enters the pool of low molecular weight iron and the iron absorbed as non-haem iron (Abboud and Haile 2000;Donovan et al. 2000;McKie et al. 2000). More recently HCP1 has been shown to have a role in proton-coupled folate transport required for folate homeostasis in man, suggesting that this gene has several functions (Qiu et al. 2006).

Thirdly, Conrad et al have proposed a model in which iron would bind to mucin in the intestinal lumen, then transfer to integrin at the cell surface, and then transfer to the intracellular protein mobilferrin, which is a calreticulin homologue (Conrad et al. 1991;Conrad et al. 1992;Conrad et al. 1993;Conrad and Umbreit 1993). Calreticulin is a multifunctional calcium binding protein involved in the folding of endoplasmic reticulum synthesized proteins. It is also a shock protein induced by heat, food deprivation and chemical stress (Szewczenko-Pawlikowski et al. 1997). When the intracellular iron increases there is a significant increase in calreticulin. As an oxidative stress-induced protein it is thought that this iron-induced calreticulin protects the ER, cytosol and nucleus against oxidative damage (Nunez et al. 2001).

1.3.3 The molecular mechanism of duodenal non-haem iron uptake (Fig.1.8)

As previously mentioned at physiological pH, and in the diet, iron is predominantly in the highly insoluble ferric (Fe^{3+}) form, whereas iron transport systems take up the ferrous (Fe^{2+}) form. Thus iron needs to be reduced by the ferric reductase Dcytb (Duodenal cytochrome b) or some other mechanism e.g. by ascorbate, before it can enter the cell. Non-haem is then transported into the cell mainly by the Divalent Metal Transporter 1 (DMT1). Once inside the cell, iron can either be stored as ferritin or be transferred across the basolateral membrane to reach the plasma. These fates are not mutually exclusive and the determining factor is thought to be decided when the enterocytes develops from the crypt cell. Iron stored as ferritin returns to the lumen when the enterocyte completes its limited life cycle and is sloughed off. The basolateral iron exporter was identified by three groups, one of whom named it Ireg1. Ireg1 is thought to require Hephaestin, a ferrous oxidase that converts Fe^{2+}

to Fe^{3+} facilitating the iron transport across the basolateral membrane of intestinal enterocytes into the bloodstream.

The proteins required for the non-haem iron absorption, transport into the enterocytes across the brush border membrane, movement of iron through the cells; transport across the basolateral membrane and passage through the intestinal space and capillary wall are described in more detail below.

1.3.3.1 Dcytb

The ferrous form of iron (Fe^{2+}) is very unstable and quickly oxidises to ferric iron. To prevent this from happening, ferric reductases (or ferric-chelate reductases) which are specialised transmembrane electron transport systems have evolved. These redox systems use intracellular reducing cofactors to reduce ferric iron (Fe^{3+}) to ferrous iron (Fe^{2+}) at the extracellular surface.

Although described since 1992 (Raja et al. 1992;Simpson et al. 2003) it was not until 2000 that the ferric reductase was isolated, cloned and named **d**uodenum **CYT**ochrome **B** (Dcytb) (McKie et al. 2001). As expected from a protein involved in iron transport, Dcytb mRNA and protein levels in the duodenum respond to changes in iron status. Both mRNA and protein levels increase in conditions that stimulate iron absorption, such as iron deficiency and hypoxia, and are reduced in iron loading conditions (Collins et al. 2005). Dcytb is highly expressed in the brush-border membrane of duodenal enterocytes but also in other tissues such as spleen, liver and brain (McKie et al. 2002).

1.3.3.2 DMT1

Ferrous Iron is then transported across the apical membrane (Fig. 1.8) by the **D**ivalent **M**etal **t**ransporter **1** (DMT1), also called Nramp2, SLC11A2, or DCT1. DMT1 is a member of the "natural resistance-associated macrophage protein" (Nramp) family and was identified by two groups in 1997 (Fleming et al. 1997;Gunshin et al. 1997). The phenotype of microcytic anaemia mice (gene symbol *mk*), characterised by an impairment in iron absorption that leads to iron deficiency, suggested that the causative mutation was likely to be in an intestinal transporter functioning at the brush border. Eventually Fleming (Fleming et al. 1997), localised the DMT1 mutation unique to the *mk* mice. In parallel experiments, Gunshin et al searched for an intestinal iron transporter using a Xenopus oocyte expression cloning system and found a single cDNA that stimulated iron transport. This cDNA encoded rat DMT1 and they went on to show that DMT1 transported not only iron but also a variety of other heavy metals including cobalt, manganese, lead, zinc, and copper (Gunshin et al. 1997).

DMT1 mRNA expression is ubiquitous and has been detected in most tissues and cell types analysed; however, it is higher in brain, thymus, proximal intestine, kidney, and bone marrow (Gunshin et al. 1997).

Two spliced products were identified for DMT1 in several species. One transcript contains a sequence that resembles an iron responsive element (IRE) within its 3'-UTR, whereas the alternatively spliced counterpart lacks this sequence and encodes a protein that is seven amino acids longer at the C-terminus (DMT1-IRE) (Fleming et al. 1997;Gunshin et al. 1997). Only the splice form containing the IRE (DMT1+IRE) is responsive to iron, both in cultured cells and in the human intestine (Byrnes et al. 2002;Canonne-Hergaux et al. 1999;Zoller et al. 1999). The level of regulation in intestine was higher compared to other tissues such as liver, kidney, heart and brain (Gunshin et al. 1997) and in iron deficiency, hypoxia, or stimulated erythropoiesis, the expression of DMT1 mRNA and protein in the duodenum is increased leading to an increase in iron absorption (Canonne-Hergaux et al. 1999).

1.3.3.3 Ferritin and Haemosiderin

Once inside the cell, iron can either be stored as ferritin or be transferred across the basolateral membrane to reach the plasma. Ferritin is a ubiquitously expressed protein and sequestration and storage of iron is its main function (Theil 1983;Theil 1990). Ferritins constitute a broad superfamily of iron-storage proteins in organisms as diverse as bacteria, fungi, plants and vertebrates and this wide distribution among living species implies a fundamental and ancient role in iron metabolism.

Ferritin (Fig. 1.7), is a large cytoplasmic protein consisting of symmetrically related subunits of two types, a light subunit (L-subunit) and a heavy subunit (H-subunit) (Arosio and Levi 2002;Harrison and Huehns 1979;Harrison et al. 1986;Harrison 1977) which assemble to form a shell of 24 subunits with a cavity capable of storing up to 4500 iron atoms as hydrous ferric oxide (Mann et al. 1986;Theil 1983;Theil 1990). The mechanism by which ferritin obtains Fe remains unknown but in vitro experiments have suggested that Fe^{2+} is more rapidly incorporated into the protein than Fe^{3+}. The protein shell seems to play an essential role in the initial oxidation of the incoming Fe (Richardson and Ponka 1997).

The amino acid sequences of the H- and L-subunits differ by approximately 50%, and the contents of the two chains vary according to the organ and its iron requirements. It appears that while H chains confer ferroxidase activity to the heteropolymer, L chains confer nucleation sites for iron binding (Levi et al. 1988;Levi et al. 1992). Despite this differences, synthesis of both subunits is translationally controlled by common cytoplasmic proteins, iron regulatory proteins (IRP-1 and IRP-2), which bind to the iron-responsive element (IRE) in the 5'-untranslated region (UTR) of messenger RNA (mRNA) (Huang et al. 1999). How IRPs with IREs regulate cellular iron uptake will be discussed in section 1.5.1.

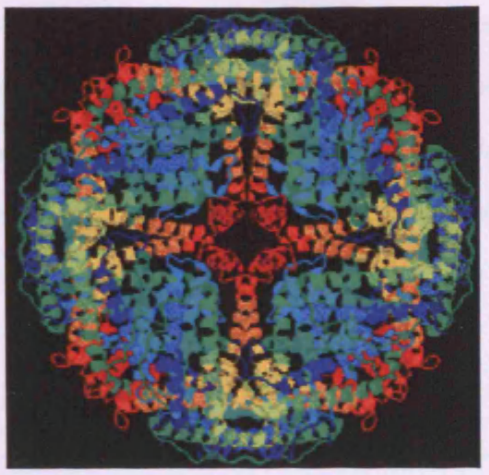

Figure 1.7 Ribbon representation of the Ferritin molecule

Ferritin is a large cytoplasmic protein consisting of symmetrically related subunits of two types, a light subunit (L-subunit) and a heavy subunit (H-subunit) which assemble to form a shell of 24 subunits with a cavity capable of storing up to 4500 iron atoms as hydrous ferric oxide. Taken from http://www.chemie.tu-darmstadt.de/akplenio/moproc/eisen/uebersicht.htm on 25/02/2007.

At normal levels of body iron, the expression of ferritin in the average cell (e.g. fibroblasts) is quite low, which contrasts with cells from tissues that have specialised functions in iron and possible oxygen homeostasis (e.g. liver and heart). Apart from storage, ferritin seems to have a protective 'anti-oxidising' function by sequestering the iron inside the cavity (Theil 2003). Ferritin has also been detected in the circulation of normal subjects but the origin and possible physiological role of plasma ferritin in normal individuals remain elusive. Linder (Linder et al. 1996), identified a number of unexpected differences between plasma and tissue ferritin, and it has been suggested that the serum ferritin may not be the product of the same genes as those encoding intracellular ferritin. The serum ferritin is a universally available and well-standardized measurement that has been the single most important laboratory measure of iron status during the past quarter century. It is used to diagnosis of patients who are suspected to have an iron overload disease (mainly hereditary haemochromatosis), or iron deficient anaemia (Beutler et al. 2003).

Haemosiderin is a poorly defined iron-protein that forms an insoluble iron storage system. Under normal homeostatic conditions the body tissues contain low amounts of haemosiderin, however under primary and secondary iron overload conditions; content of haemosiderin dramatically increases in tissues, particularly in organs such as the liver, heart and pancreas.

1.3.3.4 Hephaestin

Hephaestin (Hp) is a member of the blue multicopper oxidase family which is found in organisms as diverse as bacteria and humans. The Hp protein was found to have significant sequence identity to ceruloplasmin (Cp), a serum multicopper ferrioxidase with the ability to convert Fe^{2+} to Fe^{3+} (Syed et al. 2002). Further insights into the mechanism of hephaestin (after the Greek god of metal–working) have been obtained from the study of the sex-linked anaemia *(sla)* mouse (Bannerman et al. 1973;Chen et al. 2004b;Vulpe et al. 1999). A partial deletion of the hephaestin (Hp) gene in these mice leads to systemic iron deficiency but also iron accumulation in the enterocytes (Chen et al. 2004b;Manis 1971;Vulpe et al. 1999). The similarity between the Hp and Cp, along with the phenotype of *sla* mice, led to the conclusion that the ferrioxidase activity of Hp is critical in converting Fe^{2+} to Fe^{3+} and thus allowing iron to be released from enterocytes through the basolaterally located transporter Ireg1 prior to incorporation into transferrin (Chen et al. 2004b;Kuo et al. 2004;Syed et al. 2002;Vulpe et al. 1999).

Despite the sequence similarities, Hp expression contrasts that of Cp. Hp expression in the intestine is limited to the villi, the site of iron absorption while Cp is not expressed in the intestine but is highly expressed in liver and to a lesser extent expressed in other tissues including brain (Klomp et al. 1996;Klomp and Gitlin 1996) and lung.

1.3.3.5 Ireg1

Ireg1 (**I**ron-**reg**ulated transporter-**1**), also called ferroportin1, MTP1 (**M**etal **T**ransporter **P**rotein **1**) and Slc40a1, was identified independently by three laboratories and was shown to play a role in the export of iron (Abboud and Haile 2000;Donovan et al. 2000;McKie et al. 2000) (Fig. 1.8).

Ireg1 like DMT1 is a member of the NRAMP family of metal transporters and was found to be expressed in cells that play a critical role in mammalian iron metabolism, including placental syncyotrophoblasts, duodenal enterocytes, hepatocytes, and reticuloendothelial (RE) macrophages (Montosi et al. 2001). In the placenta, Ireg1 is involved in transfer of iron between the maternal and foetal circulations; in the macrophages of the spleen and in Kupffer cells of the liver, iron released from the breakdown of haem is transported out of the cell to the plasma via Ireg1. Duodenal Ireg1 is expressed at the basolateral membrane of mature absorptive epithelial cells of the villus (Abboud and Haile 2000) where it facilitates the transport of iron from the enterocyte to the circulation.

Ireg1 contains a functional iron responsive element (IRE) within its 5′ UTR and therefore is regulated by iron. Iron deficiency, anaemia and hypoxia increase Ireg1 mRNA and protein levels in the duodenum (Chen et al. 2003;McKie et al. 2000;Pietrangelo 2005).

In the spleen and alveolar macrophages Ireg1 is up-regulated by iron loading rather than iron deficiency indicating that there are tissue-dependent differences in the regulation of Ireg1. The protein also has been shown to be down-regulated in macrophages in mice with acute inflammation. This provides an explanation of how iron may be retained in RE cells during inflammation. The mechanism by which inflammation down-regulates Ireg1 is not yet known but recently, the protein has been shown to be the molecular target of Hepcidin the major negative regulator of duodenal iron absorption and release of iron from macrophages (Delaby et al. 2005;Means 2004;Nicolas et al. 2002b;Park et al. 2001;Pigeon et al. 2001).

Ireg1 mutations have been found to be responsible for the Ferroportin disease. In this disease iron accumulates in enterocytes, splenic macrophages but mainly in Kupffer cells. This location of iron loading probably reflects the lack of Ireg1 function in recycling iron from

the breakdown of haem. The resulting iron becomes trapped in the macrophage and thus makes it unavailable for synthesis of new haemoglobin. This confirms the physiological role of Ireg1 as the major efflux route for iron in macrophages.

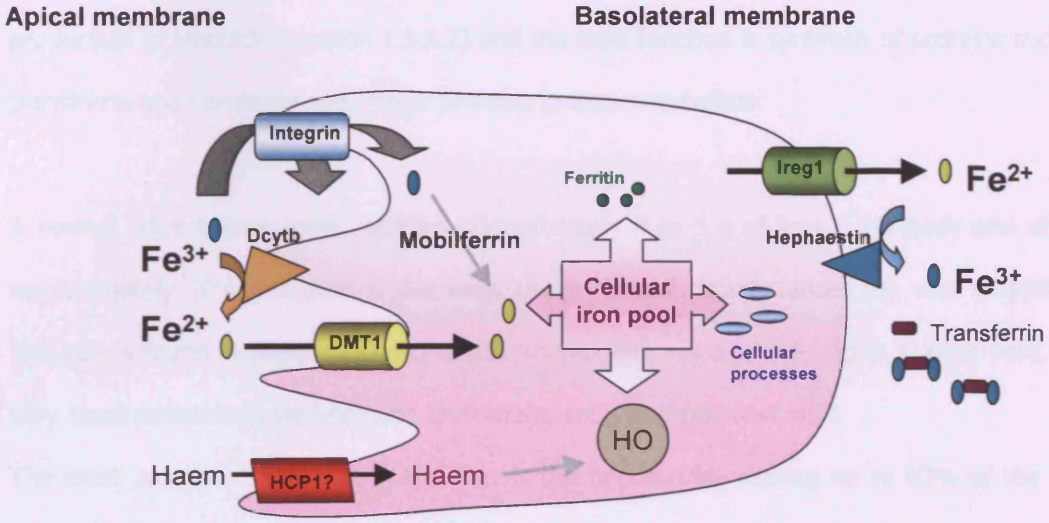

Figure 1.8 Duodenal iron transport

Three pathways have been described for the iron transport across the apical membrane also called brush border membrane. The most extensively characterised pathway involves the divalent metal transporter DMT1 which transports iron into the cell after Dcytb reduces iron to its ferrous form (Fe^{2+}). Iron can also bind mucin and be transferred into the cell by integrin. Recently it has been reported that HCP1 could be the transporter that carries haem into the cell. Once inside the cell the iron can either be stored as ferritin or be transferred across the basolateral membrane by Ireg1 coupled with hephaestin which converts iron into its ferric form (Fe^{3+}). Once in the plasma iron circulates bound to transferrin.

1.3.4 Hepatic iron metabolism

The liver has three functions in iron metabolism. The first function is iron storage, the liver being the main storage site of iron in the body. The second function of the liver in iron metabolism is the regulation of iron trafficking into and around the body through the production of Hepcidin (section 1.3.4.2) and the third function is synthesis of proteins such as transferrin and ceruloplasmin, major proteins in iron metabolism.

A normal adult human male contains approximately 4 to 5 g of iron in his body and of this approximately 10% is stored in the liver. Under normal circumstances the vast majority of this iron is found in hepatic parenchymal cells with the remainder found in Kupffer cells, and very small amounts in stellate cells, endothelial cells, and bile duct cells.

The most prominent cell type in the liver is the hepatocyte, making up to 80% of the liver mass. In iron overload conditions such as Hereditary Haemochromatosis (HH) hepatocytes are the dominant site of iron deposition.

As the main storage site, hepatocytes have a high capacity to synthesize ferritin (Harrison and Arosio 1996) but also Transferrin (TF) (Ponka et al. 1998), Ceruloplasmin (Cp) (Hellman and Gitlin 2002), haptoglobin (Wassell 2000), and hemopexin (Tolosano and Altruda 2002;Wassell 2000). As the main site of expression of the regulatory proteins HFE, transferrin receptor 2 (TFR2) and Hepcidin (Frazer and Anderson 2003;Wassell 2000) hepatocytes also play a major role in the regulation of body iron homeostasis.

Iron can be taken up by the liver in several forms and by several pathways (Figure 1.9). As the vast majority of circulating iron is Tf-bound, the dominant source of iron for the liver is diferric Tf (Trinder et al. 1996;Wassell 2000). However, in iron overload conditions when the capacity of plasma Tf to bind iron is exceeded, iron can also be taken up as non-transferrin-bound iron (NTBI) (Craven et al. 1987;Parkes et al. 1995;Randell et al. 1994;Thorstensen 1988;Thorstensen and Romslo 1988;Wright et al. 1986).

As described in section 1.2.1, uptake of iron from transferrin occurs by receptor mediated endocytosis of transferrin, release of iron within the acidic vesicles and extrusion of iron-depleted transferrin [Fig. 1.9, TfR1 Cycle (**1**) and TfR2 Cycle (**2**)].

The divalent metal transporter DMT1 responsible for iron uptake in the enterocytes is also expressed at low levels in the liver mainly in hepatocytes (Trinder et al. 2000b). In the hepatocytes, DMT1 is involved in the uptake of Tf-bound iron through the TfR1 and TfR2 pathways (Trinder and Morgan 1997) and it is thought to contribute to the uptake of NTBI at the cell surface however evidence for this is lacking. Both DMT1 splice forms (DMT1+IRE and DMT1-IRE) are expressed at similar levels in the liver (Tchernitchko et al. 2002) unlike in the duodenum, where the IRE- containing splice form is more abundant. In the duodenum DMT1 expression is upregulated by iron deficiency but in the liver DMT1 levels are enhanced by iron loading (Scheiber-Mojdehkar et al. 2003;Trinder et al. 2000b;Trinder et al. 2002a). The reason for this opposite response is unclear but it is possible that this upregulation may help reduce the circulating NTBI and therefore prevents its toxic effect in iron overload conditions.

The liver can also take up iron from circulating haem, haemoglobin, and ferritin. The levels of these molecules in the plasma is very low under normal conditions but in case of hemolysis or ferritin release from damaged tissues, the liver has a scavenging role in removing them from circulation. Haemoglobin in the circulation is readily bound to haploglobin (liver derived plasma protein) and the protein complex is taken up by macrophages by receptor–mediated endocytosis. Once inside the cell, the haemoglobin/haploglobin complex is degraded in lysosomes and haem is released. The haem is then degraded by haem oxygenase (HO) to release iron.

As excess haem is potentially toxic, most haem and its associated iron are sequestered by hemopexin, a liver derived protein. In addition, specific binding sites for hemopexin and a receptor for haem-hemopexin complexes (LRP/CD91) have been found on the plasma membrane of hepatocytes.

Another potential source of iron for the liver is ferritin. As described in section 1.3.3.3, ferritin is expressed in all body cells and is the major iron storage protein (Harrison and Arosio

1996). At normal levels of body iron, the expression of ferritin is quite low, but in various pathological situations where there is cellular damage, tissue ferritins are released into the circulation. These tissue ferritins are rapidly removed from the plasma by the liver and studies have suggested the possibility of a specific receptor for tissue ferritin (Halliday et al. 1994;Mack et al. 1981). Apart from storing iron, ferritin seems to have a protective 'anti-oxidising' function by sequestering the iron inside the cavity, away from dioxygen, hydrogen peroxide and superoxide, thus assuming a detoxification of intracellular iron function (Theil 2003).

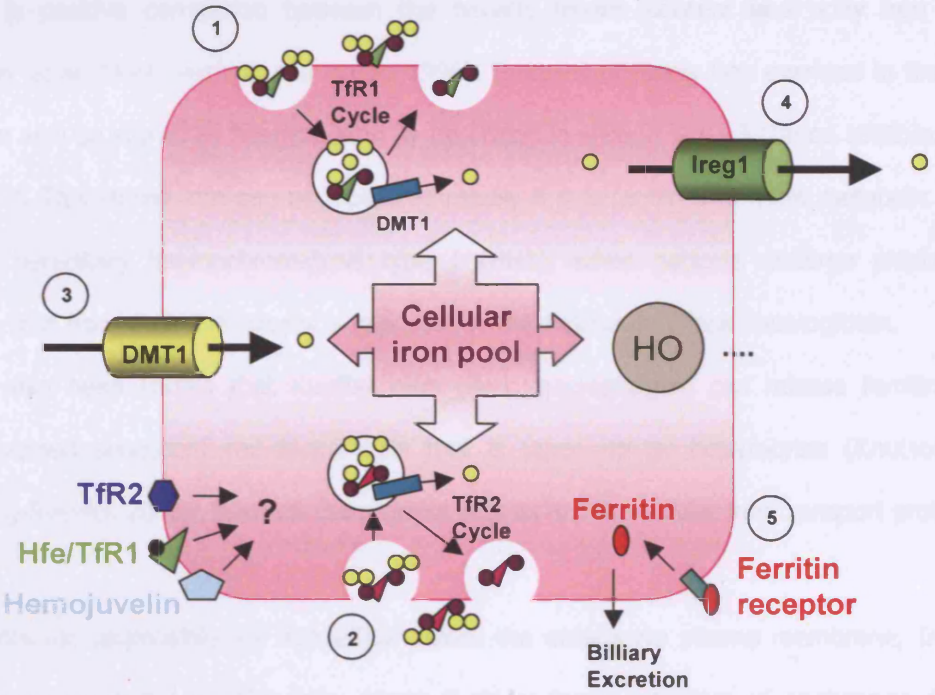

Figure 1.9 Pathways of iron homeostasis in the liver

Representative schaem showing some of the pathways of iron uptake and efflux by the hepatocyte: uptake of iron through the TfR1 pathway (1) and TfR2 pathway (2), uptake of NTBI (3), cellular iron export through Ireg1 (4), uptake of ferritin (5); and its components: Divalent metal transporter 1 (DMT1), Iron regulatory element 1 (Ireg1) and Haem oxygenase (HO).

All the iron that enters the hepatocyte, irrespective of its source enters the same intracellular pool (cellular iron pool). From here iron possibly will be used for metabolic functions, may be stored within ferritin, or may contribute to the regulation of cellular iron metabolism by influencing the activity of IRPs and likely other factors. The physical nature of this cellular iron pool, although present in most cells is poorly defined. It is unclear what happens to ferritin once inside the liver; some is probably directed to the bile but most is expected to remain within the cell to be either degraded or join the endogenous ferritin pool (Halliday et al. 1994;Ramm et al. 1994).

The level of ferritin within the cell is determined by its iron content and many studies have shown a positive correlation between the hepatic ferritin content and body iron levels (Halliday et al. 1994;Harrison and Arosio 1996). In cases of heavy iron overload in the liver, iron can also be stored as haemosiderin as described in section 1.3.3.3 (Iancu 1990;Iancu et al. 1997). This stored iron can be mobilized readily if it is required to meet metabolic needs and in hereditary haemochromatosis type 1 (HH1), when patients undergo phlebotomy therapy iron from their liver stores is released for the synthesis of new haemoglobin.
It has also been shown that Kupffer cells (liver macrophages) can release ferritin from phagocytosed senescent red blood cells that is taken up by hepatocytes (Knutson and Wessling-Resnick 2003); in which case ferritin acts as an intercellular iron transport protein.

The molecule responsible for iron efflux across the enterocyte plasma membrane, Ireg1 is also expressed in the Kupffer cells, where it clears large quantities of erythrocyte-derived iron. Ireg1 is also highly expressed in hepatocytes and hepatic stellate cells, with lower levels in sinusoidal endothelial cells (Zhang et al. 2004). How iron is released from intracellular ferritin and haemosiderin and delivered to Ireg1 is still unknown. The liver-derived plasma protein Cp also plays an important role in iron release from the liver.

The newly discovered peptide Hepcidin also plays a major role in the regulation of iron efflux. Several studies have shown that Hepcidin inhibits iron release from several cell types, such as

macrophages, enterocytes and hepatocytes (Ganz 2002;Rivera et al. 2005a). It has also been reported that Hepcidin binds to Ireg1, facilitating its internalisation thus removing it from the cell surface so that it can no longer participate in iron release (Nemeth et al. 2004b). Hepcidin will be described in more detail in the section 1.3.4.2.

The processes of hepatic iron uptake, storage, and release are vital, not just for the maintenance of hepatocyte iron homeostasis, but for the body as a whole. However, the central role played by the liver in the regulation of body iron homeostasis has only become apparent with the recent discovery of the iron regulatory hormone Hepcidin and therefore requires further investigation.

1.3.4.1 Caeruloplasmin (Cp)

Caeruloplasmin is an abundant α-glycoprotein that contains >95% of the copper found in the plasma of all vertebrate species. Surprisingly, rather than playing a role in copper metabolism, the main function of this protein appears to be to facilitate iron efflux from cells. This multicopper oxidase can oxidise several substrates in vitro, but early studies suggested a distinct role for caeruloplasmin as a ferroxidase. In these experiments, caeruloplasmin was shown to play a role in the mobilisation and oxidation of iron from tissue stores with subsequent incorporation of ferric iron into transferrin (Morgan and Oates 2002;Osaki and Johnson 1969).

The role of caeruloplasmin in iron metabolism was further confirmed as the loss of function mutations in this gene leads to acaeruloplasminemia, a disorder characterised by iron accumulation in the parenchymal and reticuloendothelial cells of the liver and pancreas. This iron overload could be the result of an inability of the cells to release iron due to the lack of the ferroxidase. It is possible that caeruloplasmin may facilitate cellular iron release by promoting the oxidation of Fe^{2+}, the redox form of intracellular iron.

Cp is regulated predominantly at the transcriptional level and its synthesis is enhanced by iron deficiency, some cytokines, and hormones (Anderson and Frazer 2005). Caeruloplasmin does not seem to be essential for export of iron from all cells of the body as dietary iron can

still cross the intestine to enter the blood of individuals with acaeruloplasminemia. This is probably due to the copper oxidase activity of hephaestin, mentioned in section 1.3.3.4 which has significant homology to caeruloplasmin in its structure and presumed function.

1.3.4.2 Hepcidin

Hepcidin was identified by two groups while they were investigating novel antimicrobial peptides in body fluids. Whilst screening human blood ultrafiltrate for antimicrobial peptides, Krause et al found a peptide that was synthesised by the liver and named it, **L**iver **E**xpressed **A**ntimicrobial **P**eptide **1** (LEAP-1) (Krause et al. 2000). Another group lead by CH Park identified the peptide they called Hepcidin (***hep***atic bacteri***cid***al prote***in***) in urine (Park et al. 2001). Even though the peptide was first isolated from urine and blood, hepcidin is predominantly expressed in liver of mice and humans. To a much less extent expression was also detectable in the intestine, stomach, colon, lungs, heart, kidney and brain (Kulaksiz et al. 2005;Pigeon et al. 2001).

The human hepcidin gene (HAMP) comprises three exons and maps to the long arm of chromosome 19 (19q13) (Park et al. 2001). The human gene encodes 84-amino acid pre-pro-hepcidin with two cleavage sites. This is then further processed to give a 25 amino acid form found in blood and urine (Ganz 2005b). The 25 amino acid contains four intra-chain disulfide bonds and eight cysteine residues that are conserved among species (Fig. 1.10).
A slightly truncated 20 amino acid peptide was also found. Hepcidin has been found to be a member of the family of cysteine rich, cationic, antimicrobial peptides which includes the defensins due to its antibacterial (Park et al. 2001) and antifungal activities (Krause et al. 2000). Members of this family of peptides have been shown to be involved in inflammation and hepcidin has been shown to be a type II acute phase protein (Nemeth et al. 2003).

The role of hepcidin in iron homeostasis was revealed by two French groups working independently on mice. Pigeon (Pigeon et al. 2001) were searching for new genes

upregulated during iron overload. They found that hepcidin mRNA was increased in the liver of experimentally (carbonyl iron) and spontaneously ($ß_2$-$m^{-/-}$ mice) iron-overloaded mice.

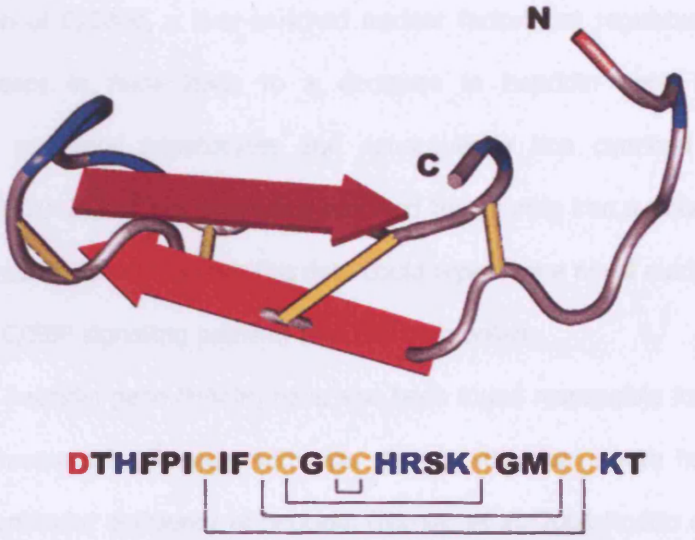

Figure 1.10 Amino acid sequence and a model of the major form of human hepcidin. *The amino and carboxy termini are labelled as N and C, respectively. Disulphide bridges are in yellow, basic amino acids in blue, and acidic in red. The pattern of disulphide linkages between the 8 cysteines is also shown in the amino acid sequence (Park et al. 2001).*

The group also found that the amount of mRNA was directly linked to liver iron concentration as evidenced by the dose dependence of mRNA induction in the carbonyl-iron–treated mice and the decreased expression of hepcidin when $ß_2$-$m^{-/-}$ mice were fed a low iron diet. From this data they concluded that hepcidin expression increases with iron overload and decreases with iron depletion (Pigeon et al. 2001).

The other group to identify the relevance of hepcidin in iron metabolism was lead by Nicolas (Nicolas et al. 2001). This group identified the murine hepcidin gene as having a role in iron homeostasis by generating USF2 null mice (Table I, appendix I) and accidentally removing

the neighbouring hepcidin genes. The USF2 null mice spontaneously became loaded with iron and the pattern of iron loading mimicked that seen in hereditary haemochromatosis (HH) (Nicolas et al. 2001). That hepcidin rather than USF2 was involved in iron homeostasis was confirmed by the same group, by showing that mice transgenic for hepcidin were severely anemic (Nicolas et al. 2002c).

Hepatic disruption of C/EBPα, a liver-enriched nuclear factor that regulates several hepatic metabolic processes in mice leads to a decrease in hepcidin gene expression, iron accumulation in periportal hepatocytes and consequently iron overload resembling HH (Courselaud et al. 2002). It has also been reported that during iron overload both C/EBP α and hepcidin increase. Taken together this data could represent a novel mechanism for cross-talk between the C/EBP signalling pathway and iron metabolism.

Mutations in the hepcidin gene (HAMP) have also been found responsible for HH2 also called juvenile haemochromatosis. Patients with this disorder develop severe haemochromatosis associated with profound deficiency of hepcidin (Nicolas et al. 2001;Roetto et al. 2003;Viatte et al. 2005).

Only one hepcidin gene exists in humans, whereas two hepcidin genes (hepcidin 1 and hepcidin 2) were reported in mice (Nicolas et al. 2001;Pigeon et al. 2001). Both hepcidin 1 and hepcidin 2 are predominantly expressed in the liver; hepcidin 2 is also present at high levels in the pancreas. The expression of both genes is controlled by USF2 transcriptional factor but whereas the role of hepcidin 1 gene product on iron metabolism is established, biological functions of hepcidin 2 remain to be fully characterised.

1.4 Iron metabolism diseases

1.4.1 Iron Deficiency diseases: Iron deficient Anaemia and Anaemia of Chronic disease (AI)

When the intake iron is not sufficient to compensate the daily losses, iron deficiency (also called "sideropenia"), develops. Iron deficiency is the most common haematological disorder encountered in general practice (World Health Organisation 2003). Worldwide, up to a billion individuals suffer adverse effects from insufficient body iron with children and women being the most susceptible. Children often become iron deficient because their rapid growth outstrips the iron supply. Similarly, premenopausal woman become iron deficient because they regularly experience menstrual blood loss. Chronic parasitosis can result in intestinal blood loss, as well as tumours, inflammation, infections, and congenital malformations, which can lead to iron deficiency (Andrews 2000).

The most common iron deficiency condition is iron deficient anaemia. This anaemia is characterized by decreased or absent iron stores, low serum iron concentration, low transferrin saturation, and low haemoglobin concentration or haematocrit value. Clinical symptoms of anaemia include paleness, fatigue, poor exercise tolerance, and decrease work performance (Leventhal and Stohlman, Jr. 1966).

Congenital and acquired abnormalities in the intestinal epithelium can also result in iron deficiency, though these are still poorly understood on a molecular level. Hypotransferrinemia, also called atransferrinemia, is a condition in which little or no plasma transferrin is produced. Although this rare disorder leads to severe iron deficiency anaemia the fact that is it characterised by parenchymal iron overload classifies it as a primary iron overload disorder and as such it will be further described in the iron overload diseases section.

In 1932, Locke et al observed that hypoferremia (low serum iron) was associated with infection which explained why it was common to find anaemia in patients with chronic infections. Later, Cartwright and Wintrobe (Cartwright and Wintrobe 1952) showed that the

anaemia associated with infection was indistinguishable from the anaemia of inflammation, and so anaemia of chronic disease (ACD) is currently known as anaemia of inflammation (AI) (reviewed in Weiss and Goodnough 2005). AI is characterised by inadequate erythrocyte production in the setting of low serum iron and low iron-binding capacity (i.e. low transferrin) despite preserved or even increased macrophage iron stores in the bone marrow. Patients with AI despite having low serum iron and low transferrin, have high serum ferritin concentration. The anaemia is caused by increased inflammation cytokines and changes in iron metabolism are due to the effects of these cytokines as they have been shown to modulate the expression of iron transport and storage proteins (Andrews 2004).

1.4.2 Iron Overload diseases: Primary and secondary iron overload diseases

Iron overload diseases are disorders characterised by an excessive storage of iron. This could be a result of excessive absorption of dietary iron or an inability of the body to properly transport iron. There are two types of iron overload diseases, primary or genetic iron overload diseases (Table 1.1) and secondary iron overload diseases. Only primary iron overload diseases will be discussed in this thesis.

Disease		**Causative gene mutations**	**Clinical features**	**Mode of Inheritance**
Haemochromatosis	HFE1 (Type 1 or HH1)	Hfe	Iron overload, late onset	AR
	HFE2 (Juvenile Haemochromatosis)	Hemojuvelin (Hjv)	Iron overload, early onset	AR
		hepcidin (HAMP)		AR
	HFE3 (TfR2-related HH)	TfR2	Iron overload, late onset	AR
	HFE4 (Ferroportin Disease)	IREG1 (SLC40A1)	Variable*	AD
Acaeruloplasminemia		caeruloplasmin (Cp)	Anaemia, iron overload	AR
Atransferrinemia		transferrin (Tf)	Anaemia, iron overload	AR

Table 1.1 Primary iron overload diseases.

*Causative gene mutations, clinical features and mode of inheritance (AR-Autosomal recessive, AD-Autosomal dominant). * There are two forms of Ferroportin disease each of them having very distinct clinical manifestations. Adapted from (Bacon et al. 2006).*

1.4.2.1 Haemochromatosis

Haemochromatosis was first described by Armand Trousseau in an article on diabetes, in 1865 (Trousseau 1865). In this article Trousseau included the notion that it was a manifestation secondary to diabetes, that it was an intrinsic liver disease, that it was due to haemolysis, to toxins, or that it was a metabolic disorder. The link of the disease with iron accumulation was not made as it was unclear whether the presence of iron was the cause of the disease or a secondary manifestation. The link was made by Daniel von Recklinghausen (von Recklinhausen 1889) who believed that the iron pigment was derived from the blood and created the term "haemochromatosis" used to this day.

The view that Haemochromatosis might be due to an inborn error of metabolism was first expressed by Joseph Harold Sheldon in 1927. in 1935 Sheldon published a monograph entitled "Haemochromatosis" describing the clinical features of the disease, suggesting mechanisms for the symptoms, a description of the metabolism of iron and other compounds, the pathological appearance of every organ system, chemical analyses of the tissues and, most important, a discussion of theories about the causes of the disease including the inability of humans to excrete iron. Despite Sheldon's complete monograph some researchers still believed that all cases of idiopathic haemochromatosis were actually acquired from ingestion of iron. Continuing support for Sheldon's genetic hypothesis was to come nearly 40 years later, when a study established a close association between haemochromatosis and HLA-A3 haplotype (Simon et al. 1976). However another 20 years were to pass before the identification of the gene that is mutated in hereditary haemochromatosis type 1, HLA-H (Burke et al. 1998;Feder et al. 1996;Jazwinska and Powell 1997). Because of the similarities between its proposed gene product and proteins of the major histocompatibility complex, the name HLA-H was soon mutated to HFE.

Most HH is caused by mutations in the Hfe gene but pathological mutations causative of the disease have been discovered in another four genes: TfR2 (encoding transferrin receptor–2), SLC40A1 (encoding Ireg1, also called ferroportin,), hepcidin or HAMP (encoding hepcidin), and HJV (encoding hemojuvelin).

Haemochromatosis caused by mutations in the TfR2, hepcidin and Hjv genes are characterized by increased intestinal iron absorption and increased levels of serum iron suggesting a defect that affects both absorptive enterocytes and tissue macrophages, which supply most of the serum iron primarily through recovery of the metal from senescent erythrocytes. Human subjects with these three disorders also produce inappropriately low amounts of the iron-regulatory hormone hepcidin. Haemochromatosis disorders due to Hfe and TfR2 mutations tend to have a later clinical onset and be less severe than those caused by hepcidin and Hjv gene mutations. Haemochromatosis caused by mutations in the Ireg1 gene can be divided into two forms of the disease, in one form patients manifest the loss of iron export function while in the other form patients retained full iron export activity (Camaschella 2005;Schimanski et al. 2005).

Organ	**Manifestations**	**Complications**
Liver	Enzyme alterations	Fibrosis, Cirrhosis, hepatocellular carcinoma
Heart	Arrhythmia, failure	Cardiomyopathy
Pancreas	Hyperglycemia	Diabetes mellitus
Pituitary	Decreased libido, impotence in men; amenorrhea in women	Hypogonadism
Thyroid gland	Decreased thyroid hormone	Hypothyroidism
Joints	Arthralgia	Arthropathy
Skin	Pigmentation	None

Table 1.2 Hereditary Haemochromatosis manifestations in the different organs. *(Adams et al. 1991;Adams et al. 1997;Bacon and Sadiq 1997;Camaschella 2005;Moirand et al. 1997;Pietrangelo 2004c).*

Hereditary haemochromatosis (HH) is now considered a group of genetic disorders characterised by increased transferrin (Tf) saturations, systemic iron overload with deposition of excess iron in parenchymal cells of the liver, heart, pancreas, and other endocrine tissues, with reticuloendothelial iron sparing. The most predominant features include hepatomegaly, hepatic dysfunction, heart failure, skin pigmentation, testicular atrophy, diabetes mellitus, and arthropathy (Table 1.2).

In haemochromatosis the total iron content of the body is usually between 20g and 40g. Particularly in the liver and pancreas, the iron concentrations may be 50 to 100 times normal (Table 1.3). If untreated, liver cirrhosis, heart disease, hepatic cancer and diabetes can develop which leads to an increased morbidity and mortality (Feder et al. 1996;Trousseau 1865). Only a fraction of patients with a haemochromatosis genotype develop iron overload and environmental factors seem to affect the disease penetrance. Other genetic factors are likely to determine individual susceptibility to iron loading.

1.4.2.1.1 Hereditary haemochromatosis Type I or Hfe-related Haemochromatosis

Hereditary haemochromatosis type 1 (HH1 or HFE1) is an autosomal recessive disorder of iron metabolism common in populations of north-west European ancestry. The estimated carrier frequency within the Caucasian population is between 1 in 8 and 1 in 10.

The causative gene of HH1, designated Hfe, was identified in 1996 by Feder et al (Feder et al. 1996). Feder described mutations associated with hereditary haemochromatosis in the MHC class I-like gene Hfe. The Hfe gene is located at 6p21.3 and the Hfe protein is a 343 residue type I transmembrane protein that associates with class I light chain β-2-microglobulin (Fig. 1.11).

Over 83% of haemochromatosis patients are homozygous for a guanine to adenine transition at nucleotide 845 in the coding sequence of HFE, resulting in the substitution of a tyrosine for cysteine at position 282 (C282Y) of the unprocessed polypeptide (Feder et al. 1996). This mutation prevents the correct folding of the alpha3 (α-3) domain altering the Hfe protein

structure, the assembly with beta-2-microglobulin (β-2m) and presentation at the cell surface (Feder 1999;Feder et al. 1996;Waheed et al 1997).

Figure 1.11 The HFE structure

HFE includes a large extracellular domain consisting of three loops (α-1 to α-3), a single transmembrane domain and a short cytoplasmic tail. Similar to other MHC class 1 molecules, Hfe physically associates with β-2-microglobulin (β-2m) via its α-3 loop. (adapted from Bennett et al. 2000).

The functional importance of such interplay in HH between β2m and some class I-type HLA molecule was suggested by studies of β-2m-deficient mice (β-2m$^{-/-}$), which develop progressive hepatic iron overload as described below.

A second mutation was found in HH1 patients, resulting in the substitution of an aspartic acid for histidine at position 63 (H63D). In contrast to C282Y, this mutation does not appear to prevent β2-microglobulin association or cell surface expression, indicating that C282Y mutation results in a greater loss of protein function than H63D. The H63D mutation is present in 17% of the normal chromosomes and was also found in a number of patients who carried only one copy of the C282Y mutation (Feder et al. 1996). These two mutations are in linkage disequilibrium and have not yet been found together in the same haplotype.

The cases reported of patients with haemochromatosis with the C282Y mutation or at least homozygous for this mutation are far from the estimated frequency of 1 in 150 in people of northern European descent (Feder et al. 1996), leading us to think that this mutation has a low penetrance and that there are a lot of asymptomatic cases of haemochromatosis (Bomford 2002). This low penetrance can lead us to consider that there are gene modulators contributing to the incomplete penetrance of the gene.

There is now a comprehensive panel of diagnostic measurements for HH 1 (Table 1.3), including serum iron indices (transferrin saturation and ferritin), hepatic iron concentration and hepatic iron index, genetic testing for Hfe mutations and evaluation of liver biopsy with iron stain. The first histological abnormality in homozygous HH1 patients is the appearance of stainable iron in periportal hepatocytes. Over time, parenchymal iron deposition increases, fibrosis develops and evolves into the characteristic cirrhosis of untreated HH1. The histological pattern of iron accumulation in HH1 will be further described in chapter 3.

Measurements			Normal subjects	HH1 subjects
Blood (fasting)		Serum iron (µg/dL)	60-80	180-300
		Serum transferrin level (mg/dL)	220-410	200-300
		Transferrin saturation (%)	20-50	80-6000
		Serum ferritin level (ng/mL)	20-200 (M) 15-150 (W)	500-6000 (M) 500-6000 (W)
Liver	Hepatic iron concentration	µg/g dry weight	300-1500	8000-30 000
		µmol/g dry weight	5-27	140-550
		Hepatic iron index*	<1.0	>1.9
	Liver histology	Perl's Prussian blue stain	0-1+	3+,4+

Table 1.3 Diagnostic measurements in the diagnostic of Haemochromatosis type 1 (HH1). ** Hepatic iron index (HII) is calculated by dividing the hepatic iron concentration (in µmol/g dry weight) by the age of the patient (in years). With the availability of genetic*

testing for Hfe mutations, the utility of HII has diminished. Serum ferritin values are given for women (W) and men (M) (Bacon et al. 2006).

If a course of phlebotomies is initiated before patients developed cirrhosis, haemochromatosis manifestations can be reverted to normal. Even among those patients with cirrhosis, phlebotomies can increase the life expectancy.

As human population studies and *ex vivo* biochemical studies had not yielded consistent results regarding the consequences of the Hfe mutations and a confirmation that it was indeed Hfe the sought after gene responsible for Haemochromatosis, Zhou and his colleagues (Zhou et al. 1998) reported the production of a mouse model in which the Hfe gene was disrupted. This knockout (KO) mouse showed increased serum transferrin saturation and increased hepatocellular iron deposition, the symptoms that are characteristic of human haemochromatosis. This Hfe KO mouse also established that the HFE gene mutations that produce HH1 in humans do so by causing a deficiency of the Hfe protein, not by changing its characteristics or location in the cell (Beutler 1998).

Further support for a causative role of HFE in HH1 disease came from the observation that β-2-microglobulin knockout (β-$2m^{-/-}$) mice, develop iron overload (De SM et al. 1994;Santos et al. 1998). As with other MHC-I molecules, Hfe needs to associate with β-2m for appropriate expression at the cell surface. This study showed that β-$2m^{-/-}$ mice, which fail to express cell surface HFE protein, shared similarities with HH1 patients.

The role of the two most common Hfe mutations, C282Y and H63D were more comprehensively studied when Tomatsu et al generated mouse models carrying the murine analogous mutations C294Y and H67D, respectively (Tomatsu et al. 2003). These mutations allowed the Hfe mutations to be investigated in an environment free of potential risk factors. Tomatsu et al demonstrated that mice homozygous for C294Y had significant higher levels of hepatic iron followed by compound heterozygous for H67D and C294Y and H67D homozygotes (Tomatsu et al. 2003). To further investigate the effect of homozygosity for the C282Y and whether this mutation results in total loss of protein function, Levy et al created

two mutant mouse strains (Levy et al. 1999b). Homozygosity for the C282Y equivalent mutation resulted in postnatal iron loading similar to the one seen in Hfe KO mice. The effects of this mutation were less severe than the effects of the null mutation; therefore, the group concluded that the C282Y mutation does not result in a null allele (Levy et al. 1999b).

The HFE null mutation has now been highly back-crossed onto an array of inbred mouse strain backgrounds (Table I, appendix I). These strains provide an approach for investigating the extent to which modifier genes play a role in normal and pathological iron regulation in the HFE deficient mouse model. Lebeau et al (Lebeau et al. 2002) showed that C57BL/6 Hfe KO mice mimic the typical features of HH in short term studies. Duodenal iron absorption and hepatic iron load were two or three times higher in C57BL/6 Hfe KO mice than in corresponding C57BL/6 controls (wt). Iron was found preferentially in periportal hepatocytes and plasma iron concentrations and transferrin saturation were elevated accordingly. The iron distribution between organs and microscopic iron deposition in the tissues of these Hfe KO mouse models resembled the patterns described in HH1. One difference between the mouse model and the HH1 patients is that Hfe KO mice do not develop fibrosis or cirrhosis despite the severe iron overload (Knutson et al. 2001). Thus, the role of iron in initiating liver fibrosis in iron overload diseases such as HH1 is not understood and an animal model that can produce the full pathological picture of the cirrhotic liver seen in HH1 is still needed. It is known that iron overload enhances liver injury, and mildly accelerates the process of fibrosis (Arezzini et al. 2003) but it is believed that other factors may be involved in this process.

In HH1 patients, the combination of iron and ethanol results in greater liver damage, than iron alone (Bassett et al. 1986;Olynyk et al. 1995;Tavill et al. 1990;Tector et al. 1995;Tsukamoto 1993). Although this does not occur in rats to the same extent, when iron acts in concert with other hepatotoxins (e.g. CCl_4 and alcohol), liver injury is enhanced (Olynyk et al. 1995;Stal and Hultcrantz 1993). In the presence of a damaging event it is possible that the pro-oxidant action of iron is amplified and the initial toxic effect is propagated.

The variation in phenotypic expression of HH1 between patients may be attributed to nongenetic factors, such as diet, alcohol intake, and iron loss (menstruation or pregnancy). However, population studies suggest that the variation in severity of iron loading in HH1 may be also caused by the additive or interactive effect of other genes (Bulaj et al. 2000;Pratiwi et al. 1999;Whitfield et al. 2000). This conclusion was also taken from Hfe KO mice studies. Inbred mouse strains exhibit considerable variability in several parameters of iron metabolism (Clothier et al. 2000;Leboeuf et al. 1995;Morse et al. 1999). Serum iron, serum transferrin saturations, and hepatic iron stores vary as much as 2-fold among inbred strains such as C57BL/6 and AKR on a basal diet (Fleming et al. 2001;Levy et al. 2000;Sproule et al. 2001). The finding that hepatic iron stores failed to reflect transferrin saturation also suggests that different genetic factors control transferrin saturation and hepatic iron stores. When mice were fed a high-iron diet, the concentration of carbonyl iron required to completely saturate transferrin with iron was 10 times greater for C57BL/6 and BALB/c mice than for DBA/2 and AKR mice (Leboeuf et al. 1995). It is hypothesized that modifier genes modulate the regulatory capacity of the Hfe gene. These modifiers could interact with HFE directly or, more likely, modify iron loading through independent mechanisms to magnify or dampen the effects of HFE. (Ajioka et al. 2002;Fleming et al. 2001). The understanding of these modifier genes will be addressed in this thesis.

1.4.2.1.2 Haemochromatosis Type 2 or Juvenile Haemochromatosis

Juvenile haemochromatosis (JH) or type 2 haemochromatosis (HFE2) is a hereditary condition characterised by severe iron overload and organ damage typically before age 30 years (De et al. 2002;Lamon et al. 1979;Rivard et al. 2003b;Rivard et al. 2000). JH is a heterogeneous genetic disorder, related to at least 2 distinct loci. The first maps to a chromosome 1q21 (Roetto et al. 2003) recently identified gene Hemojuvelin (Hjv) while the second one maps to chromosome 19q13 and is responsible for a rare subset of HH2 due to mutations in hepcidin (HAMP) gene (Camaschella et al. 2002;Papanikolaou et al. 2004;Roetto et al. 1999;Roetto et al. 2003) (Papanikolaou et al. 2001;Papanikolaou et al. 2004;Rivard et al. 2003b;Rivard et al.

2000;Roetto et al. 2002;Roetto et al. 2004). Most patients with HH2 have mutations in the Hjv gene (Lanzara et al. 2004;Papanikolaou et al. 2004).

The clinical course of HH2 is rapid and severe compared to HH1 (Feder et al. 1996;Levy et al. 2000) and transferrin receptor 2 (TFR2)-related Haemochromatosis (HH3) (Camaschella et al. 2000), indicating that the JH protein is an important regulator of iron absorption (De et al. 2002). Clinical symptoms are similar to HH1 but hypogonadism and cardiac disease are more frequent presenting symptoms. Premature deaths due to heart failure or major arrhythmias are reported in untreated or undiagnosed patients with cardiac involvement.

1.4.2.1.3 Haemochromatosis Type 3 or TFR2 –related Haemochromatosis

The first association between TfR2 gene mutations and iron overload was made by Camaschella *et al* in a study of Italian patients with no Hfe mutations but with the diagnostic criteria of HH (Camaschella et al. 2000). This new type of Haemochromatosis was named HH3. Like HH1 the clinical parameters of HH3 are increased serum iron due to increased iron absorption at the duodenal level that leads to parenchymal iron overload. TfR2 haemochromatosis seems less severe than juvenile haemochromatosis but more severe than the Hfe-related disease. The progression of iron overload is slow in HH3 patients but a constant feature is the persistently high transferrin saturation, even after treatment (Camaschella 2005).

1.4.2.1.4 Ferroportin Disease

The iron-regulated transporter 1/ferroportin/metal transporter protein 1 (IREG1/FPN/MTP-1; gene symbol SLC40A1) was reported simultaneously by three groups in 2000 (Abboud and Haile 2000;Donovan et al. 2000;McKie et al. 2000). IREG1 (the term used for the purpose of this thesis) protein is expressed in Kupffer cells and at the basolateral membrane of

enterocytes, macrophages, placental cells, and hepatocytes, where it likely plays the role of iron exporter.

At least twelve mutations in the SLC40A1 gene (previously called SLC11A3) have been implicated in an autosomal dominant inherited disorder of iron metabolism now referred as type 4 haemochromatosis (HFE4) or Ferroportin disease (Arden et al. 2003;Montosi et al. 2001;Pietrangelo et al. 1999;Pietrangelo 2006;Pietrangelo 2004b). Heterozygosity for mutations of Ireg1 generated a controversy as to whether these mutations might cause a gain or a loss of the metal exporter function (Camaschella 2005). Thus, patients with Ireg1 mutations can be separated into two groups: one group manifested the loss of iron export function; the other retained full iron export activity (Schimanski et al. 2005). One group of patients is characterized by an early rise in ferritin levels with low to normal transferrin saturation and iron accumulation predominantly in macrophages (Arden et al. 2003;Beutler et al. 2003;Cazzola et al. 2003;Devalia et al. 2002;Gordeuk et al. 2003;Jouanolle et al. 2003;Montosi et al. 2001;Njajou et al. 2001;Pietrangelo 2006;Rivard et al. 2003a;Rivard et al. 2003b;Robson et al. 2004;Roetto et al. 2002;Wallace et al. 2002;Wallace et al. 2004). The absence of an apparent increase in total body iron in this group of patients, suggests a partial loss of Ireg1 similar to that observed in mice lacking one Ireg1 allele (Donovan et al. 2005). In the other group, patients have a different constellation of Ireg1 missense mutations and present symptoms that are more similar to those of the other haemochromatosis disorders such as high transferrin saturation and prominent parenchymal iron loading (Arden et al. 2003;Cazzola et al. 2003;Njajou et al. 2001;Njajou et al. 2002;Schimanski et al. 2005;Sham et al. 2005;Wallace et al. 2004). Hyperferritinemia has been reported in patients with this type of Ferroportin disease, and in these cases a less aggressive regimen of phlebotomies is therefore needed (Jouanolle et al. 2003;Pietrangelo et al. 1999).

1.4.2.2 Acaeruloplasminemia

Acaeruloplasminemia is a late onset autosomal recessive disease of iron overload that results from loss of function mutations in the caeruloplasmin (Cp) gene (human chromosome 3q23–q24). While the iron overload associated with haemochromatosis results from increased iron absorption, the iron overload associated with acaeruloplasminemia results from aberrant iron distribution. Without caeruloplasmin iron cannot be efficiently recycled from storage sites in the liver and a seemingly inconsistent collection of iron-related symptoms develops (Harris et al. 1995). Serum ferritin is elevated, but serum iron remains low because iron is not efficiently loaded onto transferrin. Iron accumulates in the parenchymal and reticuloendothelial cells of the liver and pancreas, but anaemia results because iron is not efficiently delivered to red blood cell precursors.

1.4.2.3 Hypotransferrinemia

Hypotransferrinemia, also called atransferrinemia, is a rare autosomal recessive disease condition in which little or no plasma transferrin is produced. As previously mentioned severe iron deficiency anaemia in this disease is accompanied by iron loading of the liver and other parenchymal organs (Andrews 1999;Beutler et al. 2000;Pietrangelo 2004a). The condition emphasizes the key role of the transferrin-TFR1 pathway for iron uptake in erythroid cells and indicates the existence of alternative mechanisms for hepatocyte iron uptake. Transferrin KO mice die in utero from severe anaemia (Levy et al. 1999a), while hypotransferrinemic ($TRf^{hpx/hpx}$) mice (Table I, appendix I)) show a small amount of TF protein in the plasma and survive past birth (Bernstein 1987;Trenor, III et al. 2000). The $TRf^{hpx/hpx}$ mouse shows cytological features similar to the human congenital atransferrinemia (Raja et al. 1999). This mouse model also presents extremely low hepcidin levels which explain the intestinal iron hyperabsorption that leads to iron overload (Pietrangelo 2004a).

Other primary iron overload diseases include Neonatal haemochromatosis and African iron overload but descriptions of these disorders are beyond the scope of this thesis.

1.5 Regulation of iron uptake

Iron homeostasis depends on the regulated absorption of dietary iron as no mechanisms for the regulated excretion of iron exist. Three different regulators, namely dietary, stores and erythropoietic regulator were hypothesised almost 50 years ago to govern duodenal iron absorption. The store regulator was thought to act on a pathway that facilitated a slow accumulation of non haem dietary iron (about 1 mg/day) (Hunt and Roughead 2000) and to act in order to prevent iron overload after ensuring iron needs were met. A soluble component was hypothesized for this regulator as it must signal between the sites of absorption, usage and storage (duodenum, muscle and liver, respectively).

The fact that individuals with normal, or even increased iron stores up-regulated iron absorption as marrow iron requirements increased led to the conclusion that a erythropoietic regulator communicated the erythropoietic demand of the organism rather than reflecting the iron stores. Iron absorption in this case was not increased by erythropoiesis alone; rather, the imbalance between the rate of erythropoiesis of the marrow and its iron supply was thought to induce the iron absorption. The absorptive pathway targeted by the erythropoietic regulator was thought to be a distinct from the pathway targeted by the stores regulator but like the stores regulator, the erythropoietic regulator was hypothesized to be a soluble component of the plasma, as it must signal between the erythroid marrow and the intestine (Roy and Enns 2000).

In recent times it became clear that a more complex regulatory network is responsible for iron regulation through regulating iron traffic rather than deposition as previously thought. Today iron uptake is considered to be regulated at the mRNA, cellular and body level. Several genes appear to be involved in the feedback regulation between sites of iron utilization (primarily marrow), storage (spleen and liver), and absorption (duodenum), and the

expression of these genes seems to be regulated by the iron content of the diet, changes to the rate of erythropoiesis, hypoxia, inflammation, and pregnancy (Morgan and Oates 2002). The molecules HFE, TF, TFR2, and the antimicrobial peptide Hepcidin are now accepted to be important regulators of iron uptake and to maintain iron homeostasis for the entire organism. On a cellular level, iron uptake regulation is controlled by iron responsive proteins (IRP-1 and IRP-2) that work in conjunction with iron regulatory elements (IRE). Iron uptake regulation by these genes and the cellular iron regulation will be described in detail in the following sections.

1.5.1 Regulation of cellular iron levels by IRE-IRP interactions

In mammalian cells, cellular uptake and storage of iron are normally controlled post-transcriptionally by two cytoplasmic proteins, iron regulatory protein IRP-1 and IRP-2 that recognise iron responsive elements (IRE) on mRNA (Fig. 1.12) (Hentze and Kuhn 1996). IRP activity is determined in response to cellular iron levels and independently by signalling through nitric oxide (NO) and reactive oxygen intermediates, particularly hydrogen peroxide (H_2O_2). IRP-1 activity is controlled by all three effectors by a mechanism involving the conversion of 4Fe4S IRP-1 into 3Fe3S apoIRP-1. IRP-2 activity is regulated in response to iron levels and NO and by changes in the stability of the protein.

IREs were first identified in the 5'-UTR of ferritin H and L chain mRNAs and found to mediate inhibition of ferritin mRNA translation in iron-deprived cells. When cellular iron is abundant, ferritin synthesis is not repressed, instead newly made ferritin baskets assemble increasing the iron storage capacity of the cells (reviewed in Thomson A 1999). IREs were also found in the 3' UTR of the transferrin receptor 1 (TfR1) mRNA.

In iron deficient states, IRPs bind IREs in the 5' UTR of ferritin mRNA and the 3' UTR of transferrin receptor mRNA. Ferritin synthesis is prevented and transferrin receptor numbers increase (Casey et al. 1988;Hentze and Kuhn 1996;Koeller et al. 1989;Mullner et al. 1989). In iron overload states IRPs no longer bind IREs and ferritin is synthesised allowing storage of

excess iron and transferrin receptor number to decrease, limiting further iron uptake (Fig. 1.12).

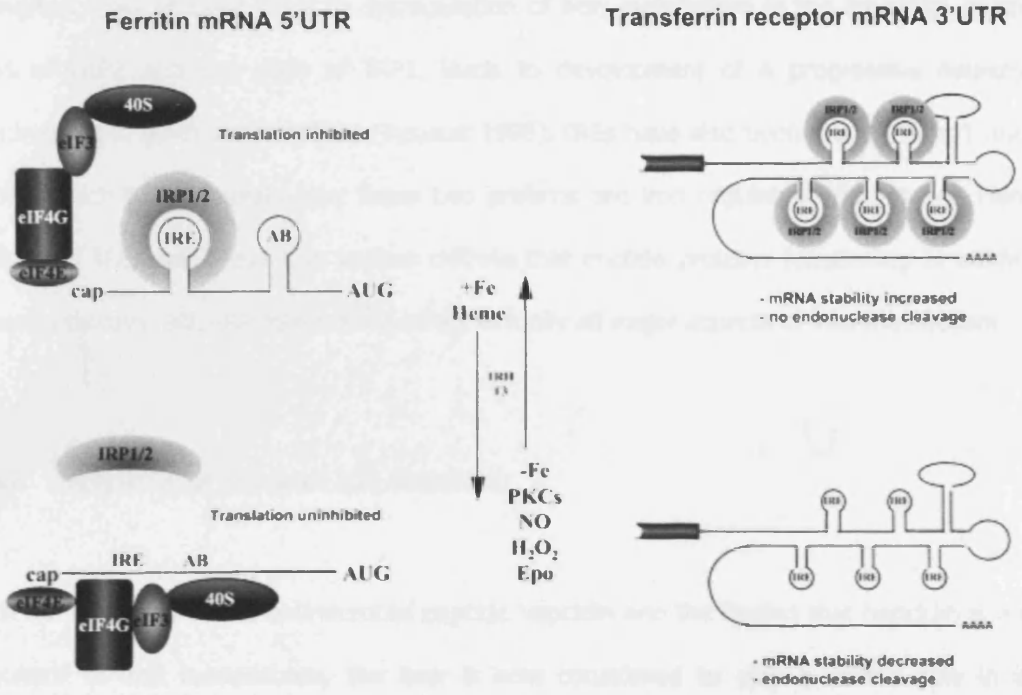

Figure 1.12 Two posttranslational controls mediated by iron

When iron concentration in the cytosol increases, the synthesis of ferritin is increased in order to bind the extra iron and the synthesis of transferrin receptors is suppressed in order for less iron to be imported across the plasma membrane. These responses are mediated by cytosolic aconitase, an iron-responsive regulatory protein. Aconitase recognises common features in a stem-loop structure in the mRNA encoding ferritin and transferrin receptor and dissociates from the mRNA when it binds iron. Although ferritin and TFR are regulated by the same iron-responsive regulatory protein, their levels respond differently to iron concentrations as they are regulated by different types of mechanisms. The binding of aconitase to the 5' -UTR of ferritin mRNA blocks translation initiation; its binding to the 3' -UTR of the transferrin receptor mRNA blocks an endonuclease cleavage site and thereby stabilizes the mRNA (Adapted from Hentze et al. 1988).

The intracellular level of iron is thus tightly regulated to permit the uptake of essential quantities of iron and to prevent the toxic effects of higher amounts by storing iron into ferritin. The interplay of IRP1 and IRP2 has been studied in mice where one of these genes is disrupted. Loss of IRP2 leads to dysregulation of iron metabolism in the intestinal mucosa. Loss of IRP2 and one copy of IRP1, leads to development of a progressive neurologic syndrome and other abnormalities (Rouault 1998). IREs have also been found in Ireg1 and in DMT1 which partly explain how these two proteins are iron regulated (Hubert and Hentze 2002). As IREs are present in various mRNAs that encode proteins functioning in either of these pathways, IRE-IRP interactions affect virtually all major aspects of iron metabolism.

1.5.2 Regulation of duodenal iron absorption

With the discovery of the antimicrobial peptide hepcidin and the finding that hepcidin is a key regulator of iron homeostasis, the liver is now considered to play a central role in iron metabolism. Variations in body iron stores, changes in rate of erythropoiesis, hypoxia, inflammation and pregnancy result in changes at the protein and mRNA level of the duodenal expression of the major enterocyte iron transport molecules, particularly, DMT1, Dcytb, and Ireg1 (Frazer and Anderson 2005).

1.5.2.1 Regulation by hepcidin

The identification of hepcidin has provided compelling evidence against the long-supported crypt hypothesis for the regulation of iron absorption. Since the 1960's it had been proposed that signals from the body to alter iron absorption were detected by enterocytes in the crypts of the duodenum, thus programming them to absorb more or less iron after they matured. This hypothesis was based on the presence of a lag period of several days between a stimulus to alter iron absorption and the actual change in absorption. The lag period was interpreted as the time required for the programmed crypt cells to mature and become

absorptive enterocytes on the villus. At the molecular level, programming in the crypt cell was presumed to involve the modulation of the gene expression of the key factors involved in iron transport. This model predicted that iron deficiency would lower crypt cell iron status such that gene expression of critical transport factors would be upregulated on cellular differentiation and migration to the villus tip. However, it has now been shown that this "lag period" for changes in iron absorption reflects the time required by the body to detect the need for a change in absorption and alter hepcidin expression (Frazer et al. 2004a). It now appears that hepcidin might be the stores regulator, the erythropoietic regulator and the "inflammation" regulator of iron absorption and recycling (Fleming and Sly 2001;Nicolas et al. 2002c;Nicolas et al. 2002a;Nicolas et al. 2002b). The changes in iron efflux due to hepcidin expression have not yet been shown but a decreased serum iron has been shown within 4 hours in mice after a single injection of Hepcidin (Rivera et al. 2005b) and a decrease in iron absorption was observed after multiple injections of Hepcidin (Laftah et al. 2004).

This small antimicrobial peptide is secreted into the circulation where it acts as an inhibitor of iron release from a variety of cell types, including the hepatocytes and Kupffer cells of the liver via its interaction with Ireg1 (Ganz 2005b;Nemeth et al. 2004b;Nicolas et al. 2001). The relevance of the interaction with Ireg1 is not yet fully understood but the fact that hepcidin is interacting with a protein expressed in the enterocytes confirms that signals from the body can be detected by mature villus enterocytes and does not have an absolute requirement for crypt cells to detect changes in body iron status (Nemeth et al. 2004b).

In humans, as described in section 1.4.2.1.2, disruption of hepcidin gene causes the most severe form of iron overload—juvenile haemochromatosis (Roetto et al. 2003) while hepcidin deficiency in mice resulted in iron overload (Nicolas et al. 2001). Conversely, overexpression of hepcidin-1 in transgenic mice caused severe iron-deficiency anaemia (Lou et al. 2004;Nicolas et al. 2004). Both dietary and parenteral iron load induced hepcidin mRNA in humans and in mice (Nemeth et al. 2004b;Pigeon et al. 2001). All these observations indicate that hepcidin is a negative regulator of iron absorption, recycling and release from iron stores and is homeostatically regulated by iron and anaemia (Millard et al. 2004;Nicolas et al.

2002c;Pigeon et al. 2001). Hepcidin has also been shown to be regulated by inflammation and hypoxia.

In hereditary haemochromatosis caused by homozygous disruption of HFE, transferrin receptor 2 (TFR2) and hemojuvelin (HJV), Hepcidin production has been found to be low in spite of iron overload, suggesting that all these molecules act as direct or indirect regulators of Hepcidin synthesis.

1.5.2.1.1 Regulation of Ireg1 expression

Ireg1 is found in all the tissues that export iron into plasma: basolateral membranes of duodenal enterocytes, and cell membranes of placental cells, hepatocytes and macrophages (Donovan et al. 2005). Here, Ireg1 is in a unique position to regulate the inflow of iron into plasma from dietary or maternal sources, from hepatic stores and from macrophages engaged in recycling senescent erythrocytes. Thus the transport of iron by Ireg1 across the enterocyte basolateral membrane determines whether iron is delivered to plasma transferrin or removed from the body with shed enterocytes.

When iron stores are high, high levels of Hepcidin are produced causing Ireg1 to be internalised, therefore blocking the pathway for the transfer of iron from the enterocyte to plasma. When iron stores are low, Hepcidin production is suppressed and Ireg1 molecules are displayed on basolateral membranes of enterocytes, where they transport iron from the enterocyte cytoplasm to plasma transferrin (Ganz and Nemeth 2006). This proposed model explains how iron recycled in macrophages is regulated and how macrophages containing iron in inflammatory status lead to high Hepcidin production. The high levels of Hepcidin block iron export and the iron remains trapped within the macrophages (Yang et al. 2002). The expression of Ireg1 on the cell membrane has also been found to be regulated by iron (Frazer et al. 2002;McKie et al. 2000). In iron deficiency conditions Ireg1 expression in the duodenum is upregulated and thus iron absorption is increased. Interestingly in the Kupffer cells of the liver, spleen and alveolar macrophages, Ireg1 protein expression is downregulated by iron deficiency and up-regulated by iron loading (Abboud and Haile 2000;Yang et al.

2002). This indicates a tissue-dependent difference in the regulation of Ireg1 protein levels. As the regulation observed in the Kupffer cells is similar to that of ferritin and both Ireg1 and ferritin contain a 5'-IRE, it is possible that the 5'-IRE may be functional in these cells.

Recently and contrasting with previous immunohistological studies, Ireg1 has been reported to localise to the apical brush border of duodenum enterocytes, where it could be modulating iron absorption possibly by modulating the activity of DMT1 (Donovan et al. 2000;McKie et al. 2000;Thomas and Oates 2004). In addition to directly regulating Ireg1 expression and thus iron export, hepcidin is expected to have an indirect effect on cellular iron intake. This indirect effect would be the result of increased iron concentrations in enterocytes, macrophages or hepatocytes that would suppress the synthesis of the splice variant of DMT1 containing an IRE (Ganz and Nemeth 2006).

1.5.2.1.2 Regulation of cellular iron intake

The mechanism by which the brush border iron uptake molecules DMT1 and Dcytb are regulated by hepcidin is not clear. It is unlikely that hepcidin has a direct effect on these molecules as these molecules seem to respond to the cell iron concentration whereas systemic signals such as hepcidin appear to modulate preferably the export of iron across the basolateral membrane which leads to alterations in enterocyte iron levels and subsequently to changes in the expression of the brush border uptake components (Abboud and Haile 2000;Frazer et al. 2001;Frazer and Anderson 2003;McKie et al. 2000). In the enterocytes the majority of DMT1 present is the splice variant containing an IRE motif and the binding of IRPs to DMT1 mRNA when intracellular iron levels are low appears to stabilize this message, increasing the level of DMT1 protein. As Dcytb does not contain an IRE motif, it cannot be regulated by the IRP activity. Although Dcytb is regulated by intracellular iron levels in the same direction as DMT1 the regulatory mechanism involved remains unknown.

1.5.3 Regulation of Hepcidin Synthesis

Different studies have revealed that hepcidin synthesis is regulated by three main factors: inflammation, oxygen concentration and iron levels (Nicolas et al. 2002b). These factors will be discussed in detail in the sections below and in the chapters 4, 5 and 6.

1.5.3.1 Inflammation and infection

Hepcidin synthesis is markedly induced by infection and inflammation. In animal models and human subjects, injection of lipopolysaccharide (LPS) (Pigeon et al. 2001), or Freund's adjuvant increased significantly hepatic hepcidin mRNA expression (Frazer et al. 2004b;Kemna et al. 2005;Nemeth et al. 2004a). Although the up regulation of hepcidin as a response to inflammation and infection is beneficial for an organism during the course of an infection (the sequestration of iron in cellular stores makes iron less accessible for invading microorganisms), this has a deleterious effect leading to the development of the anaemia of inflammation (AI).

LPS treatment stimulates IL-6 which induces an increase in production of Hepcidin by hepatocytes as mentioned previously. This Hepcidin leads to the internalisation and degradation of Ireg1 which blocks the release of iron from macrophages causing a decrease in serum iron (hypoferremia) characteristic of AI (Ganz 2006).

Turpentine oil injections in mice also increase liver hepcidin gene expression, cause hypoferremia and the resulting in anaemia (Nicolas et al. 2002b;Weinstein et al. 2002). This hypoferremic response to turpentine-induced inflammation is absent in the USF2/Hepcidin-deficient mice, confirming that this response is fully dependent on hepcidin. Neutralising antibodies against IL-6 block hepcidin in vitro, and IL-6 KO mice fail to up-regulate hepcidin in response to turpentine showing a direct effect of IL-6 on Hepcidin expression (Lee et al. 2004;Nemeth et al. 2004a). The data demonstrates that Hepcidin is a type II acute phase protein that plays a major role in the dysregulation of iron homeostasis during inflammation (Nemeth et al. 2003).

1.5.3.2 Hypoxia and Anaemia

In humans iron absorption is mainly regulated by iron stores and the rate of erythropoiesis. Erythropoiesis regulates iron absorption regardless of iron stores to provide an adequate iron supply for the production of erythrocytes. When oxygen is lacking, erythropoietin (EPO) is produced which in turn leads to the production of erythrocyte precursors in the bone marrow. The development of these erythrocyte precursors then depends on an adequate supply of iron from the diet. Previously it was thought that stimulated erythropoiesis was necessary for the induced iron uptake seen in hypoxic conditions but now it has been shown that hepcidin has a more crucial role than EPO in the response to hypoxia (Nicolas et al. 2002b;Vokurka et al. 2006). In hypoxic conditions hepcidin levels decrease, its inhibitory effects on iron absorption diminish, and more iron is made available from the diet and from the iron stores (Nicolas et al. 2002b;O'Riordan et al. 1995;Raja et al. 2005). The iron absorbed in the duodenum is then delivered to bone marrow to sustain the erythrocyte production.

Interestingly, it has been shown that turpentine-treated mice exposed to 3 days of hypoxia failed to show an increase in iron absorption. This observation can be explained by the positive response of the hepcidin gene to inflammation counterbalancing the hypoxia-dependent downregulation of this gene (Raja et al. 1990).

The human hepcidin promoter contains several binding sites for the hypoxia-inducible factor 1 (HIF-1) (Ganz 2005b) but these binding sites do not seem to be conserved in other mammals, and their role has not yet been experimentally tested. Therefore, the exact mechanism by which hypoxia down-regulates hepcidin gene is still unknown.

Anaemia regulates Hepcidin levels in a similar manner to hypoxia. In iron deficiency hepatic hepcidin mRNA levels decrease leading to an increase in iron absorption (Bondi et al. 2005;Latunde-Dada et al. 2004;Nicolas et al. 2002b;Vokurka et al. 2006). Cases of anaemia with ineffective erythropoiesis, such as β-thalassemia major are characterised by increased iron absorption and consequently iron overload (Nemeth and Ganz 2006;Papanikolaou et al.

2005). Thus, showing that anaemia is dominant over iron overload in regulating hepcidin expression in the thalassemia setting (Andrews 1999).

Although in these cases, hepcidin levels correlate with parameters of erythropoiesis and anaemia they do not correlate with indices of iron overload such as liver iron concentrations, ferritin, serum iron or transferrin saturation. There was however, a negative correlation between Non-transferrin bound iron (NTBI) and hepcidin levels, suggesting that low levels of hepcidin allow the increase of iron flow into plasma, leading to saturation of transferrin and NTBI formation.

Mice lacking the transferrin (Tf) gene develop severe iron deficiency anaemia but also develop an increased pool of non-transferrin-bound iron and tissue iron overload. Although hypotransferrinemic mouse ($TrR^{hpx/hpx}$) present extremely low hepcidin levels, in this case the hyperabsorption of iron is not solely because of the anaemia but also due to the effect of transferrin levels probably on the intestinal mucosa (Pietrangelo and Trautwein 2004;Raja et al. 1999;Trenor, III et al. 2000). The low levels of hepcidin in hypotransferrinemic mice support the notion of a dominant erythroid signal in hepcidin regulation (Roy CN 2002). One possible candidate for this dominant erythroid signal in hepcidin regulation is the soluble TfR1 (sTfR1). sTfR1 is produced by proteolytic cleavage of TfR1, and circulates in blood as a monomer bound to transferrin. When iron availability is reduced and when erythropoiesis is stimulated sTfR1 levels were found to be high (Beguin 2003;Nemeth et al. 2005). The reasons why overexpression of sTfR1 in mice did not alter hepcidin expression remains to be studied (Flanagan et al. 2006).

Recently a model has been proposed whereby TfR2, the second human transferrin receptor gene is involved in the detection of diferric TF and subsequently activation of a signal transduction pathway regulating hepcidin expression (Frazer and Anderson 2003;Johnson and Enns 2004). It is therefore possible that the low TF seen in $TrF^{hpx/hpx}$ mice leads to low hepcidin via a TfR2 signalling pathway.

1.5.3.3 Iron Overload and Transferrin

Mice injected with iron dextran presented hepcidin mRNA expression levels 4 times higher than control mice (Pigeon et al. 2001). In addition, dietary iron supplementation to both humans and mice lead to an increase in hepcidin mRNA which in turn blocks iron absorption until the normal plasma iron levels are restored (Nemeth et al. 2004b;Pigeon et al. 2001). Interestingly, in vitro exposure of hepatocytes to iron did not have a significant effect on hepcidin mRNA levels (Pigeon et al. 2001), this could be due to hepatocyte phenotypic changes that occur with time in culture, as hepatocytes when maintained for a few days in primary cultures without differentiation promoting factors lose the expression of several liver-specific genes (Glaise et al. 1998;Ilyin et al. 1998).

The hepcidin gene does not contain any iron responsive elements (IREs), suggesting that the iron status of the body is not signalled through iron regulatory proteins (IRPs), but by other signalling pathways. One suggested signalling pathway already mentioned involves diferric Tf in the circulation could provide the necessary signal for the hepatocytes to detect body iron demand and subsequently alter hepcidin expression (Frazer and Anderson 2003), but this pathway is still not fully understood.

While a role for diferric TF in the regulation of hepcidin expression remains speculative, the molecules HFE, transferrin receptor 2 (TFR2), and Hemojuvelin (HJV), are now accepted to be important regulators of Hepcidin production by hepatocytes. In Haemochromatosis disorders due to mutations in these genes, Hepcidin levels are inappropriately low, suggesting that these molecules act as direct or indirect regulators of hepcidin synthesis.

1.5.3.3.1 HFE

Changes in cellular iron status appear to have little effect on the expression of Hfe but the expression of Hfe has profound effects on cellular iron status. Haemochromatosis due to mutations in the Hfe gene is characterised by an inappropriate high iron absorption and reticuloendothelial cell iron release that leads to excess iron entering the circulation and subsequent deposition in parenchymal cells such as hepatocytes (Fleming et al. 2004). While the precise function of the Hfe protein remains unknown, recent studies have shown that Hfe gene mutations result in an inappropriately low level of hepcidin expression (Ahmad et al. 2002;Bridle et al. 2003;Muckenthaler et al. 2003). Moreover, when Hfe KO mice were crossed with mice overexpressing hepcidin their iron overload status was normalized (Nicolas et al. 2003). These studies suggest that Hfe participates in the regulation of intestinal iron absorption by modulating hepcidin expression. The fact that Hfe and Hepcidin are both expressed in the liver (Hfe in the Kupffer cells and hepcidin in hepatocytes) encourages this link (Bastin et al. 1998;Mura et al. 2004).

The decrease of circulating Hepcidin results in increased ferroportin-mediated iron efflux from reticuloendothelial cells and duodenal enterocytes increased circulating iron concentrations and eventually the saturation of TF. This leads to NTBI to be taken into tissues with a high capability for NTBI uptake such as the liver. In HH1 patients and Hfe KO mice, the increased enterocyte iron export leads to secondary increases in the expression of genes involved in intestinal iron uptake (e.g., Dcytb, DMT1) suggesting that the increased intestinal iron absorption, increased circulating iron, and sparing of RE iron loading seen in iron homeostasis abnormalities, such as HH1 are caused by an inappropriately low expression of hepcidin.

Despite the low levels of hepcidin, Hfe KO mice maintain the ability to regulate hepcidin expression when iron status changes, suggesting that Hfe loss only attenuates the signal between iron status and hepcidin expression in these mice. It has been proposed that other gene products such as TfR2 and hemojuvelin may serve as transducers to this signal. Whether HFE acts by modulating the function of either of these two molecules or acts independently of them to influence hepcidin expression is still unknown.

The Hfe gene has been identified as the second ligand for TfR. HFE lowers the affinity for Fe-TF by directly competing for TFR binding sites (Feder et al. 1998;Parkkila et al. 1997b;Waheed et al. 1999). Although previous studies have shown that HFE and TFR2 did not interact in vitro (West, Jr. et al. 2000), Andrews and her colleagues recently have shown that TFR2 competes with TFR1 for binding to HFE. It has also been found that the two molecules interact and that disease-associated mutations of Hfe and TfR2 do not abrogate this interaction (Goswami and Andrews 2006). Hence this interaction may be part of the hepatocytes mechanism of iron sensing.

Before the discovery of Hepcidin, it was thought that duodenal crypts sensed the body iron status and programmed the absorptive activity of daughter enterocytes, this way regulating the iron uptake by the duodenum. As HFE is expressed in duodenal crypt cells in physical association with TfR1, it was suggested that Hfe influences the ability of crypt cells to sense body iron status by modulating their Tf-mediated uptake of iron. This model postulates that HFE in duodenal crypt cells facilitates the TfR1-mediated uptake of plasma iron and that mutant HFE lacks this facilitating effect. The loss of functional Hfe would thereby result in a relatively iron-deficient state in these cells and daughter enterocytes which in turn would lead to an increase in expression of iron-regulated genes participating in dietary iron absorption, including DMT1, Dcytb, and/or Ireg1. This "crypt cell hypothesis" was supported by the observations that in Hfe KO mice, iron uptake from plasma TF by the duodenum is significantly decreased and that expression of the iron transport genes are increased in Hfe KO mice (Dupic et al. 2002b).

In summary, HFE clearly interacts with TFR1, changes the iron status of cells in which it is expressed, and influences hepcidin expression. However, there are difficulties in distinguishing the primary effects of Hfe on cellular iron status and its secondary effects resulting from changes in hepcidin expression. Developing cell-specific Hfe KO models may be useful is separating these influences as HFE is broadly expressed and its effects seem to be cell specific.

1.5.3.3.2 TFR2 and Hemojuvelin

The second molecule known to regulate hepcidin expression is TFR2 (Fleming et al. 2000;Kawabata et al. 2005). The disruption of the TfR2 gene leads to iron loading that is phenotypically very similar to HH1 (Camaschella et al. 2000). It has also been shown that that mutations in TfR2 also lead to inappropriately low Hepcidin levels (Nemeth et al. 2005), suggesting that like HFE, TFR2 is involved in the regulation of hepcidin expression and the two molecules may be part of the same regulatory pathway (Ganz and Nemeth 2006;Nemeth et al. 2005).

Hemojuvelin is the most recently discovered molecule in this pathway and like Hfe is expressed in hepatocytes (Papanikolaou et al. 2005;Papanikolaou et al. 2004;Roetto et al. 2001;Roetto et al. 2003). JH due to mutations in the hemojuvelin gene do not produce detectable levels of Hepcidin despite severe iron overload, suggesting that hemojuvelin is absolutely required for the production of hepcidin (Frazer and Anderson 2005). As hemojuvelin is a glycosylphasphatidylinositol (GPI)-linked plasma membrane protein that can enhance the signal produced from certain receptors, it was thought that it may also be involved in the signal transduction pathway that regulates hepcidin expression (Niederkofler et al. 2005). Recently, Babitt *et al* showed that Hemojuvelin (HJV) was also a coreceptor for BMPs and suggested that the Hjv/BMP complex regulated hepcidin expression through a BMP signal transduction pathway (Babitt et al. 2006;Truksa et al. 2006). Bone morphogenetic proteins (BMPs) are cytokines of the TGF-β superfamily that play a crucial role in the development of tissues, in regulating cell proliferation, cell differentiation, and apoptosis (Chen et al. 2004a;Gambaro et al. 2006;Varga and Wrana 2005). After activating their transmembrane receptors, TGF-β signalling is transduced into the nucleus by SMADs. SMAD4 is a tumour suppressor gene often found mutated in many cancers. Recently a group has shown that disruption of SMAD4 in mouse livers results in a significant decrease in hepcidin expression and accumulation of iron in many organs. They have also shown that SMAD4-deficient hepatocytes do not show transcriptional activation of hepcidin in response to iron

overload, TGF-β, BMP, or IL-6 (Wang et al. 2005). This new data reveals a novel role for TGF-β/BMP signalling in induction of hepcidin expression and shows that SMAD4 is required for this activity although the pathway and physiological relevance of these stimuli remains undefined. The significance of the role of Hemojuvelin in regulating hepcidin expression and systemic iron homeostasis also remains unclear.

In conclusion, Hepcidin is a key iron regulatory hormone in iron homeostasis that is up-regulated by iron and inflammation and down-regulated by anaemia and hypoxia. Two pathways are now known to be important for transcriptional regulation of Hepcidin, BMP/SMAD and IL-6/STAT3 signalling but it remains to be determined how these pathways, or others, transduce the physiologic signals (inflammation, oxygen concentration and iron levels) and regulate Hepcidin.

1.6 Aims

The discovery of the Hfe gene, the role of Hfe gene mutations as the main cause of Hereditary Haemochromatosis and the establishment of Hepcidin as the key regulator of iron homeostasis have contributed to our understanding of the molecular control of iron metabolism. The study of human diseases and animal models has led to the discovery and identification of new genes involved in iron homeostasis but much remains to be understood. The scope of this thesis is to further understand the mechanism of regulation of hepcidin mRNA expression and to study the role of HFE in the regulation of body iron levels, either in conjunction with hepcidin or as part of a cascade of modulators of hepatic iron concentrations. First, a novel animal model for Haemochromatosis type 1 (SWR Hfe KO) was created and characterised (Chapter 3). This animal mouse models was then studied in different iron status conditions (iron deficiency and iron overload) for hepcidin and iron transporter genes mRNA expression levels. The effect of transferrin in the expression of these genes was also investigated (Chapter 4). The effect of cytokines and acute inflammation on Hepcidin and iron transporter genes and the role of Hfe in the regulation of hepcidin by inflammatory settings were described (Chapter 5). The effect of anaemia and hypoxia on hepcidin and iron transporter genes mRNA expression levels *in vivo* and *in vitro* is presented and the effect of hepcidin on iron uptake is investigated (Chapter 6). Finally, in Chapter 7 the significance of the presented findings is discussed together with future studies.

CHAPTER 2
GENERAL METHODS

2.1 Gene expression levels by Reverse-Transcription Polymerase Chain reaction (RT-PCR)

2.1.1 RNA extraction

Precautions against contamination of samples with RNAses were taken. The bench working area was wiped with RNAse Zap (Ambion Ltd., UK), disposable gloves were worn at all times, glassware and pestle and mortar were baked at 150^{0}C for at least 4 hours prior to use and sterile disposable plastic wear and pipettes reserved for RNA work only were used.

Fresh tissues were snap frozen in liquid nitrogen and ground to powder using a cold pestle and mortar.

2.1.1.1 RNA extraction by the TRIzol® method

RNA was extracted using the TRIzol®/chloroform extraction and isopropyl alcohol precipitation. Powdered tissue or cells were incubated in TRIzol® reagent (Invitrogen, Ltd., Renfrew, UK) for 5 minutes at room temperature to complete the dissociation of nucleotide/protein complexes. Two hundred µl of chlorophorm (Sigma, Poole, UK) was added to the samples (20%v/v) and samples were shaken vigorously for 20 seconds. Samples were incubated at room temperature for 5 minutes then centrifuged at 12,000g for 15 minutes at 4^{0}C. The mixture separated into a lower red phenol chloroform phase which contained DNA and protein and an upper aqueous phase containing the RNA. The upper aqueous phase was removed to a separate clean tube and the lower organic phase was discarded.

The RNA was precipitated from the aqueous phase by incubating the samples with 500 µl of isopropyl alcohol (Sigma, Poole,UK) (30% v/v), for 20 minutes at room temperature (RT); and then centrifugated at 12,000 g for 15 minutes at 4^{0}C.

The resulting RNA pellet was washed in 75% ethanol and centrifuged at 8,000 g for 5 minutes at 4^{0}C. The supernatant was removed; the RNA pellet was air-dried at room temperature and resuspended in DEPC treated water (Promega UK Ltd., Southampton, UK). RNA samples were kept at -80^0 C until required.

2.1.1.2 RNA extraction by the Qiagen kit method

RNA was extracted using the Qiamp RNA blood Mini Kit (Qiagen, Crawley, UK). Samples were resuspended in Qiamp RTL buffer (Qiagen, Crawley, UK) with added β–mercaptoethanol and centrifuged at 12,000 g for 2 minutes in a Qiamp Shredder. The supernatant was transferred to a new and clean tube and the pellet was discarded. An equal volume of ice-cold 70% ethanol was added to the supernatant and transferred to the Qiamp spin column. This was centrifuged at 6,000 g for 20 seconds to bind the RNA to the column membrane. RNA bound to the membrane was washed with RW1 buffer. Contaminating DNA was digested by incubation of the membrane with Qiamp RNAse-free DNAse Set (Qiagen, Crawley, UK) for 15 minutes at room temperature. Membranes were rewashed with RW1 buffer, followed by two washes in RPE buffer containing 80% ethanol to remove contaminants. Columns were centrifuged at 12,000 g for 2 minutes to remove all traces of ethanol. RNA was reconstituted into 30 µl of DEPC treated water (Ambion Ltd., UK); this was added onto the membrane and centrifuged at 6,000 g for 2 minutes to elute. RNA samples were kept at -80^0 C until required.

2.1.1.3 RNA concentration and purity

The RNA concentration and purity were determined by measuring the absorbance of RNA in water at 260nm using a spectrophotometer (Beckman DU 650 Spectrophotometer, High Wickam, Bucks., UK). RNA concentration was calculated using the formula A_{260}*40 = µg RNA/ml. In distilled water, the RNA had an $A_{260/280}$ ratio of 1.9-2.1 indicating RNA free of contamination.

2.1.2 cDNA synthesis

Complementary DNA was synthesised using ABgene Reverse-iT 1st Strand Synthesis Kit (ABgene, Surrey, United Kingdom) using the PTC-100 thermocycler (MJ Research, NV, USA). 1µg of total RNA was used as a template and incubated with 500nM oligodT primer and H_2O

for 5 minutes at 70^0 C. to denature any secondary structure. 1^{st} strand synthesis buffer, dNTPs and reverse transcriptase were added. Reaction components were incubated at 47^0 C. for 60 minutes and then at 70^0 for 10 minutes to inactivate the Reverse-iT™ RTase Blend. Complimentary DNA was stored at -20^0C.

2.1.3 PCR

The resulting cDNA transcripts of the cells' mRNA were used for PCR amplification using the PCR Core System II (Promega UK Ltd., Southampton, UK) according to the manufacture's protocol. Each PCR reaction contained 5.0pmol of forward primer, 5.0 pmol of reverse primer, 1.5 mM $MgCl_2$, 500 µM each of dATP, dCTP, dGTP, dTTP, 0.5 units of *Taq* polymerase and 1xPCR buffer in a 20 µl reaction. The cycling parameters were initial denaturing at 95^0C for 3 minutes, unless stated 30 cycles of denaturing at 95^0C for 30 seconds, annealing for 1 minute and extension at 72^0C for 1 minute, followed by a final extension step at 72^0C for 5 minutes using a thermocycler (MJ Research, NV, USA). See table 2.1 for primer sequences, annealing temperatures and expected product sizes. The primers were synthesised by Sigma-Genosys Ltd. (Poole, Dorset, UK) according to the specific sequences. The house keeping genes β–actin, glyceraldehyde-3-phosphate dehydrogenase (GAPDH), and hypoxanthinephophoribosyltransferase (HPRT) were designed to incorporate areas of sequence that were highly conserved between species of rat, mouse and human. Primer specificity was determined by performing a BLAST search where the primer sequence can be checked against a database of all published genomic sequences (web address:http://www.ncbi.nlm.nih.gov/blast/).

2.1.4 Agarose electrophoresis

The PCR products were resolved on a 1.2% (w/v) agarose gel in TAE buffer (Tris-Acetate EDTA) containing 0.5 µg/ml ethidium bromide (Sigma-Aldrich Co., Ltd., Poole, UK). Samples were run alongside molecular weight markers (Bioline, London, UK) using a horizontal gel apparatus (BioRad, Hemel Hempstead, UK). The PCR bands were observed under ultraviolet illumination and images were captured using the Fluor-S MultiImager (Bio-Rad, Hemel Hempstead, UK).

Bands of the expected size were further analysed using MultiAnalyst (Bio-Rad, Hemel Hempstead, UK) imager analysis software. The amount of mRNA was standardised to that of the housekeeping gene. Results are therefore expressed as arbitrary optical density units of (gene of interest/housekeeper gene). In all the experiments, the presence of possible contaminants was investigated using control RT-PCR assays of samples in which either RNA had been excluded (blank) or reverse transcriptase had been omitted from the RT mixture.

2.2 Detection of gene expression mRNA levels using real-time PCR

Real time PCR allows continuous monitoring of PCR product information. Fluorescent double-stranded DNA dyes such as SYBR Green I can be used to monitor PCR product accumulation after each cycle of amplification (Wittwer et al. 1997). Real time PCR can be conducted either as a one-step or a two-step reaction. Two step RT-PCR, in which cDNA is produced in a separate reaction tube to the PCR, has the advantage over one step RT-PCR, in which the reverse transcriptase and the PCR are conducted in the same reaction tube. The cDNA template is more stable than RNA and there is often enough cDNA to perform a number of subsequent PCR reactions. Moreover, since the cDNA reaction product used as a starting template for the PCR is the same for both the control gene and for the gene of interest this eliminates variations due to fluctuations in efficiency of the reverse transcriptase step. For these reasons, the two step protocol for real time PCR was used.

2.2.1 Extraction of messenger RNA for real-time PCR

RNA was extracted by either using the TRIzol®/chloroform extraction and isopropyl alcohol precipitation as described in section 2.1.1.1; or by the Qiagen kit method, described in section 2.1.1.2.

2.2.2 cDNA synthesis

One μg of total RNA was reverse transcribed with a first-strand cDNA kit (ABgene Reverse-iT 1st Strand Synthesis Kit, ABgene, Surrey, United Kingdom) as described in section 2.1.2.

2.2.3 Real-Time PCR amplification

The resulting cDNA transcripts of the samples were used for Real Time PCR amplification using the QuantiTect SYBR® Green PCR kit (Qiagen, West Sussex UK) on a LightCycler Real Time PCR instrument (version 3.5, Roche Diagnostics, Mannheim, Germany). QuantiTect SYBR® Green I PCR master mix contains SYBR® Green I, HotStart Taq DNA Polymerase and a dNTP mix (including dUTP). SYBR® Green I present in the PCR mix only emits light when it binds to double stranded DNA, once bound it is excited at 494nm and emits light at 521nm. Monitoring of emissions at 521nm following excitation at 494nm, allows indirect quantification of the double stranded DNA concentration within the reaction capillary. Fluorescence at 521nm is quantified within each reaction capillary following the completion of every PCR extension step. The PCR cycle at which the fluorescence (product) reaches a threshold value is used as a measure of the original template concentration. When back calculated against a standard curve, the number of mRNA templates in the initial sample can be calculated. SYBR green does not interfere with PCR cycling as it dissociated from the product DNA during the denaturation step of the following PCR cycle. Each PCR reaction mix contained 1.0 μl of cDNA template, 5.0pmol forward and 5.0pmol reverse primers, 10 μl 2x QuantiTect SYBR® Green I PCR master mix and distilled water to a final volume of 20 μl.

Primers were designed using LightCycler Probe Design software version 1.01 (Roche Molecular Biochemicals, Mannheim, Germany) and synthesised by Sigma-Genosys Ltd. (Poole,

Dorset, UK) according to the specific sequences. The genes of interest and the house keeping genes were designed to incorporate areas of sequence that were highly conserved between species of rat, mouse and human. BLAST (http://www.ncbi.nlm.nih.gov/BLAST/) searcher were conducted on all primers to ensure unique specificity to the gene of interest.

Suitability of primers was determined by producing a single product of the correct length, determined by agarose gel electrophoresis, after PCR cycling with the protocol described (section 2.2.4.2). A single peak on the meltcurve analysis (section 2.2.4.3) was also required to determine suitability of primers. For primer sequences see Table 2.1.

2.2.4 Real-Time PCR cycling parameters

The RT-PCR reaction conditions were as suggested in the manufacturers protocol, this included an initial hot-start at 95^0C for 15 minutes, followed by PCR cycling of denaturation at 94^0C for 15 seconds, annealing at 60^0C for 20 minutes, extension at 72^0C for 30 seconds. The temperature of fluorescence acquisition was set at 2^0C below the product melting temperature and held for 5 seconds. The product melting temperature was determined in a test run by examining the melting curve (described in section 2.2.4.3). All experiments were performed in duplicate and for each sample the gene of interest and the control gene were run in parallel. A ratio of relative abundance of the gene of interest to the constitutively expressed gene was calculated by the Lightcycler Relative Quantification software version 1.0 (Roche Diagnostics, Germany).

2.2.4.1 The second derivative maximal method

The Lightcycler software version 3.5 (Roche Diagnostics, Germany) calculates the PCR cycle at which the maximal increase in fluorescence occurs in the log/linear phase of cycling. This is known as the second derivative maximal method, and the cycle at which this occurs can be, and is usually different for each sample. The cycle number at which maximal increase in fluorescence occurs is compared to that of standards with known concentration of PCR product using RelQuant software (Roche Diagnostics, Germany). A standard curve for each

gene was prepared with PCR products in which the concentration has been determined by spectroscopy.

Gene of interest		***Primer sequence***	
Human	**GAPDH**	F	5′ TGGTATCGTGGAAGGACTC 3′
		R	5′ AGTAGAGGCAGGGATGATG 3′
	HPRT	F	5′ TTGAGCCCTCTGTGTGCTCAAG 3′
		R	5′ GCCTGACCAAGGAAAGCAAAGTC 3′
	Hepcidin	F	5′ CTGCAACCCCAGGACAGAG 3′
		R	5′ GGAATAAATAAGGAAGGGAGG 3′
	DMT1+IRE	F	5′ AGTGGTTTATGTCCGGGACC 3′
		R	5′ TTTAACGTAGCCACGGGTGG 3′
	Ireg1	F	5′ CGTCATTGCTGCTAGAATCG 3′
		R	5′ AGACTGAAATCAATACGAGC 3′
	TfR1	F	5′ TATAGAAGGTTTGGGGGCTGTG 3′
		R	5′ GAGACCCTATGAACTTTTCCCTA 3′
	TfR2	F	5′ GAAGGGGCTGTGATTGAAGG 3′
		R	5′ GATTCAGGGTCAGGGAGGTG 3′
Mouse	**β- Actin**	F	5′ GACGGCCAAGTCATCACTATT 3′
		R	5′ CCACAGGATTCCATACCCAAGA 3′
	Hepcidin 1	F	5′ CCTATCTCCATCAACAGATG 3′
		R	5′ AACAGATACCACACTGGGAA 3′
	DMT1	F	5′ GGCTTTCTTATGAGCATTGCCTA 3′
		R	5′ GGAGCACCCAGAGCAGCTTA 3′
Mouse	**Ireg1**	F	5′ CCAGCATCAGAACAAACACG 3′
		R	5′ ACTGCAAAGTGCCACATCC 3′

Rat	**β- Actin**	F	5' GACGGCCAAGTCATCACTATT 3'
		R	5'CCACAGGATTCCATACCCAAGA 3'
	Hepcidin	F	5'CACGAGGGCAGGACAGAAGGCAAG 3'
		R	5'CAAGGTCATTGCTGGGGTAGGACAG 3'

Table 2.1 Human, mouse and rat primer sequences used in this study
Forward sequences (F) and Reverse sequences (R).

2.2.4.2 Preparation of standard curves

PCR products (dsDNA) for each gene were separated on a 1.2% agarose-TAE gel and purified using the Geneclean kit (Qbiogene, Cambridge, UK). Approximately 300 mg of the product of interest were excised from the gel using a clean scalpel and placed in a 1.5 ml tubes with 400µl of glassmilk (silica beads in high salt solution), this was incubated at 55^0C to melt the agarose gel. Glassmilk containing the DNA/gel mix was placed in the GENECLEAN spin filter column and centrifuged at 12,000g for 1 minute. DNA was retained by the membrane and the glassmilk/gel in the supernatant was discarded. The membrane-filter was washed twice with wash buffer and dried by centrifuging for further 2 minutes. DNA was resuspended in 10-25 µl of distilled water and centrifuged at 13,000 g for 1 minute. The concentration of each PCR product DNA was determined using a spectrophotometer (Beckman DU 650 Spectrophotometer, High Wycombe, Bucks., UK) and calculated using the formula A_{260}*50 = µg DNA/ml. Purified DNA was serially diluted 10-fold covering a dynamic range of 7 logarithmic orders. 1.0 µl of each standard dilution was amplified by PCR using the Lightcycler and specific primers (Fig. 2.1). One set of gene-of-interest standards were run in duplicate with the house keeping gene standards to generate two standard curves (Fig. 2.2).

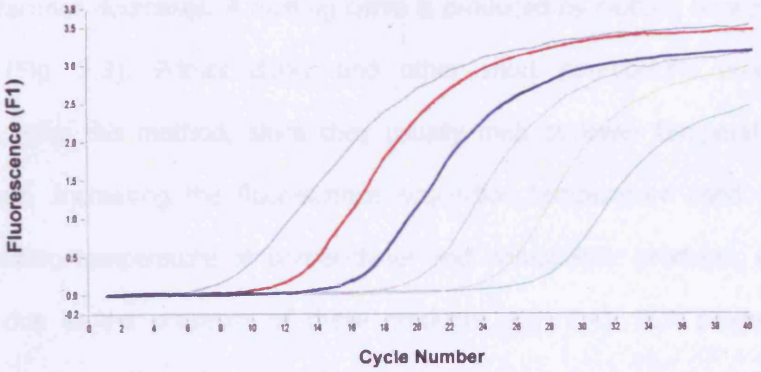

Figure 2.1 Representative graph of a gene product standard curve.

A set of standard dilutions covering a dynamic range of 6 logarithmic orders was amplified per gene of interest.

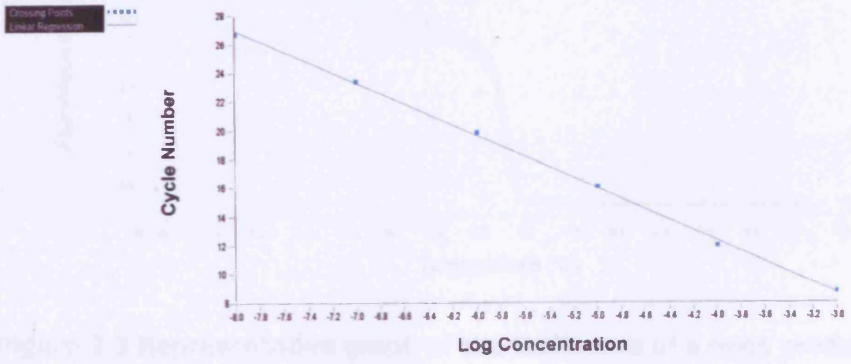

Figure 2.2 Representative graph of the linear regression of a gene product standard curve.

2.2.4.3 Analysis of the melting curve

After completion of the PCR amplification cycles, a melting curve was determined for each PCR product. Each dsDNA has its own melting temperature (TM) based on the strand length and the G-C content. Therefore melting curve analysis can be used to identify unwanted by-products of the PCR reaction such as primer dimer. The PCR products were heated to 65^0C and then the temperature was increased slowly (0.5^0C per second) whilst fluorescence was continually monitored. At low temperatures all DNA is double stranded, SYBR Green I binding and fluorescence is maximal. As the temperature is increased, DNA products are denatured,

and the fluorescence decreases. A melting curve is produced by plotting fluorescence against temperature (Fig. 2.3). Primer dimer and other short non-specific products can be distinguished using this method, since they usually melt at lower temperatures than the desired product. Increasing the fluorescence acquisition temperature used during PCR to above the melting temperature of primer-dimer and non-specific products, eliminates any fluorescence due to the presence of these products (Fig. 2.4). PCR products were also analysed by gel electrophoresis as described in section 2.1.4, and visualised using a Bio-Rad MultiImager (Bio-Rad, Hemel Hempstead, UK).

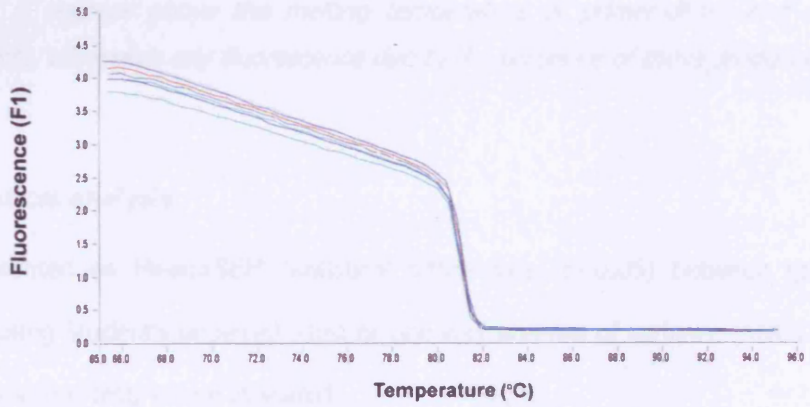

Figure 2.3 Representative graph of the meltcurve of a gene product

At low temperatures all DNA is double stranded, SYBR Green I binding and fluorescence is maximal. As the temperature is increased, DNA products are denatured, and the fluorescence decreases.

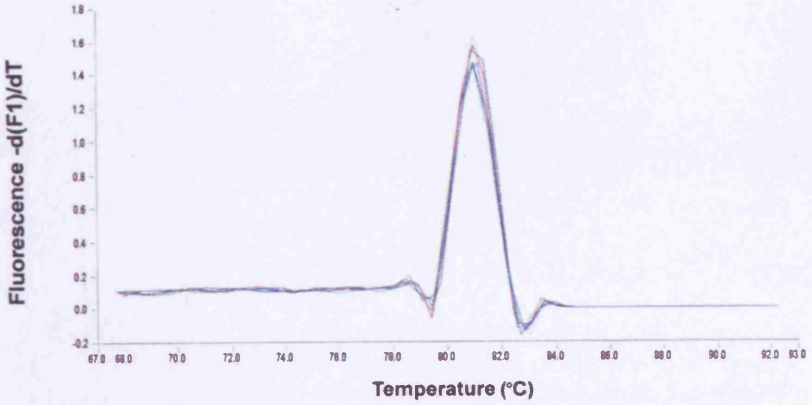

Figure 2.4 Representative graph of the meltcurve peak analysis of a gene product. *Increasing the fluorescence acquisition temperature used during PCR to about 2 degrees above the melting temperature of primer-dimer and non-specific products, eliminates any fluorescence due to the presence of these products.*

2.3 Statistical analysis

Data is presented as Mean±SEM Statistical differences ($p<0.05$) between groups were determined using Student's unpaired t-test or one-way analysis of variance (ANOVA) followed by Tukey's post hoc test, where indicated.

CHAPTER 3

CHARACTERISATION OF IRON ACCUMULATION IN THE LIVER OF WT AND HFE KO SWR MICE

3.1 Introduction

The liver

The liver is the second largest organ and the largest gland within the human body with a median weight of approximately 1600g in men and 1400g in women. The human liver lies in the right upper quadrant of the abdomen in contact with the diaphragm, under the protection of the rib cage. It lies on the right of the stomach and makes a kind of bed for the gallbladder (Fig. 3.1).

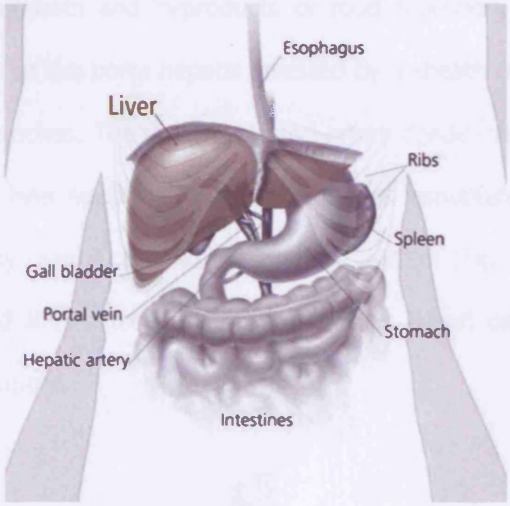

Figure 3.1 Position of the liver in the right hypochondrium and relationships to neighbouring organs and structures. *Scheme adapted from: http://www.liver-cancer.info/ on 1/09/2006.*

Apart from a section where it connects to the diaphragm, the liver is entirely covered by visceral peritoneum, a thin, double-layered membrane that reduces friction against other organs. The peritoneum folds back on itself to form the falciform ligament and the right and left triangular ligaments. Traditional gross anatomy divided the liver into four lobes based on surface features. The falciform ligament is visible on the front (anterior side) of the liver. This divides the liver into a left anatomical lobe, and a right anatomical lobe. When looking at the visceral surface of the liver, there are two additional lobes between the right and left. These are the caudate lobe (the more superior), and below this the quadrate. From behind, the

lobes are divided up by the ligamentum venosum and ligamentum teres (anything left of these is the left lobe), the transverse fissure (or *porta hepatis*) divides the caudate from the quadrate lobe, and the right sagittal fossa, which the inferior vena cava runs over, separates these two lobes from the right lobe.

The liver is supplied by two main blood vessels on its right lobe: the hepatic artery and the portal vein. The hepatic artery carries 25% of the liver's blood supply (arterial blood) and the remaining 75% (venous blood) comes through the portal vein that carries blood from the entire capillary system of the digestive tract, spleen, pancreas, and gall bladder, so that the liver can process the nutrients and byproducts of food digestion. The hepatic artery and portal vein enter the liver at the porta hepatis invested by a sheath of connective tissue which incorporates bile duct branches. The duct, vein, and artery divide into left and right branches, and the portions of the liver supplied by these branches constitute the functional left and right lobes. In the widely used Couinaud or "French" system (Fig. 3.2, 3.3), the functional lobes are further divided into a total of eight segments based on secondary and tertiary branching of the blood supply.

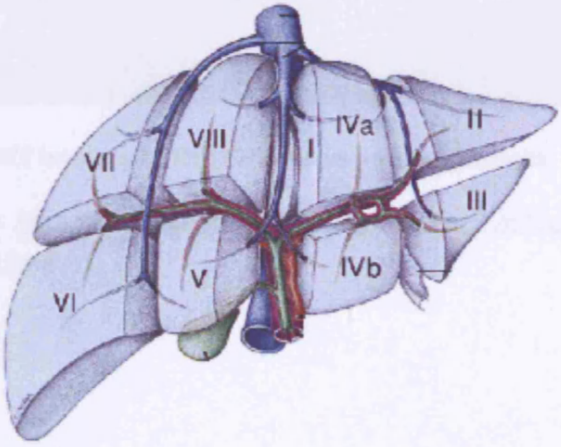

Figure 3.2 Diagrammatic representation of Couinaud liver segments. *The anterosuperior view is shown, with division of the portal and hepatic veins. The segments are indicated as: I, caudate lobe; II, III and IV, left lobe; V, VI, VII and VIII, right lobe. Scheme taken from: http://mbi.dkfz-heidelberg.de/projects/liver/medical_background.html on the 1/09/2006.*

The venous drainage from the liver operates through the hepatic veins that emerge from the posterior surface of the liver and open immediately into the inferior vena cava just before it pierces the diaphragm. There are three main hepatic veins: the left, the middle and the right. The first two usually join to form a short stalk with a common outlet. Inferior vein(s) drain the posterior segment of the right lobe and the caudate lobe directly into the vena cava. The main left vein drains the two lateral segments of the left lobe (Segments II and III), the middle vein drains segment IV and the anteromedial sector of the right lobe (segment V and VIII); the right vein drains the remainder of the right lobe (segment VI and VII). The caudate lobe has its own venous supply and drainage and so it can be regarded as a separate lobe.

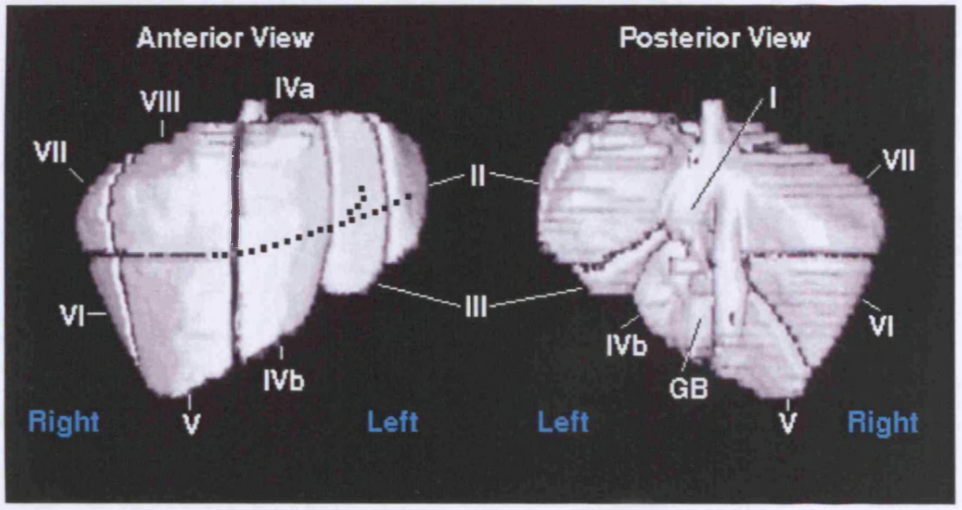

Figure 3.3 MRI images of the Couinaud liver segments

Adapted from http://dpi.radiology.uiowa.edu/nlm/app/livertoc/liver/8seg.html, taken on the 10/10/2006

Liver parenchyma

The liver is covered with a connective tissue capsule that branches and extends throughout the substance of the liver as septae. This connective tissue tree provides a scaffolding of support and the highway which along which afferent blood vessels, lymphatic vessels and bile ducts traverse the liver. Additionally, the sheets of connective tissue divide the parenchyma of the liver into very small units called lobules. Lobules, consists of a mass of cells, hepatic cells, arranged in irregular radiating columns between which are the blood channels

(sinusoids). These convey the blood from the circumference to the center of the lobule, and end in the central vein, which runs through its center, to open at its base into one of the sublobular veins. Between the cells are also the minute bile capillaries. At the vertices of the lobule are regularly distributed portal triads, containing a bile duct and a terminal branch of the hepatic artery and portal vein (Fig. 3.4, 3.6).

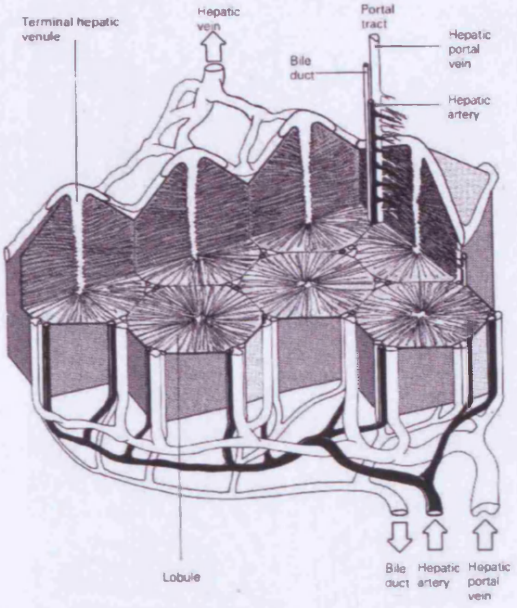

Figure 3.4 Hepatic vasculature and biliary system

Schematic diagram showing the gross arrangement of the hepatic vascular and the bile collecting systems. The hepatic portal vein and hepatic artery branch repeatedly within the liver, their terminal branches running within the portal tracts (Burkitt et al. 2007).

This basic hexagonal pattern is replicated millions of times throughout the tissue and is held together by an extremely fine areolar tissue, in which the portal vein, hepatic ducts, hepatic artery, hepatic veins, lymphatics, and nerves ramify; the whole being invested by a serous and a fibrous coat. Terminal branches of the hepatic portal vein and hepatic artery empty together and mix as they enter sinusoids in the liver. Sinusoids are distensible vascular channels lined with highly fenestrated or "holey" endothelial cells and bounded

circumferentially by hepatocytes. As blood flows through the sinusoids, a considerable amount of plasma is filtered into the space between endothelium and hepatocytes (the "space of Disse"), providing a major fraction of the body's lymph. Blood flows through the sinusoids and empties into the central vein of each lobule (Fig. 3.5). Central veins coalesce into hepatic veins, which leave the liver and empty into the vena cava.

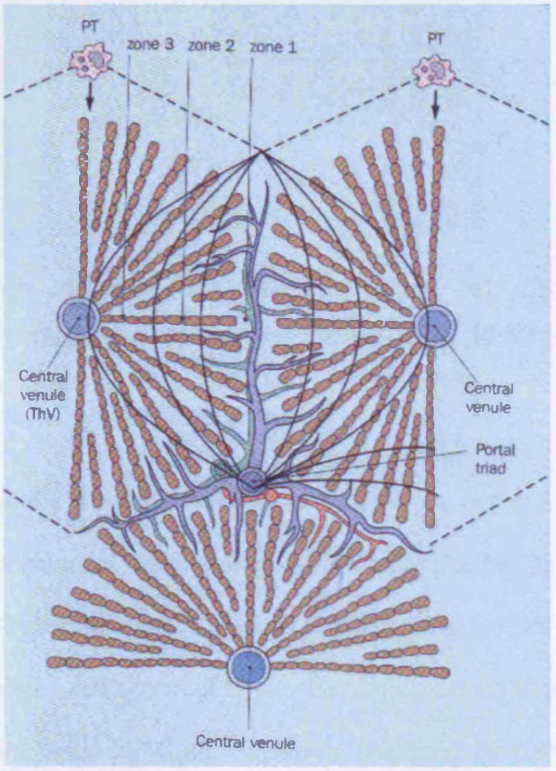

Figure 3.5 Liver simple acinus

Diagrammatic representation with the zonal arrangement of the hepatocyte and two neighbouring classic lobules outlined by a discontinuous line (Bacon et al. 2006).

A three-dimensional representation of this organisation is best illustrated by the stereoscopic reconstruction of Hans Elias (ELIAS 1949) (Fig. 3.6).

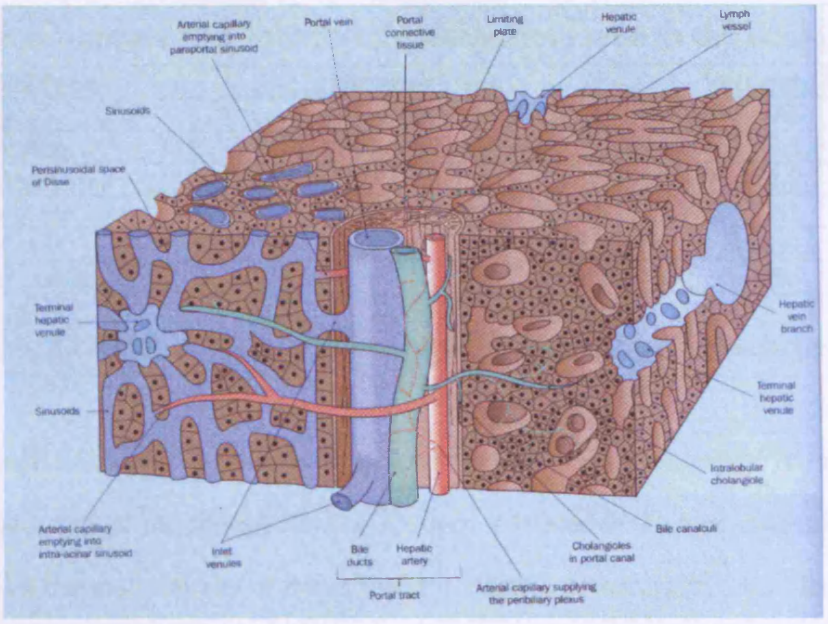

Figure 3.6 Three dimensional representation of the normal liver parenchyma. *Schematic diagram modified from (ELIAS 1949) showing the portal triad containing the hepatic artery, portal vein and bile duct.*

Hepatocytes occupy around 78% of the total liver volume in humans (Table 3.1). The individual hepatocyte is a polyhedral and highly polarized epithelial cell approximately 30-40 m^3 in diameter. Each cell contains one or more nuclei; binucleation of a minority of hepatocytes is a normal finding. Hepatocytes form interconnecting walls or plates separated from each other by the sinusoidal labyrinth. Sinusoids are lined by flattened, fenestrated endothelial cells which form an incomplete, porous barrier, allowing easy exchange of materials between blood and hepatocytes. Within the sinusoidal lumen there are phenotypically heterogeneous macrophages. The principal phagocytic reticuloendothelial cell in the liver is the Kupffer cell. Kupffer cells are more numerous near the portal tracts and so often are in direct contact with the blood. A phenotypically distinctive population of lymphocytes is also present in the sinusoidal lumens and in the portal tracts (Sheuer and Leftowitch 2000).

Relative number and volume of different cell type in the adult liver		
Cell type	**Number (%)**	**Volume (%)**
Hepatocytes	60	78
Non-hepatocytes	40	6.3
Endothelial cells	20	2.8
Kupffer cells	14	2.1
Stellate cells	6	1.4
Extracellular space		15.7

Table 3.1 Relative number and volume of different cell types in liver

As mentioned in chapter 1, the main storage site of iron in the body is in the liver. Approximately 40% of the storage iron, or 400 mg, is located in the liver, and under normal circumstances the vast majority of this is found in hepatic parenchymal cells. The remainder is found in Kupffer cells, with very small amounts in stellate cells, endothelial cells, and bile duct cells. As the major site of iron storage, hepatocytes have a high capacity to synthesize not only the iron storage protein ferritin (Harrison and Arosio 1996) but also the plasma iron transport protein, Transferrin (TF) (Ponka et al. 1998), Ceruloplasmin (Cp) (Hellman and Gitlin 2002), haptoglobin (Wassell 2000), and hemopexin (Tolosano and Altruda 2002). The hepatocyte also plays a major role in the regulation of body iron homeostasis as it is the main site of expression of the regulatory proteins HFE transferrin receptor 2 (TFR2), Hemojuvelin (HJV) and Hepcidin (Frazer and Anderson 2003).

Iron can be acquired by the liver in several ways as described in section 1.4 of Chapter 1. Irrespective of its source, it is likely that iron that enters the hepatocyte joins the same intracellular pool and from here, iron will be used for metabolic functions, may be stored within ferritin, or may contribute to the regulation of cellular iron metabolism by influencing the activity of IRPs and likely other factors. Many studies have shown a positive correlation between the hepatic ferritin content and body iron levels and so the level of ferritin within the cell is determined by intracellular iron levels (Arosio and Levi 2002;Halliday et al. 1994;Harrison and Arosio 1996). In cases of severe iron overload, iron can be stored in the liver as haemosiderin, a breakdown product of ferritin (Iancu 1990;Iancu et al. 1997).

Although it is known that processes of hepatic iron uptake, storage, and release are vital, not just for the maintenance of hepatocyte iron homeostasis but for the body as a whole. The central role played by the liver in the regulation of body iron homeostasis has only become apparent with the recent discovery of the iron regulatory hormone Hepcidin.

Hepatic iron content and Haemochromatosis

As described in section 1.4.2.1.1 of Chapter 1, hereditary Haemochromatosis type 1 (HH1) is an autosomal recessive disorder of iron metabolism caused by mutations in the Hfe gene. HH1 is characterised by defective regulation of dietary iron absorption that leads to excessive iron accumulation, mainly in the liver. The increased iron absorption in haemochromatosis is in part responsible for elevated transferrin saturation and transferrin-bound iron transport, which leads to cellular uptake of excess circulating iron and pathological expansion of body iron stores. This in turn results in the increased formation of the iron storage molecules ferritin and haemosiderin, especially in parenchymal cells of the liver. Progressive hepatic iron accumulation in humans leads to fibrosis, cirrhosis and subsequent increased morbidity and mortality.

The first histological abnormality in haemochromatosis patients homozygous for the C282Y mutation is the appearance of stainable iron in periportal hepatocytes. At this stage the diagnosis should be confirmed by genetic testing as heterozygous patients have very sparse or absent stainable liver iron. As parenchymal iron deposition increases, fibrosis begins to expand the portal tracts and Kupffer cells and portal tract macrophages start to also accumulate iron. As fibrosis and hepatocellular hyperplasia start to alter the normal architectural relationship of the parenchyma, cirrhosis slowly starts to develop. The onset of cirrhosis results in a fall in life expectancy and an increased risk of hepatocellular carcinoma (Sheuer and Leftowitch 2000).

Kupffer cells are the principal macrophages of the liver, they are important in phagocytosing senescent red blood cells and recycling the iron back to the plasma and around 15% of this traffic occurs in the liver. Under iron overload conditions such as HH1, the proportion of

Kupffer cells storing iron can increase considerably, but hepatocytes remain the dominant site of iron deposition. The iron accumulated by Kupffer cells leads to production of cytokines that can play an important role in activating hepatic stellate cells and thus in the genesis of liver fibrosis.

The presence of iron stores in humans has been characterised by using invasive methods such as biopsies and non-invasive techniques such as MRI (Magnetic Resonance Imaging) scans. These methods are not able to give a full account of how much and where the iron stores are located and therefore the pattern of iron accumulation in the different lobes in the liver of patients has not been fully investigated. In clinical practice, the iron concentration determined in a small part of a needle biopsy or in a fine needle biopsy is considered to be representative of the mean iron concentration in the whole liver. When a non-uniform pattern of iron distribution was observed in haemochromatosis and in cirrhosis, the possibility of sampling errors was reported (Emond et al. 1999). Emond et al investigated the accuracy of iron measurements by taking multiple biopsy-sized and microtome samples at random sites from the livers of 11 patients undergoing liver transplantation. They found an average coefficient of variation of liver iron concentration of 41% when measured via multiple needle biopsies, and 30% when measured from larger microtome samples showing that single biopsies are very imprecise to measure hepatic iron concentrations (Emond et al. 1999). Ambu (Ambu et al. 1995) and Clark (Clark et al. 2003) had already shown this differential distribution of iron in the liver by studying non-cirrhotic B-thalassaemic autopsy liver specimens and by studying patients with Thalassaemia major by MRI, respectively. Although the hepatic variation of iron accumulation has been reported, there is no information on iron levels in the different hepatic lobes.

In order to study Haemochromatosis type 1 (HH1), the Hfe gene was knocked out in several mouse strains, such as C57BL/6 and DBA/2 (Lebeau et al. 2002). These strains provide an approach for investigating the extent to which modifier genes play a role in normal and pathological iron regulation in the Hfe KO mouse model. Duodenal iron absorption and hepatic iron load have been found to be two or three times higher in Hfe KO mice (C57BL/6 X

129/OLa) than in corresponding controls. Iron was found preferentially in periportal hepatocytes and plasma iron concentrations and transferrin saturation were elevated accordingly. The iron distribution between organs and microscopic iron deposition in the hepatocytes of these Hfe KO mouse models resembled the patterns described in HH1. One difference between the mouse model and the HH1 patients is that the Hfe KO mice do not develop fibrosis or cirrhosis despite the severe iron overload (Knutson et al. 2001). Thus, the role of iron in initiating liver fibrosis in iron overload diseases such as HH1 is not fully understood and an animal model that can produce the full pathological picture of the cirrhotic liver seen in HH1 is still needed. It is known that iron overload enhances liver injury, mildly accelerates the process of fibrosis and can be directly carcinogenic in the absence of cirrhosis or fibrosis (Arezzini et al. 2003;Asare et al. 2006) but it is believed that other factors may be involved in this process (Roberts et al. 1993). The insufficiently high levels of iron accumulation might account for the lack of fibrosis and cirrhosis seen in these animal models. It has been reported that the severity of iron accumulation when the Hfe gene is disrupted is dependent on the mouse strain used (Clothier et al. 2000;Leboeuf et al. 1995;Morse et al. 1999). The difference in iron loading in different mouse strains is probably dependent on modifier genes (Fleming et al. 2001) and in most strains, levels of iron never reach the levels seen in HH1. In order to reach high levels of liver iron in a mouse strain model, the murine Hfe allele was disrupted in the SWR strain. The SWR mouse strain has been described as having a higher basal iron status in the liver (190±6 μg/g dry weight) than other strains, namely DBA/2 (103±8 μg/g dry weight), and C57BL/6 (44±3 μg/g dry weight) mouse strains (Clothier et al. 2000).

The aim of this study is to accurately characterise the pattern of iron accumulation in wt and Hfe KO SWR mice and to investigate if the high levels of hepatic iron content in this mouse strain together with the disruption of the Hfe allele lead to fibrosis or other pathological abnormalities in the liver making the SWR Hfe KO mice a more accurate animal model for the study of HH1.

3.2 Methods

3.2.1 SWR Hfe Knockout (KO) mice

C57BL/6 mice lacking the Hfe gene were donated by Susan Gilfillan, Department of Immunology, Washington University, St Louis, MO). Cloning and sequence analysis of the murine Hfe gene from a 129/SvJ library has been previously described (Bahram et al. 1999); a 2.5-kb BglII fragment encompassing the second and third exons (α1 and α2 domains) was replaced with a 2-kb pgk-neo^r gene flanked by loxP sites. The targeting fragment was excised from the vector and correctly targeted HFE alleles were detected by Southern blot analysis in 6 of 240 G418-resistant clones, two of which (with normal karyotypes) were subsequently injected into C57BL/6 blastocysts. Chimeric, heterozygous, and homozygous mice were generated according to standard procedures and were obtained in Mendelian ratios; genotyping was assessed by PCR.

SWR mice Hfe KO mice were generated by intercrossing heterozygous animals (with 129/Ola-C57BL/6 mixed background) with wt SWR mice (Charles River Lab, Inc., USA) for 9 generations. This number of generations is expected to generate mice 99.9% Hfe KO when homozygous for the Hfe mutation. Wild-type and homozygous Hfe KO littermates were identified at 3 to 4 weeks of age. Mice were fed CRM diet (Scientific Diet Supplies (SDS), Witham, Essex, United Kingdom) ad lib and males were studied at 12 weeks of age. All experimental procedures were conducted in accordance with the UK animals (Scientific Procedures), Act, 1986.

3.2.1.1 SWR mice genotyping

DNA was prepared from mouse tail fragments using a DNeasy Tissue kit (Qiagen, Crawley, UK). The tails were digested overnight at 55^{0}C in ATL buffer and protease K. Once the tails were fully digested, AL-Ethanol buffer was added to the samples. The samples were then centrifuged at 12,000 g for 2 minutes in a Qiamp Shredder. The resulting sample was transferred to a new and clean tube and the Qiamp Shredder column was discarded. An equal volume of ice-cold 70% ethanol was added to the supernatant and transferred to the Qiamp spin column. This was centrifuged at 6,000 g for 20 seconds to bind the DNA to the

column membrane. DNA bound to the membrane was washed with AW1 buffer to remove contaminants. Columns were centrifuged at 12,000 g for 2 minutes to remove all traces of washing buffer. DNA was reconstituted into 200 µl of AE buffer; this was added onto the membrane and centrifuged at 6,000 g for 2 minutes to elute. The concentration of the DNA samples was determined using a spectrophotometer (Beckman DU 650 Spectrophotometer, High Wickam, Bucks., UK) and calculated using the formula A_{260}*50 = µg DNA/ml.

The resulting DNA samples were used for PCR amplification using the PCR Core System II (Promega UK Ltd., Southampton, UK) according to the manufacture's protocol. The cycling parameters were initial denaturing at 95^0C for 3 minutes, unless stated 30 cycles of denaturing at 95^0C for 30 seconds, annealing for 1 minute and extension at 72^0C for 1 minute, followed by a final extension step at 72^0C for 5 minutes using a thermocycler (MJ Research, NV, USA).

Radiolabeled primers were designed to amplify the murine Hfe gene: 5'-GAATTAACAGGCCGTTTCTAAAG-3'(HFE forward), 5'-CTTGGAGTAGTGGCTCACACT-3' (HFE reverse), and 5'-GAGATCAGCAGCCTCTGTTCC-3' (pgk-neo^r). The primers were synthesised by Sigma-Genosys Ltd. (Poole, Dorset, UK) according to the specific sequences. Primer specificity was determined as stated in section 2.1.3.

The PCR products were resolved on a 1.2% (w/v) agarose gel in TAE buffer (Tris-Acetate EDTA) containing 0.5 µg/ml ethidium bromide (Sigma-Aldrich Co., Ltd., Poole, UK). Samples were run alongside molecular weight markers (Bioline, London, UK) using a horizontal gel apparatus (BioRad, Hemel Hempstead, UK). The PCR bands were observed under ultraviolet illumination and images were captured using the Fluor-S MultiImager (Bio-Rad, Hemel Hempstead, UK). The disruption of the Hfe gene was confirmed by a single band 350 bp (Fig. 3.2.1).

Wild-type Heteroz Hfe KO

Figure 3.2.1 Interpretation of agarose gel band results in SWR mice genotyping. *SWR wt (band size= 320 bp), SWR heterozygous for Hfe disruption (320 bp, 350 bp) and SWR Hfe KO (350 bp).*

3.2.2 Tissue iron quantification in SWR wt and Hfe KO mice by a modified Torrance & Bothwell method (Torrance and Bothwell 1980).

In order to characterise the iron accumulation in the whole of the SWR mice liver accurately, the livers were divided into five lobes and named A to E (Fig. 3.2.2, Table 3.2.1). Tissue non-haem iron determination was performed by a modified Torrance and Bothwell colorimetric method (Torrance and Bothwell 1980).

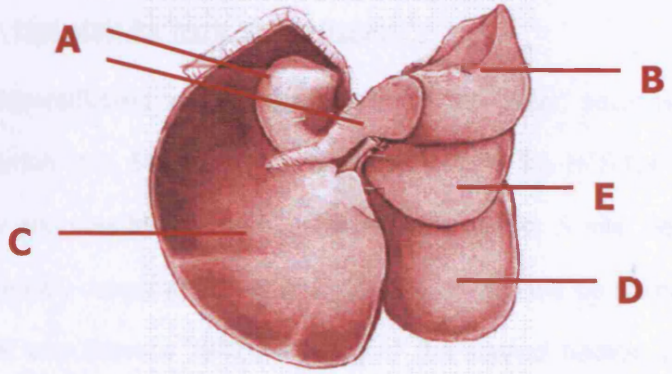

Figure 3.2.2 Posterior view of the mouse liver

The mouse liver was sectioned into five different lobes, designated A to E.

Lobe	Couinaud segments	S
Caudate	1	A, B
Left	2, 3	E
Quadrate	4	D
Right	5, 6, 7, 8	C

Table 3.2.1 Hepatic lobes, corresponding Couinaud Segments and corresponding sections used in this study (S).

Tissue samples were dried at 50°C for four days. Dried samples were weighed and digested in acid digestion mixture (3 M hydrochloric acid, 10% trichloroacetic acid) at 65°C for 20 hours. 75µl of each acid extract was mixed with 0.3 ml of bathophenanthroline chromagen reagent and the absorbance was measured at 535 nm in a spectrophotometer (Beckman DU 650 Spectrophotometer, High Wycombe, Bucks., UK). Results are expressed per g dry weight of tissue.

3.2.3 Histological stains used on SWR mice tissue sections

3.2.3.1 Perl's Prussian blue stain for ferric iron in tissues

Tissue sections were deparaffinised and hydrated with distilled water, sections were then placed in the Perl's solution (1:1, 5% potassium ferrocyanide and 5% HCl) for 10 minutes, rinsed in distilled water and counterstained with nuclear fast red for 5 min. Sections were then in rinsed distilled water, dehydrated, and mounted. Ferric iron will be stained blue and the nuclei red (Bancroft and Stevens 1982). Grading of the stained hepatic sections was performed according to Scheuer's grading table shown on Table 3.2.2.

Grade	Magnification required (eye piecex objective)
0	Granules absent or barely discernable x400
1	Barely discernable x250 Easily confirmed x400
2	Discrete granules resolved x100
3	Discrete granules resolved x25
4	.....visible x10 or naked eye

Table 3.2.2 Grading of iron deposition according to Scheuer (personal communication by Prof. P. Dhillon).

3.2.3.2 Massom Trichrome stain for the histological hepatic assessment of fibrosis/cirrhosis in SWR Hfe KO mice

Liver sections were deparaffinised and hydrated with distilled water. Sections were fixed with Bouins solution overnight. Sections were then washed in running water until clear then placed in Weigerts hematoxylin for 10 minutes which will stain the nuclei. Sections were then again washed in running water for 10 minutes, rinsed in distilled water and placed in Biebrich Scarlet-acid fuchsin solution for 15 minutes. After rinsing in distilled water sections were differentiated in Phosphotungstic-phosphomolybdic acid for 10-15 minutes (at this point sections were checked under the microscope to assess if collagen tissue was clear if positive results are expected sections are differentiated for 5-10 more minutes until collagen is clear). Sections are counterstained in aniline blue for 2 minutes, rinsed in distilled water, dehydrated and mounted. Collagen will be stained blue or green, the nuclei dark brown and the cytoplasm red.

3.3 Results

3.3.1 Perl's Prussian Blue staining of whole liver sections of SWR wt and Hfe KO mice

Histological examination of SWR Hfe KO mice liver with Perl's reaction for ferric iron showed iron accumulation is unevenly distributed within the different lobes (Fig. 3.3.1b). Iron in these mice accumulated primarily in the hepatocytes with scarce Kupffer cell accumulation (Fig. 3.3.2). No positive staining was observed in endothelial cells or in bile ducts. Representative sections of SWR wt mouse liver (a) and SWR Hfe KO mouse liver (b) are shown in Fig. 3.3.1.

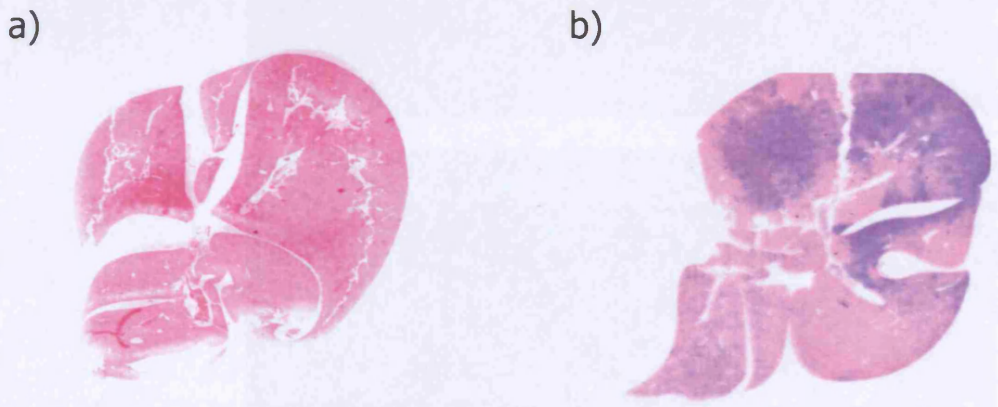

Figure 3.3.1 Perl's Prussian blue staining of the whole SWR mouse liver

SWR wt mouse showing no positive staining confirming the lack of iron stores (A), SWR Hfe KO showing positive patchy staining showing a differential distribution of iron stores in different lobes (B).

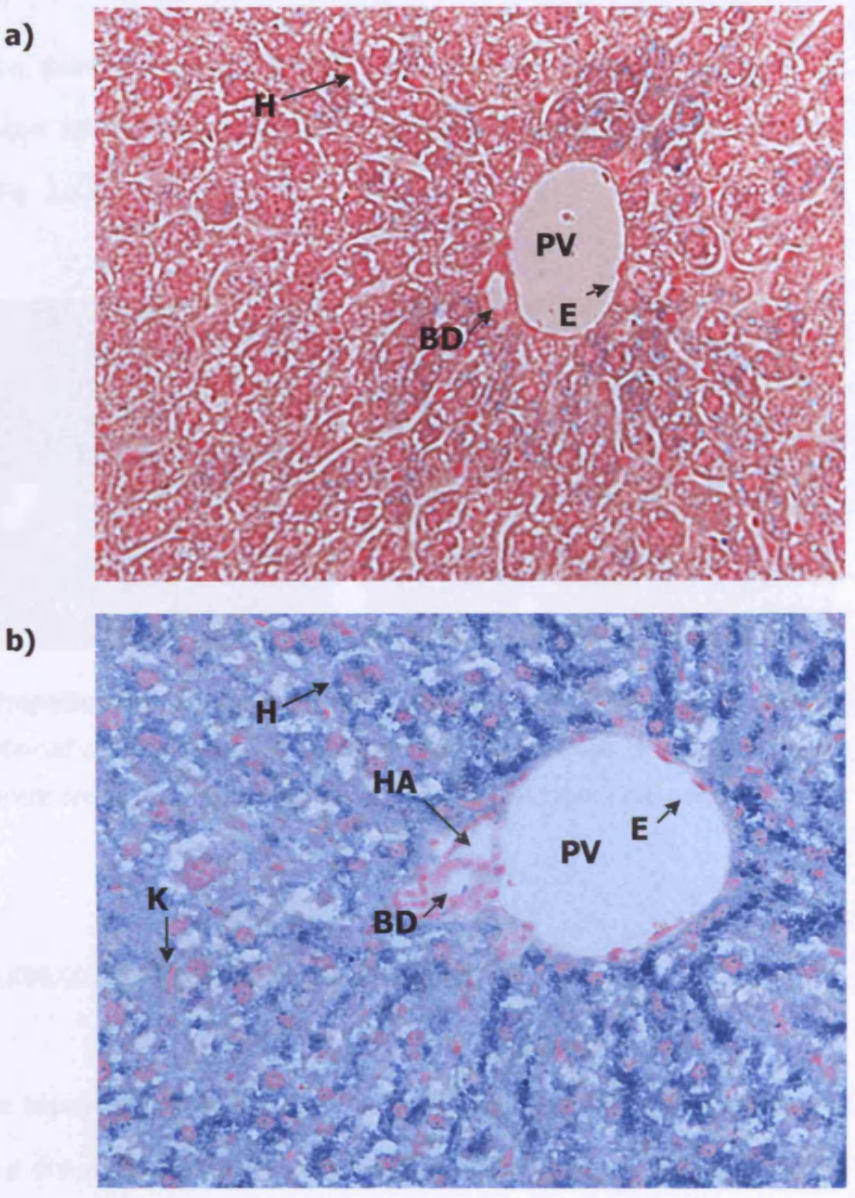

Figure 3.3.2 Perl's Prussian blue staining of wt and Hfe KO SWR mouse liver. *Light microscopy of liver parenchyma showing the portal vein (PV), hepatic artery (HA) and bile duct (BD) in wt (a) and Hfe KO SWR mice (b). Positive staining for ferric iron was observed in the hepatocytes (H) but not in the endothelial cells (E) or Kupffer cells (K) in the Hfe KO SWR mice. No positive staining was seen in wt SWR mice for ferric iron (x40 original magnification (OM).*

3.3.2 Histological staining of liver sections for fibrosis in wt and Hfe KO SWR mice

Masson trichrome staining of wt and Hfe KO SWR mice liver sections at 12 weeks of age showed no positive staining of collagen fibers signifying that no fibrosis had developed in these animals (Fig. 3.3.3).

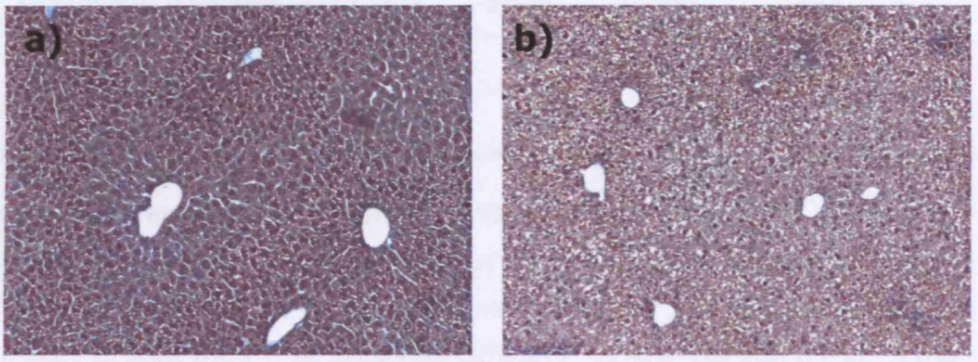

Figure 3.3.3 Hepatic staining of wt and Hfe KO SWR mice for collagen fibers *Liver sections were stained using the Masson trichrome staining protocol. No positive staining for collagen fibers were seen in wt (a) or Hfe KO (b) mice liver sections (x10 OM).*

3.3.3 Hepatic iron content in wt and Hfe KO SWR mice

In SWR wt mice hepatic iron in all the lobes (A-E) ranged from 100 to 290 µg/g dry weight (195.4±47.6µg/g dry weight) while in SWR Hfe KO liver iron levels in lobes B to E iron content levels ranged from 350 to 500 µg/g dry weight (438±15.6µg/g dry weight). Interestingly, lobe A had a significantly higher content of iron than any of the other lobes (821.6±102.8µg/g dry weight) as seen in Fig. 3.3.4.

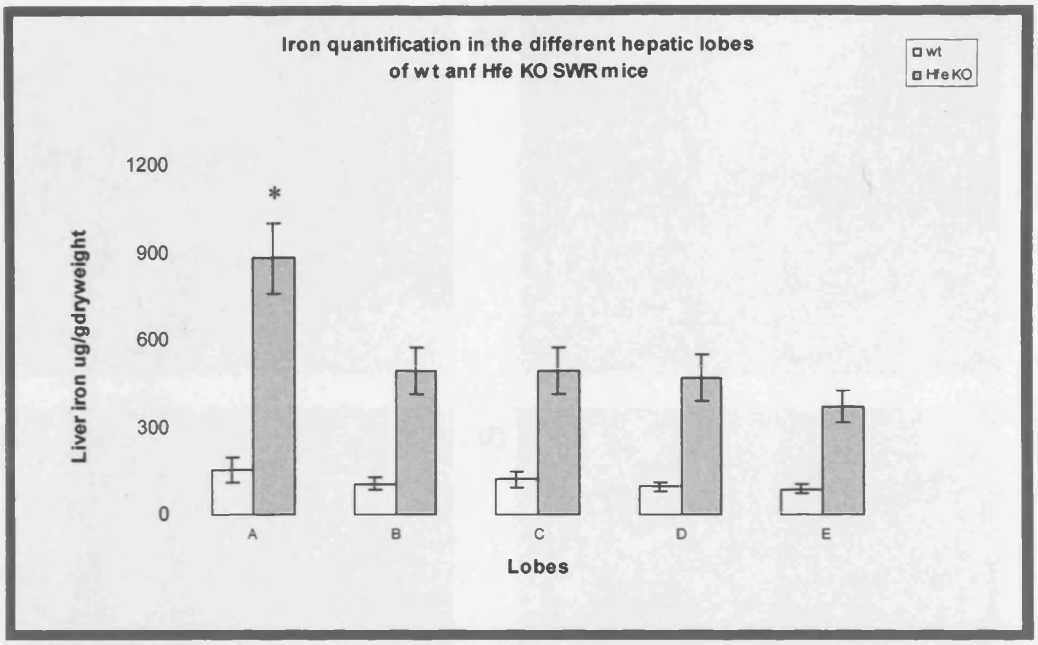

Figure 3.3.4 Iron stores in the different lobes of SWR wt and Hfe KO mouse. *Mouse livers were divided into five lobes and named A to E and non-haem iron determination was performed by a modified Torrance and Bothwell colorimetric method as described in chapter 2. In SWR wt mice there is no significant difference between the iron content levels of the hepatic lobes, however in Hfe KO mice; lobe A has significantly higher iron levels compared to the remaining lobes (B-E). Data is presented as Means±SEM, n=8 per group, *p<0.05.*

3.3.4 Perl's Prussian Blue and haematoxylin and eosin (H&E) staining of spleen sections of SWR wt and Hfe KO mice

Histological staining of spleen sections with Perl's Prussian blue showed that wt SWR mice accumulate iron in the splenic macrophages (Fig. 3.3.5a, b). In contrast Hfe KO mice do not accumulate iron significantly in the spleen (Fig. 3.3.5c).

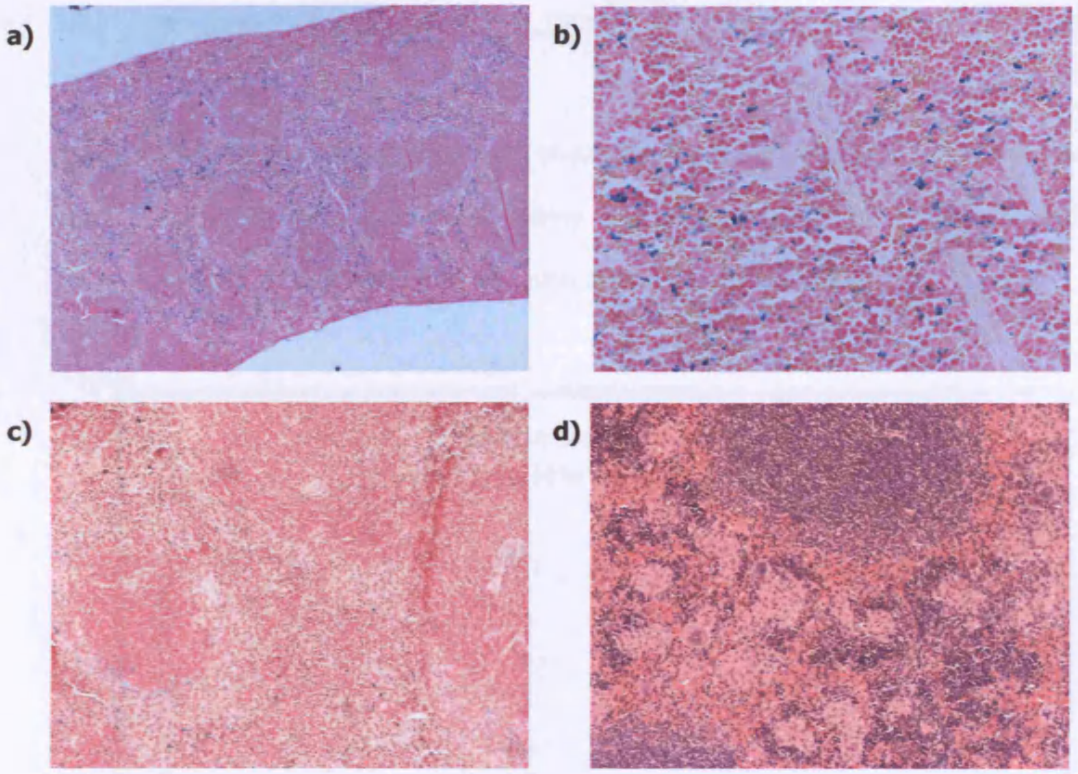

Figure 3.3.5 Histological staining of spleen sections of wt and Hfe KO mice. *Perl's staining of spleen section of wt SWR showed positive staining for iron in the spleen macrophages (a=x10 original magnification (OM), b=x40 OM) while staining of spleen section in Hfe KO SWR mice was generally non-significant (c=x20 OM). A small number of cases of splenomegaly were found in Hfe KO mice, H&E staining showed an enlargement of the white pulp of the spleen in this cases (d=x20 OM).*

Interestingly, a small number of Hfe KO SWR mice were found to have an enlargement of the spleen (splenomegaly) but failed to show any symptoms of the associated pathological characteristics (Fig. 3.3.5d).

3.3.5 Iron content of whole gut, spleen, kidney and pancreas in wt and Hfe KO SWR mice

Quantification of tissue iron in SWR mice showed that Hfe KO mice have higher iron content levels in the whole gut, pancreas and kidney than wt mice (Fig. 3.3.6). Interestingly in the spleen, wt mice had significantly higher levels of iron accumulation than Hfe KO mice.

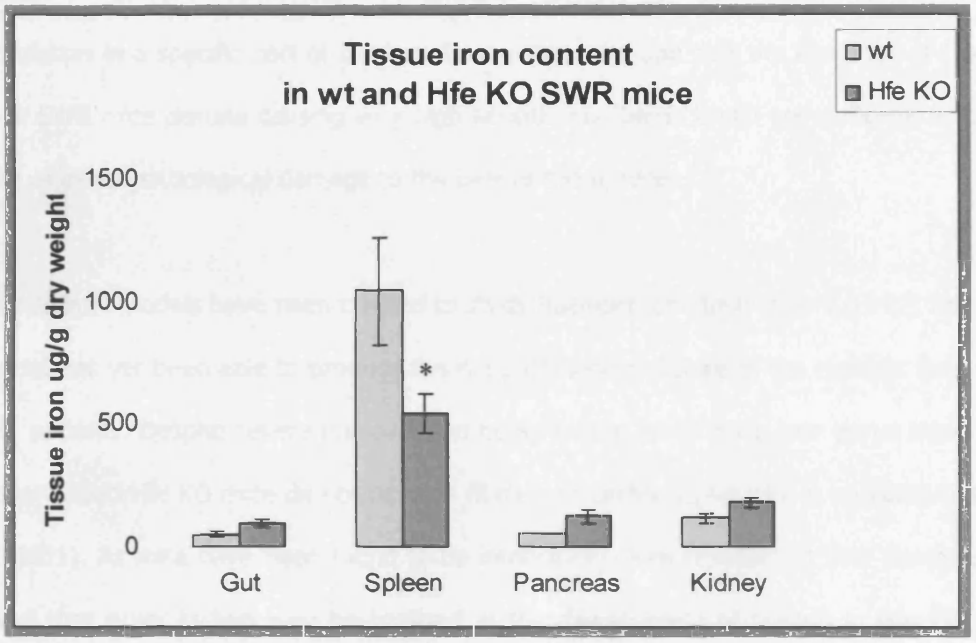

Figure 3.3.6 Iron content in the whole gut, spleen, pancreas and kidney of SWR mice. *Tissues were removed and prepared for iron quantification by a modified Torrance & Bothwell method as described in section 3.2.2. Iron content levels are higher in the gut, pancreas and kidney of Hfe KO mice compared to wt mice. SWR wt mice however accumulate significantly higher levels of iron in the spleen than Hfe KO mice. Data are Mean±SEM, n=5 per group, *p<0.05.*

3.4 Discussion

In this chapter the hepatic iron accumulation of wt SWR mice and a novel haemochromatosis type 1 mouse model, Hfe KO SWR mice, was characterised. Our data shows that in wt SWR mice iron accumulation is evenly distributed between the different hepatic lobes while in SWR Hfe KO mice the hepatic iron accumulation is uneven and patchy within the lobes of the liver. In addition we have shown that the disruption of the Hfe gene causes a preferential accumulation in a specific part of the hepatic caudate lobe and that the knockout of the Hfe gene in SWR mice despite causing very high hepatic iron levels is still not sufficient to cause fibrosis or other pathological damage to the liver of these mice.

Several animal models have been created to study haemochromatosis type 1 (HH1), however no model has yet been able to produce the full pathological picture of the cirrhotic liver seen in HH1 patients. Despite severe iron overload being known to enhance liver tissue injury, the iron overloaded Hfe KO mice do not develop fibrosis or cirrhosis (Arezzini et al. 2003;Knutson et al. 2001). As mice have been found to be intrinsically more resistant to liver damage it is believed that other factors may be involved in the development of fibrosis in Hfe KO mice such as the severity of iron overload or genetic background. The SWR mouse strain has been previously shown to have a higher basal iron status in the liver than other mouse strains (Clothier et al. 2000). We hypothesised that, together with the high levels of iron loading caused by the disruption of the Hfe allele, the hepatic iron accumulation in SWR Hfe KO mice would result in the development of fibrosis.

The present study shows that as previously reported Hfe KO mice like HH1 patients accumulate excess iron in the liver but not in the spleen. HH1 patients have also been found to accumulate iron in the pancreas (Sherlock and Dooley 2002) however, this was not observed in SWR Hfe KO mice. Interestingly here we show that SWR wt mice accumulate significantly higher iron levels in the spleen compared to Hfe KO mice with the site of iron deposition being splenic macrophages. Untreated and severe haemochromatosis in patients often results in an enlarged spleen and this was observed in a small percentage (5%) of SWR

Hfe KO mice in this study. These mice were excluded from the study despite there being no other physiological difference or pathologies such as inflammation observed in these mice.

This study has shown that liver iron content in wt SWR mice is higher (185.8±25.4 µg/g dry weight) than hepatic iron levels seen in other mouse strains such as C57BL/6 (35±4 µg/g dry weight) and DBA/2 (107±9 µg/g dry weight) as previously demonstrated (Clothier 2000). We have also shown that SWR mice liver iron content is 3-fold higher in Hfe KO compared with wild type (wt) mice. In addition we have shown that despite this high increase of hepatic iron observed in Hfe KO mice, SWR mice did not develop fibrosis or any other liver damage pathology due to iron stores suggesting that genetic iron overload does not appear to be sufficient for this pathology.

A literature survey on hepatic iron content of wt and Hfe KO mice of different strains reveals that an array of methods for the quantification of non-haem iron is used and therefore it is difficult to compare the results obtained in this study with previous reports. For this reason the results obtained in this study are only compared to studies describing iron content levels measured using the Torrance & Bothwell method.

In HH1 patients, the pattern of accumulation of iron in the liver has not been fully investigated and so there is no information on iron content levels in the different hepatic lobes. In this study the pattern of iron accumulation in the liver of Hfe KO mice is described for the first time. The presence of ferric iron in the whole liver tissue was analysed by Perl's staining showing that in SWR Hfe KO mice, iron accumulates predominantly in periportal hepatocytes with no staining seen in endothelial cells or in the bile duct similarly to other Hfe KO mice or HH1 patients. Interestingly, despite the periportal iron accumulation, iron content levels within the hepatic lobes were found to be unevenly distributed.

The quantification of the iron stores by the spectrophotometric assay in each lobe not only confirmed the differential distribution of iron in the liver of the SWR Hfe KO mice, but it also showed that lobe A accumulated significantly more iron (821.6±102.8µg/g dry weight) than the remaining lobes (438±15.6µg/g dry weight). Lobe A in the mouse liver corresponds to

the caudate lobe in the human liver. The caudate lobe is also called Spigelius' lobe and is situated upon the posterior surface of the right lobe between the liver and the vena cava. This lobe is composed of three different parts based on the portal blood supply: the first called Spiegel's lobe includes the caudate lobe and papillary process, the second is termed paracaval portion, and the third is called the caudate process. The caudate lobe as a whole (or segment I) is unique in its blood supply and venous drainage in that it receives blood from both the right and left branches of the portal vein and drains directly into the inferior vena cava through the main caudate vein and minor hepatic veins (Kanamura et al. 2001;Kogure et al. 2000).

In the present study, lobe A consists only of Spiegel's lobe (caudate lobe and papillary process) and the paracaval portion of the caudate lobe, while the caudate process, a tail-like strip of liver tissue is here considered to be lobe B. In lobe A, it is not possible to know in which of the two parts (Spiegel lobe or paracaval portion) of the caudate lobe is the one demonstrating particularly high levels of iron accumulation.

Although the iron distribution in HH1 has not been investigated in individual lobes, the differential distribution of iron content in the liver has been reported by Ambu et al when studying non-cirrhotic β-thalassaemic autopsy liver specimens (Ambu et al. 1995) and by Clark et al when studying patients with Thalassaemia Major by MRI (Clark et al. 2003).

In this study, although SWR Hfe KO mice did not develop fibrosis, the finding that the caudate lobe accumulates significantly higher levels of iron might help us start to understand how fibrosis develops in mice. In human patients one imaging sign for diagnosing cirrhosis is the caudate–right lobe ratio (C/RL) (Harbin et al. 1980). When cirrhosis develops it was observed that the right lobe exhibited shrinkage, the caudate lobe undergoes a relative enlargement (Awaya et al. 2002). Measuring the caudate–right lobe ratio (C/RL) using CT, ultrasound, and MRI, has shown to be 94% accurate in diagnosing liver cirrhosis (Harbin et al. 1980;Hess et al. 1989;Honda et al. 1990). One cause of hypertrophy of the caudate lobe and atrophy of the right is thought to be changes in their blood supply. As mentioned before the caudate lobes receives blood from both the right and left branches of the portal vein, and

therefore it receives blood from the entire gastrointestinal tract, while the right lobe receives blood from the right branch of the portal vein only. This differential blood supply might account for the different iron accumulation levels of lobe A compared to the remaining lobes. Other factors such as gene expression of iron transporters might be responsible for this differential iron accumulation between the lobes and this hypothesis will be investigated in chapter 4.

Another reason for the lack of liver tissue damage in SWR Hfe KO mice is that fibrosis is commonly seen in HH1 patients with hepatic iron levels >8000 µg of iron per gram of dry weight (Bassett et al. 1986) and hepatic iron levels in SWR Hfe KO mice levels were not found higher than 4000 µg of iron per gram of dry weight (in lobe A). A recent paper by Asare and colleagues has shown that dietary iron supplementation for 32 months led to hepatocellular cancer in the absence of fibrosis (Asare et al. 2006), suggesting that in order to accurately assess if SWR mice develop fibrosis or hepatocellular cancer as a result of iron, mice would have to be fed an iron loaded diet and their hepatic iron levels would have to be higher than the ones observed in this study. This hypothesis is further investigated in chapter 4.

In conclusion, this study shows that the disruption of the Hfe gene causes a preferential accumulation of iron in the caudate lobe of the SWR mouse liver. Interestingly, the caudate lobe is one of the lobes studied when investigating cirrhosis in HH1 patients and consequently, although SWR Hfe KO did not develop fibrosis or cirrhosis the significantly higher accumulation of iron is this lobe might be of relevance. Overall the data obtained suggests that the SWR Hfe KO mouse is not the ideal and most accurate mouse model for studying HH1. Furthermore our data confirms the findings of Edmond (Edmond et al. 1999) that one measurement of hepatic iron in a single sample results in misleading conclusions and that iron levels obtained this way do not correspond to the actual hepatic iron accumulation levels.

CHAPTER 4

REGULATION OF HEPCIDIN MRNA EXPRESSION LEVELS IN RESPONSE TO:

- **DIETARY IRON, HOLOTRANSFERRIN AND APOTRANSFERRIN IN WT AND HFE KO MICE AND**
- **IRON LOADING AND IRON DEFICIENCY IN HUH7 CELLS AND MOLECULES PRODUCED BY HEREDITARY HAEMOCHROMATOSIS MACROPHAGES**

4.1.1 Regulation of hepcidin mRNA expression levels in response to: dietary iron, holotransferrin and apotransferrin in wt and Hfe KO mice

Hepcidin an antimicrobial peptide is now accepted to be the key negative regulator of iron homeostasis. A detailed description of hepcidin identification and mode of action as a regulator of duodenal iron uptake has been described in section 1.3.4.2. Hepcidin has been found to be upregulated in iron overload conditions and downregulated in iron deficiency conditions such as anaemia. Iron dextran injections and dietary iron supplementation were shown to increase hepcidin levels in mice (Pigeon et al. 2001) and humans (Nemeth et al. 2004b) while in iron deficiency conditions such as anaemia, hepatic hepcidin mRNA levels were found to be downregulated. The low levels of hepcidin expression seen in anaemia remove the inhibitory effects of this peptide on iron absorption and as a result more iron is absorbed and delivered to bone marrow to sustain the erythrocyte production. (Bondi et al. 2005;Latunde-Dada et al. 2004;Nicolas et al. 2002b;O'Riordan et al. 1995;Raja et al. 1990;Vokurka et al. 2006).

No iron responsive elements (IREs) have been found in the hepcidin gene suggesting that the iron status of the body is not signalled through iron regulatory proteins (IRPs), but by other signalling pathways.

The decrease in transferrin saturation during iron deficiency and the increase in iron loading would make it suitable as an indicator of body iron status (Frazer and Anderson 2003). In addition, mice lacking the transferrin (Tf) gene develop anaemia in the presence of iron overload and low expression of hepcidin (Roy et al. 2002). Transferrin (TF) exists in the serum in three forms: diferric TF, monoferric TF, and apotransferrin (Leibman and Aisen 1979). The distribution of iron between diferric TF and monoferric TF is dependent on TF saturation such that a lowering of TF saturation shifts the ratio of the two forms in favor of monoferric TF (Huebers and Finch 1984). All three forms of TF can bind to transferrin receptor 1 (TFR1) at the cell surface, although diferric TF has a higher affinity to TFR1 than monoferric TF and apotransferrin as described in chapter 1. Despite this higher affinity of diferric TF to TFR1 the proportion of iron delivered from monoferric TF increases as TF saturation decreases (Huebers and Finch 1984). Under normal conditions there is sufficient

circulating diferric TF to totally saturate the cell surface TFR1 in the body (Cazzola et al. 1985) and thus the Tf saturation in normal conditions determines the ratio of diferric to monoferric TF that is bound to its receptor at any one time.

A correlation between Hepcidin expression and diferric TF levels (Frazer et al. 2004b;Frazer et al. 2002;Frazer and Anderson 2003) has been reported. Therefore it is plausible that the level of diferric transferrin in the plasma could provide the signal between the body iron requirements and the hepatocytes and consequently the appropriate production of hepcidin.

Several proteins expressed in the liver, such as HFE and transferrin receptor 2 (TFR2), have also been implicated in sensing the body's iron status to signal the production of an appropriate level of hepcidin (Johnson and Enns 2004;Nemeth et al. 2005). In addition, mutations in TfR2, Hfe and hepcidin genes have been found to cause hereditary haemochromatosis with similar iron loading of the liver and low levels of hepcidin expression, suggesting that these molecules act as upstream regulators of hepcidin synthesis.

In the duodenum HFE has been found to competitively inhibit the binding of diferric transferrin to transferrin receptor 1 (TFR1) (Feder et al. 1998;Giannetti and Bjorkman 2004;Lebron and Bjorkman 1999;Parkkila et al. 1997a;Waheed et al. 1999) suggesting that the function of Hfe is to inhibit the uptake of diferric transferrin. This would explain why the disruption of the Hfe gene in HH1 patients results in an inappropriate high uptake of iron. In HH1 patients, however, the crypt enterocytes and reticuloendothelial cells behave as though starved of iron (Andrews 1999;Fleming et al. 1999;Zhou et al. 1998) while hepatocytes of the liver accumulate excess iron. As HFE has been detected in all these cell types (Bastin et al. 1998;Parkkila et al. 1997b) and the exposure of wt HFE to HH1 monocytes in vitro resulted in an accumulation of iron and ferritin (Drakesmith et al. 2002;Montosi et al. 2000), the notion that HFE is a competitive inhibitor of transferrin binding to TFR1 cannot be accepted. Instead the findings suggest that HFE either enhances uptake of iron, as suggested by Waheed and colleagues (Waheed et al. 1999) or inhibits the release of iron from cells (Bastin et al. 1998). A mechanism for the detection of TF saturation by HFE and TFR2 was proposed (Townsend and Drakesmith 2002) with the site of HFE and TFR2 action placed in the crypt cells of the

duodenum and in the macrophages of the reticuloendothelial system but as there is compelling evidence against the direct involvement of the intestinal crypts in the regulation of iron absorption this could not be accepted either. More recently, Frazer & Anderson (Frazer and Anderson 2003) have suggested yet another model this time shifting the site of HFE and TFR2 activity to the liver. Evidence for the important role of Hfe in the liver came from transplantation studies. When iron loaded livers from HH1 patients were transplanted into normal individuals they retained their iron, whereas normal livers grafted into HH1 subjects did not accumulate significant amounts of iron suggesting that the main site of action for the Hfe gene is the liver (McCullen et al. 2002). Besides HFE (Frazer et al. 2001) the liver is also the main site of expression of TFR2 (Kawabata et al. 1999) and Hepcidin (Pigeon et al. 2001) with HFE being expressed mainly in Kupffer cells (Bastin et al. 1998;Parkkila et al. 1997b) and TFR2 and Hepcidin being expressed in hepatocytes (Fleming et al. 2000;Pigeon et al. 2001). HFE has also been shown to be expressed in the hepatocytes (Fleming et al. 2000;Holmstrom et al. 2003;Zhang et al. 2004), sinusoidal lining cells and bile duct epithelial cells in the liver.

In the Frazer & Anderson model of detection of TF saturation by HFE and TFR2, the body iron requirements are detected by the liver as alterations in the ratio of diferric TF to TFR1. This model assumes that diferric TF can outcompete HFE for TFR1 binding and that TFR1 can outcompete TFR2 for diferric TF binding. According to the proposed model, in normal situations the levels of diferric transferrin favours the binding to TFR1; the unbound Hfe on the cell surface and the binding of TFR2 to excess diferric TF upregulates hepcidin expression. In iron deficiency the decreased levels of diferric TF and the increased expression of TFR1 on the cell surface allows Hfe to bind to TFR1. This leads to TFR1 to outcompete TFR2 for diferric TF binding and therefore the signal from HFE and TFR2 to produce hepcidin is decreased. In iron loaded conditions the level of diferric TF is increased and the cell surface TFR1 levels are decreased. This greatly reduces the binding of HFE to TFR1 and allows TFR2 to be fully saturated with diferric TF. This results in an increase in the signal from HFE and TFR2 to produce Hepcidin (Fleming et al. 2000;Frazer and Anderson

2003). In HH1 patients as no HFE exists on the cell surface; the signal to produce Hepcidin does not increase appropriately.

The role of TFR2 sensing the body iron status by sensing the concentration of diferric transferrin also called holotransferrin or iron-saturated transferrin has been reported (Camaschella 2005;Johnson and Enns 2004;Robb and Wessling-Resnick 2004). In hepatocyte-derived cell lines and animal models, increasing concentrations of holotransferrin but not apotransferrin increases TFR2 protein levels (Johnson and Enns 2004;Robb and Wessling-Resnick 2004). In addition it has been reported that the cytoplasmic domain of TfR2 is essential for its stabilization by diferric TF (Chen and Enns 2007;Frazer and Anderson 2003;Johnson and Enns 2004;Robb and Wessling-Resnick 2004).

In this chapter, the effect of iron status on hepcidin 1 expression levels will be investigated by feeding different iron content diets ranging from low to high iron to SWR mice. To investigate whether the response to iron status is regulated by HFE, Hfe KO SWR mice were also investigated for hepatic hepcidin 1 and hepatic iron transporter gene expression. To investigate the effect of transferrin on hepcidin and hepatic iron transporter gene expression levels, SWR mice were injected with human apotransferrin and holotransferrin (diferric TF). These treatments were also performed on Hfe KO mice to investigate the role of Hfe gene in the regulation of Hepcidin by transferrin levels.

4.1.2 Methods

4.1.2.1 Dietary iron studies: iron deficiency and iron supplementation in SWR wt and Hfe KO mice

After being weaned at 3 weeks of age, SWR wild type (wt) and Hfe KO male mice were fed the stated diet ad lib for 9 weeks. At the age of 12 weeks mice were anaesthetised with pentobarbitone sodium (60 mg/kg, i.p.) and sacrificed. Blood was removed by cardiac puncture for serum iron measurements by means of a ferrozine-based assay (Randox Laboratories Ltd. Antrim, UK).

Fresh liver sections were snap frozen in liquid nitrogen and prepared for Real Time PCR as described in section 2.2. Liver samples were also collected for iron quantification by a modified Torrance & Bothwell method (described in section 3.2.2). Iron staining of livers was performed by using Perl's Prussian blue method, using the standard procedures as described in section 3.2.3.1. Experimental procedures were conducted in accordance with the UK animals (Scientific Procedures), Act, 1986. The iron content of diets is shown in table 4.1.2.1.

Diet	**Iron content**
Control Diet (CD)	160 mg iron/Kg
Iron Deficient Diet (IDD)	6 mg iron/Kg
Iron Loaded Diet (ILD)	40g carbonyl iron/Kg

Table 4.1.2.1 Diets used in this study and their iron content

4.1.2.2 Treatment of wt and Hfe KO SWR mice with Apotransferrin and Holotransferrin

Male SWR mice aged 3 weeks were placed on an iron adjusted diet (44 mg of iron/Kg of diet) for 9 weeks. At the age of 12 weeks SWR wt and Hfe KO mice were injected with apotransferrin (4 mg), holotransferrin/diferric transferrin (4 mg) or an equivalent volume of the diluent (saline). After 5 hours mice were anaesthetised with pentobarbitone sodium (60 mg/kg, i.p.) and sacrificed. Blood was removed by cardiac puncture for serum iron and transferrin saturation measurements.

4.1.3 Results

4.1.3.1 Effect of different iron content diets in wt and Hfe KO SWR mice

4.1.3.1.1 Changes in serum iron, transferrin saturation and liver iron content in wt and Hfe KO mice fed on diets containing variable amounts of iron

4.1.3.1.1.1 Serum iron and transferrin saturation levels in wt and Hfe KO mice fed different iron content diets

When fed on normal diet (OD), IDD or ILD, serum total iron levels are higher in Hfe KO SWR mice than in wt SWR mice (Table 4.1.3.1). Iron deficiency diet did not have a significant effect on serum iron levels or transferrin saturation in wt mice. In Hfe KO mice iron deficient diet increased transferrin saturation significantly despite having no significant effect on serum iron levels.

		Control Diet (CD)	Iron deficient diet (IDD)	Iron loaded diet (ILD)
wt	***Serum total iron (µmol/L)***	182.8±14.2 (8)	160.0±21.1 (4)	445.8±52.3 § (4)
	Transferrin Saturation (%)	78.8±2.8 (6)	75.3±5.0 (4)	93.8±1.7 $^{\S,\beta}$ (5)
Hfe KO	***Serum total iron (µmol/L)***	265.4±20.5$^{\alpha}$ (20)	208.4±49.0 (5)	630.3±38.0 $^{\alpha,\S}$(4)
	Transferrin Saturation (%)	84.9±1.9 (7)	91.4±3.6$^{\alpha}$ (4)	88.5±4.5 (4)

Table 4.1.3.1 Total serum iron in SWR wt and Hfe KO mice after being fed different iron content diets. *SWR mice wt and Hfe KO mice were fed the described diets for 9 weeks after weaning. Mice were culled at 12 weeks of age and blood was removed for haematological parameters by cardiac puncture.* $^{\alpha}$ *Denotes a statistical significance of $p<0.05$ between serum iron levels/transferrin saturation of wt and Hfe KO SWR mice fed the same diet,* $^{\beta}$ *denotes a statistical significance of $p<0.01$ between transferrin saturation in wt SWR mice fed CD and ILD,* § *denotes a statistical significance of $p<0.05$ between serum iron/transferrin saturation levels in SWR mice fed CD and ILD. Data are Means±SEM, number of samples analysed per group shown in brackets.*

ILD in wt mice increased significantly the serum iron levels and transferrin saturation. In Hfe KO mice however, ILD increased significantly serum iron levels but had no effect on transferrin saturation.

4.1.3.1.1.2 Liver iron concentration in wt and Hfe KO mice fed different iron content diets

As described in chapter 3, SWR Hfe KO mice have significantly higher hepatic iron content than wt SWR mice. When SWR mice were fed on an iron deficient diet (IDD) for 9 weeks after weaning both wt and Hfe KO mice showed a decreased in iron content in the whole liver (Fig. 4.1.3.1). SWR wt and Hfe KO mice fed an iron loaded diet (ILD) for 9 weeks showed a significant increase in the total liver iron content.

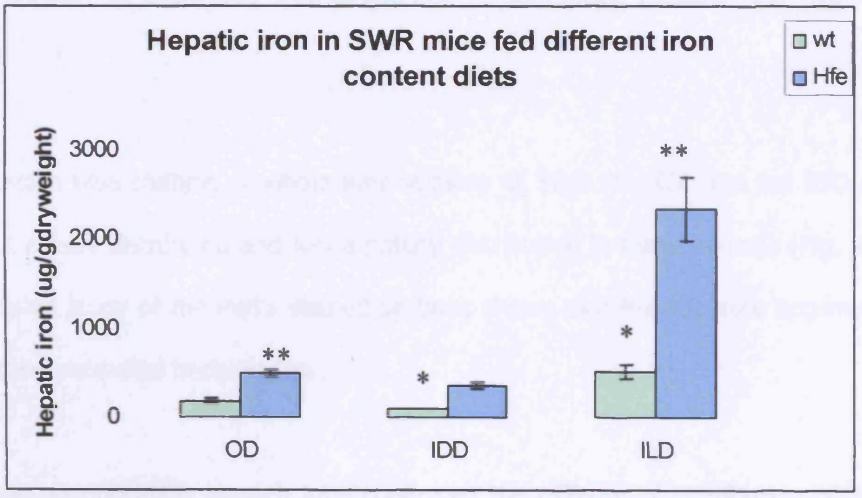

Figure 4.1.3.1 Hepatic iron content in SWR mice fed different diets

*SWR wt and Hfe KO mice were fed either an iron deficient diet (IDD) or an iron loaded diet (ILD) for 9 weeks after weaning. The whole liver was removed and divided into five lobes. Iron was quantified in each lobe and the average of the iron content in each whole liver was calculated. Hepatic iron content decreased by iron deficient diet and increased by iron loaded diet in wt and Hfe KO mice. Data are Mean±SEM, n=4 per group, *p<0.05, **p<0.005.*

4.1.3.1.1.3 Prussian blue iron staining and pattern of iron accumulation in the liver of wt and Hfe KO mice fed different iron content diets

Prussian staining and iron quantification in each lobe showed that SWR wt mice fed on normal iron content diet (CD) have an even distribution of iron between the hepatic lobes as mentioned in chapter 3. Interestingly in Hfe KO mice iron is not uniformly distributed and has a patchy distribution. Iron stores quantification of each lobe confirmed this differential distribution of iron in the liver, and showed that a specific lobe, named A has significantly higher levels of iron than the rest of the lobes (described in chapter 3).

SWR mice were fed an iron deficient diet (IDD) for 9 weeks after weaning. Using Perl's Prussian blue method wt SWR mice hepatic sections showed no positive staining and when the iron content of each lobe was quantified, no difference between the five lobes was observed.

Perl's Prussian blue staining of whole liver sections of SWR Hfe KO mice fed IDD show that iron is not evenly distributed and has a patchy distribution in these animals (Fig. 4.1.3.2). A more detailed study of the Perl's stained sections shows that Hfe KO mice accumulated iron mainly at the periportal hepatocytes.

Iron stores quantification in each lobe confirmed the differential distribution of iron in the liver of SWR Hfe KO mice, and showed that lobe A again, had significantly higher levels of iron than the rest of the lobes (Fig. 4.1.3.3).

Figure 4.1.3.2 Representative section of a whole liver of Hfe KO SWR mice fed on IDD. *SWR Hfe KO mice were fed on an IDD diet containing 6 mg iron/kg for 9 weeks after weaning. Whole liver sections were stained by Perl's Prussian blue method. The distribution of iron between the different lobes was found to be patchy and uneven (original size).*

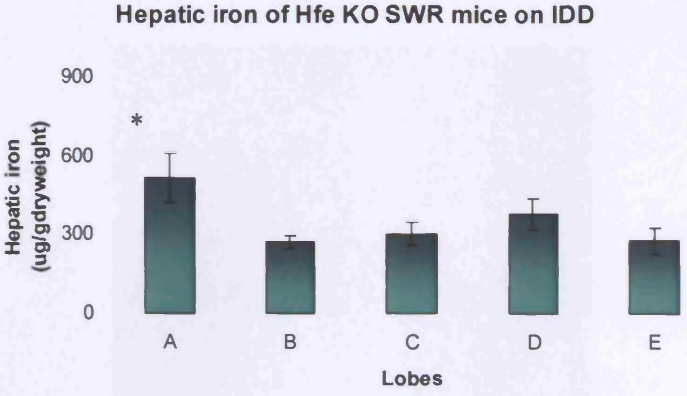

Figure 4.1.3.3 Iron stores in the different lobes of Hfe KO SWR mice fed IDD. *The whole liver was removed, divided into five lobes and iron was quantified in each lobe as previously described. In SWR Hfe KO mice hepatic iron content in lobe A was significantly different to the rest of the lobes (B-E) (*p<0.05). Data is presented as Means±SEM, n=5 per group.*

SWR mice were also fed an iron loaded diet (ILD) containing 40g carbonyl iron/kg. When SWR wt mice were fed a high iron diet, although there was a greater accumulation of iron in the liver, no differences were seen between the different lobes. This result was confirmed by staining a whole liver section with Perl's Prussian blue staining (Fig. 4.1.3.4). On a higher magnification, iron deposition in SWR wt mice fed ILD was predominantly observed in periportal hepatocytes. When SWR Hfe KO mice were fed on ILD no difference in iron content between the five lobes was observed.

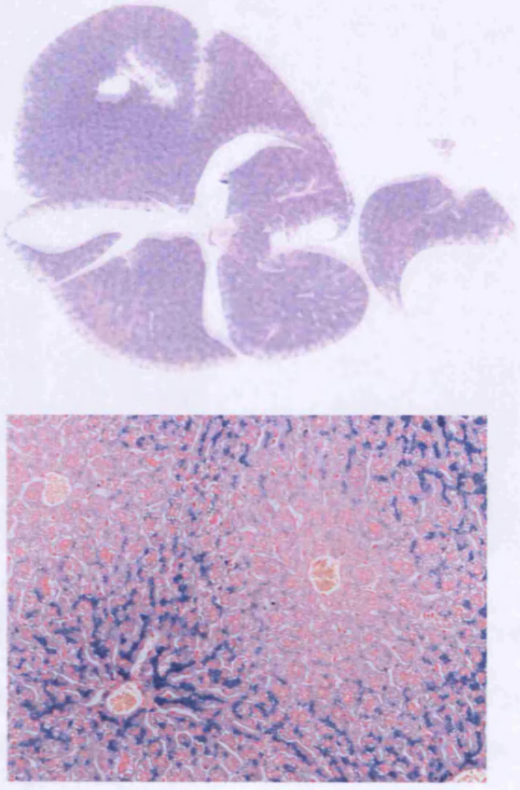

Figure 4.1.3.4 Perl's staining of wt SWR mice fed on ILD. *SWR wt mice were fed on an ILD diet for 9 weeks after weaning. Whole liver sections were stained by Perl's Prussian blue method. Representative section of a wt mice fed ILD shows no difference in the distribution of iron between the lobes (a= original size). On higher power, iron is seen predominantly in periportal hepatocytes (b= x20 OM).*

Duodenum sections of SWR wt and Hfe KO mice fed ILD were also analysed. Perl's Prussian blue staining showed that wt mice fed ILD accumulate more iron in the intestinal villus than Hfe KO mice on a normal diet (Fig. 4.1.3.5).

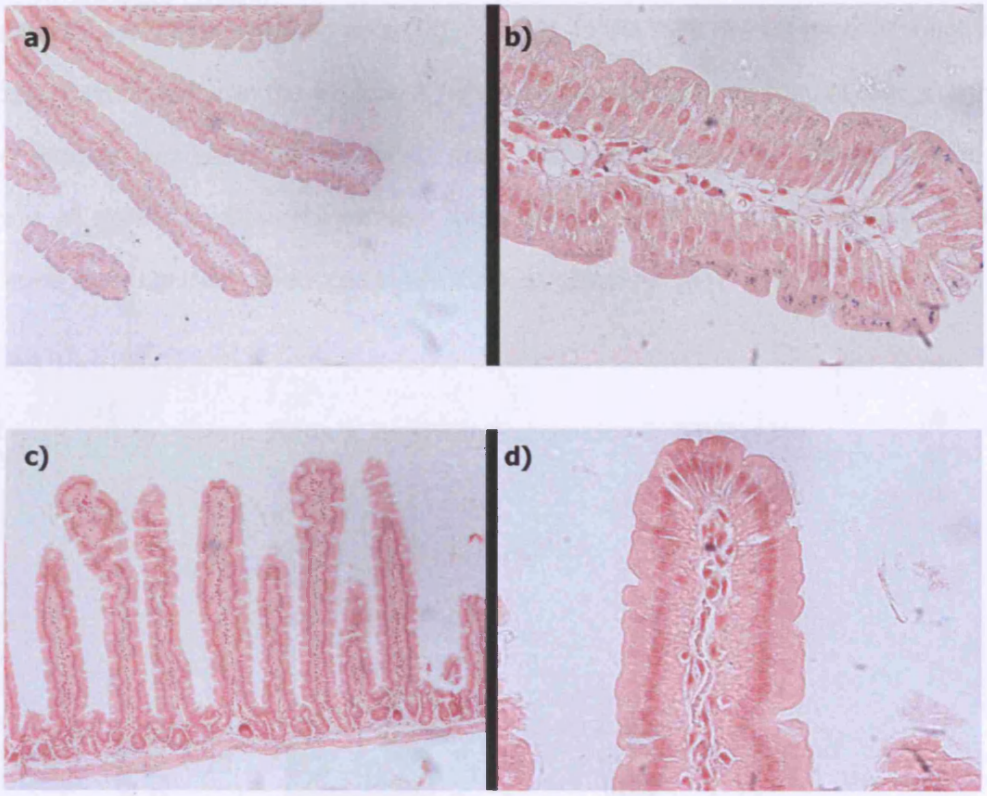

Figure 4.1.5 Perl's staining of duodenum sections of wt and Hfe KO mice.

The villus of wt SWR mice fed ILD (a=x10 OM; b=x20 OM) showed positive staining for ferric iron while Hfe KO (c=x10 OM; d=x20 OM) fed a normal diet shown no positive staining for iron in the duodenum.

4.1.3.1.2 Hepatic hepcidin 1, DMT1 and Ireg1 gene expression in wt and Hfe KO SWR fed on control diet (CD)

Analysis of hepcidin 1 gene expression levels showed no significant difference between the different lobes in the SWR wt mice (Fig. 4.1.3.6). In the SWR Hfe KO mice, although hepcidin levels were lower than the wt, lobe A (which had the highest iron content) had a higher level of hepcidin expression but this did not reach statistical significance. Although in lobe A there was no significant difference between wild type and Hfe KO mice in all other lobes, hepcidin levels were significantly reduced in Hfe KO mice compared to wt mice.

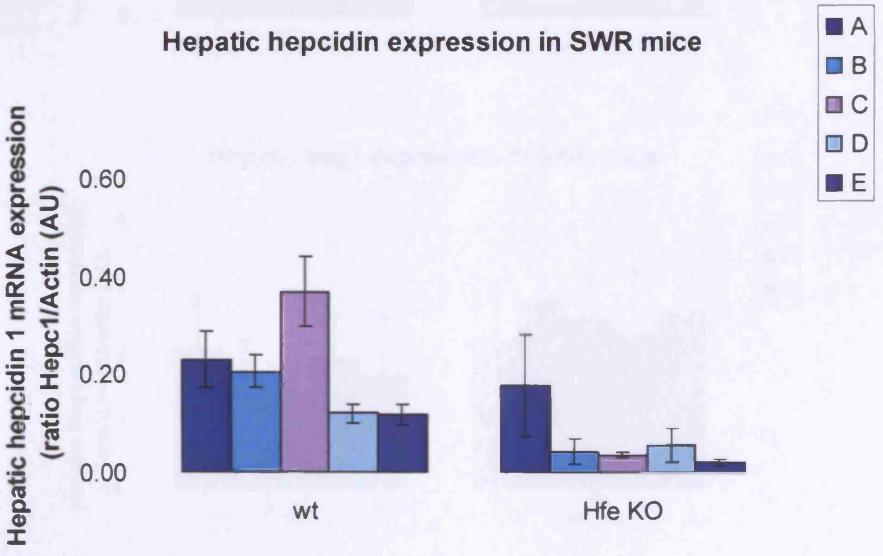

Figure 4.1.3.6 Hepatic hepcidin 1 mRNA expression in SWR mice

SWR mice fed on control diet (CD) were sacrificed at 12 weeks of age. Hepatic hepcidin expression levels were analysed by Real Time PCR. Although hepcidin levels were lower in Hfe KO mice this did not reach statistical significance. Data are Mean±SEM, n=8.

Hepatic DMT1 and Ireg1 mRNA expression was also analysed in wt and Hfe KO mice. No overall difference was found between hepatic DMT1 expression levels of wt and Hfe KO SWR mice. When each lobe was analysed for DMT1 levels, once again no difference was seen

between each lobe in wt mice (Fig. 4.1.3.7a). In Hfe KO mice, lobe C was found to have significant higher mRNA expression levels of DMT1 due a small number of samples of Hfe KO mice lobe C having high DMT1 expression levels.

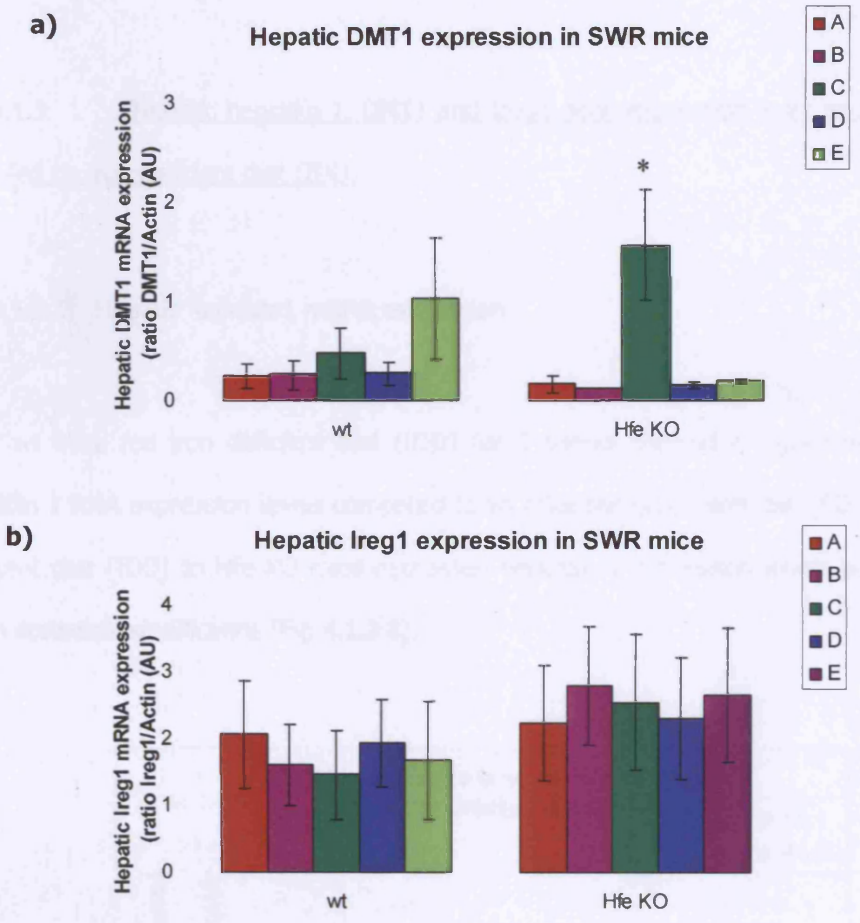

Figure 4.1.7 Hepatic iron transporter mRNA expression in SWR mice

SWR mice fed on control diet (CD) were sacrificed at 12 weeks of age. Hepatic DMT1 (a) and Ireg1 (b) expression levels were analysed by Real Time PCR. No difference between Ireg1 expression in wt and Hfe KO mice was observed. In addition, no difference was seen between Ireg1 levels of the five lobes in both wt and Hfe KO SWR mice. Data are Mean±SEM, n=8.

Hepatic Ireg1 expression levels were not different in wt and Hfe KO mice and in both of these mice (Fig. 4.1.3.7b), no difference between each lobe was found regarding Ireg1 mRNA expression levels.

4.1.3.1.3 Hepatic hepcidin 1, DMT1 and Ireg1 gene expression in wt and Hfe KO SWR mice fed on iron deficient diet (IDD)

4.1.3.1.3.1 Hepatic hepcidin1 mRNA expression

SWR wt mice fed iron deficient diet (IDD) for 9 weeks showed a significant decrease in hepcidin 1 RNA expression levels compared to wt mice fed on control diet (CD). Feeding iron deficient diet (IDD) to Hfe KO mice decreased hepcidin 1 expression levels but this did not reach statistical significance (Fig 4.1.3.8).

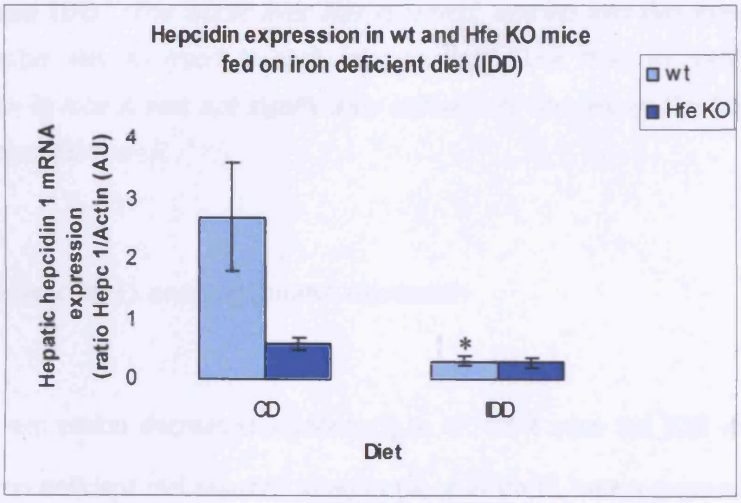

Figure 4.1.3.8 Hepcidin expression in SWR mice fed iron deficient diet (IDD). *SWR mice fed on IDD for 9 weeks were sacrificed at 12 weeks of age. Hepatic hepcidin expression levels were analysed by Real Time PCR. In wt SWR IDD leads to a significant decrease in hepcidin mRNA expression levels while in Hfe KO mice IDD did not have a significant effect on hepcidin expression. Data are Mean±SEM, n=5.*

Hepcidin mRNA expression levels were also analysed in each lobe. In wt SWR mice fed IDD no difference between hepcidin expression levels was observed in the five hepatic lobes. In Hfe KO mice although lobe A shows a higher expression level of hepcidin this failed to reach statistical significance and therefore no significant difference was observed between the hepcidin mRNA expression levels in the hepatic lobes (Fig. 4.1.3.9).

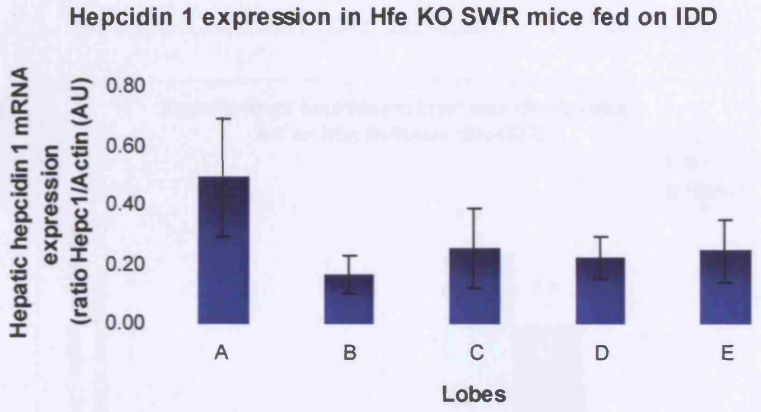

Figure 4.1.3.9 Hepcidin expression in the different lobes of Hfe KO SWR mice fed IDD. *The whole liver was removed, divided into five lobes and hepcidin expression was analysed in each lobe by Real Time PCR. In SWR Hfe KO mice hepcidin in lobe A was not significantly different to the rest of the lobes (B-E). Data are Mean±SEM, n=5.*

4.1.3.1.3.2 Hepatic DMT1 and Ireg1 mRNA expression

Hepatic DMT1 expression decreased significantly in wt SWR mice fed IDD while in Hfe KO mice feeding iron deficient diet resulted in an increase in DMT1 mRNA expression levels (Fig. 4.1.3.10a).

a)

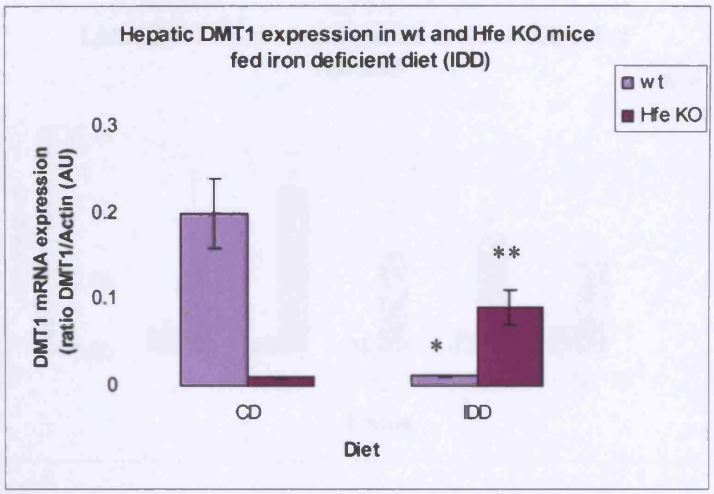

b)

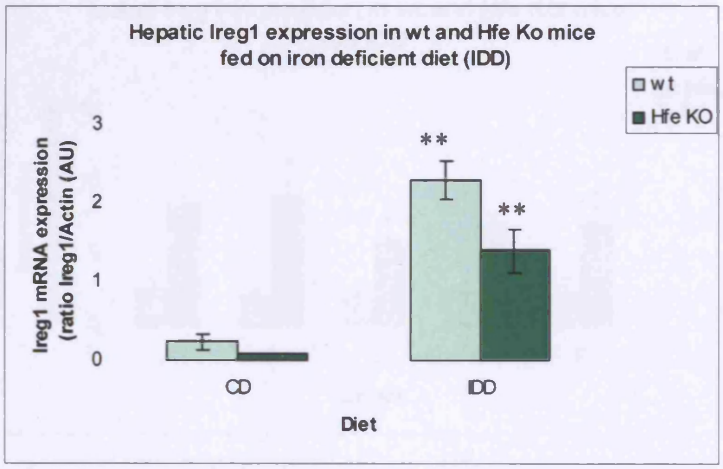

Figure 4.1.3.10 Hepatic iron transporter genes expression in SWR mice fed iron deficient diet (IDD). *SWR mice fed on IDD for 9 weeks were sacrificed at 12 weeks of age. Hepatic DMT1 and Ireg1 expression levels were analysed by Real Time PCR. In SWR mice IDD results in a significant increase in DMT1 and Ireg1 mRNA expression levels. Data are Mean±SEM, n=5, *p<0.05, **P<0.01.*

Feeding wt and in Hfe KO SWR mice an iron deficiency diet for 9 weeks upregulated hepatic Ireg1 mRNA expression levels significantly (Fig. 4.1.3.10b).

a)

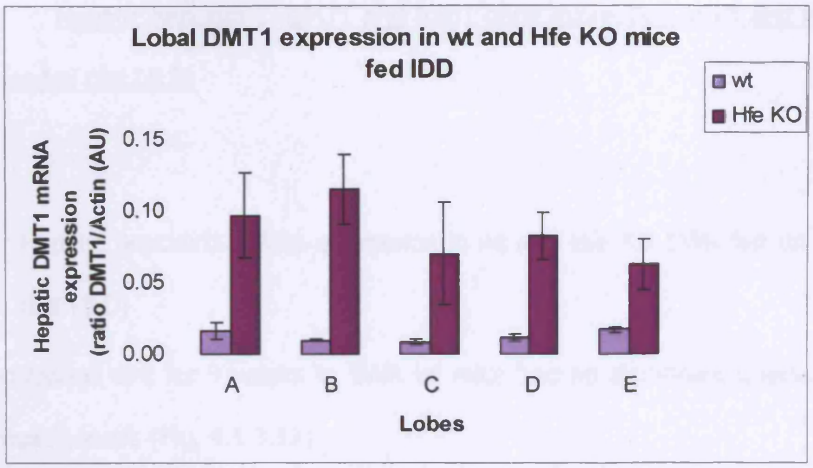

b)

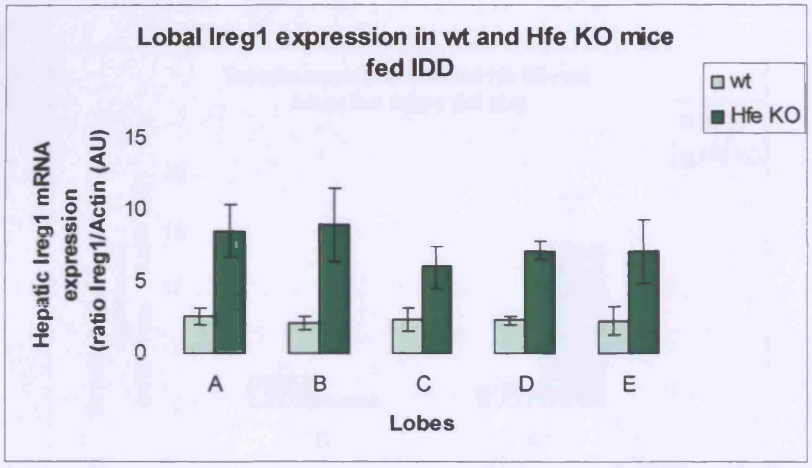

Figure 4.1.3.11 Hepatic DMT1 and Ireg1 expression in the different lobes of wt and Hfe KO SWR mice fed IDD. *The whole liver was removed, divided into five lobes and DMT1 and Ireg1 expression was analysed in each lobe by Real Time PCR. No difference was observed between the mRNA expression levels of DMT1 and Ireg1 in the five lobes. Data are Mean±SEM, n=5.*

Analysis of DMT1 expression in each lobe of the liver showed no differences in mRNA expression levels of the iron transporter in wt and Hfe KO SWR mice (Fig. 4.1.3.11a). There was also no difference in Ireg1 mRNA expression levels in the different lobes in wt and Hfe KO mice (Fig. 4.1.3.11b).

4.1.3.1.4 Hepatic hepcidin 1, DMT1 and Ireg1 gene expression in wt and Hfe KO SWR fed on iron loaded diet (ILD)

4.1.3.1.4.1 Hepatic hepcidin1 mRNA expression in wt and Hfe KO SWR fed on iron loaded diet (ILD)

Feeding iron loaded diet for 9 weeks to SWR wt mice had no significant effect on hepcidin mRNA expression levels (Fig. 4.1.3.12).

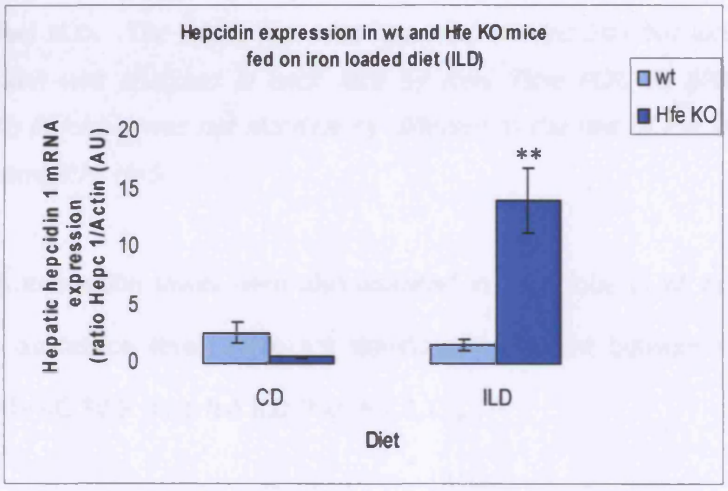

Figure 4.1.3.12 Hepcidin expression in SWR mice fed iron loaded diet (ILD). *SWR mice fed on ILD for 9 weeks were sacrificed at 12 weeks of age. Hepatic hepcidin expression levels were analysed by Real Time PCR. In wt SWR ILD had no significant effect on hepcidin expression whereas in Hfe KO mice iron loaded diet up regulated significantly hepcidin mRNA expression levels. Data are Mean±SEM, n=5, **p<0.01.*

In contrast Hfe KO mice fed an iron loaded diet showed a significant increased in hepcidin mRNA expression levels (Fig. 4.1.3.12).

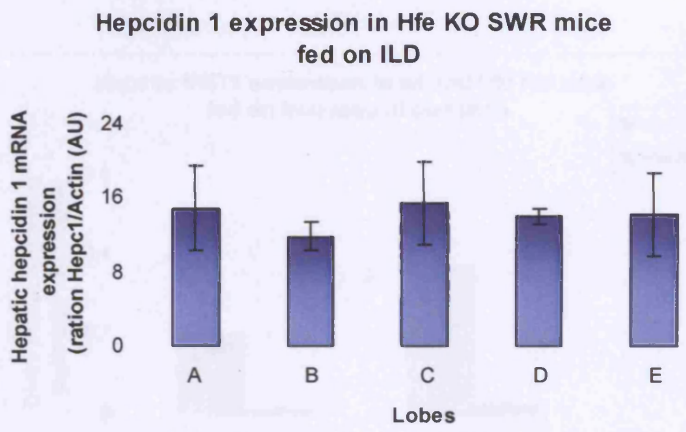

Figure 4.1.3.13 Hepcidin expression in the different lobes of Hfe KO SWR mice fed ILD. *The whole liver was removed, divided into five lobes and hepcidin expression was analysed in each lobe by Real Time PCR. In SWR Hfe KO mice hepcidin in lobe A was not significantly different to the rest of the lobes (B-E). Data are Mean±SEM, n=5.*

Hepcidin mRNA expression levels were also analysed in each lobe in wt and Hfe KO SWR mice. Hepcidin expression levels were not significantly different between the five hepatic lobes in wt or Hfe KO SWR mice fed ILD (Fig. 4.1.3.13).

4.1.3.1.4.2 Hepatic DMT1 and Ireg1 mRNA expression

Hepatic DMT1 expression significantly increased in wt SWR mice fed ILD (Fig. 4.1.3.14a) but feeding Hfe KO mice on an iron loaded diet had no effect on DMT1 expression levels.

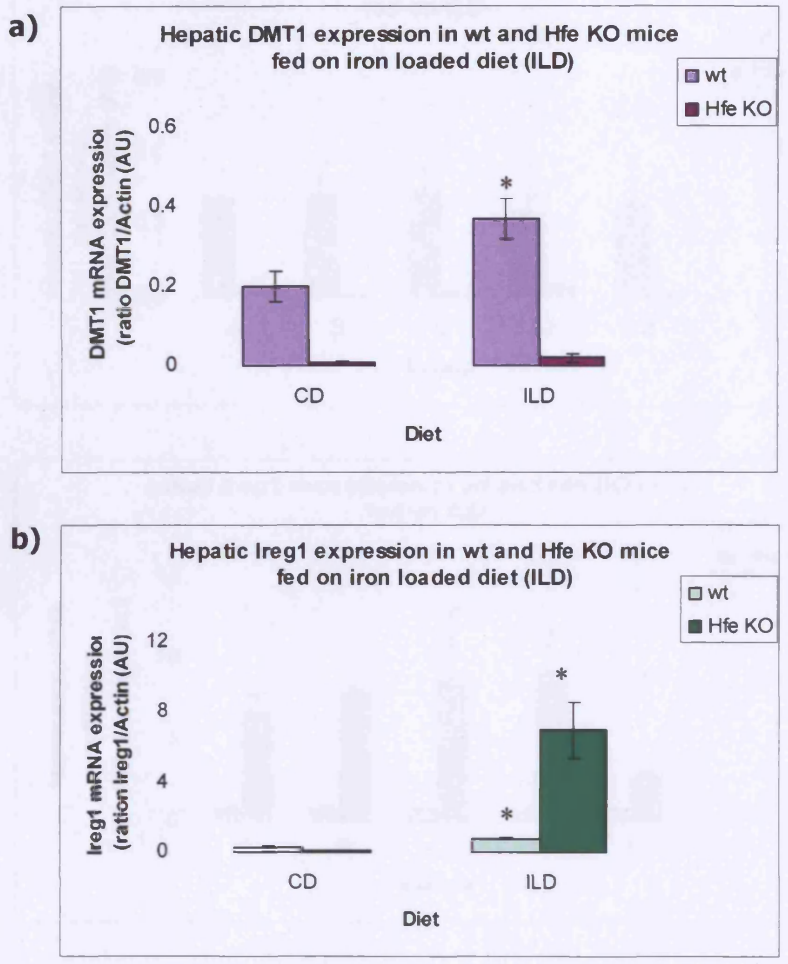

Figure 4.1.3.14 Hepatic iron transporter genes expression in SWR mice fed iron loaded diet (ILD). *SWR mice fed on ILD for 9 weeks were sacrificed at 12 weeks of age. Hepatic DMT1 (a) and Ireg1 (b) expression levels were analysed by Real Time PCR. In SWR mice ILD results in a significant increase in DMT1 and Ireg1 mRNA expression levels. Data are Means±SEM, n=5, *p<0.05.*

In SWR wt mice hepatic Ireg1 mRNA expression levels did not change significantly with iron loading while in Hfe KO mice, Ireg1 expression levels increased significantly with ILD (Fig. 4.1.3.14b).

a)

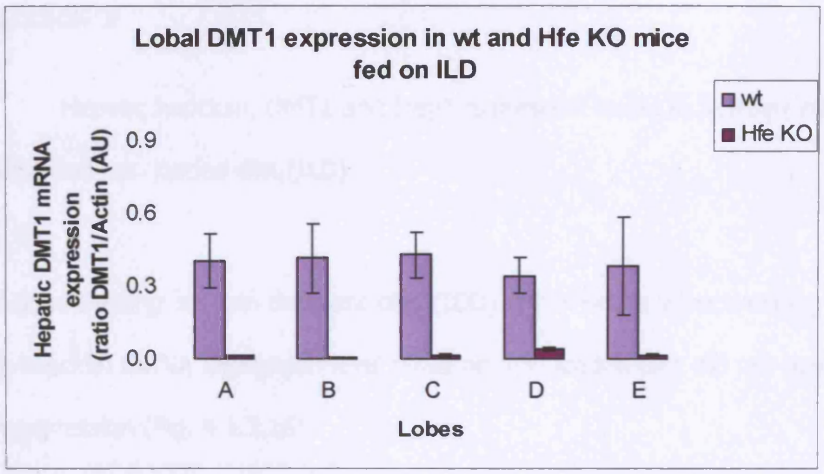

b)

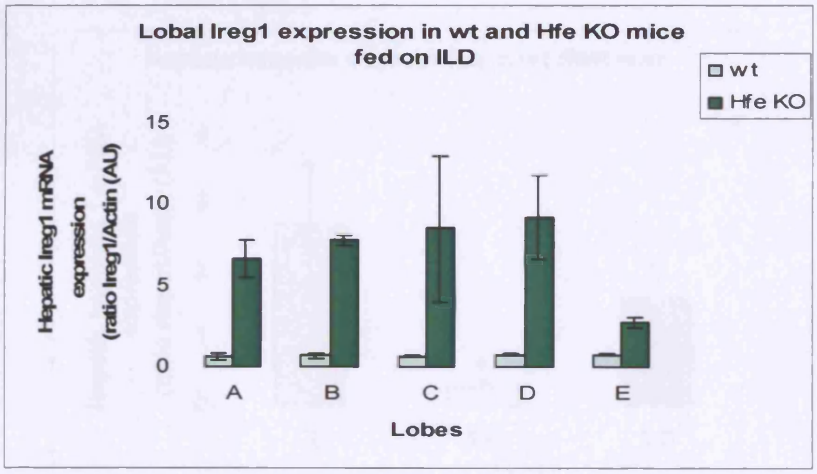

Figure 4.1.3.15 Hepatic DMT1 and Ireg1 expression in the different lobes of wt and Hfe KO SWR mice fed ILD. *The whole liver was removed, divided into five lobes and DMT1 (a) and Ireg1 (b) expression was analysed in each lobe by Real Time PCR. No difference was observed between the mRNA expression levels of DMT1 and Ireg1 in the five lobes. Data are Mean±SEM, n=5.*

When hepatic DMT1 and Ireg1 expression levels were analysed in each lobe of the liver, no difference was found on expression levels of either iron transporter in wt or Hfe KO SWR mice (Fig. 4.1.3.15).

4.1.3.2 Conclusions

4.1.3.2.1 Hepatic hepcidin, DMT1 and Ireg1 expression levels in SWR wt mice fed iron deficient (IDD) and iron loaded diet (ILD)

In SWR wt mice feeding an iron deficient diet (IDD) for 9 weeks after weaning decreased significantly hepcidin mRNA expression level while an iron loaded diet did not have an effect on hepcidin expression (Fig. 4.1.3.16).

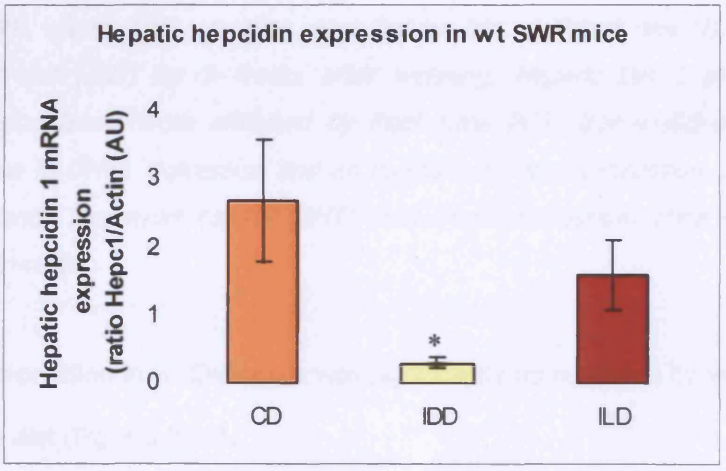

Figure 4.1.3.16 Dietary iron and hepcidin expression in wt SWR mice

*SWR wt mice were fed an iron deficient diet (IDD) and an iron loaded diet (ILD) for 9 weeks after weaning. Hepcidin 1 mRNA expression levels were analysed by Real Time PCR. IDD led to a significant decrease (*p<0.05) while ILD had no effect on hepcidin expression levels. Data are Mean±SEM, n=6.*

Iron deficient diet decreased significantly DMT1 expression in the liver of wt mice whereas iron loaded diet resulted in a significant increase in DMT1 mRNA expression levels in these mice (Fig. 4.1.3.17).

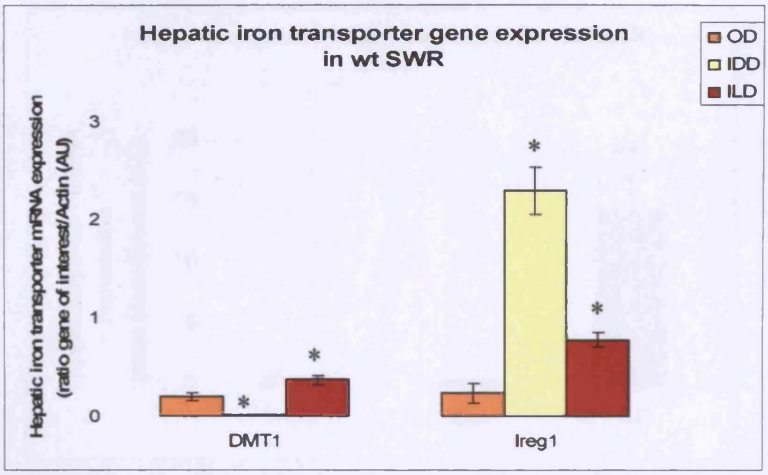

Figure 4.1.3.17 Effect of dietary iron in iron transporter gene expression in wt SWR mice. *SWR wt mice were fed an iron deficient diet (IDD) and an iron loaded diet (ILD) for 9 weeks after weaning. Hepatic DMT1 and Ireg1 mRNA expression levels were analysed by Real Time PCR. Iron deficient diet led to a decrease in DMT1 expression and an increase in Ireg1 expression. Iron loaded diet significantly increased hepatic DMT1 and Ireg1 expression. Data are Mean±SEM, n=6, *p<0.05.*

Hepatic Ireg1 expression in wt SWR mice was significantly up regulated by iron deficient diet and iron loaded diet (Fig. 4.1.3.17).

4.1.3.2.2 Hepatic hepcidin, DMT1 and Ireg1 expression levels in SWR Hfe KO mice fed iron deficient (IDD) and iron loaded diet (ILD)

In Hfe KO SWR mice, feeding an iron deficient diet did not have an effect on hepcidin expression levels whereas feeding an iron loaded diet resulted in a significant increase in hepcidin mRNA expression levels (Fig. 4.1.3.18).

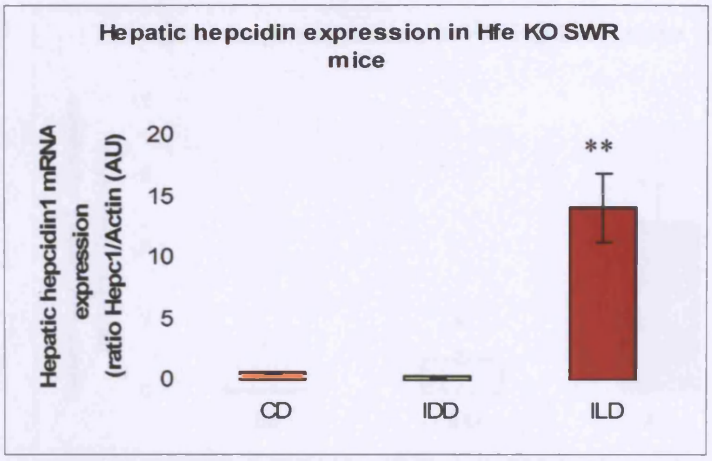

Figure 4.1.3.18 Dietary iron and hepcidin expression in Hfe KO SWR mice. *SWR Hfe KO mice were fed an iron deficient diet (IDD) and an iron loaded diet (ILD) for 9 weeks after weaning. Hepcidin 1 mRNA expression levels were analysed by Real Time PCR. ILD led to a significant increase (**p<0.001) while IDD had no effect on hepcidin expression levels. Data are Mean±SEM, n=6.*

Hepatic DMT1 expression levels were increased significantly when Hfe KO mice were fed on an iron deficient diet while an iron loaded diet did not have an effect on DMT1 expression (Fig. 4.1.3.19a). Feeding iron deficient and iron loaded diet increased hepatic Ireg1 expression levels in Hfe KO SWR mice (Fig. 4.1.3.19b).

a)

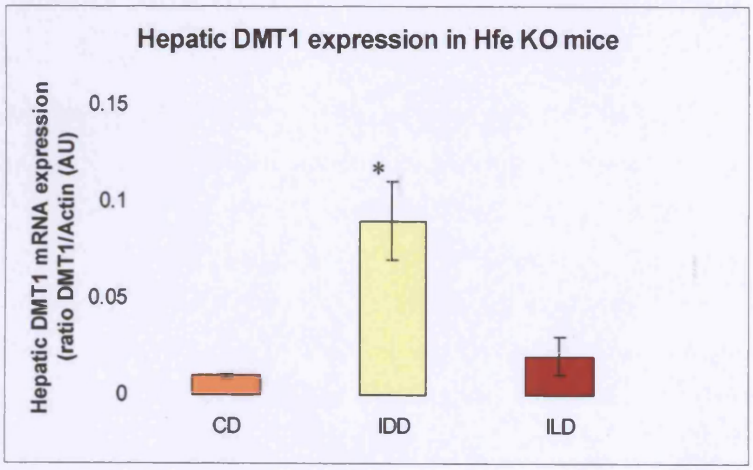

b)

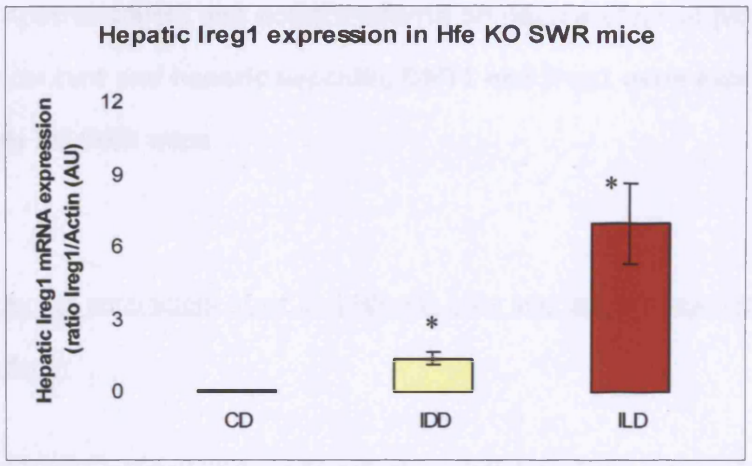

Figure 4.1.3.19 Effect of dietary iron on iron transporter gene expression in Hfe KO mice. *SWR Hfe KO mice were fed an iron deficient diet (IDD) and an iron loaded diet (ILD) for 9 weeks after weaning. Hepatic DMT1 and Ireg1 mRNA expression levels were analysed by Real Time PCR. An iron deficient diet increased significantly DMT1 expression levels while an iron loaded diet had no effect on hepatic DMT1 expression. Hepatic Ireg1 levels were increased significantly by IDD and ILD (*p<0.05). Data are Mean±SEM, n=6.*

4.2.1 Effect of Apotransferrin and holotransferrin on haematological parameters, liver iron content and hepatic hepcidin, DMT1 and Ireg1 gene expression in wt and Hfe KO SWR mice

4.2.1.1 Haematological parameters of wt and Hfe KO mice injected with apotransferrin or holotransferrin

SWR wt and Hfe KO mice injected with apotransferrin or holotransferrin were culled after 4 hours. Serum iron levels in saline-treated Hfe KO SWR mice were higher than the ones seen in saline-treated wt SWR animals (wt 178.6±5.3; Hfe KO 216.6±27.4, n=4 per group) though not significantly while transferrin saturation was not different between wt and Hfe KO mice. Serum total iron and transferrin saturation did not change significantly in wt or Hfe KO mice following treatment with apotransferrin or holotransferrin (Table 4.2.1).

		CONTROL	APOTRANSFERRIN	HOLOTRANSFERRIN
wt	***Serum total iron (µmol/L)***	178.6±5.3 (4)	280.7±24.4 (3)	187.3±38.0 (5)
	Transferrin Saturation (%)	88.0±3.8 (4)	84.9±4.5 (3)	73.9±4.2 (5)
Hfe KO	***Serum total iron (µmol/L)***	216.6±27.4 (4)	308.6±2.0 (3)	264.7±21.8 (7)
	Transferrin Saturation (%)	84.9±3.6 (4)	86.6±3.6 (3)	82.6±3.4 (4)

Table 4.2.1 Serum total iron and transferrin saturation in wt and Hfe KO SWR mice treated with saline (controls), apotransferrin or holotransferrin. *SWR mice were injected at 12 weeks of age with apotransferrin (4 mg), holotransferrin/diferric transferrin (4 mg) or the equivalent volume of the diluent (saline). Mice were culled 4 hours later and blood was used for haematological parameters. No significant change in serum iron or transferrin saturation was found in animals injected with apotransferrin or holotransferrin. Data are Mean±SEM, with the number of samples analysed shown in brackets.*

4.2.1.2 Liver iron content in wt and Hfe KO SWR mice injected with apotransferrin and holotransferrin

Injection with apotransferrin or holotransferrin had no significant effect on the hepatic iron content of wt or Hfe KO SWR mice (Fig. 4.2.1).

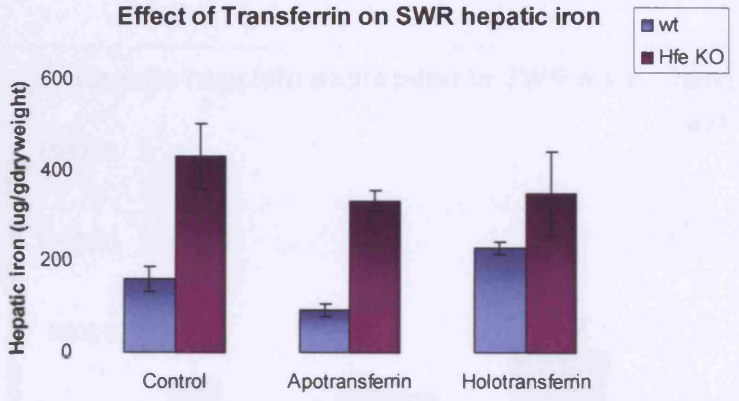

Figure 4.2.1 Hepatic iron content in response to apotransferrin and holotransferrin injections. *SWR wt and Hfe KO mice were injected with either saline (Control), Apotransferrin or Holotransferrin. Animals were culled after 4 hours and hepatic iron content was quantified by modified Torrance & Bothwell method. There was no significant change in hepatic iron content after injections in wt or Hfe KO SWR mice. Data are Mean±SEM, n=5.*

4.2.1.3 Hepatic Hepcidin 1 gene expression in wt and Hfe KO SWR mice injected with apotransferrin and holotransferrin

Hepatic hepcidin 1 in saline treated animals was found to be lower in Hfe KO mice compared to controls (Fig. 4.2.2). Injection of apotransferrin and holotransferrin was found to have no effect on hepcidin expression in either wt or Hfe KO mice.

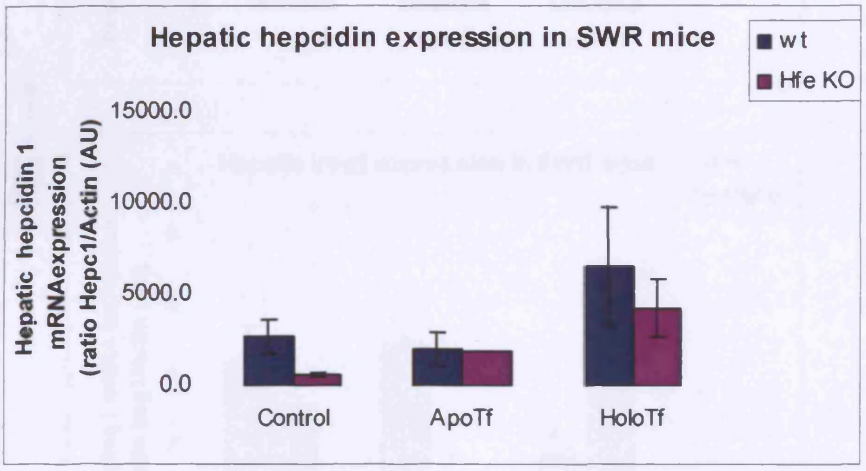

Figure 4.2.2 Hepatic hepcidin 1 mRNA expression in SWR mice injected with apotransferrin and holotransferrin

Hepatic hepcidin 1 expression levels were determined by Real Time-PCR analysis. No significant difference on hepcidin was found after injection of apotransferrin or holotransferrin in wt and Hfe KO SWR mice. Results are expressed as Mean±SEM, n=4.

4.2.1.4 Hepatic DMT1 and IREG1 gene expression in wt and Hfe KO SWR mice injected with apotransferrin and holotransferrin

Hepatic DMT1 expression did not change with transferrin treatments in either wt or Hfe KO mice (Fig. 4.2.3a). Ireg1 expression levels in wt mice decrease significantly after injection with holotransferrin while apotransferrin injection had no effect (Fig. 4.2.3b). In Hfe KO mice Ireg1 expression was not change by either transferrin treatments.

a)

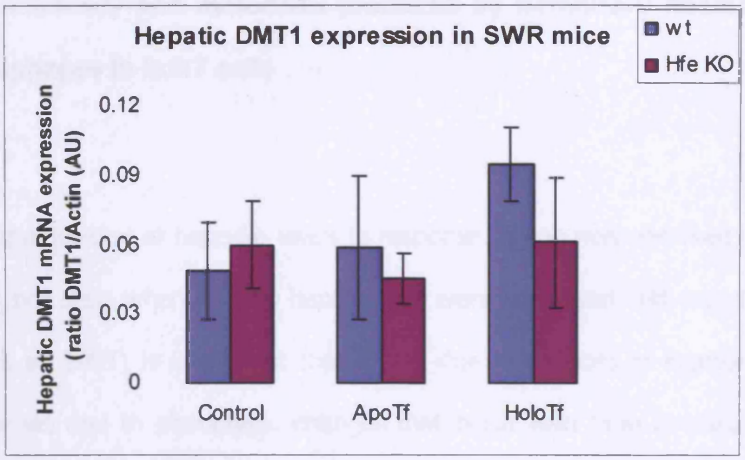

b)

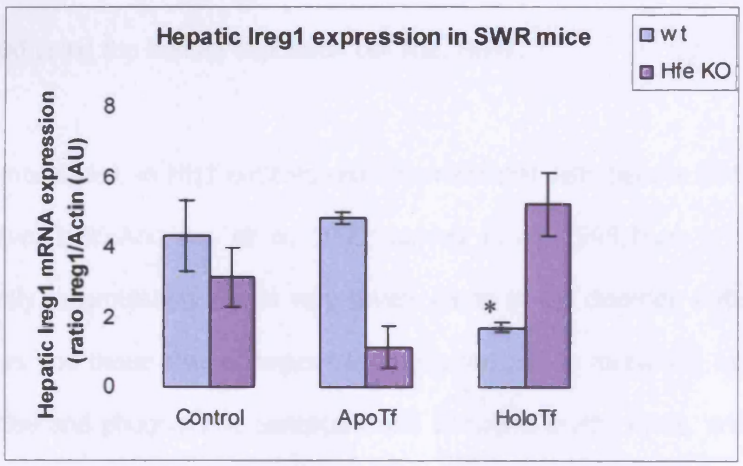

Figure 4.2.3 Expression of mRNA iron transporter genes after transferrin injections. *SWR wt and Hfe KO mice were injected with saline (Control), apotransferrin (ApoTf) or holotransferrin (HoloTf) and sacrificed after 4 hours. Hepatic DMT1 (a) and Ireg1 (b) expression levels were analysed by Real Time PCR. Hepatic DMT1 expression did not change with transferrin injections in either wt or Hfe KO animals. Ireg1 expression levels in wt mice were decreased significantly by holotransferrin (*p<0.05) while apotransferrin injection had no effect. Transferrin treatments had no effect on Hfe KO mice Ireg1 expression. Results are expressed as Mean±SEM, n=4.*

4.3.1 Regulation of hepcidin mRNA expression levels in response to iron loading, iron deficiency and molecules produced by hereditary haemochromatosis macrophages in huh7 cells

Although the upregulation of hepcidin levels in response to iron was observed in humans and in mice it was not seen when *in vitro* hepatocytes were incubated with iron (Nemeth et al. 2003;Pigeon et al. 2001) It is thought that this is due to the loss of expression of several liver-specific genes due to phenotypic changes that occur with time in culture (Ilyin et al. 1998). In this study the effect of high iron and low iron levels on hepcidin expression *in vitro* was investigated using the human hepatoma cell line, Huh7.

As previously mentioned, in HH1 patients reticuloendothelial cells behave as though starved of iron (Andrews 1999;Andrews et al. 1999;Fleming et al. 1999;Zhou et al. 1998) with Kupffer cells only accumulating iron in very severe cases of the disorder. Reticuloendothelial cells, monocytes and tissue macrophages have a central role in regulating iron homeostasis as they recognise and phagocytose senescent and damaged erythrocytes, process iron from haem and return the iron to circulation for reuse by red cell precursors during erythropoiesis (Knutson and Wessling-Resnick 2003).

The importance of the Hfe gene in macrophages is not fully understood. Makui and colleagues (Makui et al. 2005) have shown that Hfe in macrophages participates in the regulation of splenic and liver iron concentrations and liver hepcidin while Montosi and colleagues have shown that when Kupffer cells are inactivated, hepcidin mRNA expression fails to respond to inflammation by cytokines. In addition this group has shown that the inactivation of Kupffer cells does not abrogate the response of hepcidin expression to iron overload suggesting that Kupffer cells are necessary for the hepcidin response to inflammation but not to its response to iron overload (Montosi et al. 2005). The relevance of Hfe in the upregulation of hepcidin expression in response to inflammation was reported by other groups (Roy et al. 2004) however contradictory results by Lou 2005 and Nemeth 2004

have shown that iron- and inflammation-induced hepcidin gene expression is normal in Kupffer cell-depleted mice (Lou et al. 2005;Nemeth et al. 2004a).

In this study, the functional role of Hfe in peripheral macrophages and the contribution of the molecules produced by this cell type to the regulation of liver hepcidin are further investigated. Macrophages were isolated from HH1 patients with high levels of circulating iron and saturated transferrin. A human hepatoma cell line was then incubated with the conditioned medium collected from the macrophages culture and hepcidin expression levels were determined.

4.3.2 Methods

4.3.2.1 Iron loading by ferric ammonium citrate (FAC) and iron deficiency by Desferoxamine (DFO) in human hepatoma cell line

The Huh7 human hepatoma cell line was obtained from Dr. Roozina Rafique (Department of Haematology, UCL, London, UK). HuH7 cells were grown in monolayer culture in RPMI 1640 medium containing L-glutamine and 25 mM HEPES buffer, supplemented with 10% heat-inactivated foetal calf serum, 100 U/ml penicillin and 50 µg/ml gentamicin. Cells were seeded at a density of 1.5-2.0 x 10^5 cells per 80-cm^2 flask (Nunclon, Nunc Brand) and grown at 37°C in a humidified atmosphere of 5% CO_2 in air. Cell viability was determined by Trypan blue dye exclusion.

Iron loaded cells were obtained by incubating Huh7 monolayers (in 60 mm cell culture dishes) with supplemented RPMI medium containing 10 µg/ml of Ferric Ammonium Citrate (FAC) for 24 hours (as described by Parkes et al (Parkes et al. 1995)). For the iron deficient studies, cells were incubated with 100 µM of Desferoxamine (DFO) for 24 hours. At the end of the incubation period, the FAC/DFO media was removed and the Huh7 cells were washed with PBS extensively and prepared for mRNA analysis as described in chapter 2.2.

4.3.2.2 Preparation of conditioned medium from macrophages of HH1 patients for Huh7 cell culture

Hereditary haemochromatosis patients attending the Division of Hepatology and Transplantation (King's College Hospital, London, UK) homozygous for the C282Y mutation of the Hfe gene were selected. Blood samples were taken and mononuclear cells were isolated by the Ficoll-Paque Plus method (Amersham Biosciences UK Ltd., UK). These monocytes were then incubated with Lipoposaccharide (LPS) (Sigma, Poole, UK) for 20 hours in order to

isolate and differentiate macrophages. Cell free-medium was collected for treatment of Huh7 cultures (M1). Macrophages were cultured for a further 24 hours and the medium was collected for treatment of Huh 7 cells cultures (M2). The mediums collected were then used in the culture of Huh7 cells with 5% autonomous serum or serum from a subject with a different genotype. After further 24 hours the medium was removed and cells were used for mRNA analysis (Fig. 4.3.1).

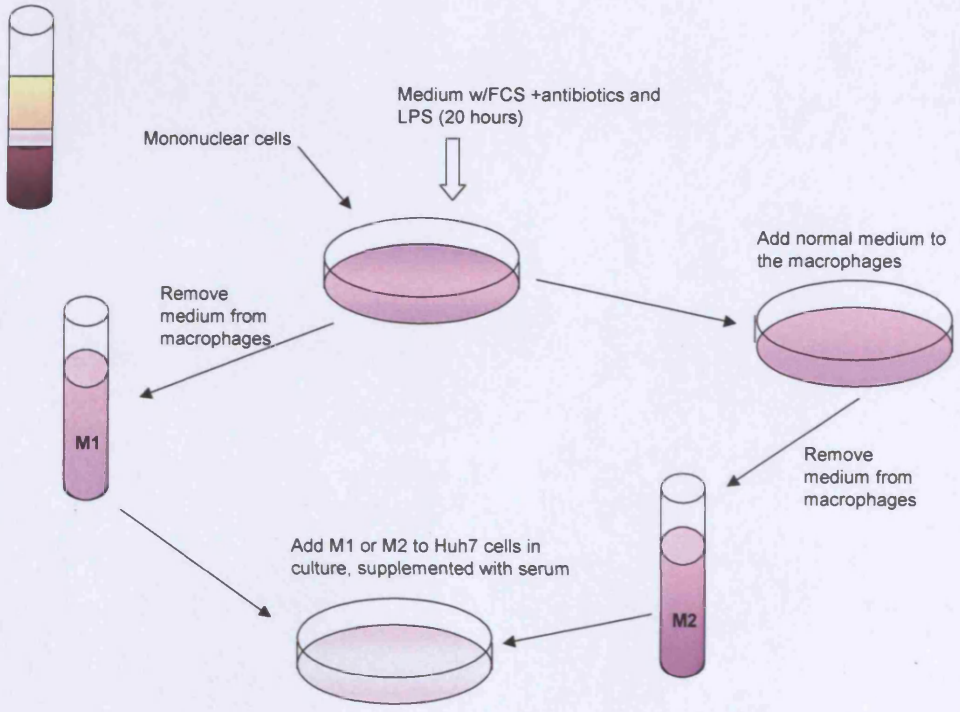

Figure 4.3.1 Preparation of the conditioned mediums used.

4.3.3 Results

4.3.3.1 Modulation of Iron Status in Huh7 cells: effect of iron on hepcidin and iron transporters mRNA expression levels

Huh7 cells were treated with Ferric Ammonium Citrate (FAC) to increase iron content of the cell and with Desferoxamine (DFO) to decrease iron content for 24 hours. Hepcidin mRNA expression levels were analysed by Real Time PCR. Treatment with FAC for 24 hours was shown to significantly decrease hepcidin expression (Fig. 4.3.2) and to stimulate NTBI uptake in Huh7 cells. Further investigation from our group has shown that this NTBI uptake stimulation occurs in a time- and concentration- dependent manner (personal communication by Dr. Roozina Rafique).

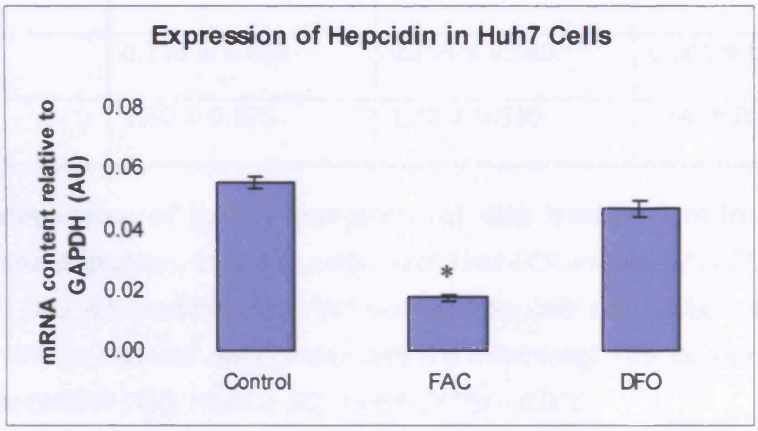

Figure 4.3.2 Effect of iron loading and iron depletion on hepcidin expression in vitro. *Hepcidin mRNA expression was determined by Real Time-PCR analysis on Huh7 cells pre-incubated with 10 μg Fe/ml FAC or 100 μM DFO for 24h at 37°C. Hepcidin mRNA expression levels decrease significantly in response to iron loading but not in response to iron depletion (*p<0.05). Results are expressed as Mean±SEM, n=6.*

Our group has also shown that treating Huh7 cells with 100 μM DFO for 24 hours resulted in no detectable levels of iron, when measured by the total cellular iron assay (personal communication by Dr. Roozina Rafique). In this study we have shown that treatment of Huh7 cells with DFO does not have a significant effect on hepcidin mRNA expression (Fig. 4.3.2).

Iron transporters were also analysed in Huh 7 cells treated with FAC and DFO. No statistically significant changes were observed in the expression of DMT1 (+IRE) or DMT1 (-IRE) in response to iron loading and iron depletion, however DMT1 (-IRE) was down regulated by 32% in response to 24 hours treatment with 100 μM DFO. In response to iron depletion a significant 3-fold increase in TfR1 expression was observed whilst no effect resulted from iron loading. TfR2 which is highly expressed in hepatocytes, was unaffected by changes in iron status (Table 4.3.1).

	Control	FAC	DFO
DMT1+IRE	0.710 ± 0.09	0.840 ± 0.260	0.680 ± 0.100
DMT1 -IRE	0.470 ± 0.160	0.380 ± 0.180	0.320 ± 0.270
TfR1	0.110 ± 0.010	0.104 ± 0.020	0.301 ± 0.05***
TfR2	1.80 ± 0.370	1.70 ± 0.510	1.90 ± 0.380

Table 4.3.1 Regulation of mRNA expression of iron transporters in response to iron loading and depletion, in HuH7 cells. *Real Time-PCR analysis of DMT1 (+IRE and –IRE), TfR1 and TfR2 was performed on RNA isolated from cells iron loaded with FAC or iron depleted with DF0 for 24h and from control cells (no treatment). Results expressed as ratio Gene of interest/GAPDH (AU), Mean ± SD, n=4-9. (***p <0.001)*

4.3.3.2 Regulation of hepcidin mRNA expression levels in response to serum iron levels and soluble factors produced by hereditary haemochromatosis macrophages

Huh7 cells were incubated with serum from healthy subjects or serum from HH1 patients in addition to conditioned medium obtained from macrophages from healthy subjects or HH1 patients macrophages in the presence (M1) or absence (M2) of LPS. When Huh7 cells were incubated with conditioned medium obtained from macrophages from healthy subjects and autologous serum or serum from HH1 patients, no difference was found in hepcidin mRNA expression levels (Fig. 4.3.3).

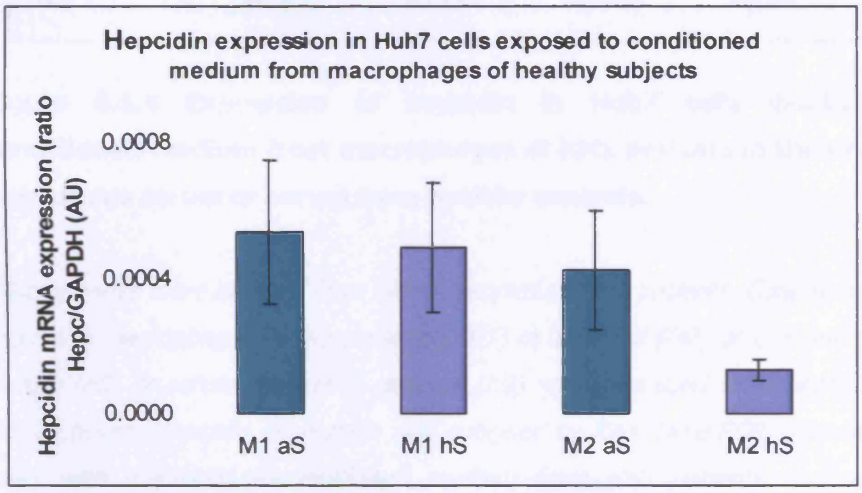

Figure 4.3.3 Expression of hepcidin in Huh7 cells incubated with conditioned medium from macrophages of healthy controls in the presence of autologous serum or serum from HH1 patients.

Macrophages were isolated from blood samples of healthy controls. Conditioned medium from the macrophages in the presence (M1) or absence (M2) of LPS and autologous serum (aS) or serum from HH1 patients (hS) was then used to incubate Huh7 cells for 24 hours. Hepcidin expression was analysed by Real Time PCR. Incubating Huh7 cells with macrophage-conditioned medium from healthy controls and serum from HH1 patients had no significant effect on hepcidin expression. Data are Mean±SEM, n=5.

Incubating Huh7 cells with conditioned medium obtained from HH1 patients macrophages and serum from healthy subjects upregulated hepcidin mRNA expression levels (Fig. 4.3.4).

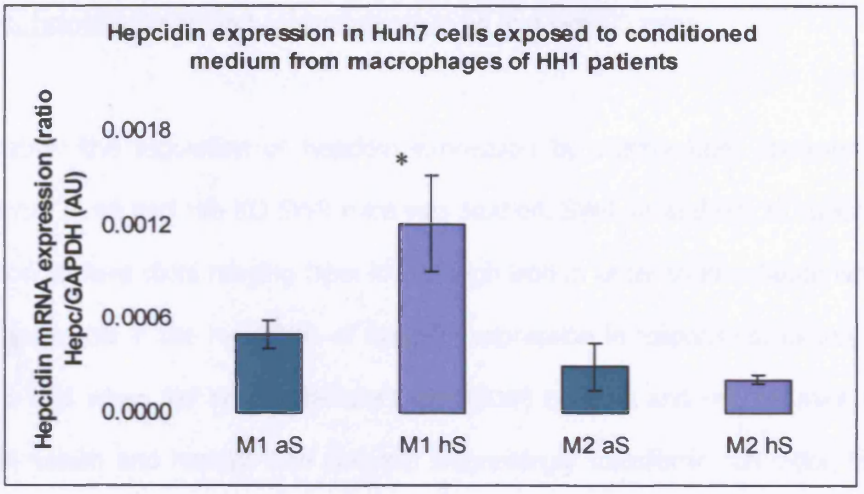

Figure 4.3.4 Expression of hepcidin in Huh7 cells incubated with conditioned medium from macrophages of HH1 patients in the presence of autologous serum or serum from healthy controls.

Macrophages were isolated from blood samples of HH1 patients. Conditioned medium from the macrophages in the presence (M1) or absence (M2) of LPS and autologous serum (aS) or serum from HH1 patients (hS) was then used to incubate Huh7 cells for 24 hours. Hepcidin expression was analysed by Real Time PCR. Incubating Huh7 cells with macrophage-conditioned medium from HH1 patients and serum from healthy controls significantly increased hepcidin expression. Data are Mean±SEM, n=5.

4.4 Discussion

Regulation of hepatic hepcidin, DMT1 and Ireg1 mRNA expression levels in response to dietary iron, holotransferrin and apotransferrin in wt and Hfe KO mice

In this chapter the regulation of hepcidin expression by dietary iron, apotransferrin and holotransferrin in wt and Hfe KO SWR mice was studied. SWR wt and Hfe KO mice were fed different iron content diets ranging from low to high iron in order to investigate whether the Hfe gene has a role in the regulation of hepcidin expression in response to dietary iron. Our data shows that when fed an iron deficient diet (IDD) both wt and Hfe KO mice showed a decrease in serum and hepatic iron content. Interestingly transferrin saturation in wt mice decreased with IDD but in Hfe KO mice transferrin saturation increased though not significantly. When wt mice were fed ILD serum iron levels, transferrin saturation and hepatic iron content levels increased significantly in wt mice while in Hfe KO mice ILD increased serum iron levels and hepatic iron content levels but had no effect on transferrin saturation. Our data also shows that on a normal diet (OD), hepcidin expression levels are lower in the Hfe KO mice compared to wt mice and hepcidin expression is inappropriately low for the hepatic iron levels found in these animals. Although these low levels of hepcidin in Hfe KO mice have already been described (Ahmad et al. 2002;Bridle et al. 2003), there is no information on hepcidin expression levels in relation to different lobes of the liver. In this study we have shown that higher levels of hepcidin expression were found in lobe A, the hepatic lobe with the highest iron content although this did not reach statistical significance.

In SWR wt mice fed IDD hepcidin expression levels decreased significantly but this iron deficiency failed to have an effect on hepcidin expression in Hfe KO mice. Iron deficiency has been shown to downregulate hepcidin in other mouse strains (Bondi et al. 2005;Latunde-Dada et al. 2004;Nicolas et al. 2002b;Vokurka et al. 2006). It is thought that the low hepcidin levels lead to an increase in iron absorption to allow more iron to the bone marrow to sustain the erythrocyte production. As Hfe KO mice accumulate higher levels of iron in the liver it is

possible that these iron stores prevent iron deficiency to upregulate hepcidin expression in these mice.

Iron loading by ILD in wt mice did not have an effect on hepcidin expression while in Hfe KO mice ILD for 9 weeks upregulated hepcidin mRNA expression levels. In iron overload conditions the increased hepcidin expression levels in iron overload conditions is thought to block iron absorption until the normal plasma iron levels are restored (Mazur et al. 2003;Nemeth et al. 2004b;Pigeon et al. 2001). It has also been reported that in Hfe KO mice duodenal iron absorption decreases with age suggesting that Hfe KO mice down-regulate iron absorption when body iron stores reach certain levels (Ajioka et al. 2002). As hepatic iron stores increase in Hfe KO mice with age it is possible that this severe iron stores increases hepcidin expression which consequently results in a decrease in duodenal iron uptake. In support of this theory, the disruption of the Hfe gene in the AKR mouse strain has been found to have no significant effect on hepcidin expression levels in some experiments (Ahmad et al. 2002). AKR Hfe KO mice have been reported to have 2-3 fold higher hepatic iron content than wt ARK mice. In addition AKR mice like SWR mice have been shown to have a higher basal iron level than C57BL/6 or DBA/2 mouse strains (Fleming et al. 2001).

When fed a normal diet (CD) hepatic DMT1 and Ireg1 expression levels were not significantly different in wt and Hfe KO mice and no difference was observed between levels of expression of hepatic DMT1 or Ireg1 in the different hepatic lobes studied. In wt mice fed IDD, hepatic DMT1 expression was decreased as previously described (Scheiber-Mojdehkar et al. 2003;Trinder et al. 2000b) while in Hfe KO mice hepatic DMT1 was upregulated by iron deficiency.

Hepatic Ireg1 expression was found to be upregulated in both wt and Hfe KO mice fed IDD. The increased erythropoiesis in mice fed an iron deficient diet might explain the upregulation of hepatic Ireg1 expression as more iron in the circulation would be necessary for the production of erythrocytes precursors.

In wt mice, ILD led to an upregulation of DMT1 expression as previously reported (Scheiber-Mojdehkar et al. 2003;Trinder et al. 2000b). Interestingly hepatic DMT1 expression was also upregulated in Hfe KO mice fed on ILD. In the liver DMT1 is thought to be involved in the uptake of Tf-bound iron through the TfR1 and TfR2 pathways (Trinder et al. 2000a;Trinder and Morgan 1997) and it has been thought to contribute to the uptake of NTBI at the cell surface although further investigation is required. Although DMT1 expression is upregulated by iron deficiency in the duodenum, in the liver DMT1 levels have been described to be enhanced by iron loading (Scheiber-Mojdehkar et al. 2003;Trinder et al. 2000b). It has been hypothesised that this upregulation of hepatic DMT1 in iron loaded conditions helps reduce the circulating NTBI and prevents its toxic effect; however DMT1 has been shown to have a limited role in iron loading of the liver. Inactivation of DMT1 in animal models (Gunshin et al. 2005) and DMT1 mutations in humans (Beaumont et al. 2006;Iolascon et al. 2006;Mims et al. 2005) result in severe microcytic anaemia accompanied with severe iron overload. Furthermore although DMT1 expression levels in the liver are upregulated by iron loading, Trinder et al (Trinder et al. 2002b) have shown that there are no significant differences in the rate of NTBI uptake by the liver in the Hfe KO mice compared to control mice. All these findings suggest that DMT1 in the liver is not involved in iron uptake and therefore the possibility of alternative mechanisms of NTBI uptake into the liver needs to be considered. In conclusion the present study and the already published data (Chua et al. 2004) show that to date it is not possible to determine whether the increase in hepatic DMT1 expression and the increase in uptake by the hepatocytes are the primary cause of iron loading or the secondary to iron loading by another mechanism.

Iron loading had no significant effect on hepatic Ireg1 expression in wt mice but in Hfe KO mice ILD for 9 weeks upregulated Ireg1 expression significantly. As in enterocytes, Ireg1 is considered to be an iron exporter in the hepatocytes. The finding that Ireg1 was upregulated in Hfe KO mice fed ILD suggests that the hepatocytes have an excretion mechanism to avoid severe iron accumulation and subsequent liver damage. In support of this hypothesis, Bonkovsky et al observed that when iron loaded rats were changed to a carbonyl-free diet

there was a 50% reduction in total liver iron. More recently Oates et al have shown that within two days of changing from an iron loaded diet to an iron deficient diet, non-haem iron levels significantly fall by 30%. Bonkovsky and Oates also observed that in animals fed on ILD iron accumulation stabilised after falling to a certain level of liver iron with animals fed on ILD having 10-times higher liver iron content than animals fed on a normal diet (Bonkovsky et al. 1987;Oates et al. 2000).

The upregulation of hepatic Ireg1 expression seen in the Hfe KO mice in this study has also been reported in HH1 patients (Bridle et al. 2003). This finding together with the discovery that mutations to a single copy of the Ireg1 gene result in tissue iron loading and the data from Bonkovsky and Oates on iron excretion confirms that Ireg1 plays a protective role by facilitating the release of iron from the liver in iron overload conditions.

The loss of the Hfe gene in Haemochromatosis type 1 patients results in a defective regulation of dietary iron absorption that leads to increased serum transferrin saturation. It also results in a decrease in circulating hepcidin, which leads to increased ferroportin-mediated iron efflux from reticuloendothelial cells and duodenal enterocytes (Ahmad et al. 2002;Bridle et al. 2003;Muckenthaler et al. 2003). This increased Ireg1-mediated iron efflux eventually leads to increased circulating iron concentrations and Tf to become saturated.

Therefore, circulating diferric transferrin is thought to be a candidate for the erythroid regulator. It is possible that the levels of diferric Tf in the circulation could provide the necessary signal for the hepatocytes to detect body iron demand and subsequently alter hepcidin expression (Frazer and Anderson 2003). Here we have shown that injections of wt and Hfe KO SWR mice with apotransferrin and holotransferrin (diferric transferrin) have no significant effect on serum iron, transferrin saturation or hepatic iron content.

Apotransferrin injection in wt SWR mice had no effect on hepcidin expression mRNA levels while holotransferrin upregulated hepcidin expression levels though not significantly. The same response was observed in Hfe KO mice suggesting that Hfe is not involved in the regulation of hepcidin expression by apotransferrin or holotransferrin.

Hepatic DMT1 expression did not change in either wt or Hfe KO after apotransferrin and holotransferrin injections while hepatic Ireg1 expression levels decreased significantly after holotransferrin treatment. Apotransferrin injection had no effect on the expression of Ireg1 iron exporter in wt or Hfe KO mice. Iron stores have been reported not reflect transferrin saturation, suggesting that different genetic factors control transferrin saturation and hepatic iron stores. When mice were fed a high-iron diet, the concentration of carbonyl iron required to completely saturate transferrin with iron was significantly different between mouse strains (Leboeuf et al. 1995) and in this study, injections of apotransferrin and holotransferrin did not have an effect on transferrin saturation. It is therefore hypothesized that the concentration of holotransferrin in the present study was insufficient to cause a significant effect on hepcidin or iron transporter gene expression in the SWR mice. Or that SWR mouse strain requires a higher concentration of carbonyl iron to saturate transferrin with iron. However the data suggests that holotransferrin, also called diferric transferrin might be regulated by iron and this requires further investigation.

Regulation of hepcidin and iron transporter gene mRNA expression levels in response to iron loading, iron deficiency and molecules produced by macrophages from hereditary haemochromatosis patients in Huh7 cells

In this chapter how hepcidin mRNA expression is regulated by iron in a hepatoma cell line was also investigated. The differential effect of blood macrophages from HH1 and controls on hepcidin mRNA expression levels in Huh7 cells in culture was also examined.

Hepcidin expression levels in response to iron deficiency and to iron loading was investigated by exposing a hepatoma cell line (Huh7) to Desferoxamine (DFO) and to ferric ammonium citrate (FAC). In this study Huh7 cells treated with DFO showed a decrease in hepcidin expression levels though this failed to reach significance while Huh7 cells treated with FAC showed a significant decrease in hepcidin expression levels.
The upregulation of hepcidin in response to high iron has been observed in mice (after iron dextran injections) and humans (dietary iron), but not when hepatocytes are exposed to iron *in vitro* (Pigeon et al. 2001). The results of this study support the idea that Huh7 cells lose expression of several liver-specific genes due to phenotypic changes that occur with time in culture and therefore do not respond to iron as *in vivo* cells (Ilyin et al. 1998).

Although DMT1 has been proposed as an obvious candidate for NTBI uptake by hepatocytes (Chua et al. 2004;Trinder et al. 2000b) due to its optimal iron transport activity at acid pH of 5.5 (Gunshin et al. 1997) several lines of evidence from cell culture studies do not support this notion and therefore it is unlikely that DMT1 contributes to the iron uptake in Huh7 cells. Studies from our group have shown that at low pH, when transport by proton-dependent DMT1 is optimal, ferrous iron uptake was significantly blocked in differentiated Caco-2 cells expressing DMT1 but not in Huh7 cells. This finding suggests that iron uptake in Caco-2 cells and in Huh7 cells is pH dependent that although DMT1 is involved in iron uptake in Caco-2 cells, in Huh7 cells an alternative iron transporter must exist. There was no significant increase in DMT1 (+ire) or DMT1 (-ire) expression in Huh7 cells in response to iron loading in

this study, confirming that DMT1 is not responsible for the FAC-stimulated NTBI uptake rate. These findings are consistent with those of Gunshin *et al* (Gunshin et al. 2001) who observed no change in mRNA DMT1 expression levels in Hep3B cells in response to iron loading with FAC. Exposure of Huh7 cells to DFO had no effect on DMT1 (+ire) expression while DMT1 (-ire) expression was slightly (32%) decreased.

The expression of TfR1 and TfR2 were also analysed in Huh7 cells after treatment with FAC and DFO. Iron depletion caused a significant increased in TfR1 although this was accompanied by down regulation of iron uptake rate. Expression levels of TfR2 did not change with FAC and DFO exposure suggesting that TfR2 does not mediate FAC-induced NTBI uptake nor is regulated by iron as reported previously in mouse liver (Fleming et al. 2000).

As transferrin levels did not have a significant effect on hepcidin expression levels we hypothesised that macrophages of HH1 patients could be producing soluble factors that regulate hepcidin expression differently in HH1 patients and healthy subjects. In this study, Huh7 cells were incubated with conditioned medium from HH1 patients and healthy subjects macrophages and either autologous serum or serum from a different genotype. Data shows that serum iron levels or conditioned medium from macrophages does not have an effect on hepcidin expression levels. Huh7 cells incubated with macrophage-conditioned medium from HH1 patients and serum from healthy subjects up regulated significantly hepcidin expression although this could be a secondary effect of the presence of LPS in the culture medium. Overall, data suggests that peripheral macrophages do not have a role in the production of soluble factors that could regulate hepcidin expression levels in HH1 patients.

Conclusions

In conclusion the study of the regulation of hepcidin and iron transporter genes expression in response to dietary iron, apotransferrin and holotransferrin in wt and Hfe KO mice and the regulation of hepcidin and iron transporter genes expression in response to iron loading and iron depletion in Huh7 cells suggest the presence of a regulatory iron pool in hepatocytes that directly regulates hepcidin expression levels.

Our data also suggests that iron regulates hepatic Ireg1 mRNA expression in a direct manner and not through the regulation of hepcidin expression levels. Furthermore our data shows that Hfe gene is not necessary for the regulation of Ireg1 in response to iron in accordance with the findings of Bridle and colleagues (Bridle et al. 2003) showing that in HH1 patients and in Hfe KO C57BL/6 mice, iron stores regulate hepcidin expression but have no effect on Ireg1 expression. We hypothesised that in cases of disruption of Hfe or when mice are fed an iron loaded diet, hepatocytes accumulate the iron in this "regulatory iron pool". When this pool reaches a yet unknown iron content level, Ireg1 expression level in hepatocytes is upregulated and the excess iron is exported to avoid oxidative stress and lipid peroxidation in the liver. The iron accumulation in this "regulatory iron pool" would regulate hepcidin in the same manner, when iron stores reach a certain level, hepcidin is upregulated in order to decrease duodenal iron uptake. This would explain why iron loaded diet in Hfe KO mice upregulates hepcidin expression.

Taken together from the previously published data and the results obtained in this study we can conclude that dietary iron (in SWR mice) or iron loading (in Huh7 cells) does not have a direct effect on hepatic DMT1 expression and therefore it is possible that in the case of the Hfe KO mice, the Hfe gene might have a role in the regulation of this iron transporter gene expression, but this requires further investigation.

In addition we have shown that iron deficient peripheral macrophages lacking the Hfe gene do not produce any soluble factors that regulate hepcidin expression in the setting of hereditary haemochromatosis compared to healthy subjects.

CHAPTER 5

INFLAMMATION AND HEPCIDIN

5.1 Introduction

In cases of infection and inflammation the maintenance of body iron homeostasis is disregulated resulting in anaemia of inflammation (AI). Anaemia of Inflammation is characterised by inadequate erythrocyte production in the setting of low serum iron and low iron-binding capacity (i.e. low transferrin) despite preserved or even increased macrophage iron stores in the bone marrow. Despite having low serum iron and low transferrin, patients with AI have high serum ferritin concentration. The anaemia is caused by increased inflammatory cytokines and the changes in iron metabolism are due to the effects of these cytokines as described in chapter 1.

Pro-inflammatory cytokines have been shown to act on a number of cell types to decrease iron release (Johnson et al. 2004;Ludwiczek et al. 2003;varez-Hernandez et al. 1989;Yang et al. 2002) and promote the cellular sequestration of iron in ferritin (Miller et al. 1991;Torti et al. 1988). More specifically the pro-inflammatory cytokine IL-6 induces an increased production of the iron regulatory hormone hepcidin by hepatocytes, which blocks the release of iron from macrophages, hepatocytes, and enterocytes causing hypoferraemia (low serum iron). Although this hypoferraemia provides protection against proliferating microorganisms (Ashrafian 2003) it also results in the iron deprivation of the developing erythrocytes and leads to the development of anaemia (Ganz 2005b).

As iron homeostasis is tightly regulated at the intestinal level and therefore it is important to assess the influence of inflammatory cytokines on this transport pathway. Previous work has demonstrated that a mixture of pro-inflammatory cytokines (that includes tumour necrosis factor α (TNF-α) and interleukin 6 (IL-6) are produced in inflammatory conditions such as acute inflammation due to LPS injection (Ganz 2003). TNF-α and IL-6 treatment has shown to decrease iron transport in intestinal Caco-2 cells (Han et al. 1997). Furthermore, studies by our group and those of others have shown that TNF-α alone can act directly on intestinal epithelial cells to regulate the expression of iron transport proteins (Johnson et al. 2004;Sharma et al. 2005).

As mentioned previously, hepcidin expression dramatically increases with the onset of inflammation (Frazer et al. 2004b;Johnson et al. 2004;Nemeth et al. 2004a;Nicolas et al. 2002b;Park et al. 2001;Pigeon et al. 2001;Rivera et al. 2005a) and this appears to be co-ordinated, at least in part, through the actions of IL-6 released by Kupffer cells/ macrophages (Nemeth et al. 2003;Nemeth et al. 2004a). High levels of hepcidin, in turn, are known to decrease intestinal iron absorption (Laftah et al. 2004;Roy et al. 2004;Roy and Andrews 2005;Yamaji et al. 2004), and hence this represents an alternative route by which IL-6 might influence intestinal iron metabolism. A LPS injection in human subjects dramatically induces IL-6 within 3 hours, induces urinary hepcidin and leads to a significant decrease in serum iron (Kemna et al. 2005) while IL-6 injection in human volunteers induces hepcidin and hypoferremia within just 2 hrs (Nemeth et al. 2004a).

Mice with disruption of the gene encoding IL-6 have been reported to have a small response to LPS which makes it unclear whether LPS is stimulating the secretion of cytokines other than IL-6 that may stimulate hepcidin transcription (Nemeth et al. 2004a).

Recently, it has been reported that IL-6 directly induces hepcidin through STAT3 activation and subsequent hepcidin promoter binding. This provides a mechanism by which hepcidin can be regulated by inflammation or, in the absence of inflammatory stimuli, by alternative mechanisms leading to STAT3 activation (Pietrangelo et al. 2007;Wrighting and Andrews 2006).

Turpentine injections in mice also result in increased liver hepcidin gene expression, a reduction in RBC mass, haemoglobin, and serum iron (hypoferremia), leading to anaemia (Nicolas et al. 2002b;Weinstein et al. 2002) The finding that the hypoferraemic response to turpentine-induced inflammation was absent in the USF2/hepcidin-deficient mice, confirms that this response is fully dependent on hepcidin.

In vivo inactivation of Kupffer cells abrogates the stimulatory effect of both LPS and turpentine on hepcidin expression confirming that macrophages are releasing cytokines that up regulate hepcidin in inflammation conditions (Montosi et al. 2005). High levels of hepcidin lead to Ireg1 internalisation and degradation, therefore blocking the pathway for the transfer of iron from the enterocyte to plasma (Ganz 2005a) and trapping the iron within the

macrophages. This proposed model confirms the earlier finding that during inflammation, Ireg1 is downregulated in macrophages (Yang et al. 2002).

The effect of LPS stimulation on hepcidin expression levels in Hfe KO mice and the requirement of Hfe or other genes for the up-regulation of hepcidin in inflammation conditions is less clear. Some reports have shown that Hfe KO mice do not respond to LPS stimulation or develop hypoferremia (Roy et al. 2004), in other reports the response to LPS injections differs strikingly from animal to animal (Lee et al. 2004) and a recently published paper has reported that although basal hepcidin levels were manifestly dependent on the presence of Hfe and on the mouse background, Hfe KO mice were still able to regulate hepcidin in situations of altered iron homeostasis such as inflammation by LPS (Constante et al. 2006). Injection of IL-6 in TfR2 mutated mice had an effect on hepcidin levels suggesting that the signalling pathway activated by IL-6 does not require TfR2 (Lee et al. 2004). The contradictory results on the role of Hfe in up regulation of hepcidin by acute inflammation suggest that the study of Hfe KO mice in the inflammatory setting requires further investigation.

To investigate whether IL-6, like TNF-α could directly regulate intestinal iron transporter expression, Caco-2 cells, a model human intestinal epithelial cell line which phenotypically resembles small intestinal enterocytes (Chantret et al. 1994;Sharp et al. 2002) were used. This cell line was also used to investigate the effect of hepcidin on iron transporter genes, namely DMT1 and IREG1. A human hepatoma cell line (Huh7 cells) was also used to determine how pro-inflammatory interleukins regulate hepcidin expression levels.

To investigate the effect of acute inflammation on hepcidin expression levels, SWR wt mice were injected with Lipopolysaccharide (LPS) for 1.5 hours, 6 hours, the time at which maximal response of hepcidin transcription has been noted (Yeh et al. 2004) and 16 hours. Mice were also injected with Turpentine oil for 16 hours. To further understand the role of the Hfe gene and the up regulation of hepcidin, SWR Hfe KO was also subjected to acute

inflammation by LPS and Turpentine. The expression of iron transporter genes and liver iron content was also studied in both wt and Hfe KO SWR mice after acute inflammation treatment.

5.2 Methods

5.2.1 Pro-inflammatory cytokines treatment of hepatocytes and enterocytes

Caco-2 cells were grown in Dulbecco's modified Eagle's medium (DMEM) containing 10% fetal bovine serum for 21 days on Transwell inserts (Corning-Costar, High Wycombe, UK) to achieve a fully differentiated monolayer. For the final 24 h of the culture period, the cells were incubated in serum-free medium containing 10ng/ml of IL-6 (or an equal volume of the vehicle in the control groups) added to the basolateral chamber. Huh7 cells were cultured in RPMI1640 medium (Sigma) containing L-Glutamine (Sigma), antibiotics and 10% FCS (Sigma) and maintained in 5% CO2 at 37oC. The cells were seeded in $5cm^2$ wells till confluent. Once confluent, cells were treated with IL-6 (0.5ng/ml & 10ng/ml), and TNF-α (10ng/ml) for 24 hours. After removing the culture medium, Huh7 and Caco-2 cells were washed with PBS and prepared for Real Time PCR amplification as described in section 2.1.

5.2.2 IL-6-stimulated Huh 7 cells conditioned medium treatments of Caco-2 cells

Conditioned medium (CM) was collected from IL-6 stimulated Huh7 cells and added to the basolateral chamber of Caco-2 cell containing Transwell plates for 24 hours. In addition the produced conditioned medium was incubated in the presence and absence of hepcidin anti-human antibody (raised in-house) for 20 minutes at room temperature. This conditioned medium containing the hepcidin antibody (Hepc Ab-medium) was then added to the Caco-2 cells for 24 hours as described above. Cells were harvested and prepared for Real Time PCR amplification as described in section 2.1.

5.2.3 Inflammation by LPS and Turpentine in SWR mice

SWR mice were fed on an iron adjusted diet (44 mg iron/kg) for 9 weeks after being weaned (3 weeks of age). Two different strategies were used to induce inflammation: lipopolysaccharide (LPS) or turpentine oil injections. SWR male mice were given one intraperitoneal injection of 5µg of LPS (Sigma, Poole, UK) or an interscapular fat pad injection of 0.1mL/20g of body weight of Turpentine oil (Sigma, Poole, UK) in a buffered saline. Mice were sacrificed 16 hours after injection; tissues were collected and snap frozen for mRNA studies. RNA was extracted and prepared for Real Time PCR analysis as described in section 2.2.

Liver samples were also collected for hepatic iron content levels as described in section 3.2.2. Blood was collected by cardiac puncture and serum iron and transferrin saturation was analysed using a commercially available assay (Randox Laboratories Ltd. Antrim, UK).

5.3 Results

5.3.1 Effect of pro-inflammatory cytokines

5.3.1.1 Duodenal iron transporter gene expression

Treatment of Caco-2 cells with the cytokine interleukin 6 had no effect on the mRNA expression of iron transporters DMT1+IRE or Ireg1 (Fig. 5.3.1). Work from our group has shown that interleukin 6 treatment has also no effect on the protein levels of DMT1 or Ireg1 (personal communication by Dr. Paul Sharp).

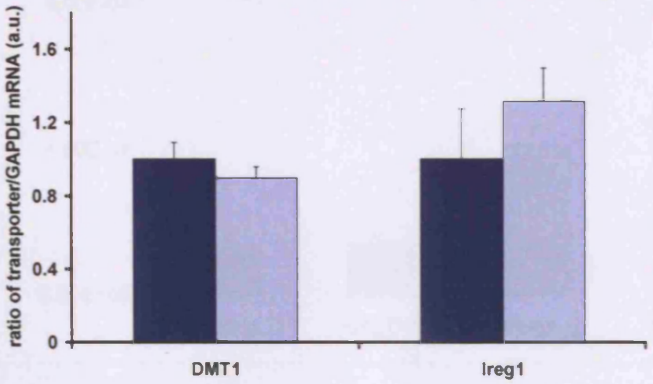

Figure 5.3.1 Effect of IL-6 on mRNA expression levels of iron transporters in Caco-2 cells. *Quantitative PCR analysis of iron transporter transcripts in Caco-2 cells demonstrated that DMT1 (+IRE) and IREG1 mRNA expression was unaltered following incubation with IL-6 (light blue bars) compared with untreated control cells (dark blue bars). Data are expressed as Mean± SEM from 4 separate experiments.*

5.3.1.2 Hepatic hepcidin mRNA expression

Inflammation studies in Huh7 cells demonstrated that hepcidin mRNA expression levels significantly increase following exposure to IL-6 but not to TNF-α compared to unstimulated Huh7 cells. Interleukin 6 treatment of 0.5ng/ml increased the mRNA expression of Hepcidin by 2-fold and the treatment of 10ng/ml of IL-6, caused a 4-fold increase in Huh7 cells compared to non-treated Huh7 Cells. Hepcidin expression was not significantly altered in Huh7 cells incubated in the presence of TNF-α (Fig 5.3.2).

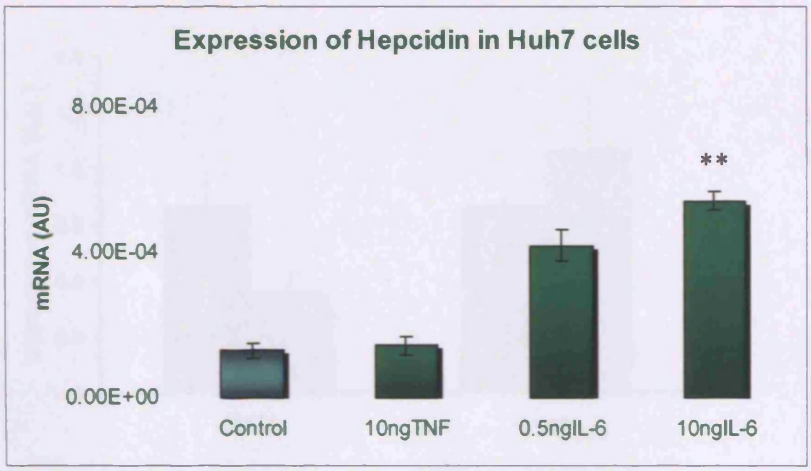

Figure 5.3.2 Quantitative PCR analysis of hepcidin expression in Huh7 cells following cytokine treatment. *Huh7 cells were incubated for 24 h in the presence of either TNF-α (10ng/ml) or IL-6 (0.5ng/ml and 10ng/ml). Quantitative PCR analysis of total RNA isolated from Huh7 cells demonstrated that hepcidin mRNA levels were significantly increased following exposure to IL-6. Hepcidin expression in cells stimulated with TNF-α was not significantly different from the unstimulated controls. Data are Mean± SEM from 4 separate experiments, **p<0.005.*

5.3.1.3 Duodenal iron transporter gene expression in Caco-2 cells exposed to IL-6-stimulated Huh7 cells conditioned medium

Caco-2 cells that were exposed (at their basolateral surface) to conditioned medium from IL-6-stimulated Huh7 cells showed a decreased in DMT1 (+IRE) mRNA expression though not significantly compared to the Caco-2 cells that were exposed to quiescent cells (Fig. 5.3.3). Ireg1 mRNA expression levels were not changed by the conditioned medium containing Hepcidin.

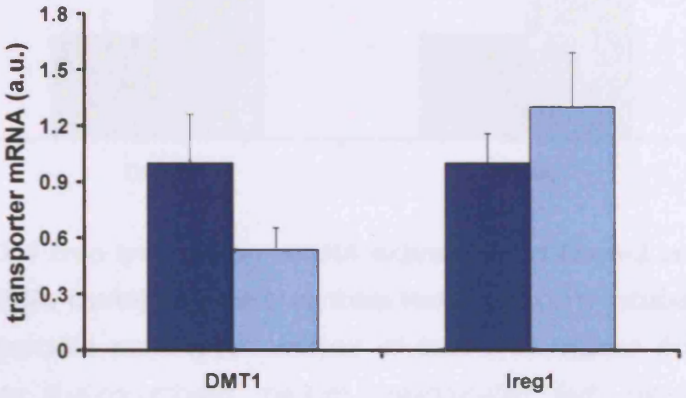

Figure 5.3.3 Iron transporter mRNA expression in Caco-2 cells stimulated with hepcidin-containing medium from IL-6 stimulated HuH7 cells. *Analysis of total RNA isolated from Caco-2 cells exposed to IL-6-conditioned medium demonstrated that DMT1 (+IRE) mRNA expression was decreased though not significantly, in cells exposed to the hepcidin-containing medium (light blue bars) compared with those incubated medium from unstimulated HuH7 cells (dark blue bars). IREG1 expression was not altered in these cells. Data are Mean±SEM of 3-4 measurements in each experimental group.*

To further investigate whether the release of hepcidin due to IL-6 treatment was responsible for the changes in duodenal DMT1 and Ireg1 expression, CM (conditioned medium from IL-6-stimulated Huh7 cells) was incubated with an anti-human Hepcidin antibody prior to its addition to the basolateral chamber of the Caco-2 cell-containing Transwell plates. Results

show that DMT1 and Ireg1 expression levels increase significantly in Caco-2 cells treated with conditioned medium pre-incubated with an anti-human Hepcidin antibody (Fig. 5.3.4).

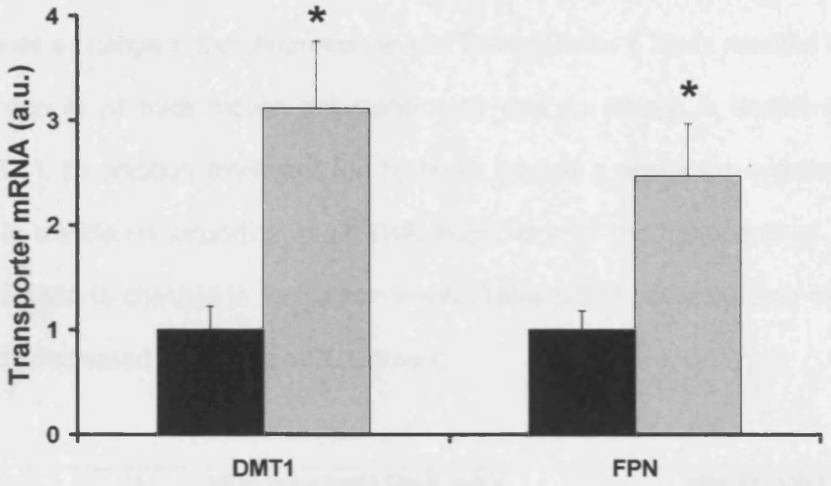

Figure 5.3.4 Iron transporter mRNA expression in Caco-2 cells stimulated with hepcidin-containing medium from HuH7 cells pre-incubated with anti-human hepcidin antibody. *Analysis of total RNA isolated from Caco-2 cells exposed to IL-6-conditioned medium pre-incubated with anti-human hepcidin antibody (Hepc Ab-medium) demonstrated that DMT1 (+IRE) and Ireg1 (FPN) mRNA expression was significantly upregulated in cells exposed to Hepc Ab-medium (grey bars) compared with those incubated with CM alone (black bars). Data are Mean±SEM of 3-4 measurements in each experimental group, *p<0.05).*

5.3.2 Effect of inflammation on serum iron levels in SWR wt and Hfe KO mice

Two different strategies were used to induce inflammation in SWR wt and Hfe KO mice: lipopolysaccharide (LPS) or turpentine oil (Turps) injections. SWR wt and Hfe KO mice were treated with LPS for 1.5, 6 and 16 hours. Treatment for 1.5 hours with LPS in SWR wt mice did not cause a change in the serum iron levels. Treatment for 6 hours resulted in a decrease in serum iron in wt mice though not significantly and no change in transferrin saturation (Table 5.3.1). In addition treatment for 16 hours caused a significant hypoferremia and a decrease in transferrin saturation in wt SWR mice. None of the treatments of LPS given to Hfe KO mice led to changes in serum iron levels (Table 5.3.1) but transferrin saturation was significantly decreased 16 hours post-treatment.

Treatment		Wild type (wt) SWR mice		Hfe KO SWR mice	
		Total Serum iron (µmol/L)	***Transferrin Saturation (%)***	***Total Serum iron (µmol/L)***	***Transferrin Saturation (%)***
6 hours	**Control**	89.4-126.1 (2)	74.5-83.2 (4)	181.5-192.3(2)	77.7-93.5 (4)
	LPS	47.5-57.7 (2)	68.9-72.0 (3)	69.7-150.4(3)	85.3-92.4 (3)
16 hours	**Control**	130.1-205.0 (3)	68.8-84.1 (4)	200.7-499.0(6)	80.0-87.4 (4)
	LPS	24.2-49.7(3)**	39.2-40.3 (3)**	61.8-286.0(4)	45.6-62.2 (3)**

Table 5.3.1 Total Serum iron and transferrin saturation after LPS treatment. *Male SWR wt and Hfe KO mice 12 weeks old were injected with 5µg of LPS and sacrificed after 1.5, 6 and 16 hours. Treatment for 1.5 hours did not change the serum iron levels or transferrin saturation in either wt or Hfe KO SWR mice. Treatment for 6 hours caused a decrease in serum iron in both wt and Hfe KO mice though not significantly and treatment for 16 hours led to a significant hypoferremia in wt SWR mice (*p<0.05, **p<0.005). Treatment for 16 hours with LPS did not have a significant effect on serum iron levels in Hfe KO mice although transferrin saturation was significantly decreased in these mice compared with non-treated animals. Data are Mean±SEM, number of samples stated in brackets.*

Treatment with turpentine resulted in a significant decrease in total serum iron and transferrin saturation in wt SWR mice (Table 5.3.2). Treatment of Hfe KO SWR mice with LPS for 16 hours had no effect on serum iron levels or transferrin saturation.

SWR MICE		CONTROL	TURPENTINE	P
wt	Serum total iron (µmol/L)	85.2-177.1 (4)	43.1-84.8 (5)	<0.01
	Transferrin Saturation (%)	70.3-83.2 (3)	41.3-44.0 (3)	<0.05
Hfe KO	Serum total iron (µmol/L)	221.5-326.6 (6)	274.8-462.0 (7)	>0.05
	Transferrin Saturation (%)	81.0-92.0 (4)	79.4-95.1 (3)	>0.05

Table 5.3.2 Total serum iron and transferrin saturation after Turpentine injection. *SWR wt and Hfe KO mice were injected with turpentine oil (0.1ml/20g body weight) and sacrificed after 16 hours. Injection of Turpentine resulted in a significant hypoferremia in wt SWR mice accompanied with a significant decrease in transferrin saturation. No change in serum iron levels or transferrin saturation was observed in Hfe KO SWR mice injected with turpentine oil. Data are Mean±SEM, number of samples described in brackets.*

5.3.3 Effect of acute inflammation by LPS and Turpentine on hepatic iron content, hepatic hepcidin, DMT1 and Ireg1 gene expression in wt SWR mice

5.3.3.1 Effect of acute inflammation on hepatic iron content in wt SWR mice

Liver iron content was analysed in wt SWR treated with LPS and Turpentine oil for 16 hours. Acute inflammation induced by both LPS and turpentine oil treatment had no effect on hepatic iron content levels (Fig. 5.3.5).

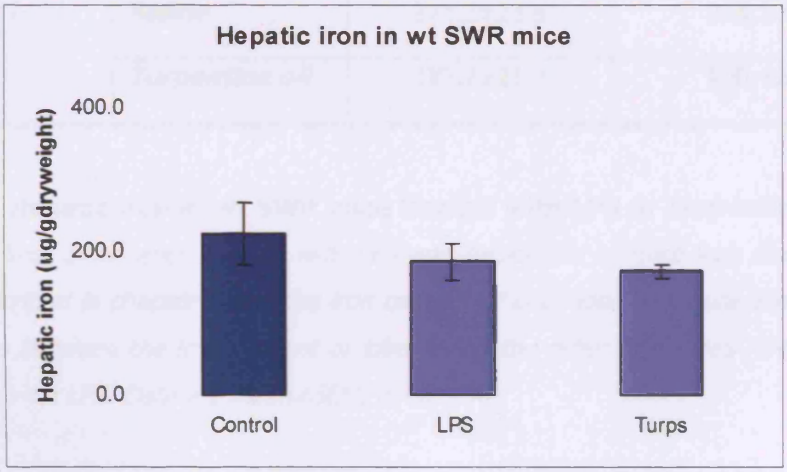

Figure 5.3.5 Liver iron content levels in wt SWR mice in acute inflammation

Mice injected with LPS and turpentine were sacrificed after 16 hours; the whole liver was removed and divided into five lobes. Iron was quantified in each lobe and the average of the iron content in each whole liver was calculated. Treatment of wt SWR mice with LPS and turpentine oil had no effect on hepatic iron content levels. Data are Mean±SEM, Control n=6; LPS n=3; Turps n=3.

Hepatic iron content was analysed in each lobe of the liver and no difference was found between the iron content of lobe A and the other four lobes (B-E) in wt SWR mice treated with LPS or turpentine oil (Table 5.3.3).

SWR MICE	TREATMENT	LOBE A IRON CONTENT (µg/gdryweight)	LOBE B-E IRON CONTENT (µg/gdryweight)
wt	***Saline***	136.2±13.4	180.2±22.1
	LPS	272.8±14.5	185.6±26.1
	Saline	271.2±23.5	265.1±61.8
	Turpentine oil	183.2±21.3	126.4±17.9

Table 5.3.3 Hepatic iron in wt SWR mice treated with LPS or Turpentine oil for 16 hours. *The liver of wt mice treated with LPS and turpentine oil mice was divided into five lobes as described in chapter 3 and the iron content of each lobe was quantified. There was no difference between the iron content of lobe A and the other four lobes (B-E) in wt SWR mice treated with LPS. Data are Mean±SEM, n=3.*

5.3.3.2 Effect of inflammation on hepatic hepcidin 1 gene expression in wt SWR mice

Hepcidin mRNA expression levels were analysed by Real Time PCR. Treatment with LPS for 1.5 hours had no effect on hepcidin levels while treatment for 6 hours increased hepcidin expression though not significantly. Treatment for 16 hours was found to significantly decrease mRNA expression levels (Fig. 5.3.5).

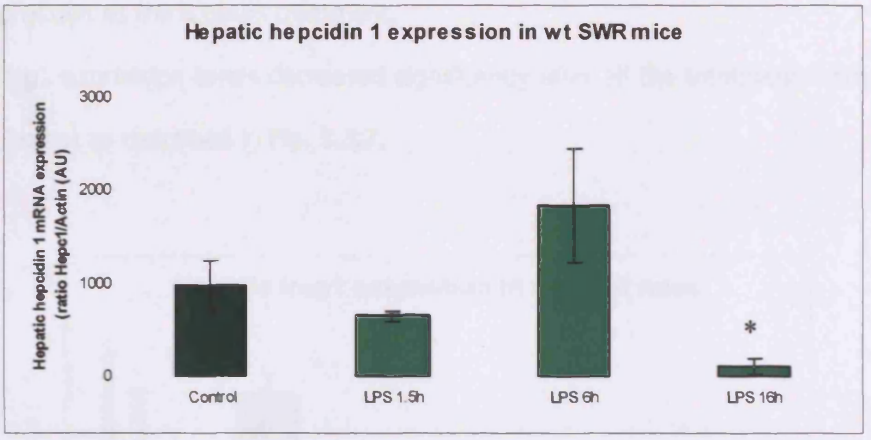

Figure 5.3.6 Time course effect of acute inflammation on hepatic hepcidin expression levels. *SWR wt mice were injected with LPS and sacrificed after 1.5, 6 and 16 hours. Hepcidin mRNA expression levels were analysed by Real Time PCR. Treatment for 1.5 hours had no effect while treatment for 6 hours showed an increase in hepcidin expression. Treatment for 16 hours decreased significantly hepcidin levels *p<0.05. Data are Mean±SEM, n=6 per group.*

Treatment of wt SWR mice with turpentine oil for 16 hours did not have a significant effect on hepatic hepcidin mRNA expression compared to non-treated mice.

5.3.3.3 Effect of inflammation on hepatic DMT1 and Ireg1 gene expression in wt SWR mice

Hepatic iron transporters gene expression, namely DMT1 and Ireg1 mRNA gene expression was analysed in wt SWR mice injected with LPS and Turpentine oil. Hepatic DMT1 decreased significantly after the 1.5 hours treatment with LPS compared to control (Control 0.085±0.029; LPS-treated 0.011±0.003, $p<0.05$). LPS treatment for 6 hours increased DMT1 though not significantly. In addition, treatment for 16 hours caused the same increase in DMT1 expression as the 6 hours treatment.

Hepatic Ireg1 expression levels decreased significantly after all the treatments with LPS (1.5, 6 and 16 hours) as described in Fig. 5.3.7.

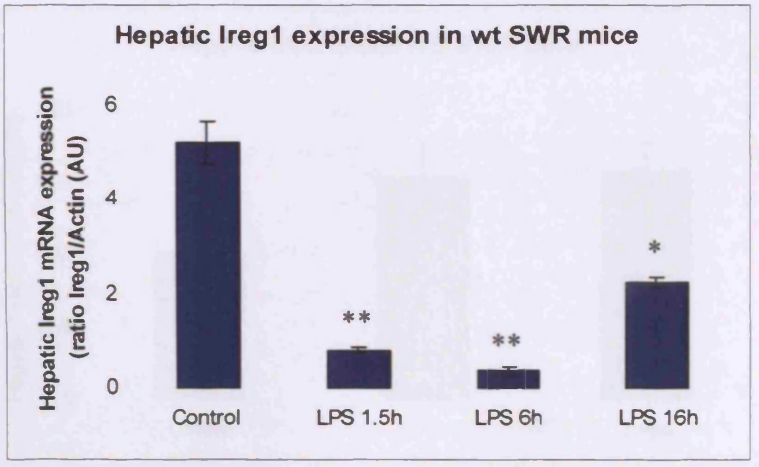

Figure 5.3.7 Effect of acute inflammation on hepatic Ireg1 expression.

*SWR wt mice were injected with LPS and sacrificed after 1.5, 6 and 16 hours. Ireg1 mRNA expression levels were analysed by Real Time PCR. All treatments with LPS lead to a reduction on hepatic Ireg1 expression levels. Data are Mean±SEM, n=6 per group, *p<0.05, **p<0.01.*

Turpentine treatment of wt SWR for 16 hours led to an increase in hepatic DMT1 expression compared to non-treated mice though not significant (Control 0.09±0.02; Turpentine-treated 0.22±0.05). Acute inflammation caused by turpentine injection also resulted in a significant decrease in hepatic Ireg1 expression levels (Control 9.04±2.27, turpentine-treated 0.96±0.14, n= 4 per group, $p<0.01$).

5.3.4 Effect of acute inflammation by LPS and Turpentine on hepatic iron content, hepatic hepcidin, DMT1 and Ireg1 gene expression in Hfe KO SWR mice

5.3.4.1 Effect of acute inflammation on hepatic iron content in Hfe KO mice

Iron content was analysed in Hfe KO SWR treated with LPS and Turpentine oil for 16 hours. Contrary to what it was found in wt mice, acute inflammation induced by both LPS and turpentine treatment had no significant effect on hepatic iron content (Fig. 5.3.8).

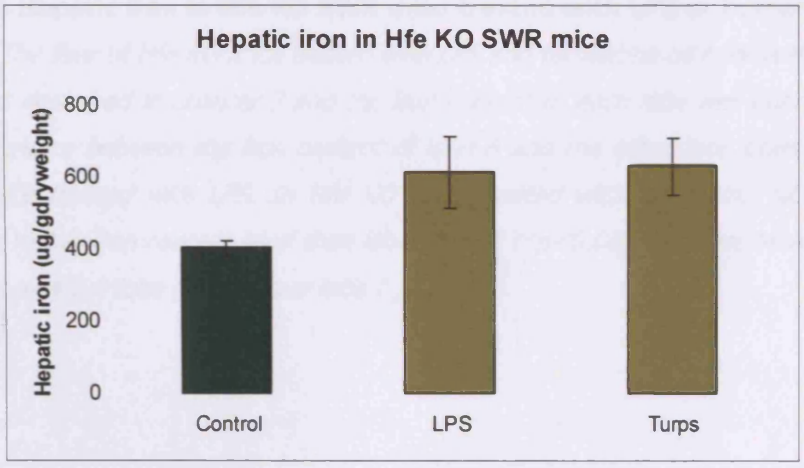

Figure 5.3.8 Liver iron content in Hfe KO SWR mice in acute inflammation. *Mice injected with LPS and turpentine were sacrificed after 16 hours; the whole liver was removed and divided into five lobes. Iron was quantified in each lobe and the average of the iron content in each whole liver was calculated. Treatment of Hfe KO SWR mice with LPS and turpentine oil had no significant effect on hepatic iron content. Data are Mean±SEM, Control n=6; LPS n=4; Turps n=6.*

When the iron content in each lobe was analysed in LPS and turpentine treated mice, there was no difference between the iron content of the five lobes of non-treated mice. In LPS-treated Hfe KO mice there was no significant difference between the iron content of lobe A

the remaining lobes was observed (Table 5.3.4) while in turpentine-treated Hfe KO mice iron content of lobe A was significantly higher.

SWR MICE	TREATMENT	LOBE A IRON CONTENT (µg/gdryweight)	LOBE B-E IRON CONTENT (µg/gdryweight)
Hfe Knockout	*Saline*	608.2±139.1 [a]	376.5±66.2 [a]
	LPS	1030.1±248.3 [b]	472.8±79.3 [b]
	Saline	488.5±61.8 [a]	367.7±43.2 [a]
	Turpentine oil	1101.5±144.7 [c] *	513.3±44.1 [c]

Table 5.3.4 Hepatic iron in Hfe KO SWR mice treated with LPS or Turpentine oil for 16 hours. *The liver of Hfe KO mice treated with LPS and turpentine oil mice was divided into five lobes as described in chapter 3 and the iron content of each lobe was quantified. There was no difference between the iron content of lobe A and the other four lobes (B-E) in Hfe KO SWR mice treated with LPS. In Hfe KO mice treated with turpentine oil, lobe A had significantly higher iron content level than lobes B to E (*p<0.05). Data are Mean±SEM, n=3 per lobe ([a]), n=4 per lobe ([b]), n=6 per lobe ([c]).*

5.3.4.2 Effect of inflammation on hepatic hepcidin 1 gene expression in wt SWR mice

Treatment of Hfe KO mice with LPS for 1.5 hours increased hepcidin mRNA expression though not significantly (Fig. 5.3.9). Hepcidin expression was also increased after LPS treatment for 6 hours but to a lesser extent. Interestingly LPS treatment for 16 hours of Hfe KO mice showed significantly lower hepcidin 1 expression levels than non-treated animals (Fig. 5.3.9). Treatment of SWR Hfe KO mice with Turpentine oil for 16 hours had no effect on hepcidin mRNA expression levels.

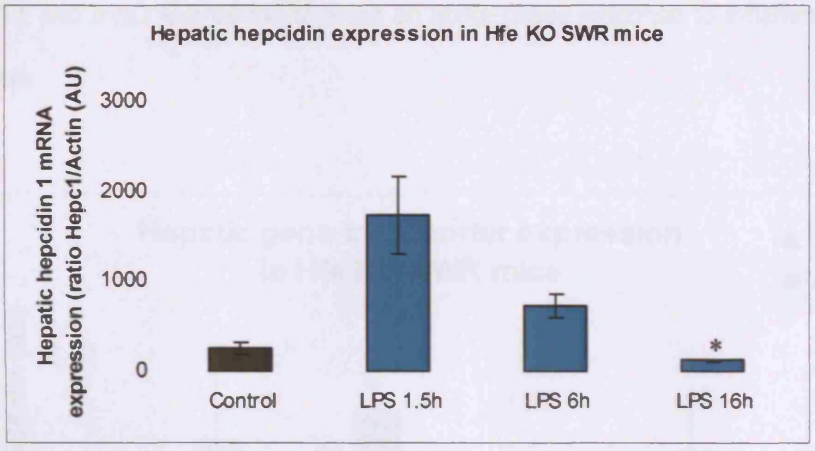

Figure 5.3.9 Effect of acute inflammation on hepatic hepcidin expression in Hfe KO SWR mice. *SWR Hfe KO mice were injected with LPS, sacrificed after 1.5, 6 and 16 hours and hepcidin 1 mRNA expression levels were analysed by Real Time PCR. Treatment for 1.5 hours increased hepcidin expression levels though not significantly. Treatment for 6 hours was also found to up regulate hepcidin levels but to a lesser extent. Treatment for 16 hours significantly decreased hepcidin 1 expression levels* $*p<0.05$*. Data are Mean±SEM, n=6 per group.*

5.3.4.3 Effect of inflammation on hepatic DMT1 and Ireg1 gene expression in Hfe KO SWR mice

Hepatic mRNA expression levels of DMT1 and Ireg1 were analysed in Hfe KO mice treated with LPS for 1.5, 6 and 16 hours (Fig. 5.3.10). Hepatic DMT1 RNA expression following LPS injection increased significantly after one and an half hours and decreased significantly after 6 hours remaining at the same level after the 16 hours treatment. Hepatic Ireg1 did not change after the 1.5 hours treatment with LPS but decreased in animals injected with LPS for 6 hours. Treatment for 16 hours with LPS increased Ireg1 expression to control levels. Both hepatic DMT1 and Ireg1 expression showed an acute-phase response to inflammation in Hfe KO SWR mice.

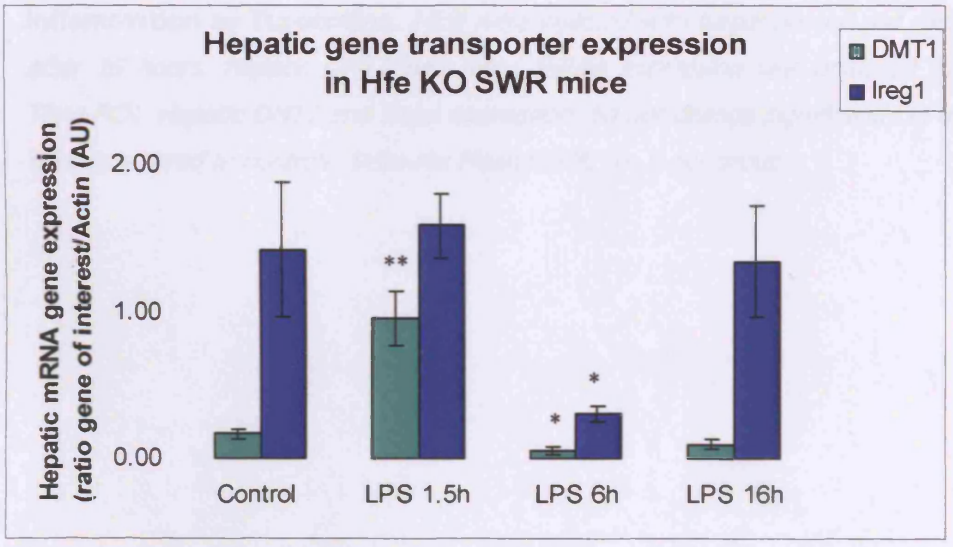

Figure 5.3.10 Expression of mRNA iron transporter genes after acute inflammation for 1.5, 6 and 16 hours. *Mice were injected with LPS for 1.5, 6 and 6 hours. Hepatic DMT1 and Ireg1 mRNA expression were analysed by Real Time PCR. Both hepatic DMT1 and Ireg1 expression showed an acute-phase response to inflammation in Hfe KO SWR mice. Data are Mean±SEM, n= 3 per group; *p<0.05, **p<0.01.*

Turpentine injection resulted in a decrease of both hepatic DMT1 and Ireg1 expression in Hfe KO mice though not significantly (Fig. 5.3.11).

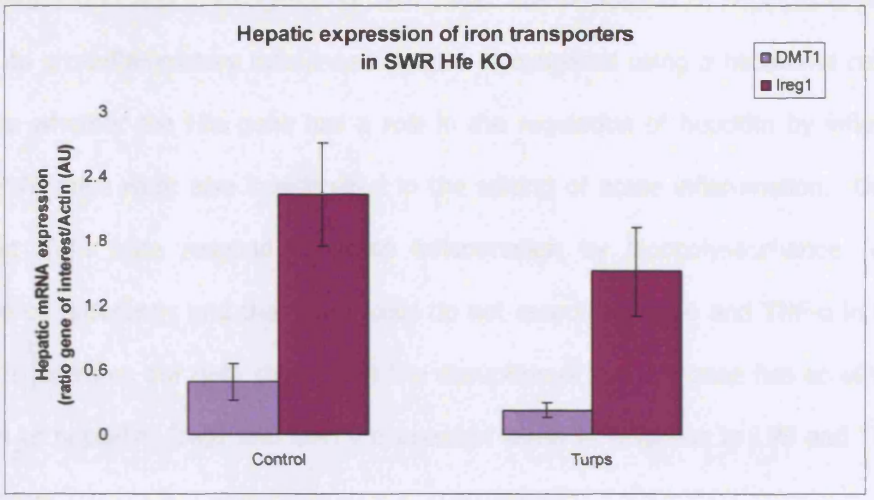

Figure 5.3.11 Hepatic iron transporters mRNA expression in acute inflammation by Turpentine. *Mice were injected with turpentine oil and sacrificed after 16 hours. Hepatic DMT1 and Ireg1 mRNA expression was analysed by Real Time PCR. Hepatic DMT1 and Ireg1 expression did not change significantly in treated mice compared to controls. Data are Mean±SEM, n= 5 per group.*

5.4 Discussion

In this chapter the regulation of hepcidin expression in response to two different models of acute inflammation was investigated in SWR mice. The regulation of hepcidin expression in response to pro-inflammatory cytokines was also investigated using a hepatoma cell line. To investigate whether the Hfe gene has a role in the regulation of hepcidin by inflammation, Hfe KO SWR mice were also investigated in the setting of acute inflammation. Our results show that SWR mice respond to acute inflammation by Lipopolysaccharide (LPS) and turpentine oil differently and that Huh7 cells do not respond to IL-6 and TNF-α in the same manner. In addition, our data shows that the disruption of the Hfe gene has an effect in the regulation of hepcidin, Ireg1 and DMT1 expression levels in response to LPS and Turpentine oil treatment.

In this study we have shown that in wt SWR mice, acute inflammation by either LPS or Turpentine oil injection for longer than six hours decreases serum iron and transferrin saturation levels but has no effect on the hepatic iron content levels. Injection of LPS in Hfe KO mice decreased significantly transferrin saturation after 16 hours and serum iron levels although this failed to reach statistical significance. In contrast, turpentine injection of Hfe KO mice had no effect no serum iron levels. As observed in wt SWR mice, LPS and turpentine oil injection had no effect of hepatic iron content of Hfe KO mice.

Hepatic hepcidin expression in wt SWR mice was upregulated up to 6 hours post-treatments with LPS in this study in accordance with previously published reports (Pigeon et al. 2001;Sheikh et al. 2007). In addition, LPS injections for 6 hours was found to upregulate hepcidin expression levels in Hfe KO SWR mice. Interestingly hepcidin mRNA expression levels were found to be significantly downregulated in both wt and Hfe KO SWR mice 16 hours after LPS injections.

Turpentine oil injection for 16 hours decreased hepcidin mRNA expression levels in wt SWR mice though this failed to reach statistical significance while in Hfe KO mice, turpentine treatment was found to have no effect on hepcidin expression levels.

Contradictory reports have been published on the effect of LPS stimulation on hepcidin expression levels in Hfe KO mice and the requirement of Hfe or other genes for the up-regulation of hepcidin in inflammation conditions. In some reports, a response to LPS stimulation and hypoferremia are absent (Roy et al. 2004), in others this lack of response is attributed to differences from animal to animal (Lee et al. 2004) and in a recently published paper it was reported that although basal hepcidin levels are dependent on the presence of the Hfe gene, Hfe KO mice are still able to regulate hepcidin in acute inflammation (Constante et al. 2006). Here we have shown that Hfe KO mice upregulating hepcidin expression in response to LPS-induced inflammation but in turpentine-induced acute inflammation no change is observed in hepcidin mRNA expression levels.

Injected LPS is mainly taken up by the Kupffer cells and is responsible for the upregulation of IL-6 in the liver (Ganz 2003) while turpentine oil injections lead to an induced local irritation which results in the recruitment of inflammatory cells and the upregulation of IL-6 in the injured muscle. In addition turpentine oil injection results in the production of IL-6, IL-1β and TNF-α in hepatocytes (Sheikh et al. 2007). In this study we have shown that when hepatocytes are exposed to IL-6, hepcidin expression levels increased by 4-fold confirming findings by other groups that IL-6 has a direct effect on hepcidin expression (Nemeth et al. 2003;Nemeth et al. 2004a).

Our results show that Hfe is not necessary for the upregulation of hepcidin by LPS injection as previously shown by other groups (Lee et al. 2004). In addition we have shown that the disruption of the Hfe gene abrogates the regulation of hepcidin by turpentine injection. Studies in human hepatoma (Huh7) cells have shown that IL-1β induces hepcidin expression in an IL-6 independent mechanism (Inamura et al. 2005). In this study we have shown that TNF-α does not upregulate hepcidin expression in Huh7 cells and therefore it is possible that the disruption of the Hfe gene prevents the release of IL-1β in response to acute inflammation by turpentine oil injection preventing hepcidin upregulation in Hfe KO mice but this requires further investigation.

In cells transfected with the iron exporter Ireg1 and in macrophages, hepcidin has been shown to interact directly with the Ireg1 protein (De, I et al. 2005;Delaby et al.

2005;Drakesmith et al. 2005;Knutson et al. 2005;Nemeth et al. 2004b). Our group has shown that a course of injections of recombinant hepcidin (synthesised in-house) into mice results in a decreased in iron uptake (Laftah et al. 2004). In addition a single injection of hepcidin into rats has been shown to downregulate duodenal Ireg1 mRNA expression (Rivera et al. 2005b). Here have shown that IL-6-induced production of hepcidin by hepatocytes does not alter hepatic DMT1 or Ireg1 protein expression. In addition, acute inflammation by LPS or turpentine oil injection in wt SWR mice was shown to decrease hepatic Ireg1 as previously shown (Krijt et al. 2006;Sheikh et al. 2007;Yang et al. 2002). In contrast, LPS injection in Hfe KO SWR mice was found to only significantly downregulate hepatic Ireg1 expression 6 hours pos-treatment while turpentine injection for 16 hours had no effect on Ireg1 expression in these mice. As observed with hepcidin expression the results suggest that Hfe gene has a vital role in the regulation of Ireg1 expression in the liver in a turpentine-induced inflammatory setting. This finding together with some published reports, also suggest that the regulation of hepatic Ireg1 expression is independent of hepcidin expression in an inflammatory setting (Mena et al. 2006;Yeh et al. 2004).

The spleen is one of the major sites of Ireg1 expression and hypoferremia is thought to occur as a consequence of hepcidin mediated inhibition of iron release from reticuloendothelial macrophages (resident in spleen and liver) through Ireg1. Our group has shown that hepcidin treatment of mice and a human macrophage cell line results in a significant decrease in Ireg1 expression in the spleen (personal communication by Dr. Paul Sharp). To investigate further the effect of inflammation and the increase of hepcidin expression levels on iron uptake and retention in the spleen, we quantified the iron content of the spleen following LPS and turpentine treatment. Here we show that LPS and turpentine injection has no significant effect on splenic iron content in wt or Hfe KO SWR mice 16 hours post-treatment suggesting that although hepcidin injections cause splenic Ireg1 expression to decrease and thus reticuloendothelial macrophages accumulate iron in the spleen, the hepcidin produced as a result of inflammatory inducers does not have the same effect. As our results show that hepcidin expression levels are decreased after 16 hours post-injection with LPS and

turpentine oil, it is possible that the levels of hepcidin produced in this setting were not sufficiently high to have a significant effect on Ireg1 expression and thus splenic iron content.

As previously shown in wt rats (Sheikh et al. 2007) our study shows that acute inflammation upregulates hepatic DMT1 expression in wt mice. In contrast hepatic DMT1 expression was found to be downregulated by LPS and turpentine treatment in Hfe KO SWR mice. Similarly to hepatic Ireg1 expression, hepatic DMT1 expression appears to be dependent on the presence of the Hfe gene and independent of hepcidin expression in an inflammatory setting although this requires further investigation.

In this study we have also investigated the role of hepcidin in duodenal iron uptake in an inflammatory setting using Huh7 cells. Incubation of an intestinal epithelial cell line (Caco-2) with IL-6 had no effect on intestinal DMT1 or Ireg1 expression, confirming the previous findings that IL-6 has no direct effect on duodenal iron uptake (Raja et al. 2005).
To investigate the possibility that IL-6 is regulating intestinal iron absorption through hepcidin expression, conditioned medium from Huh7 cells was used as a source of hepcidin to determine its effects on intestinal iron transporter expression.
Applying the conditioned medium from IL-6-stimulated HuH7 cells to the basolateral surface of the Caco-2 monolayer for 24 hours significantly decreased the expression of DMT1 (+IRE) compared with transporter levels in cells incubated in medium from unstimulated Huh7 cell cultures. To further investigate whether the induced hepcidin was responsible for the downregulation of duodenal DMT1 and Ireg1 expression, medium was collected from IL-6 stimulated Huh7 cells, incubated with anti-human hepcidin antibody and added to Caco-2 cell monolayers. Duodenal DMT1 and Ireg1 was significantly greater in cells exposed to conditioned medium pre-treated with the hepcidin antibody suggesting that Hepcidin might be the possible component in the medium inhibiting intestinal iron uptake. Recently a report has shown that hepcidin released from IL-6-stimulated Huh7 cells decreased iron export in THP-1 macrophages using similar methodology to this study (Andriopoulos and Pantopoulos 2006).

In conclusion, the results from the present study taken together with previous work from our group (Johnson et al. 2004) demonstrate that the pro-inflammatory cytokines TNF-α and IL-6 can both regulate intestinal iron metabolism. TNF-α seems to act directly with intestinal epithelial cells to decrease the expression of the apical iron transporter DMT1, while IL-6 seems to influence intestinal iron absorption via stimulating the release of hepatic hepcidin.

Our study of acute inflammation by LPS and Turpentine oil in SWR mice has shown that although hepcidin expression is upregulated rapidly as a result of inflammation, hepcidin expression levels decreases around 16 hours post-treatment suggesting a feedback loop response to the hypoferremia caused by the inflammation. In addition our study has confirmed that the two models of inflammation regulate gene expression very differently. Our data suggests that the disruption of the Hfe gene abrogates the gene expression of hepcidin, hepatic DMT1 and Ireg1 in response to acute inflammation by turpentine oil but not by LPS injection. Furthermore, we have provided evidence that although hepcidin expression levels in the inflammatory setting leads to hypoferremia, hepcidin expression does not have a direct effect on hepatic DMT1 or Ireg1 expression levels. Instead the data suggests that the changes in hepatic DMT1 and Ireg1 expression results from a hepcidin independent effect of the cytokines produced in acute inflammation.

CHAPTER 6

HYPOXIA AND ANAEMIA AS HEPCIDIN EXPRESSION MODULATORS

&

HEPCIDIN AS A DUODENAL IRON ABSORPTION REGULATOR

6.1 Hypoxia and Anaemia as hepcidin expression modulators & Hepcidin as a duodenal iron absorption regulator

In humans iron absorption is mainly regulated by iron stores (stores regulator) and the rate of erythropoiesis (erythroid regulator). Erythroid stimulation of iron absorption occurs regardless of body iron stores, aiming to provide an adequate iron supply for red blood cell (erythrocytes) production. Tissue hypoxia is the main stimulus of Erythropoeitin (EPO) production. EPO is a glycoprotein hormone produced by the kidneys and the liver that is a cytokine that induces the production of erythrocyte precursors in the bone marrow (Jelkmann 2004;Tan and Ratcliffe 1992). The subsequent development of the erythrocytes depends on an iron supply from the diet or from the iron storage pool in macrophages and hepatocytes.
In 1988 Peters et al provided evidence that hypoxia enhances iron uptake by a mechanism that is independent of stimulated erythropoiesis (Peters et al. 1988;Raja et al. 1988;Raja et al. 1986). The group demonstrated that exposure of splenectomized 89Sr-treated mice to hypoxia resulted in an increase in the total intestinal iron uptake, without any change in erythropoiesis. This suggested that the increase in intestinal mucosal iron uptake which follows hypoxia was not mediated by erythropoietin or other factors associated with increased erythropoiesis (Raja et al. 1986). These authors also demonstrated that transgenic mice with partial deficiency of erythropoietin due to hypoplastic anemia have increased iron absorption, with no increased erythropoiesis (Raja et al. 1997).

Hepcidin has been shown to be homeostatically regulated by hypoxia and anaemia. In hypoxic conditions it has been reported that hepcidin expression levels decrease, its inhibitory effects on iron absorption diminish and more iron is acquired from the diet and from the storage pool in macrophages and hepatocytes (Nicolas et al. 2002b). The low levels of hepcidin will allow iron uptake from intestine and recirculation from macrophages and iron will be delivered to bone marrow to sustain the production of erythrocytes (erythropoiesis). Mice exposed to hypoxia for 3 days have been shown to exhibit a two- to threefold increase in iron absorption (Raja et al. 1990). For this reason Hepcidin is suggested to act as the

erythroid regulator that transmits the erythroid demand of the organism to the enterocyte (Fleming and Sly 2001;Nicolas et al. 2001;Nicolas et al. 2002b) and not EPO as previously suggested.

Treatment of mice with synthetic hepcidin led to the reduction in iron uptake seen in the intestinal cell line and in mice. Injection of Erythropoietin (EPO) in mice was found to also decrease liver hepcidin expression but the finding that irradiation prevented this hepcidin suppression, ruled out a direct effect of EPO on hepcidin synthesis (Nicolas et al. 2002b;Vokurka et al. 2006).

Anaemia has been found to regulate hepcidin levels in a similar manner to hypoxia. Mice that were bled or had undergone phenylhydrazine-induced hemolysis showed a decrease in hepcidin mRNA levels in the liver and duodenum while iron absorption was increased (Bondi et al. 2005;Frazer et al. 2004b;Latunde-Dada et al. 2004;Nicolas et al. 2002b;Vokurka et al. 2006). Anaemia induced by mouse mutations that restrict the uptake of iron in the small intestine (*sla* and *mk* mice) also show a significant decrease in hepatic hepcidin mRNA. Importantly, anaemia has a stronger effect in the suppression of hepcidin than iron overload has on the stimulation of hepcidin, as seen in hemolytic phenylhydrazine-induced iron-overloaded mice (with the exception of thalassaemic mice).

Thalassaemia syndromes belong to a group of conditions characterised by anaemia with ineffective erythropoiesis which leads to an increased absorption of dietary iron and a consequently iron overload (reviewed by Andrews 1999). In β- thalassaemia major, hepcidin levels correlated with parameters of erythropoiesis and anaemia but not with indices of iron overload such as liver iron concentrations, ferritin, serum iron or transferrin saturation. There was however, a negative correlation between hepcidin levels and Non-Transferrin Bound Iron (NTBI) which suggested that low levels of Hepcidin allow the increase of iron flow into plasma, leading to saturation of transferrin and NTBI formation. It has been suggested that hypoxia and other still undefined signals from the erythroid activity, downregulate hepcidin

production which then allows the iron overload of patients with thalassaemia to develop (Papanikolaou et al. 2005).

In the murine model of human thalassaemia, the $Hbb^{th3/+}$ mice, hepcidin mRNA expression was found to be decreased despite the iron overload (Adamsky et al. 2004). Although it has been reported that urinary Hepcidin is decreased in patients with Thalassaemia Major, hepcidin mRNA expression levels have not yet been described (Papanikolaou et al. 2005).
Occurrence of anaemia and tissue iron overload is also encountered in mice with transferrin deficiency (hpx/hpx) mice. In these mice erythropoiesis is functional though iron restricted or ineffective and Hepcidin expression is decreased (Adamsky et al. 2004;Weinstein et al. 2002). These findings confirm that the iron overload is less dominant than the anaemia in regulating Hepcidin expression in the anaemia setting (Andrews 1999;Finch 1994).

In this study, the human hepatoma-derived cell line, HepG2 was used to investigate the effect of hypoxia on hepcidin mRNA expression levels. An animal model of chronic hypoxia, equivalent to the partial pressure of inspired oxygen at an altitude of 5000 m above sea level was also studied to investigate the changes in iron uptake from the duodenal lumen and its transfer to the blood. Hepcidin mRNA expression levels in rat liver before and after direct exposure to reduced oxygen were quantified by Real Time-PCR.
Urinary Hepcidin has been reported to be decreased in patients with Thalassaemia Major and Thalassaemia Intermedia, but hepcidin mRNA expression levels have not yet been described. In this study we investigate hepcidin mRNA expression levels in thalassaemia major and thalassaemia minor patients receiving different treatments.
To further investigate the effect of Hepcidin on intestinal iron transport *in vivo* iron uptake was measured and serum iron levels and transferrin saturation were quantified in mice injected with Hepcidin.

6.2 Methods

6.2.1 Short term hypoxia of hepatoma cell line

HepG2 cells were cultured in RPMI1640 medium (Sigma, Poole, UK) containing L-Glutamine (Sigma, Poole, UK), antibiotics and 10% FCS (Sigma, Poole, UK) and maintained in 5% CO2 at 37^0C till confluent. The medium was changed every 2-3 days. Cells were passaged at confluence using 0.5mg/ml trypsin (Sigma, Poole, UK). Prior to the experiment HepG2 cells were seeded in $5cm^2$ wells. Cells were cultured to confluency and the medium was changed immediately prior to exposure to hypoxia. HepG2 cells were made hypoxic by placing them in stainless steel hypoxia chambers as previously described (Mazure et al. 2002). The chambers were evacuated until the desired oxygen partial pressure, deduced by measuring the pressure with an electronic pressure sensor (SMC digital pressure sensor; SMCCorporation, Tokyo, Japan) was reached. The chambers were then refilled with a gas mixture containing 5% CO_2 and 95% N_2 and a final concentration of oxygen (O_2) of 1% used. The chambers were then placed in an incubator at 37°C for 24 hours and 48 hours. After hypoxia, the culture medium was removed, cells were washed with PBS and RNA was extracted.

Figure 6.2.1 Hypoxic chamber. *Photograph of an incubator taken from the web page: (hht://www.brincubator.com/hypoxiachamber.htm) on the 12/08/2006.*

6.2.2 Long term hypoxia of Sprague-Dawley rats

Sprague-Dawley rats (initial weight 90-100 g) supplied by the Animal Services Centre of the Chinese University of Hong Kong, were exposed for 4 weeks to room air mixed with nitrogen to reduce oxygen concentration to 10%, or room air alone (Leung et al. 2000). Cages containing four rats were kept in sealed Perspex chambers with inflow and outflow ports for inspired normal or hypoxic air. Water and rat chow were supplied *ad libitum* to the hypoxic group and the weight of chow consumed was monitored so that the normoxic group was supplied the same amount of chow. Animals were weighed twice-weekly. At the end of 4 weeks, rats were anaesthetized with pentobarbitone sodium (40mg/kg, i.p.) and sacrificed. Livers were removed for gene expression analysis by Real Time PCR. RNA was extracted as described in chapter 2.2 and frozen at -80^0 until required for PCR analysis.

All experimental procedures were approved by the Animal Experimentation Ethics Committee of the Chinese University of Hong Kong.

6.2.3 Hepcidin injections of C57BL/6 mice

Male C57BL/6 mice aged 4 weeks were placed on an iron adjusted diet (44mg Fe/Kg diet) for 3 weeks prior to experimentation. Mice were given a single intraperitoneal injection of either 10µg hepcidin (Peptides International Inc. Louisville, KY) or an equivalent volume of the diluent (saline).

6.2.4 Iron uptake across duodenum in C57BL/6 injected with Hepcidin

After four hours, mice were anaesthetized with pentobarbitone sodium (40mg/kg, i.p.) and the duodenum was washed through with warm 0.15M NaCl followed by air. The lower end of the duodenum segment (proximal to the ligament of Treitz) was tied off and uptake buffer (Hepes-buffered saline containing 0.2mM $^{59}Fe^{2+}$ complexed with 4mM ascorbate, pH 6.5) was instilled proximally from a tied-in syringe. After 15 minutes, during which the animal body temperature was maintained at 37^0 with a thermostatically controlled heating blanket, blood samples and the duodenal segment were removed. The tissue was then washed free of surface bound iron using a solution containing 2 mM unlabelled iron followed by 0.15 M NaCl, and finally dried overnight. The mucosal layer was scraped off, weighed and together with weighed blood samples and the animal carcass, was gamma-counted (Packard 5003, Cobra II Auto-Gamma, Global Medical Instrumentation, Inc., Minnesota, USA) for the determination of ^{59}Fe.

Livers were removed for gene expression analysis. RNA was extracted as described in chapter 2.2 and frozen at -80^0 until required for Real Time PCR analysis. Blood was removed by cardiac puncture and serum iron and transferrin saturation was analysed using a commercially available assay (Randox Laboratories Ltd. Antrim, UK).

6.2.5 Liver biopsies of Thalassaemic Major (TM) and Thalassaemia Intermedia (TI) patients

Liver biopsies were obtained from thalassaemia major (TM) patients (n=14, male= 8, female= 6) on regular transfusion programmes (3-4 weekly) and from thalassaemia intermedia (TI) patients (n=6, male= 4, female= 2) receiving different treatment regimes. Of the 6 thalassaemia intermedia (TI) patients two were not currently receiving transfusion. The mean average age of the patients was 25.6±5.1 years of age for the TM patients and 30±10.5 years of age for TI patients. Data on liver iron, ferritin levels and haemoglobin of the patients are described on Table I of appendix I. Ethical permission was obtained from all the subjects mentioned in this study. RNA from liver biopsies was extracted as described in chapter 2.2 and frozen at -80^0 until required for Real Time PCR analysis.

6.3 Results

6.3.1 Hepcidin mRNA expression levels in response to hypoxia *in vitro*

Hepcidin mRNA expression levels of HepG2 cells were determined by Real Time-PCR after the cells were exposed to 1% oxygen for up to 48 hours. When compared to the housekeeping gene HPRT, hepcidin mRNA expression was reduced by 24.8% and 50.0% after 24 and 48 hours of hypoxia respectively, the value at 48 hours being significantly different to the control value (Fig. 6.3.1).

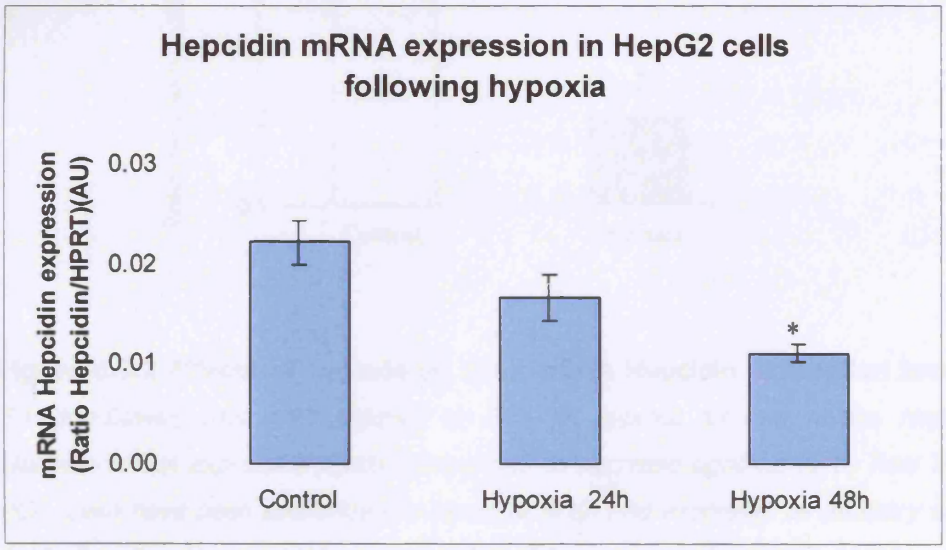

Figure 6.3.1 Effect of hypoxia on hepatocytes mRNA hepcidin expression levels *HepG2 cells were exposed to 1% oxygen for 24 and 48 hours. Hypoxia for 48 hours was shown to significantly decrease hepcidin mRNA expression levels by Real Time PCR. Data have been normalized to levels of HPRT and expressed as arbitrary units (AU). Results are expressed as Mean±SEM of samples from each 3 (control and 24 hour hypoxia) and 4 (48 hours hypoxia) cells, *p<0.02.*

6.3.2 Effect of hypoxia *in vivo* on hepcidin mRNA expression levels

Sprague-Dawley rats made hypoxic for four weeks showed significant reduction in hepcidin mRNA expression levels (Fig. 6.3.5). Hypoxia was confirmed by the increased expression of the housekeeping gene GAPDH mRNA expression.

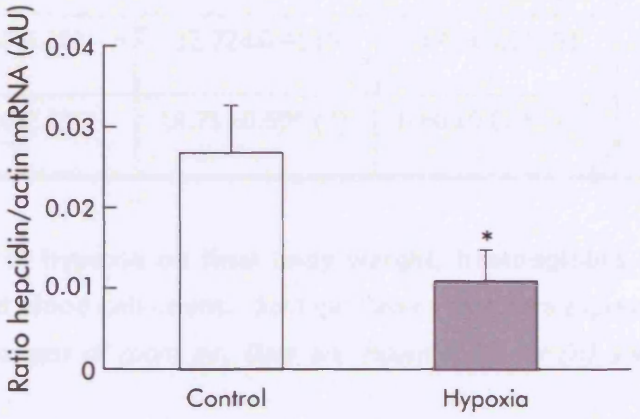

Figure 6.3.2 Effects of hypoxia on liver mRNA Hepcidin expression levels. *Sprague-Dawley rats were exposed to 10% O_2 hypoxia for four weeks. Hepatic Hepcidin mRNA expression levels were shown to decrease significantly by Real Time PCR. Data have been normalized to levels of Actin and expressed as arbitrary units (AU). Results are expressed as Mean±SEM of liver samples from each of 3 (control) and 4 (hypoxia) animals, *p<0.01.*

The four weeks hypoxia treatment had no effect on animal body weight but caused significant increases in blood haemoglobin concentration, haematocrit and erythrocyte count (Table 6.3.1).

	FINAL BODY WEIGHT (g)	HAEMOGLOBIN (g/dL)	HAEMATOCRIT	RED BLOOD CELL COUNT (x 10^{12}/L)
Control	210.4±5.6 (18)	12.72±0.41 (5)	0.41±0.01 (5)	7.33±0.48 (5)
Hypoxic	223.6±6.2 (21)	18.71±0.59* (7)	0.60±0.02* (7)	9.43±0.18* (7)

Table 6.3.1 Effects of hypoxia on final body weight, haemoglobin concentration, haematocrit and red blood cell count. *Sprague-Dawley rats were exposed for 30 days to air containing 10% oxygen or room air. Data are Means±SEM for (n) animals. *p<0.001 compared to control.*

6.3.3 Hepatic hepcidin expression levels in the Thalassaemia setting

Three patients with high transaminase levels (>80 iu/ml) had low hepcidin mRNA levels (77 ± 16 %) and increased levels of fibrosis compared to those with lower transaminase levels (106 ± 55%) and only mild fibrosis (personal communication by Dr. Farrah Shah).

Hepcidin mRNA expression levels were not significantly different between the two thalassemia groups; Thalassemia Intermedia (3.84±0.83) compared to Thalassemia Major (4.06±0.99). However hepcidin mRNA expression levels was significantly lower in thalassemia patients with liver iron concentrations >10mg/gdryweight compared to those with lower iron concentrations (85 vs 131%, p=0.05) (Table II in appendix I).

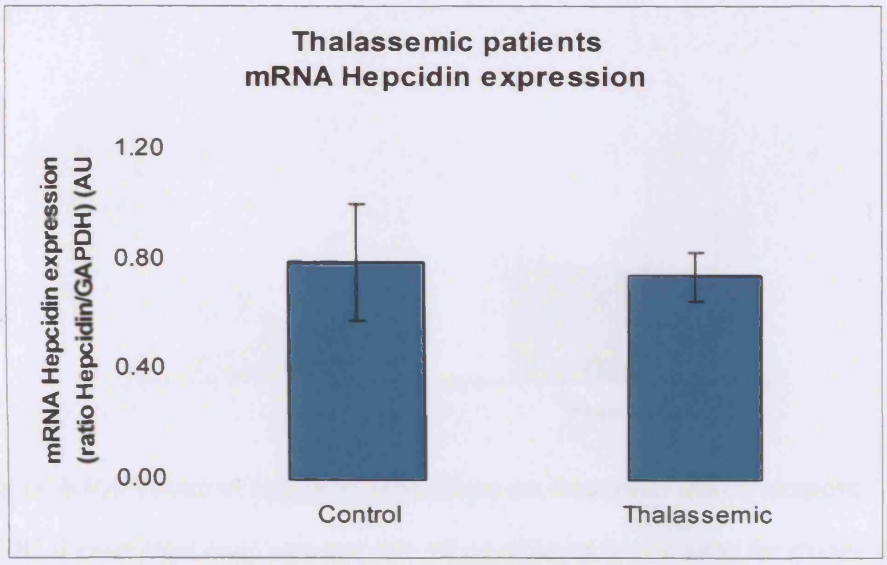

Figure 6.3.3 Hepcidin mRNA expression levels in thalassemic patients. *Hepcidin expression was investigated in biopsies from thalassemia major (TM) and thalassemia intermedia (TI) patients (n=14 and n=6, respectively). Data expressed as Mean±SEM.*

Hepcidin expression did not vary significantly with anaemia, with ferritin > 3000ng/ml or <1500ng/ml (p=0.99). Moreover there was no significant difference between the thalassaemia patients (TM and TI) compared with controls (Fig. 6.3.3).

6.3.4 Hepcidin as a regulator of intestinal iron transport

Mice injected with hepcidin show after 4 hours a significant decrease in serum iron content (5.7±2.4 µmol/L) compared to control animals (14.7±0.9 µmol/L). Hypoferremia was accompanied by a 27% decrease in transferrin saturation in the hepcidin treated mice (control 60.7±9.3%; hepcidin treated 34.0±10.2%. $p<0.05$).

Uptake and transfer of iron across the duodenal mucosa (Fig. 6.3.4) showed no significant difference between control and hepcidin-treated animals (duodenal counts, $p>0.93$; blood/carcass counts, $p>0.11$ respectively).

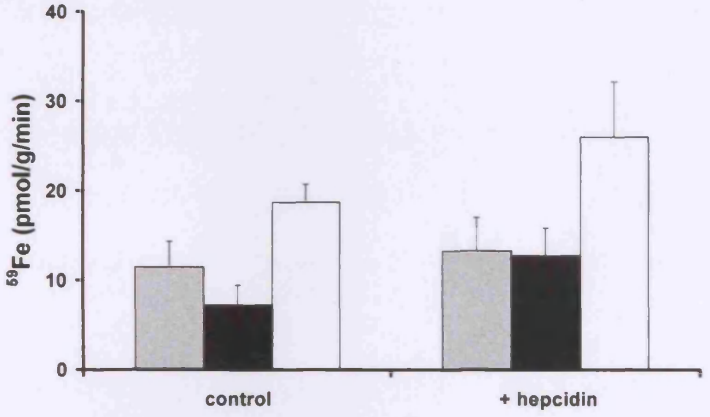

Figure 6.3.4 Effect of hepcidin injections on duodenal iron transport

C57BL/6 male mice were injected with 10 µg of hepcidin and used for studies 4 hours later. The duodenum lumen was filled with 200µM $^{59}Fe^{2+}$ for 15 minutes and the subsequent levels of ^{59}Fe in duodenal mucosa, blood and carcass determined by gamma counting. There was no significant difference in mucosal iron retention (grey bars), mucosa iron transfer (black bars) and total mucosal uptake (white bars) between control and hepcidin-treated animals. Data are Mean±SEM of 6 observations in each group.

The effect of hepcidin on Ireg1 protein expression in the duodenum and in the spleen was investigated by other members of the group and therefore is not shown here. It was however found that in the duodenum hepcidin treatment had no effect on Ireg1 protein expression

levels while in the spleen hepcidin-treated animals revealed a 50% reduction in Ireg1 protein levels (personal communication Dr. Paul Sharp).

6.4 Discussion

Chronic hypoxia requires the erythroid regulator to increase the production of red blood cells to carry more oxygen. The subsequent production and development of the erythrocytes cannot be compensated by the iron storage pool and therefore depends on an iron supply from the diet. Therefore an increase in iron absorption is required to enable the iron to be delivered to bone marrow to sustain the production of erythrocytes (erythropoiesis). Recent work from our laboratory on rats has shown that increased entry of iron in the body during hypoxia occurs by both stimulation of iron entry across luminal membrane into the enterocyte and enhanced iron transfer across the basolateral membrane into the perfusing blood (Leung et al. 2005). The changes in iron uptake caused by hypoxia were independent of villus length implying altered function of individual enterocytes. Previous studies by the same group on hypoxia responses suggest that the increased iron movement across the brush border is due in part to an increased electrical driving force for proton -mediated iron transport across this membrane (O'Riordan et al. 1995). Interestingly in the present study (Leung et al. 2005), significantly lower levels of absorbed iron in hypoxic mucosa were found following the in vivo transfer study despite the high iron uptake by isolated duodenum. This implies a proportionally greater effect of hypoxia on iron transfer across the basolateral membrane to the blood.

Hypoxia stimulates the secretion of erythropoietin (EPO) and although the increase in iron uptake seen in these hypoxic rats could be a result of stimulated erythropoiesis, studies have shown that EPO does not have a direct effect on the regulation of iron absorption (Peters et al. 1988;Raja et al. 1988;Raja et al. 1986;Raja et al. 1997).

Evidence is emerging that intestinal iron transport is under hormonal control; studies suggest a humoral effect on iron transport is linked to an inflammatory response (Raja et al. 1990). Since then Hepcidin has been identified as a negative regulator of duodenal iron transport homeostatically regulated by hypoxia and anaemia. In hypoxic conditions it has been reported that hepcidin expression levels decrease, its inhibitory effects on iron absorption diminish and more iron is acquired from the diet and from the storage pool (Laftah et al.

2004;Nicolas et al. 2002b). These low levels of Hepcidin will then allow iron uptake from intestine to increase as required. Consequently Hepcidin is thought to act as the erythroid regulator that transmits the erythroid demand of the organism to the enterocyte (Fleming and Sly 2001;Nicolas et al. 2001;Nicolas et al. 2002b).

In this study, four weeks hypoxia significantly decreased hepatic hepcidin mRNA expression levels in rats. The increased iron transport seen could therefore be a consequence of the decrease in hepcidin expression. However, this increase in iron absorption could also be a consequence of low levels of iron in the liver due to its mobilization to the erythroid marrow. The published autoradiographic findings of our group (Leung et al. 2005) show that hypoxia stimulates iron uptake by both mature enterocytes at the upper villus as well as newly differentiated cells at the base of the villus. Although previous studies have shown a close relationship between hepcidin expression, duodenal iron transporters and iron absorption (Frazer et al. 2002), how hypoxia-induced changes in transport along the villus relate to the distribution profile of the hepcidin receptor is still unknown due to the lack of a suitable antibody to Hepcidin.

The effect of hypoxia on hepcidin mRNA expression levels was further investigated in HepG2 cells and Huh7 cells, human hepatoma-derived cell lines. Hepcidin mRNA expression was significantly reduced after 48 hours of exposure to 1% oxygen. Our data suggests that at least part of the response to hypoxia in rats is due to a direct action of low oxygen partial pressure on hepatocytes. Cell culture experiments used a lower level of oxygen (approximately 7.6 mm Hg partial pressure), than that used in the rat study because, even under normal conditions, the partial pressure of oxygen in blood supplying hepatocytes is considerably lower than the value present in systemic blood since a large proportion of hepatic blood has undergone partial deoxygenation during its passage through the mesenteric circulation. The level of oxygen in blood supplying hepatocytes in rats breathing normal or 10% oxygen is unknown.

The human Hepcidin promoter contains several binding sites for the hypoxia-inducible factor 1 (HIF-1) and it has been reported that iron deficiency activates HIF-1. A direct action of hypoxia on hepcidin expression involving the binding of HIF to a hypoxia response element

on hepcidin mRNA is unlikely as this would result in an increase of hepcidin expression. It is therefore likely that HIF works through another transcription factor to regulate hepcidin levels.

In iron deficient conditions without changes in iron stores or increased erythropoiesis, iron uptake increases significantly, duodenal expression of DcytB, DMT1 and Ireg1 increases while hepatic hepcidin and transferrin saturation decreases (Frazer et al. 2002). As all these changes happen before any haematological or iron storage changes it is likely that there is another factor regulating gene expression. Serum transferrin saturation was a possible candidate for this regulatory factor as transferrin saturation was the only parameter to correlate with gene expression (Frazer et al. 2002) but this is not yet fully understood.

Hepcidin expression levels have been shown to respond to anaemia in a similar manner to the response to hypoxia. Mice that were bled or had undergone phenylhydrazine-induced hemolysis showed a decrease in hepcidin mRNA levels in the liver while iron absorption increased (Bondi et al. 2005;Latunde-Dada et al. 2004;Nicolas et al. 2002b;Vokurka et al. 2006). In thalassaemia syndromes despite the anaemia, an increased absorption of dietary iron leads to iron overload (reviewed by Andrews 1999). Although it has been shown that urinary hepcidin is decreased in patients with Thalassaemia Major and Thalassaemia Intermedia, hepcidin mRNA expression levels have not yet been described (Papanikolaou et al. 2005). Our results show that hepcidin mRNA expression levels were not significantly different between the two thalassaemia groups; Thalassaemia Intermedia compared to Thalassaemia Major and that overall there was no significant difference between the thalassaemia patients (TM and TI) compared with healthy controls. The finding that hepcidin mRNA expression levels were significantly lower in thalassaemia patients with high liver iron concentrations and that hepcidin expression did not vary significantly with ferritin greater than 3000ng/ml or less than 1500ng/ml, suggests that hepcidin expression becomes disregulated above a critical level of iron burden.

A recent paper on the iron metabolism in a mouse model of β-thalassaemia reported intriguing results. In the early stages of the disease, hepcidin is low and this is associated with increased iron absorption, however, in older animals Hepcidin levels are raised and

duodenal Ireg1 expression and intestinal iron absorption are also increased (Gardenghi et al. 2007). Again it is possible that in this case Hepcidin expression becomes disregulated above a critical level of iron burden resulting from the iron accumulation through time. This would explain the failure of Hepcidin expression to increase with further elevations in the iron accumulation and the inappropriately high iron absorption in already heavily iron-loaded patients.

To investigate the direct effects of hepcidin on intestinal iron transport we injected Hepcidin into male C57BL/6 mice fed on an iron adjusted diet and measured in vivo duodenal iron transport and changes in serum iron levels. Following administration of hepcidin mice showed a rapid decrease in serum iron, in accordance with published data reporting the association of high levels of hepcidin and hypoferremia (Rivera et al. 2005a). Our group has found that Ireg1 expression was significantly decreased in the spleen of mice injected with hepcidin which confirms that hypoferremia occurs as a consequence of hepcidin-mediated inhibition of iron release from reticuloendothelial macrophages through Ireg1. Previous data from our group have also shown that in a macrophage cell line Ireg1 expression decreases significantly after treatment with Hepcidin for 24 hours (personal communication by Dr. Paul Sharp).

Despite the presence of hypoferremia, there was no difference in duodenal iron transport between the hepcidin-treated and control animals. Hepcidin treatment was also found to have no effect on Ireg1 expression in mice duodenum or in Caco-2 cells (personal communication by Dr. Paul Sharp).

Previous work from our group has shown that mice subjected to prolonged exposure to Hepcidin and Caco-2 cell monolayers expososed to high levels of Hepcidin, significantly decrease duodenal iron transport (Yamaji et al. 2004). The analysis of the iron transport data from both of our previous reports (Laftah et al. 2004;Yamaji et al. 2004) and from the study by Mena *et al* (Mena et al. 2006) suggests that the major effect of Hepcidin in intestinal epithelia is on the DMT1 uptake pathway and not on the Ireg1-mediated efflux.

A survey of the literature on the association between hepcidin levels and intestinal transport reveals a cloudy picture. When hepcidin expression is low as is the case in anaemia and in

hypoxic conditions, intestinal iron transport is elevated (Frazer et al. 2004b;Leung et al. 2005) however, the significant molecular changes were in the expression of DMT1 and Dcytb and not in the Ireg1 expression.

From this study, we have shown that the decrease in hepcidin mRNA expression levels seen in both the hypoxic animals and hypoxic cells may be responsible for the increased iron uptake reported (Leung et al. 2005). The events that culminate in reduced expression of the peptide at the hepatocyte level are still unknown and so the increase in iron transport might be a consequence of a direct effect of low oxygen via the transcription factor HIF and not the decrease in hepcidin expression levels.

Our study has also shown that hepcidin mRNA expression is not decreased in patients with Thalassaemia Major and Thalassaemia Intermedia. We have also shown that Hepcidin expression was significantly lower in thalassaemia patients with high liver iron concentrations, suggesting that hepcidin expression becomes disregulated above a critical level of iron content. In addition, the fact that thalassaemia patients still accumulated a high concentration of iron confirms that iron overload in the thalassaemia setting is less dominant than the anaemia in regulating Hepcidin expression.

The intestinal iron transport data obtained from the Hepcidin treated mice together with previous work from our group showing that the onset of hypoferremia does not coincide temporally with changes in duodenal iron transport, suggest that there is either a differential sensitivity to Hepcidin and/or a different mode of action of hepcidin at the recycling macrophage and the duodenal enterocyte. As mentioned in chapter 1, Ireg1 mutations lead to Ferroportin disease which is characterised by severe iron loading of the reticuloendothelial macrophages (reviewed by Pietrangelo 2004b). Interestingly in this disease enterocytes do not become iron loaded (Corradini et al. 2004) suggesting that Ireg1 expression in different cells respond differently to a Hepcidin challenge. This possibility is supported in part by the work of Drakesmith and colleagues who demonstrated that some mutant forms of Ireg1 are partially resistant to the actions of Hepcidin (Drakesmith et al. 2005). In addition, it might be possible that another as yet unidentified hepcidin "receptor", in addition to Ireg1 may be

present on the plasma membranes of different cell types. Further studies will be required to clarify these important issues and some of them will be discussed in chapter 7 of this thesis.

Chapter 7

General Discussion

Regulation of iron homeostasis

The discovery of the Hfe gene, the identification of Hfe gene mutations as the main cause of hereditary Haemochromatosis and the identification of Hepcidin as a key regulator of iron homeostasis have contributed to our understanding of the molecular control of iron metabolism in recent years. In addition, the study of human diseases and the generation of genetically altered mice have led to the discovery and identification of new genes involved in iron homeostasis, but much remains to be understood.

The studies described in this thesis are aimed to analyse some regulatory components of iron homeostasis in a newly generated mouse model for hereditary Haemochromatosis type 1, SWR Hfe KO mice.

SWR Hfe KO as an animal model for hereditary haemochromatosis type 1

Hereditary Haemochromatosis type 1 (HH1) is an autosomal recessive disorder of iron metabolism caused by mutations in the Hfe gene. HH1 is characterised by defective regulation of dietary iron absorption that leads to excessive iron accumulation, mainly in the liver. The increased iron absorption in hemochromatosis is in part responsible for elevated transferrin saturation and transferrin-bound iron transport, which leads to cellular uptake of excess circulating iron and pathological expansion of body iron stores. This in turn results in the increased formation of the iron storage molecules ferritin and haemosiderin, especially in parenchymal cells of the liver. Progressive hepatic iron accumulation in humans leads to fibrosis, cirrhosis and subsequent increased morbidity and mortality. Several mouse strains have had their Hfe gene knocked out in order to study this disease but the full pathological picture of the cirrhotic liver seen in HH1 is still not observed in these animal models (Knutson et al. 2001). To address this problem we generated a new mouse model for HH1, the SWR Hfe KO mice. SWR mouse strain has been reported to have a higher basal iron status in the liver than other mouse strains (Clothier et al. 2000) and therefore could be an ideal candidate for the study of the development of fibrosis due to iron overload. In this study we have

shown that when the murine Hfe allele was disrupted in the SWR strain, despite the higher basal iron status of this strain, hepatic iron contents were not similar to the ones seen in HH1 patients nor were significantly higher than Hfe KO mice of other strains (Chapter 3). Iron loading in SWR Hfe KO mice was also shown to be insufficient to cause fibrosis. In humans it has been shown a differential distribution of iron content in the liver of patients with iron overload conditions (Ambu et al. 1995;Clark et al. 2003) but there is no information on iron content levels in the different hepatic lobes. Here we have shown that the disruption of the Hfe gene causes a preferential accumulation of iron in the caudate lobe of the SWR mouse liver. As the caudate lobe is one of the lobes studied when investigating cirrhosis in HH1 patients the significantly higher accumulation of iron is this lobe might be of relevance for the study of how iron overload leads to the development of fibrosis. Overall our study suggests that the SWR Hfe KO mouse is not the ideal and most accurate mouse model for studying HH1 but it might help us elucidate the role of Hfe in the regulation of hepcidin expression in mice.

Regulation of hepcidin expression by dietary iron, apotransferrin, holotransferrin in SWR wt and Hfe KO mice

How hepcidin expression levels are regulated is still not clear and although the study of human diseases and animal models has led to the discovery and identification of new genes involved in iron homeostasis much remains to be understood. The expression of Hfe has profound effects on cellular iron status although changes in cellular iron status have little effect on the expression of Hfe. The precise function of the Hfe protein remains unknown but the discovery of hepcidin has contributed to our understanding of this protein. In hereditary haemochromatosis caused by Hfe mutations (HH1), inappropriately low levels of hepcidin expression have been observed (Ahmad et al. 2002;Bridle et al. 2003;Muckenthaler et al. 2003). In addition, when Hfe KO mice were crossed with mice overexpressing hepcidin their iron overload status was normalized (Nicolas et al. 2003). These studies suggest that Hfe participates in the regulation of intestinal iron absorption by modulating hepcidin expression.

To understand the role of Hfe in the regulation of hepcidin expression by iron, wt and Hfe KO SWR mice were fed diets with different iron contents (Chapter 4). Our data suggests the presence of a "regulatory iron pool" that directly regulates the expression of hepcidin, DMT1 and Ireg1 expression in the liver. According to this proposed mechanism, the accumulation of a yet unknown level of iron content in this "regulatory iron pool" would result in an upregulation of Ireg1 and hepcidin expression in order to export the excess iron to avoid oxidative stress and lipid peroxidation in the liver and; decrease duodenal iron uptake, respectively. No difference in gene expression was found that could account for the differential iron accumulation between the lobes of Hfe KO SWR mice and therefore further investigation is required on the physiology of the murine liver. In SWR mice fed an iron overload diet the Hfe gene was shown not to be necessary for the regulation of Ireg1 in response to iron in accordance to the findings of Bridle and colleagues (Bridle et al. 2003). In contrast dietary iron was found to have no effect on hepatic DMT1 expression and therefore it is possible that Hfe might have a role in the regulation of this iron transporter in the liver. We have also found that apotransferrin or holotransferrin injections have no effect on hepcidin, hepatic DMT1 or Ireg1 expression in SWR mice and that iron deficient peripheral macrophages lacking the Hfe gene and do not produce any soluble factors that regulate Hepcidin expression in the setting of hereditary haemochromatosis differently to healthy subjects.

Regulation of hepcidin expression by acute inflammation in SWR mice and pro-inflammatory cytokines in Huh7 cells

Injected LPS is mainly taken up by the Kupffer cells and is responsible for the upregulation of IL-6 in the liver (Ganz 2003) while turpentine oil injections lead to an induced local irritation which results in the recruitment of inflammatory cells and the upregulation of IL-6 in the injured muscle. In addition turpentine oil injection results in the production of IL-6, IL-1β and TNF-α in hepatocytes (Sheikh et al. 2007). In this study acute inflammation by LPS and turpentine oil was shown to be very different as models of inflammation in SWR mice

(Chapter 5). Inflammation by LPS injection in wt and Hfe KO mice was similar suggesting that Hfe does not have a role in the upregulation of hepcidin in response to LPS inflammation. In contrast, the disruption of the Hfe gene in SWR Hfe KO mice was shown to abrogate the gene expression of hepcidin, hepatic DMT1 and Ireg1 in response to turpentine oil injection. We have also found that TNF-α does not have an effect on hepcidin, hepatic DMT1 or Ireg1 despite having a direct effect on duodenal DMT1+ire expression. In addition IL-6 was shown to upregulate hepcidin levels on hepatocytes but have no effect on the expression of iron transporter genes in the enterocyte as previously suggested (Raja et al. 2005). Studies in human hepatoma (Huh7) cells have shown that IL-1β induces hepcidin expression in an IL-6 independent mechanism (Inamura et al. 2005). Taken together the data obtained in this study suggest that the disruption of the Hfe gene prevents the release of IL-1β in response to acute inflammation by turpentine oil injection preventing hepcidin upregulation in Hfe KO mice (Fig. 7.1).

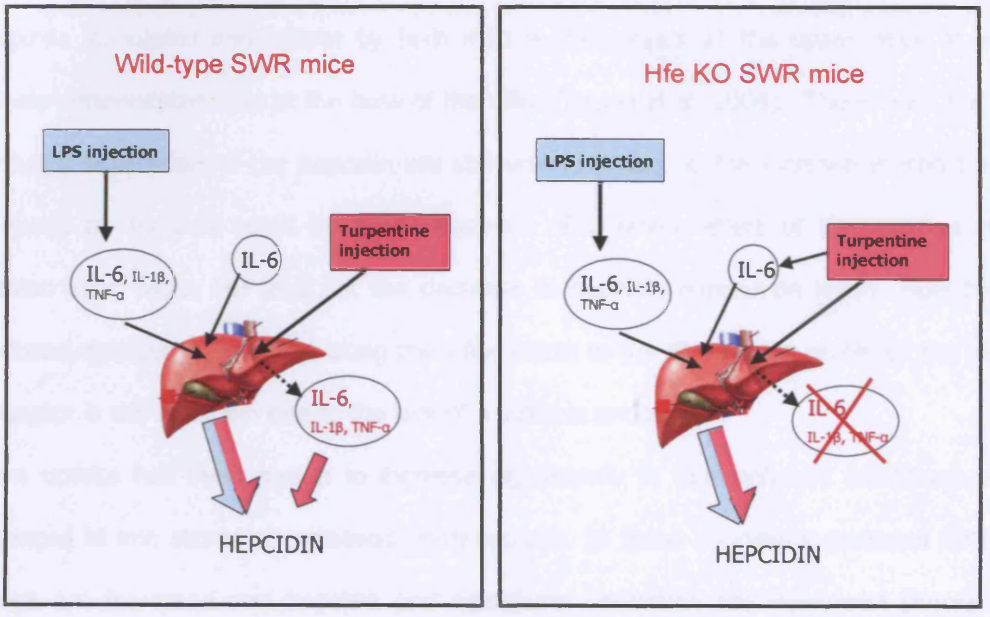

Figure 7.1 Proposed mode of action of LPS and Turpentine oil-induced cytokines in the regulation of Hepcidin. *Injected LPS is mainly taken up by the Kupffer cells and is responsible for the upregulation of IL-6 while turpentine oil injections lead to an induced local irritation which results in the recruitment of inflammatory cells and the upregulation of IL-6 in the injured muscle. In addition turpentine oil injection results in the production of IL-6, IL-1β and TNF-α in hepatocytes. Our findings lead us to postulate that the disruption of the Hfe*

gene prevents the release of cytokines such as IL-1β in response to acute inflammation by turpentine oil injection preventing hepcidin upregulation in Hfe KO SWR mice.

Regulation of hepcidin expression by hypoxia and anaemia

Hypoxia and anaemia have been shown to decrease hepcidin expression levels and it is thought that by doing so iron absorption increases to enable the iron to be delivered to bone marrow to sustain the production of erythrocytes (erythropoiesis) (Bondi et al. 2005;Latunde-Dada et al. 2004;Nicolas et al. 2002b;Vokurka et al. 2006). Recent work from our laboratory on rats has shown that increased entry of iron in the body during hypoxia occurs by both stimulation of iron entry across luminal membrane into the enterocyte and enhanced iron transfer across the basolateral membrane into the perfusing blood (Laftah et al. 2004;Leung et al. 2005;Nicolas et al. 2002b). In this study we describe for the first time the long term effect of hypoxia on hepcidin levels in rats (Chapter 6). We have shown that not only does hepcidin decrease significantly after 4 weeks hypoxia but work by our group has shown that hypoxia stimulates iron uptake by both mature enterocytes at the upper villus as well as newly differentiated cells at the base of the villus (Leung et al. 2005). The events that cause reduced expression of the hepcidin are still unknown and so the increase in iron transport induced by hypoxia could be a consequence of a direct effect of low oxygen via the transcription factor HIF and not the decrease in hepcidin expression levels. How hypoxia-induced changes in transport along the villus relate to the distribution profile of the hepcidin receptor is still unknown due to the lack of a suitable antibody.

Iron uptake has been shown to increase significantly in iron deficient conditions without changes in iron stores or increased erythropoiesis. In these conditions duodenal DMT1 and Ireg1 are increased and hepcidin and transferrin saturation are decreased (Frazer et al. 2002). One such condition is thalassaemia where despite of the anaemia setting, an increased absorption of dietary iron leads to iron overload (Andrews 1999). Although it has been shown that urinary hepcidin is decreased in patients with Thalassaemia Major (TM) and Thalassaemia Intermedia (TI) (Papanikolaou et al. 2005), hepcidin mRNA expression levels have not yet been described. Our study shows that mRNA expression of the peptide is not

different between thalassaemia patients and healthy controls or even between the two types of thalassaemia (TM and TI). An interesting finding was that hepcidin expression levels were significantly lower in thalassaemia patients with high liver iron concentrations suggesting that hepcidin expression becomes disregulated above a critical level of iron burden. Recently a mouse model of β-thalassaemia demonstrated that in the early stages of the disease, hepcidin is low and this is associated with increased iron absorption, however, in older animals hepcidin levels are raised and duodenal Ireg1 expression and intestinal iron absorption were also increased (Gardenghi et al. 2007). It is possible that the iron accumulation through time in thalassaemia patients results in the failure of hepcidin expression to increase with further elevations in the iron accumulation and with the inappropriately high iron absorption in already heavily iron-loaded patients.

Hepcidin as a regulator of iron metabolism

After studying the modulators of hepcidin expression, we investigated the direct effect of Hepcidin on iron metabolism. Our results show that administration of Hepcidin in mice decreases serum iron levels as shown in inflammatory conditions. Work by our group has also shown that Ireg1 expression was significantly decreased in the spleen of mice injected with hepcidin which confirms that hypoferremia occurs as a consequence of hepcidin-mediated inhibition of iron release from reticuloendothelial macrophages through Ireg1. Despite becoming hypoferremic, there was no difference in duodenal iron transport between the Hepcidin-treated and control animals or in duodenal Ireg1 expression levels. This data suggests that there is either a differential sensitivity to Hepcidin and/or a different mode of action of Hepcidin at the recycling macrophage and the duodenal enterocyte. Some mutant forms of Ireg1 have been shown to be partially resistant to the actions of Hepcidin (Drakesmith et al. 2005) and this could explain the lack of Ireg1 expression changes after Hepcidin treatment. In addition, it might be possible that other as yet unidentified Hepcidin "receptor", in addition to Ireg1 may be present on the plasma membranes of different cell types.

Conclusions

From the collective studies described in this thesis we can conclude that:

- SWR Hfe KO mice does not produce the full pathological features seen in HH1 patients liver,
- the disruption of the Hfe gene causes a preferential accumulation of iron in the caudate lobe of the SWR mouse liver and this differential deposition of iron is not due to gene expression differences in the hepatic lobes,
- Upregulation of hepcidin expression in iron loaded condition or in inflammation does not have a direct effect on hepatic DMT1 and Ireg1 instead it is possible that a "regulatory iron pool" exists in the hepatocytes that could regulate these iron transporter genes expression in the liver,
- Constant high levels of hepcidin appear to have a direct effect on duodenal iron transporter gene expression although this requires further investigation,
- Hfe gene has a vital role in the upregulation of hepcidin in acute inflammation induced by turpentine oil but not by LPS, suggesting that IL-1β might have a relevant role in the up regulation of hepcidin caused by turpentine oil-induced inflammation,

And finally, our knowledge of the regulation of duodenal iron uptake, the relevant modulator genes and the recent finding that the liver plays a central role in iron homeostasis, signify that the role of hepatic iron transporter gene expression and how they are regulated deserves further investigation. Studies described here contribute to the understanding of how the hepatocyte responds to iron status, hypoxia and inflammation and the relevance of the Hfe gene in the regulation of hepcidin, DMT1 and Ireg1 expression in the liver however, further studies are required to elucidate the systemic and integrative homeostasis of iron.

Future Work

The development of the SWR Hfe KO mice resulted in elevated liver iron levels but this did not lead to fibrosis. This might be due to the inability to reach high liver iron levels equivalent to those found in HH1 patients. More likely it is due to other modifier genes and environmental factors. In order to improve this model, SWR Hfe KO mice should be studied at later stages (two years), and fed on iron overload diet for longer periods of time. In addition, other factors such as alcohol and viral infections should be introduced to this model on top of gene knockout.

We were unable to say whether holotransferrin or apotransferrin are detected by the liver to sense body iron status. Therefore further studies investigating the effect of holotransferrin and apotransferrin together with studying the resulting levels of TfR2, Hfe, hemojuvelin, iron transporters and hepcidin expression need to be studied at both mRNA and protein levels to determine if there is a sensing mechanism involving holotransferrin and if so what is the mechanism.

In order to investigate further the role of Hfe in the turpentine oil effect on hepcidin expression, more experiments need to be performed. The effect of turpentine oil in a time dependent manner on cytokines and hepcidin expression needs to be investigated.
Once an array of cytokines which are produced and their appearance and disappearance with time is worked out then individual cytokines need to be injected into mice to investigate their effect on hepcidin and serum iron status. The link between hepcidin and iron efflux from duodenum and macrophages needs to be further investigated.

In this study we have clearly shown that expression of hepcidin and iron transporters in hepatocytes is not dependent of total liver iron levels but possibly on a "regulatory iron pool". This pool needs to be defined in the Hfe KO model and wild type mice.

Reference List

Abboud S, Haile DJ. A novel mammalian iron-regulated protein involved in intracellular iron metabolism. J Biol Chem 2000;275:19906-19912.

Adams PC, Deugnier Y, Moirand R, Brissot P. The relationship between iron overload, clinical symptoms, and age in 410 patients with genetic hemochromatosis. Hepatology 1997;25:162-166.

Adams PC, Kertesz AE, Valberg LS. Clinical presentation of hemochromatosis: a changing scene. Am J Med 1991;90:445-449.

Adamsky K, Weizer O, Amariglio N, Breda L, Harmelin A, Rivella S, Rachmilewitz E, Rechavi G. Decreased hepcidin mRNA expression in thalassemic mice. Br J Haematol 2004;124:123-124.

Ahmad KA, Ahmann JR, Migas MC, Waheed A, Britton RS, Bacon BR, Sly WS, Fleming RE. Decreased liver hepcidin expression in the hfe knockout mouse. Blood Cells Mol Dis 2002;29:361-366.

Aisen P. Transferrin receptor 1. Int J Biochem Cell Biol 2004;36:2137-2143.

Ajioka RS, Levy JE, Andrews NC, Kushner JP. Regulation of iron absorption in Hfe mutant mice. Blood 2002;100:1465-1469.

Ambu R, Crisponi G, Sciot R, Van EP, Parodo G, Iannelli S, Marongiu F, Silvagni R, Nurchi V, Costa V, . Uneven hepatic iron and phosphorus distribution in beta-thalassemia. J Hepatol 1995;23:544-549.

Anderson GJ, Frazer DM. Hepatic iron metabolism. Semin Liver Dis 2005;25:420-432.

Andrews NC. Disorders of iron metabolism. N Engl J Med 1999;341:1986-1995.

Andrews NC. Iron metabolism: iron deficiency and iron overload. Annu Rev Genomics Hum Genet 2000;1:75-98.

Andrews NC. Anemia of inflammation: the cytokine-hepcidin link. J Clin Invest 2004;113:1251-1253.

Andrews NC, Fleming MD, Levy JE. Molecular insights into mechanisms of iron transport. Curr Opin Hematol 1999;6:61-64.

Andriopoulos B, Pantopoulos K. Hepcidin generated by hepatoma cells inhibits iron export from co-cultured THP1 monocytes. J Hepatol 2006;44:1125-1131.

Arden KE, Wallace DF, Dixon JL, Summerville L, Searle JW, Anderson GJ, Ramm GA, Powell LW, Subramaniam VN. A novel mutation in ferroportin1 is associated with haemochromatosis in a Solomon Islands patient. Gut 2003;52:1215-1217.

Arezzini B, Lunghi B, Lungarella G, Gardi C. Iron overload enhances the development of experimental liver cirrhosis in mice. Int J Biochem Cell Biol 2003;35:486-495.

Arosio P, Levi S. Ferritin, iron homeostasis, and oxidative damage. Free Radic Biol Med 2002;33:457-463.

Asare GA, Paterson AC, Kew MC, Khan S, Mossanda KS. Iron-free neoplastic nodules and hepatocellular carcinoma without cirrhosis in Wistar rats fed a diet high in iron. J Pathol 2006;208:82-90.

Ashrafian H. Hepcidin: the missing link between hemochromatosis and infections. Infect Immun 2003;71:6693-6700.

Awaya H, Mitchell DG, Kamishima T, Holland G, Ito K, Matsumoto T. Cirrhosis:modified caudate-right lobe ratio. Radiology 2002 Sep;224 (3): 769-774

Babitt JL, Huang FW, Wrighting DM, Xia Y, Sidis Y, Samad TA, Campagna JA, Chung RT, Schneyer AL, Woolf CJ, Andrews NC, Lin HY. Bone morphogenetic protein signaling by hemojuvelin regulates hepcidin expression. Nat Genet 2006;38:531-539.

Bacon BR, O'Grady JG, DiBisceglie AM, Lake JR. Comprehensive clinical hepatology. (2nd ed.). 2006.

Bacon BR, Sadiq SA. Hereditary hemochromatosis: presentation and diagnosis in the 1990s. Am J Gastroenterol 1997;92:784-789.

Bahram S, Gilfillan S, Kuhn LC, Moret R, Schulze JB, Lebeau A, Schumann K. Experimental hemochromatosis due to MHC class I HFE deficiency: immune status and iron metabolism. Proc Natl Acad Sci U S A 1999;96:13312-13317.

Bailey S, Evans RW, Garratt RC, Gorinsky B, Hasnain S, Horsburgh C, Jhoti H, Lindley PF, Mydin A, Sarra R, . Molecular structure of serum transferrin at 3.3-A resolution. Biochemistry 1988;27:5804-5812.

Bancroft JD, Stevens A. Theory and Practice of Histological Techniques . (2nd ed.). 1982. Churchill Livingstone.

Bannerman RM, Bannerman CE, Kingston PJ. Hereditary iron deficiency: X-linked anaemia (sla) in newborn and suckling mice. Br J Haematol 1973;25:280.

Bassett ML, Halliday JW, Powell LW. Value of hepatic iron measurements in early hemochromatosis and determination of the critical iron level associated with fibrosis. Hepatology 1986;6:24-29.

Bastin JM, Jones M, O'Callaghan CA, Schimanski L, Mason DY, Townsend AR. Kupffer cell staining by an HFE-specific monoclonal antibody: implications for hereditary haemochromatosis. Br J Haematol 1998;103:931-941.

Beaumont C, Delaunay J, Hetet G, Grandchamp B, de MM, Tchernia G. Two new human DMT1 gene mutations in a patient with microcytic anemia, low ferritinemia, and liver iron overload. Blood 2006;107:4168-4170.

Beguin Y. Soluble transferrin receptor for the evaluation of erythropoiesis and iron status. Clin Chim Acta 2003;329:9-22.

Bennett MJ, Lebron JA, Bjorkman PJ. Crystal structure of the hereditary haemochromatosis protein HFE complexed with transferrin receptor. Nature 2000;403:46-53.

Bensaid M, Fruchon S, Mazeres C, Bahram S, Roth MP, Coppin H. Multigenic control of hepatic iron loading in a murine model of hemochromatosis. Gastroenterology 2004;126:1400-1408.

Bernstein SE. Hereditary hypotransferrinemia with hemosiderosis, a murine disorder resembling human atransferrinemia. J Lab Clin Med 1987;110:690-705.

Beutler E. Targeted disruption of the HFE gene. Proc Natl Acad Sci U S A 1998;95:2033-2034.

Beutler E, Gelbart T, Lee P, Trevino R, Fernandez MA, Fairbanks VF. Molecular characterization of a case of atransferrinemia. Blood 2000;96:4071-4074.

Beutler E, Hoffbrand AV, Cook JD. Iron deficiency and overload. Hematology Am Soc Hematol Educ Program 2003;40-61.

Bomford A. Genetics of haemochromatosis. Lancet 2002;360:1673-1681.

Bondi A, Valentino P, Daraio F, Porporato P, Gramaglia E, Carturan S, Gottardi E, Camaschella C, Roetto A. Hepatic expression of hemochromatosis genes in two mouse strains after phlebotomy and iron overload. Haematologica 2005;90:1161-1167.

Bonkovsky HL, Healey JF, Lincoln B, Bacon BR, Bishop DF, Elder GH. Hepatic haem synthesis in a new model of experimental hemochromatosis: studies in rats fed finely divided elemental iron. Hepatology 1987;7:1195-1203.

Bothwell TH, Charlton RW. Current problems of iron overload. Recent Results Cancer Res 1979;69:87-95.

Bridle KR, Frazer DM, Wilkins SJ, Dixon JL, Purdie DM, Crawford DH, Subramaniam VN, Powell LW, Anderson GJ, Ram GA. Disrupted hepcidin regulation in HFE-associated

haemochromatosis and the liver as a regulator of body iron homoeostasis. Lancet 2003;361:669-673.

Bulaj ZJ, Ajioka RS, Phillips JD, LaSalle BA, Jorde LB, Griffen LM, Edwards CQ, Kushner JP. Disease-related conditions in relatives of patients with hemochromatosis. N Engl J Med 2000;343:1529-1535.

Burke W, Thomson E, Khoury MJ, McDonnell SM, Press N, Adams PC, Barton JC, Beutler E, Brittenham G, Buchanan A, Clayton EW, Cogswell ME, Meslin EM, Motulsky AG, Powell LW, Sigal E, Wilfond BS, Collins FS. Hereditary hemochromatosis: gene discovery and its implications for population-based screening. JAMA 1998;280:172-178.

Burkitt HG, Young B, Heath JW. Wheater's Functional Histology: a text and colour atlas. (3rd ed.). 2007. Churchill Livingstone.

Byrnes V, Barrett S, Ryan E, Kelleher T, O'Keane C, Coughlan B, Crowe J. Increased duodenal DMT-1 expression and unchanged HFE mRNA levels in HFE-associated hereditary hemochromatosis and iron deficiency. Blood Cells Mol Dis 2002;29:251-260.

Camaschella C. Understanding iron homeostasis through genetic analysis of hemochromatosis and related disorders. Blood 2005;106:3710-3717.

Camaschella C, Roetto A, Cali A, De GM, Garozzo G, Carella M, Majorano N, Totaro A, Gasparini P. The gene TFR2 is mutated in a new type of haemochromatosis mapping to 7q22. Nat Genet 2000;25:14-15.

Camaschella C, Roetto A, Papanikolaou G. Commentary: Juvenile hemochromatosis in a Spanish family (by Montes-Cano et al.). Blood Cells Mol Dis 2002;29:83-84.

Canonne-Hergaux F, Gruenheid S, Ponka P, Gros P. Cellular and subcellular localization of the Nramp2 iron transporter in the intestinal brush border and regulation by dietary iron. Blood 1999;93:4406-4417.

Cartwright GE, Wintrobe MM. The anemia of infection. XVII. A review. Adv Intern Med 1952;5:165-226.

Casey JL, Hentze MW, Koeller DM, Caughman SW, Rouault TA, Klausner RD, Harford JB. Iron-responsive elements: regulatory RNA sequences that control mRNA levels and translation. Science 1988;240:924-928.

Cavell PA, Widdowson EM. Intakes and excretions of iron, copper, and zinc in the neonatal period. Arch Dis Child 1964;39:496-501.

Cazzola M, Huebers HA, Sayers MH, MacPhail AP, Eng M, Finch CA. Transferrin saturation, plasma iron turnover, and transferrin uptake in normal humans. Blood 1985;66:935-939.

Cazzola M, Invernizzi R, Bergamaschi G, Levi S, Corsi B, Travaglino E, Rolandi V, Biasiotto G, Drysdale J, Arosio P. Mitochondrial ferritin expression in erythroid cells from patients with sideroblastic anemia. Blood 2003;101:1996-2000.

Chantret I, Rodolosse A, Barbat A, Dussaulx E, Brot-Laroche E, Zweibaum A, Rousset M. Differential expression of sucrase-isomaltase in clones isolated from early and late passages of the cell line Caco-2: evidence for glucose-dependent negative regulation. J Cell Sci 1994;107 (Pt 1):213-225.

Chen D, Zhao M, Mundy GR. Bone morphogenetic proteins. Growth Factors 2004a;22:233-241.

Chen H, Attieh ZK, Su T, Syed BA, Gao H, Alaeddine RM, Fox TC, Usta J, Naylor CE, Evans RW, McKie AT, Anderson GJ, Vulpe CD. Hephaestin is a ferroxidase that maintains partial activity in sex-linked anemia mice. Blood 2004b;103:3933-3939.

Chen H, Su T, Attieh ZK, Fox TC, McKie AT, Anderson GJ, Vulpe CD. Systemic regulation of Hephaestin and Ireg1 revealed in studies of genetic and nutritional iron deficiency. Blood 2003;102:1893-1899.

Chen J, Enns CA. The Cytoplasmic domain of transferrin receptor 2 dictates its stability and response to holo-transferrin in Hep3B cells. J Biol Chem 2007;282:6201-6209.

Chua AC, Olynyk JK, Leedman PJ, Trinder D. Nontransferrin-bound iron uptake by hepatocytes is increased in the Hfe knockout mouse model of hereditary hemochromatosis. Blood 2004;104:1519-1525.

Clark PR, Chua-anusorn W, St PT. Proton transverse relaxation rate (R2) images of liver tissue; mapping local tissue iron concentrations with MRI [corrected]. Magn Reson Med 2003;49:572-575.

Clothier B, Robinson S, Akhtar RA, Francis JE, Peters TJ, Raja K, Smith AG. Genetic variation of basal iron status, ferritin and iron regulatory protein in mice: potential for modulation of oxidative stress. Biochem Pharmacol 2000;59:115-122.

Collins JF, Franck CA, Kowdley KV, Ghishan FK. Identification of differentially expressed genes in response to dietary iron deprivation in rat duodenum. Am J Physiol Gastrointest Liver Physiol 2005;288:G964-G971.

Conrad ME, Jr., Crosby WH. Intestinal mucosal mechanisms controlling iron absorption. Blood 1963;22:406-415.

Conrad ME, Umbreit JN. A concise review: iron absorption--the mucin-mobilferrin-integrin pathway. A competitive pathway for metal absorption. Am J Hematol 1993;42:67-73.

Conrad ME, Umbreit JN, Moore EG. A role for mucin in the absorption of inorganic iron and other metal cations. A study in rats. Gastroenterology 1991;100:129-136.

Conrad ME, Umbreit JN, Moore EG. Rat duodenal iron-binding protein mobilferrin is a homologue of calreticulin. Gastroenterology 1993;104:1700-1704.

Conrad ME, Umbreit JN, Moore EG, Harper KP. Iron absorption via the mucin-integrin mobilferrin pathway. Trans Assoc Am Physicians 1992;105:133-148.

Conrad ME, Weintraub LR, Sears DA, Crosby WH. Absorption of haemoglobin iron. Am J Physiol 1966;211:1123-1130.

Constante M, Jiang W, Wang D, Raymond VA, Bilodeau M, Santos MM. Distinct requirements for Hfe in basal and induced hepcidin levels in iron overload and inflammation. Am J Physiol Gastrointest Liver Physiol 2006;291:G229-G237.

Cook JD, Barry WE, Hershko C, Fillet G, Finch CA. Iron kinetics with emphasis on iron overload. Am J Pathol 1973;72:337-343.

Corradini E, Ferrara F, Pietrangelo A. Iron and the liver. Pediatr Endocrinol Rev 2004;2 Suppl 2:245-248.

Courselaud B, Pigeon C, Inoue Y, Inoue J, Gonzalez FJ, Leroyer P, Gilot D, Boudjema K, Guguen-Guillouzo C, Brissot P, Loreal O, Ilyin G. C/EBPalpha regulates hepatic transcription of hepcidin, an antimicrobial peptide and regulator of iron metabolism. Cross-talk between C/EBP pathway and iron metabolism. J Biol Chem 2002;277:41163-41170.

Craven CM, Alexander J, Eldridge M, Kushner JP, Bernstein S, Kaplan J. Tissue distribution and clearance kinetics of non-transferrin-bound iron in the hypotransferrinemic mouse: a rodent model for hemochromatosis. Proc Natl Acad Sci U S A 1987;84:3457-3461.

De D, I, Ward DM, Nemeth E, Vaughn MB, Musci G, Ganz T, Kaplan J. The molecular basis of ferroportin-linked hemochromatosis. Proc Natl Acad Sci U S A 2005;102:8955-8960.

De GM, Roetto A, Piperno A, Mariani R, Alberti F, Papanikolaou G, Politou M, Lockitch G, Girelli D, Fargion S, Cox TM, Gasparini P, Cazzola M, Camaschella C. Natural history of juvenile haemochromatosis. Br J Haematol 2002;117:973-979.

De SM, Reimao R, Lacerda R, Hugo P, Kaufmann SH, Porto G. Iron overload in beta 2-microglobulin-deficient mice. Immunol Lett 1994;39:105-111.

Delaby C, Pilard N, Goncalves AS, Beaumont C, Canonne-Hergaux F. Presence of the iron exporter ferroportin at the plasma membrane of macrophages is enhanced by iron loading and down-regulated by hepcidin. Blood 2005;106:3979-3984.

Demaeyer EM. Epidemiologic, traitement et prevention de la carence ferriprive. Rev.Epiden et Sante Publ. 28, 235. 1980.

Devalia V, Carter K, Walker AP, Perkins SJ, Worwood M, May A, Dooley JS. Autosomal dominant reticuloendothelial iron overload associated with a 3-base pair deletion in the ferroportin 1 gene (SLC11A3). Blood 2002;100:695-697.

Donovan A, Brownlie A, Zhou Y, Shepard J, Pratt SJ, Moynihan J, Paw BH, Drejer A, Barut B, Zapata A, Law TC, Brugnara C, Lux SE, Pinkus GS, Pinkus JL, Kingsley PD, Palis J, Fleming MD, Andrews NC, Zon LI. Positional cloning of zebrafish ferroportin1 identifies a conserved vertebrate iron exporter. Nature 2000;403:776-781.

Donovan A, Lima CA, Pinkus JL, Pinkus GS, Zon LI, Robine S, Andrews NC. The iron exporter ferroportin/Slc40a1 is essential for iron homeostasis. Cell Metab 2005;1:191-200.

Drakesmith H, Schimanski LM, Ormerod E, Merryweather-Clarke AT, Viprakasit V, Edwards JP, Sweetland E, Bastin JM, Cowley D, Chinthammitr Y, Robson KJ, Townsend AR. Resistance to hepcidin is conferred by hemochromatosis-associated mutations of ferroportin. Blood 2005;106:1092-1097.

Drakesmith H, Sweetland E, Schimanski L, Edwards J, Cowley D, Ashraf M, Bastin J, Townsend AR. The hemochromatosis protein HFE inhibits iron export from macrophages. Proc Natl Acad Sci U S A 2002;99:15602-15607.

Dupic F, Fruchon S, Bensaid M, Borot N, Radosavljevic M, Loreal O, Brissot P, Gilfillan S, Bahram S, Coppin H, Roth MP. Inactivation of the hemochromatosis gene differentially regulates duodenal expression of iron-related mRNAs between mouse strains. Gastroenterology 2002a;122:745-751.

Dautry-Varsat A, Ciechanover A, Lodish HF. pH and the recycling of transferrin during receptor-mediated endocytosis. Proc Natl Acad Sci U S A 1983;80:2258-2262.

Dupic F, Fruchon S, Bensaid M, Loreal O, Brissot P, Borot N, Roth MP, Coppin H. Duodenal mRNA expression of iron related genes in response to iron loading and iron deficiency in four strains of mice. Gut 2002b;51:648-653.

Duthie HL. The relative importance of the duodenum in the intestinal absorption of iron. Br J Haematol 1964;10:59-68.

Elias H. A re-examination of the structure of the mammalian liver; the hepatic lobule and its relation to the vascular and biliary systems. Am J Anat 1949;85:379-456, 15.

Emond MJ, Bronner MP, Carlson TH, Lin M, Labbe RF, Kowdley KV. Quantitative study of the variability of hepatic iron concentrations. Clin Chem 1999;45:340-346.

Feder JN. The hereditary hemochromatosis gene (HFE): a MHC class I-like gene that functions in the regulation of iron homeostasis. Immunol Res 1999;20:175-185.

Feder JN, Gnirke A, Thomas W, Tsuchihashi Z, Ruddy DA, Basava A, Dormishian F, Domingo R, Jr., Ellis MC, Fullan A, Hinton LM, Jones NL, Kimmel BE, Kronmal GS, Lauer P, Lee VK, Loeb DB, Mapa FA, McClelland E, Meyer NC, Mintier GA, Moeller N, Moore T, Morikang E, Prass CE, Quintana L, Starnes SM, Schatzman RC, Brunke KJ, Drayna DT, Risch NJ, Bacon BR, Wolff RK. A novel MHC class I-like gene is mutated in patients with hereditary haemochromatosis. Nat Genet 1996;13:399-408.

Feder JN, Penny DM, Irrinki A, Lee VK, Lebron JA, Watson N, Tsuchihashi Z, Sigal E, Bjorkman PJ, Schatzman RC. The hemochromatosis gene product complexes with the transferrin receptor and lowers its affinity for ligand binding. Proc Natl Acad Sci U S A 1998;95:1472-1477.

Finch C. Regulators of iron balance in humans. Blood 1994;84:1697-1702.

Finch CA, Hegsted M, Kinney TD, Thomas ED, Rath CE, Haskins D, Finch S, Fluharty RG. Iron metabolism; the pathophysiology of iron storage. Blood 1950;5:983-1008.

Flanagan JM, Peng H, Wang L, Gelbart T, Lee P, Johnson SB, Beutler E. Soluble transferrin receptor-1 levels in mice do not affect iron absorption. Acta Haematol 2006;116:249-254.

Fleming MD, Romano MA, Su MA, Garrick LM, Garrick MD, Andrews NC. Nramp2 is mutated in the anemic Belgrade (b) rat: evidence of a role for Nramp2 in endosomal iron transport. Proc Natl Acad Sci U S A 1998;95:1148-1153.

Fleming MD, Trenor CC, III, Su MA, Foernzler D, Beier DR, Dietrich WF, Andrews NC. Microcytic anaemia mice have a mutation in Nramp2, a candidate iron transporter gene. Nat Genet 1997;16:383-386.

Fleming RE, Ahmann JR, Migas MC, Waheed A, Koeffler HP, Kawabata H, Britton RS, Bacon BR, Sly WS. Targeted mutagenesis of the murine transferrin receptor-2 gene produces hemochromatosis. Proc Natl Acad Sci U S A 2002;99:10653-10658.

Fleming RE, Britton RS, Waheed A, Sly WS, Bacon BR. Pathogenesis of hereditary hemochromatosis. Clin Liver Dis 2004;8:755-73, vii.

Fleming RE, Holden CC, Tomatsu S, Waheed A, Brunt EM, Britton RS, Bacon BR, Roopenian DC, Sly WS. Mouse strain differences determine severity of iron accumulation in Hfe knockout model of hereditary hemochromatosis. Proc Natl Acad Sci U S A 2001;98:2707-2711.

Fleming RE, Migas MC, Holden CC, Waheed A, Britton RS, Tomatsu S, Bacon BR, Sly WS. Transferrin receptor 2: continued expression in mouse liver in the face of iron overload and in hereditary hemochromatosis. Proc Natl Acad Sci U S A 2000;97:2214-2219.

Fleming RE, Migas MC, Zhou X, Jiang J, Britton RS, Brunt EM, Tomatsu S, Waheed A, Bacon BR, Sly WS. Mechanism of increased iron absorption in murine model of hereditary hemochromatosis: increased duodenal expression of the iron transporter DMT1. Proc Natl Acad Sci U S A 1999;96:3143-3148.

Fleming RE, Sly WS. Hepcidin: a putative iron-regulatory hormone relevant to hereditary hemochromatosis and the anemia of chronic disease. Proc Natl Acad Sci U S A 2001;98:8160-8162.

Fontes G, Thivolle L. Trace elements in milk. J.Dairy Sci. 20, 802-812. 1925.

Frazer DM, Anderson GJ. The orchestration of body iron intake: how and where do enterocytes receive their cues? Blood Cells Mol Dis 2003;30:288-297.

Frazer DM, Anderson GJ. Iron imports. I. Intestinal iron absorption and its regulation. Am J Physiol Gastrointest Liver Physiol 2005;289:G631-G635.

Frazer DM, Inglis HR, Wilkins SJ, Millard KN, Steele TM, McLaren GD, McKie AT, Vulpe CD, Anderson GJ. Delayed hepcidin response explains the lag period in iron absorption following a stimulus to increase erythropoiesis. Gut 2004a;53:1509-1515.

Frazer DM, Vulpe CD, McKie AT, Wilkins SJ, Trinder D, Cleghorn GJ, Anderson GJ. Cloning and gastrointestinal expression of rat hephaestin: relationship to other iron transport proteins. Am J Physiol Gastrointest Liver Physiol 2001;281:G931-G939.

Frazer DM, Wilkins SJ, Becker EM, Vulpe CD, McKie AT, Trinder D, Anderson GJ. Hepcidin expression inversely correlates with the expression of duodenal iron transporters and iron absorption in rats. Gastroenterology 2002;123:835-844.

Frazer DM, Wilkins SJ, Millard KN, McKie AT, Vulpe CD, Anderson GJ. Increased hepcidin expression and hypoferraemia associated with an acute phase response are not affected by inactivation of HFE. Br J Haematol 2004b;126:434-436.

Gambaro K, Aberdam E, Virolle T, Aberdam D, Rouleau M. BMP-4 induces a Smad-dependent apoptotic cell death of mouse embryonic stem cell-derived neural precursors. Cell Death Differ 2006;13:1075-1087.

Ganz T. The role of hepcidin in iron sequestration during infections and in the pathogenesis of anemia of chronic disease. Isr Med Assoc J 2002;4:1043-1045.

Ganz T. Hepcidin, a key regulator of iron metabolism and mediator of anemia of inflammation. Blood 2003.

Ganz T. Cellular iron: ferroportin is the only way out. Cell Metab 2005a;1:155-157.

Ganz T. Hepcidin--a regulator of intestinal iron absorption and iron recycling by macrophages. Best Pract Res Clin Haematol 2005b;18:171-182.

Ganz T. Molecular pathogenesis of anemia of chronic disease. Pediatr Blood Cancer 2006;46:554-557.

Ganz T, Nemeth E. Iron imports. IV. Hepcidin and regulation of body iron metabolism. Am J Physiol Gastrointest Liver Physiol 2006;290:G199-G203.

Gardenghi S, Marongiu MF, Ramos P, Guy E, Breda L, Chadburn A, Liu Y, Amariglio N, Rechavi G, Rachmilewitz EA, Breuer W, Cabantchik ZI, Wrighting DM, Andrews NC, de SM, Giardina PJ, Grady RW, Rivella S. Ineffective erythropoiesis in {beta}-thalassemia is characterized by increased iron absorption mediated by down-regulation of hepcidin and up-regulation of ferroportin. Blood 2007.

Giannetti AM, Bjorkman PJ. HFE and transferrin directly compete for transferrin receptor in solution and at the cell surface. J Biol Chem 2004;279:25866-25875.

Girelli D, Bozzini C, Roetto A, Alberti F, Daraio F, Colombari R, Olivieri O, Corrocher R, Camaschella C. Clinical and pathologic findings in hemochromatosis type 3 due to a novel mutation in transferrin receptor 2 gene. Gastroenterology 2002;122:1295-1302.

Glaise D, Ilyin GP, Loyer P, Cariou S, Bilodeau M, Lucas J, Puisieux A, Ozturk M, Guguen-Guillouzo C. Cell cycle gene regulation in reversibly differentiated new human hepatoma cell lines. Cell Growth Differ 1998;9:165-176.

Gordeuk VR, Caleffi A, Corradini E, Ferrara F, Jones RA, Castro O, Onyekwere O, Kittles R, Pignatti E, Montosi G, Garuti C, Gangaidzo IT, Gomo ZA, Moyo VM, Rouault TA, MacPhail P, Pietrangelo A. Iron overload in Africans and African-Americans and a common mutation in the SCL40A1 (ferroportin 1) gene. Blood Cells Mol Dis 2003;31:299-304.

Goswami T, Andrews NC. Hereditary hemochromatosis protein, HFE, interaction with transferrin receptor 2 suggests a molecular mechanism for mammalian iron sensing. J Biol Chem 2006;281:28494-28498.

Gruenheid S, Canonne-Hergaux F, Gauthier S, Hackam DJ, Grinstein S, Gros P. The iron transport protein NRAMP2 is an integral membrane glycoprotein that colocalizes with transferrin in recycling endosomes. J Exp Med 1999;189:831-841.

Gunshin H, Allerson CR, Polycarpou-Schwarz M, Rofts A, Rogers JT, Kishi F, Hentze MW, Rouault TA, Andrews NC, Hediger MA. Iron-dependent regulation of the divalent metal ion transporter. FEBS Lett 2001;509:309-316.

Gunshin H, Fujiwara Y, Custodio AO, Direnzo C, Robine S, Andrews NC. Slc11a2 is required for intestinal iron absorption and erythropoiesis but dispensable in placenta and liver. J Clin Invest 2005;115:1258-1266.

Gunshin H, Mackenzie B, Berger UV, Gunshin Y, Romero MF, Boron WF, Nussberger S, Gollan JL, Hediger MA. Cloning and characterization of a mammalian proton-coupled metal-ion transporter. Nature 1997;388:482-488.

Halliday JW, Ramm GA, Moss D, Powell LW. A new look at ferritin metabolism. Adv Exp Med Biol 1994;356:149-156.

Halliwell B. Free radicals and antioxidants: a personal view. Nutr Rev 1994;52:253-265.

Han O, Failla ML, Smith CJr. Transferrin-iron and pro-inflammatory cytokines influence iron status and apical iron transport efficiency of Caco-2 intestinal cell line. J.Nutr.Biochem. 8, 585-591. 1997. Elsevier.

Harbin WP, Robert NJ, Ferrucci JT, Jr. Diagnosis of cirrhosis based on regional changes in hepatic morphology: a radiological and pathological analysis. Radiology 1980;135:273-283.

Harris ZL, Durley AP, Man TK, Gitlin JD. Targeted gene disruption reveals an essential role for ceruloplasmin in cellular iron efflux. Proc Natl Acad Sci U S A 1999;96:10812-10817.

Harris ZL, Takahashi Y, Miyajima H, Serizawa M, MacGillivray RT, Gitlin JD. Aceruloplasminemia: molecular characterization of this disorder of iron metabolism. Proc Natl Acad Sci U S A 1995;92:2539-2543.

Harrison P, Huehns ER. Proteins of iron metabolism. Nature 1979;279:476-477.

Harrison PM. Ferritin: an iron-storage molecule. Semin Hematol 1977;14:55-70.

Harrison PM, Arosio P. The ferritins: molecular properties, iron storage function and cellular regulation. Biochim Biophys Acta 1996;1275:161-203.

Harrison PM, Treffry A, Lilley TH. Ferritin as an iron-storage protein: mechanisms of iron uptake. J Inorg Biochem 1986;27:287-293.

Hellman NE, Gitlin JD. Ceruloplasmin metabolism and function. Annu Rev Nutr 2002;22:439-458.

Hentze MW, Caughman SW, Casey JL, Koeller DM, Rouault TA, Harford JB, Klausner RD. A model for the structure and functions of iron-responsive elements. Gene 1988;72:201-208.

Hentze MW, Kuhn LC. Molecular control of vertebrate iron metabolism: mRNA-based regulatory circuits operated by iron, nitric oxide, and oxidative stress. Proc Natl Acad Sci U S A 1996;93:8175-8182.

Hess CF, Schmiedl U, Koelbel G, Knecht R, Kurtz B. Diagnosis of liver cirrhosis with US: receiver-operating characteristic analysis of multidimensional caudate lobe indexes. Radiology 1989;171:349-351.

Holmstrom P, Dzikaite V, Hultcrantz R, Melefors O, Eckes K, Stal P, Kinnman N, Smedsrod B, Gafvels M, Eggertsen G. Structure and liver cell expression pattern of the HFE gene in the rat. J Hepatol 2003;39:308-314.

Honda H, Onitsuka H, Masuda K, Nishitani H, Nakata H, Watanabe K. Chronic liver disease: value of volumetry of liver and spleen with computed tomography. Radiat Med 1990;8:222-226.

Huang FW, Pinkus JL, Pinkus GS, Fleming MD, Andrews NC. A mouse model of juvenile hemochromatosis. J Clin Invest 2005;115:2187-2191.

Huang TS, Melefors O, Lind MI, Soderhall K. An atypical iron-responsive element (IRE) within crayfish ferritin mRNA and an iron regulatory protein 1 (IRP1)-like protein from crayfish hepatopancreas. Insect Biochem Mol Biol 1999;29:1-9.

Hubert N, Hentze MW. Previously uncharacterized isoforms of divalent metal transporter (DMT)-1: implications for regulation and cellular function. Proc Natl Acad Sci U S A 2002;99:12345-12350.

Huebers HA, Finch CA. Transferrin: physiologic behavior and clinical implications. Blood 1984;64:763-767.

Hunt JR, Roughead ZK. Adaptation of iron absorption in men consuming diets with high or low iron bioavailability. Am J Clin Nutr 2000;71:94-102.

Iancu TC. Biological and ultrastructural aspects of iron overload: an overview. Pediatr Pathol 1990;10:281-296.

Iancu TC, Deugnier Y, Halliday JW, Powell LW, Brissot P. Ultrastructural sequences during liver iron overload in genetic hemochromatosis. J Hepatol 1997;27:628-638.

Ilyin GP, Langouet S, Rissel M, Delcros JG, Guillouzo A, Guguen-Guillouzo C. Ribavirin inhibits protein synthesis and cell proliferation induced by mitogenic factors in primary human and rat hepatocytes. Hepatology 1998;27:1687-1694.

Imlay JA, Linn S. DNA damage and oxygen radical toxicity. Science 1988;240:1302-1309.

Inamura J, Ikuta K, Jimbo J, Shindo M, Sato K, Torimoto Y, Kohgo Y. Upregulation of hepcidin by interleukin-1beta in human hepatoma cell lines. Hepatol Res 2005;33:198-205.

Iolascon A, d'Apolito M, Servedio V, Cimmino F, Piga A, Camaschella C. Microcytic anemia and hepatic iron overload in a child with compound heterozygous mutations in DMT1 (SCL11A2). Blood 2006;107:349-354.

Ito E, Terao K. Injury and recovery process of intestine caused by okadaic acid and related compounds. Nat Toxins 1994;2:371-377.

Jazwinska EC, Powell LW. Hemochromatosis and "HLA-H": definite! Hepatology 1997;25:495-496.

Jelkmann W. Molecular biology of erythropoietin. Intern Med 2004;43:649-659.

Johnson D, Bayele H, Johnston K, Tennant J, Srai SK, Sharp P. Tumour necrosis factor alpha regulates iron transport and transporter expression in human intestinal epithelial cells. FEBS Lett 2004;573:195-201.

Johnson G, Jacobs P, Purves LR. Iron binding proteins of iron-absorbing rat intestinal mucosa. J Clin Invest 1983;71:1467-1476.

Johnson MB, Enns CA. Diferric transferrin regulates transferrin receptor 2 protein stability. Blood 2004;104:4287-4293.

Jouanolle AM, Douabin-Gicquel V, Halimi C, Loreal O, Fergelot P, Delacour T, de Lajarte-Thirouard AS, Turlin B, Le Gall JY, Cadet E, Rochette J, David V, Brissot P. Novel mutation in ferroportin 1 gene is associated with autosomal dominant iron overload. J Hepatol 2003;39:286-289.

Kanamura T, Murakami G, Hirai I, Hata F, Sato TJ, Kumon M, Nakajima Y. High dorsal drainage routes of Spiegel's lobe. J Hepatobiliary Pancreat Surg 2001;8:549-556.

Kawabata H, Fleming RE, Gui D, Moon SY, Saitoh T, O'Kelly J, Umehara Y, Wano Y, Said JW, Koeffler HP. Expression of hepcidin is down-regulated in TfR2 mutant mice manifesting a phenotype of hereditary hemochromatosis. Blood 2005;105:376-381.

Kawabata H, Germain RS, Ikezoe T, Tong X, Green EM, Gombart AF, Koeffler HP. Regulation of expression of murine transferrin receptor 2. Blood 2001;98:1949-1954.

Kawabata H, Germain RS, Vuong PT, Nakamaki T, Said JW, Koeffler HP. Transferrin receptor 2-alpha supports cell growth both in iron-chelated cultured cells and in vivo. J Biol Chem 2000;275:16618-16625.

Kawabata H, Yang R, Hirama T, Vuong PT, Kawano S, Gombart AF, Koeffler HP. Molecular cloning of transferrin receptor 2. A new member of the transferrin receptor-like family. J Biol Chem 1999;274:20826-20832.

Kemna E, Pickkers P, Nemeth E, van der HH, Swinkels D. Time-course analysis of hepcidin, serum iron, and plasma cytokine levels in humans injected with LPS. Blood 2005;106:1864-1866.

Killisch I, Steinlein P, Romisch K, Hollinshead R, Beug H, Griffiths G. Characterization of early and late endocytic compartments of the transferrin cycle. Transferrin receptor antibody blocks erythroid differentiation by trapping the receptor in the early endosome. J Cell Sci 1992;103 (Pt 1):211-232.

Klomp LW, Farhangrazi ZS, Dugan LL, Gitlin JD. Ceruloplasmin gene expression in the murine central nervous system. J Clin Invest 1996;98:207-215.

Klomp LW, Gitlin JD. Expression of the ceruloplasmin gene in the human retina and brain: implications for a pathogenic model in aceruloplasminemia. Hum Mol Genet 1996;5:1989-1996.

Knutson M, Wessling-Resnick M. Iron metabolism in the reticuloendothelial system. Crit Rev Biochem Mol Biol 2003;38:61-88.

Knutson MD, Levy JE, Andrews NC, Wessling-Resnick M. Expression of stimulator of Fe transport is not enhanced in Hfe knockout mice. J Nutr 2001;131:1459-1464.

Knutson MD, Oukka M, Koss LM, Aydemir F, Wessling-Resnick M. Iron release from macrophages after erythrophagocytosis is up-regulated by ferroportin 1 overexpression and down-regulated by hepcidin. Proc Natl Acad Sci U S A 2005;102:1324-1328.

Koeller DM, Casey JL, Hentze MW, Gerhardt EM, Chan LN, Klausner RD, Harford JB. A cytosolic protein binds to structural elements within the iron regulatory region of the transferrin receptor mRNA. Proc Natl Acad Sci U S A 1989;86:3574-3578.

Kogure K, Kuwano H, Fujimaki N, Makuuchi M. Relation among portal segmentation, proper hepatic vein, and external notch of the caudate lobe in the human liver. Ann Surg 2000;231:223-228.

Krause A, Neitz S, Magert HJ, Schulz A, Forssmann WG, Schulz-Knappe P, Adermann K. LEAP-1, a novel highly disulfide-bonded human peptide, exhibits antimicrobial activity. FEBS Lett 2000;480:147-150.

Krijt J, Vokurka M, Sefc L, Duricova D, Necas E. Effect of lipopolysaccharide and bleeding on the expression of intestinal proteins involved in iron and haem transport. Folia Biol (Praha) 2006;52:1-5.

Kulaksiz H, Theilig F, Bachmann S, Gehrke SG, Rost D, Janetzko A, Cetin Y, Stremmel W. The iron-regulatory peptide hormone hepcidin: expression and cellular localization in the mammalian kidney. J Endocrinol 2005;184:361-370.

Kuo YM, Su T, Chen H, Attieh Z, Syed BA, McKie AT, Anderson GJ, Gitschier J, Vulpe CD. Mislocalisation of hephaestin, a multicopper ferroxidase involved in basolateral intestinal iron transport, in the sex linked anaemia mouse. Gut 2004;53:201-206.

Laftah AH, Ramesh B, Simpson RJ, Solanky N, Bahram S, Schumann K, Debnam ES, Srai SK. Effect of hepcidin on intestinal iron absorption in mice. Blood 2004;103:3940-3944.

Lamon JM, Marynick SP, Roseblatt R, Donnelly S. Idiopathic hemochromatosis in a young female. A case study and review of the syndrome in young people. Gastroenterology 1979;76:178-183.

Lanzara C, Roetto A, Daraio F, Rivard S, Ficarella R, Simard H, Cox TM, Cazzola M, Piperno A, Gimenez-Roqueplo AP, Grammatico P, Volinia S, Gasparini P, Camaschella C. Spectrum of hemojuvelin gene mutations in 1q-linked juvenile hemochromatosis. Blood 2004;103:4317-4321.

Latunde-Dada GO, Vulpe CD, Anderson GJ, Simpson RJ, McKie AT. Tissue-specific changes in iron metabolism genes in mice following phenylhydrazine-induced haemolysis. Biochim Biophys Acta 2004;1690:169-176.

Lebeau A, Frank J, Biesalski HK, Weiss G, Srai SK, Simpson RJ, McKie AT, Bahram S, Gilfillan S, Schumann K. Long-term sequelae of HFE deletion in C57BL/6 x 129/O1a mice, an animal model for hereditary haemochromatosis. Eur J Clin Invest 2002;32:603-612.

Leboeuf RC, Tolson D, Heinecke JW. Dissociation between tissue iron concentrations and transferrin saturation among inbred mouse strains. J Lab Clin Med 1995;126:128-136.

Lebron JA, Bjorkman PJ. The transferrin receptor binding site on HFE, the class I MHC-related protein mutated in hereditary hemochromatosis. J Mol Biol 1999;289:1109-1118.

Lee P, Peng H, Gelbart T, Beutler E. The IL-6- and lipopolysaccharide-induced transcription of hepcidin in HFE-, transferrin receptor 2-, and beta 2-microglobulin-deficient hepatocytes. Proc Natl Acad Sci U S A 2004;101:9263-9265.

Leibman A, Aisen P. Distribution of iron between the binding sites of transferrin in serum: methods and results in normal human subjects. Blood 1979;53:1058-1065.

Leung PS, Lam SY, Fung ML. Chronic hypoxia upregulates the expression and function of AT(1) receptor in rat carotid body. J Endocrinol 2000;167:517-524.

Leung PS, Srai SK, Mascarenhas M, Churchill LJ, Debnam ES. Increased duodenal iron uptake and transfer in a rat model of chronic hypoxia is accompanied by reduced hepcidin expression. Gut 2005;54:1391-1395.

Leventhal B, Stohlman F, Jr. Regulation of erythropoiesis XVII: the determinants of red cell size in iron-deficiency states. Pediatrics 1966;37:62-67.

Levi S, Luzzago A, Cesareni G, Cozzi A, Franceschinelli F, Albertini A, Arosio P. Mechanism of ferritin iron uptake: activity of the H-chain and deletion mapping of the ferro-oxidase site. A study of iron uptake and ferro-oxidase activity of human liver, recombinant H-chain ferritins, and of two H-chain deletion mutants. J Biol Chem 1988;263:18086-18092.

Levi S, Yewdall SJ, Harrison PM, Santambrogio P, Cozzi A, Rovida E, Albertini A, Arosio P. Evidence of H- and L-chains have co-operative roles in the iron-uptake mechanism of human ferritin. Biochem J 1992;288 (Pt 2):591-596.

Levy JE, Jin O, Fujiwara Y, Kuo F, Andrews NC. Transferrin receptor is necessary for development of erythrocytes and the nervous system. Nat Genet 1999a;21:396-399.

Levy JE, Montross LK, Andrews NC. Genes that modify the hemochromatosis phenotype in mice. J Clin Invest 2000;105:1209-1216.

Levy JE, Montross LK, Cohen DE, Fleming MD, Andrews NC. The C282Y mutation causing hereditary hemochromatosis does not produce a null allele. Blood 1999b;94:9-11.

Linder MC, Schaffer KJ, Hazegh-Azam M, Zhou CY, Tran TN, Nagel GM. Serum ferritin:does it differ from tissue ferritin? J. Gastroenterol. Hepatol. 1996 Nov; 11(11): 1033-6

Lou DQ, Lesbordes JC, Nicolas G, Viatte L, Bennoun M, Van RN, Kahn A, Renia L, Vaulont S. Iron- and inflammation-induced hepcidin gene expression in mice is not mediated by Kupffer cells in vivo. Hepatology 2005;41:1056-1064.

Lou DQ, Nicolas G, Lesbordes JC, Viatte L, Grimber G, Szajnert MF, Kahn A, Vaulont S. Functional differences between hepcidin 1 and 2 in transgenic mice. Blood 2004;103:2816-2821.

Ludwiczek S, Aigner E, Theurl I, Weiss G. Cytokine-mediated regulation of iron transport in human monocytic cells. Blood 2003;101:4148-4154.

Mack U, Cooksley WG, Ferris RA, Powell LW, Halliday JW. Regulation of plasma ferritin by the isolated perfused rat liver. Br J Haematol 1981;47:403-412.

Makui H, Soares RJ, Jiang W, Constante M, Santos MM. Contribution of Hfe expression in macrophages to the regulation of hepatic hepcidin levels and iron loading. Blood 2005;106:2189-2195.

Manis J. Intestinal iron-transport defect in the mouse with sex-linked anemia. Am J Physiol 1971;220:135-139.

Mann S, Bannister JV, Williams RJ. Structure and composition of ferritin cores isolated from human spleen, limpet (Patella vulgata) hemolymph and bacterial (Pseudomonas aeruginosa) cells. J Mol Biol 1986;188:225-232.

Mazur A, Feillet-Coudray C, Romier B, Bayle D, Gueux E, Ruivard M, Coudray C, Rayssiguier Y. Dietary iron regulates hepatic hepcidin 1 and 2 mRNAs in mice. Metabolism 2003;52:1229-1231.

Mazure NM, Chauvet C, Bois-Joyeux B, Bernard MA, Nacer-Cherif H, Danan JL. Repression of alpha-fetoprotein gene expression under hypoxic conditions in human hepatoma cells: characterization of a negative hypoxia response element that mediates opposite effects of hypoxia inducible factor-1 and c-Myc. Cancer Res 2002;62:1158-1165.

McCullen MA, Crawford DH, Hickman PE. Screening for hemochromatosis. Clin Chim Acta 2002;315:169-186.

McKie AT, Barrow D, Latunde-Dada GO, Rolfs A, Sager G, Mudaly E, Mudaly M, Richardson C, Barlow D, Bomford A, Peters TJ, Raja KB, Shirali S, Hediger MA, Farzaneh F, Simpson RJ. An iron-regulated ferric reductase associated with the absorption of dietary iron. Science 2001;291:1755-1759.

McKie AT, Latunde-Dada GO, Miret S, McGregor JA, Anderson GJ, Vulpe CD, Wrigglesworth JM, Simpson RJ. Molecular evidence for the role of a ferric reductase in iron transport. Biochem Soc Trans 2002;30:722-724.

McKie AT, Marciani P, Rolfs A, Brennan K, Wehr K, Barrow D, Miret S, Bomford A, Peters TJ, Farzaneh F, Hediger MA, Hentze MW, Simpson RJ. A novel duodenal iron-regulated transporter, IREG1, implicated in the basolateral transfer of iron to the circulation. Mol Cell 2000;5:299-309.

Means RT. Hepcidin and cytokines in anaemia. Hematology 2004;9:357-362.

Mena NP, Esparza AL, Nunez MT. Regulation of transepithelial transport of iron by hepcidin. Biol Res 2006;39:191-193.

Millard KN, Frazer DM, Wilkins SJ, Anderson GJ. Changes in the expression of intestinal iron transport and hepatic regulatory molecules explain the enhanced iron absorption associated with pregnancy in the rat. Gut 2004;53:655-660.

Miller LL, Miller SC, Torti SV, Tsuji Y, Torti FM. Iron-independent induction of ferritin H chain by tumor necrosis factor. Proc Natl Acad Sci U S A 1991;88:4946-4950.

Mims MP, Guan Y, Pospisilova D, Priwitzerova M, Indrak K, Ponka P, Divoky V, Prchal JT. Identification of a human mutation of DMT1 in a patient with microcytic anemia and iron overload. Blood 2005;105:1337-1342.

Minot GR. The development of liver therapy in pernicious anemia. extract from Nobel Prize Lecture. Nobel Prize winners in medicine and physiology 1901-1950 , 175-177. 1934.

Minot GR, Murphy LP. Treatment of pernicious anaemia by special diet JAMA. 470-476. 1926.

Moirand R, Adams PC, Bicheler V, Brissot P, Deugnier Y. Clinical features of genetic hemochromatosis in women compared with men. Ann Intern Med 1997;127:105-110.

Montosi G, Corradini E, Garuti C, Barelli S, Recalcati S, Cairo G, Valli L, Pignatti E, Vecchi C, Ferrara F, Pietrangelo A. Kupffer cells and macrophages are not required for hepatic hepcidin activation during iron overload. Hepatology 2005;41:545-552.

Montosi G, Donovan A, Totaro A, Garuti C, Pignatti E, Cassanelli S, Trenor CC, Gasparini P, Andrews NC, Pietrangelo A. Autosomal-dominant hemochromatosis is associated with a mutation in the ferroportin (SLC11A3) gene. J Clin Invest 2001;108:619-623.

Montosi G, Paglia P, Garuti C, Guzman CA, Bastin JM, Colombo MP, Pietrangelo A. Wild-type HFE protein normalizes transferrin iron accumulation in macrophages from subjects with hereditary hemochromatosis. Blood 2000;96:1125-1129.

Morgan EH, Oates PS. Mechanisms and regulation of intestinal iron absorption. Blood Cells Mol Dis 2002;29:384-399.

Morse AC, Beard JL, Jones BC. A genetic developmental model of iron deficiency: biological aspects. Proc Soc Exp Biol Med 1999;220:147-152.

Muckenthaler M, Roy CN, Custodio AO, Minana B, DeGraaf J, Montross LK, Andrews NC, Hentze MW. Regulatory defects in liver and intestine implicate abnormal hepcidin and Cybrd1 expression in mouse hemochromatosis. Nat Genet 2003;34:102-107.

Mullner EW, Neupert B, Kuhn LC. A specific mRNA binding factor regulates the iron-dependent stability of cytoplasmic transferrin receptor mRNA. Cell 1989;58:373-382.

Mura C, Le GG, Jacolot S, Ferec C. Transcriptional regulation of the human HFE gene indicates high liver expression and erythropoiesis coregulation. FASEB J 2004;18:1922-1924.

Nemeth E, Ganz T. Hepcidin and iron-loading anemias. Haematologica 2006;91:727-732.

Nemeth E, Rivera S, Gabayan V, Keller C, Taudorf S, Pedersen BK, Ganz T. IL-6 mediates hypoferremia of inflammation by inducing the synthesis of the iron regulatory hormone hepcidin. J Clin Invest 2004a;113:1271-1276.

Nemeth E, Roetto A, Garozzo G, Ganz T, Camaschella C. Hepcidin is decreased in TFR2 hemochromatosis. Blood 2005;105:1803-1806.

Nemeth E, Tuttle MS, Powelson J, Vaughn MB, Donovan A, Ward DM, Ganz T, Kaplan J. Hepcidin regulates cellular iron efflux by binding to ferroportin and inducing its internalization. Science 2004b;306:2090-2093.

Nemeth E, Valore EV, Territo M, Schiller G, Lichtenstein A, Ganz T. Hepcidin, a putative mediator of anemia of inflammation, is a type II acute-phase protein. Blood 2003;101:2461-2463.

Nicolas G, Andrews NC, Kahn A, Vaulont S. Hepcidin, a candidate modifier of the hemochromatosis phenotype in mice. Blood 2004;103:2841-2843.

Nicolas G, Bennoun M, Devaux I, Beaumont C, Grandchamp B, Kahn A, Vaulont S. Lack of hepcidin gene expression and severe tissue iron overload in upstream stimulatory factor 2 (USF2) knockout mice. Proc Natl Acad Sci U S A 2001;98:8780-8785.

Nicolas G, Bennoun M, Porteu A, Mativet S, Beaumont C, Grandchamp B, Sirito M, Sawadogo M, Kahn A, Vaulont S. Severe iron deficiency anemia in transgenic mice expressing liver hepcidin. Proc Natl Acad Sci U S A 2002a;99:4596-4601.

Nicolas G, Chauvet C, Viatte L, Danan JL, Bigard X, Devaux I, Beaumont C, Kahn A, Vaulont S. The gene encoding the iron regulatory peptide hepcidin is regulated by anemia, hypoxia, and inflammation. J Clin Invest 2002b;110:1037-1044.

Nicolas G, Viatte L, Bennoun M, Beaumont C, Kahn A, Vaulont S. Hepcidin, a new iron regulatory peptide. Blood Cells Mol Dis 2002c;29:327-335.

Nicolas G, Viatte L, Lou DQ, Bennoun M, Beaumont C, Kahn A, Andrews NC, Vaulont S. Constitutive hepcidin expression prevents iron overload in a mouse model of hemochromatosis. Nat Genet 2003;34:97-101.

Niederkofler V, Salie R, Arber S. Hemojuvelin is essential for dietary iron sensing, and its mutation leads to severe iron overload. J Clin Invest 2005;115:2180-2186.

Njajou OT, de JG, Berghuis B, Vaessen N, Snijders PJ, Goossens JP, Wilson JH, Breuning MH, Oostra BA, Heutink P, Sandkuijl LA, van Duijn CM. Dominant hemochromatosis due to N144H mutation of SLC11A3: clinical and biological characteristics. Blood Cells Mol Dis 2002;29:439-443.

Njajou OT, Vaessen N, Joosse M, Berghuis B, van Dongen JW, Breuning MH, Snijders PJ, Rutten WP, Sandkuijl LA, Oostra BA, van Duijn CM, Heutink P. A mutation in SLC11A3 is associated with autosomal dominant hemochromatosis. Nat Genet 2001;28:213-214.

Nunez MT, Osorio A, Tapia V, Vergara A, Mura CV. Iron-induced oxidative stress up-regulates calreticulin levels in intestinal epithelial (Caco-2) cells. J Cell Biochem 2001;82:660-665.

O'Riordan DK, Sharp P, Sykes RM, Srai SK, Epstein O, Debnam ES. Cellular mechanisms underlying the increased duodenal iron absorption in rats in response to phenylhydrazine-induced haemolytic anaemia. Eur J Clin Invest 1995;25:722-727.

Oates PS, Trinder D, Morgan EH. Gastrointestinal function, divalent metal transporter-1 expression and intestinal iron absorption. Pflugers Arch 2000;440:496-502.

Ohgami RS, Campagna DR, Greer EL, Antiochos B, McDonald A, Chen J, Sharp JJ, Fujiwara Y, Barker JE, Fleming MD. Identification of a ferrireductase required for efficient transferrin-dependent iron uptake in erythroid cells. Nat Genet 2005;37:1264-1269.

Olynyk J, Hall P, Reed W, Williams P, Kerr R, Mackinnon M. A long-term study of the interaction between iron and alcohol in an animal model of iron overload. J Hepatol 1995;22:671-676.

Osaki S, Johnson DA. Mobilization of liver iron by ferroxidase (ceruloplasmin). J Biol Chem 1969;244:5757-5758.

Papanikolaou G, Politou M, Roetto A, Bosio S, Sakelaropoulos N, Camaschella C, Loukopoulos D. Linkage to chromosome 1q in Greek families with juvenile hemochromatosis. Blood Cells Mol Dis 2001;27:744-749.

Papanikolaou G, Samuels ME, Ludwig EH, MacDonald ML, Franchini PL, Dube MP, Andres L, MacFarlane J, Sakellaropoulos N, Politou M, Nemeth E, Thompson J, Risler JK, Zaborowska C, Babakaiff R, Radomski CC, Pape TD, Davidas O, Christakis J, Brissot P, Lockitch G, Ganz T, Hayden MR, Goldberg YP. Mutations in HFE2 cause iron overload in chromosome 1q-linked juvenile hemochromatosis. Nat Genet 2004;36:77-82.

Papanikolaou G, Tzilianos M, Christakis JI, Bogdanos D, Tsimirika K, MacFarlane J, Goldberg YP, Sakellaropoulos N, Ganz T, Nemeth E. Hepcidin in iron overload disorders. Blood 2005;105:4103-4105.

Park CH, Valore EV, Waring AJ, Ganz T. Hepcidin, a urinary antimicrobial peptide synthesized in the liver. J Biol Chem 2001;276:7806-7810.

Parkes JG, Randell EW, Olivieri NF, Templeton DM. Modulation by iron loading and chelation of the uptake of non-transferrin-bound iron by human liver cells. Biochim Biophys Acta 1995;1243:373-380.

Parkkila S, Waheed A, Britton RS, Bacon BR, Zhou XY, Tomatsu S, Fleming RE, Sly WS. Association of the transferrin receptor in human placenta with HFE, the protein defective in hereditary hemochromatosis. Proc Natl Acad Sci U S A 1997a;94:13198-13202.

Parkkila S, Waheed A, Britton RS, Feder JN, Tsuchihashi Z, Schatzman RC, Bacon BR, Sly WS. Immunohistochemistry of HLA-H, the protein defective in patients with hereditary hemochromatosis, reveals unique pattern of expression in gastrointestinal tract. Proc Natl Acad Sci U S A 1997b;94:2534-2539.

Peters TJ, Raja KB, Simpson RJ, Snape S. Mechanisms and regulation of intestinal iron absorption. Ann N Y Acad Sci 1988;526:141-147.

Pietrangelo A. Non-HFE hemochromatosis. Semin Liver Dis 2005;25:450-460.

Pietrangelo A. Molecular insights into the pathogenesis of hereditary haemochromatosis. Gut 2006;55:564-568.

Pietrangelo A. Non-HFE hemochromatosis. Hepatology 2004a;39:21-29.

Pietrangelo A. The ferroportin disease. Blood Cells Mol Dis 2004b;32:131-138.

Pietrangelo A. Hereditary hemochromatosis--a new look at an old disease. N Engl J Med 2004c;350:2383-2397.

Pietrangelo A, Dierssen U, Valli L, Garuti C, Rump A, Corradini E, Ernst M, Klein C, Trautwein C. STAT3 is required for IL-6-gp130-dependent activation of hepcidin in vivo. Gastroenterology 2007;132:294-300.

Pietrangelo A, Montosi G, Totaro A, Garuti C, Conte D, Cassanelli S, Fraquelli M, Sardini C, Vasta F, Gasparini P. Hereditary hemochromatosis in adults without pathogenic mutations in the hemochromatosis gene. N Engl J Med 1999;341:725-732.

Pietrangelo A, Trautwein C. Mechanisms of disease: The role of hepcidin in iron homeostasis--implications for hemochromatosis and other disorders. Nat Clin Pract Gastroenterol Hepatol 2004;1:39-45.

Pigeon C, Ilyin G, Courselaud B, Leroyer P, Turlin B, Brissot P, Loreal O. A new mouse liver-specific gene, encoding a protein homologous to human antimicrobial peptide hepcidin, is overexpressed during iron overload. J Biol Chem 2001;276:7811-7819.

Ponka P, Beaumont C, Richardson DR. Function and regulation of transferrin and ferritin. Semin Hematol 1998;35:35-54.

Pratiwi R, Fletcher LM, Pyper WR, Do KA, Crawford DH, Powell LW, Jazwinska EC. Linkage disequilibrium analysis in Australian haemochromatosis patients indicates bipartite association with clinical expression. J Hepatol 1999;31:39-46.

Qiu A, Jansen M, Sakaris A, Min SH, Chattopadhyay S, Tsai E, Sandoval C, Zhao R, Akabas MH, Goldman ID. Identification of an intestinal folate transporter and the molecular basis for hereditary folate malabsorption. Cell 2006;127:917-928.

Raffin SB, Woo CH, Roost KT, Price DC, Schmid R. Intestinal absorption of haemoglobin iron-haem cleavage by mucosal haem oxygenase. J Clin Invest 1974;54:1344-1352.

Raja KB, Duane P, Peters TJ. Effects of turpentine-induced inflammation on the hypoxic stimulation of intestinal Fe3+ absorption in mice. Int J Exp Pathol 1990;71:785-789.

Raja KB, Latunde-Dada O, Peters TJ, McKie AT, Simpson RJ. Role of interleukin-6 in hypoxic regulation of intestinal iron absorption. Br J Haematol 2005;131:656-662.

Raja KB, Maxwell PH, Ratcliffe PJ, Salisbury JR, Simpson RJ, Peters TJ. Iron metabolism in transgenic mice with hypoplastic anaemia due to incomplete deficiency of erythropoietin. Br J Haematol 1997;96:248-253.

Raja KB, Pippard MJ, Simpson RJ, Peters TJ. Relationship between erythropoiesis and the enhanced intestinal uptake of ferric iron in hypoxia in the mouse. Br J Haematol 1986;64:587-593.

Raja KB, Pountney DJ, Simpson RJ, Peters TJ. Importance of anemia and transferrin levels in the regulation of intestinal iron absorption in hypotransferrinemic mice. Blood 1999;94:3185-3192.

Raja KB, Simpson RJ, Peters TJ. Investigation of a role for reduction in ferric iron uptake by mouse duodenum. Biochim Biophys Acta 1992;1135:141-146.

Raja KB, Simpson RJ, Pippard MJ, Peters TJ. In vivo studies on the relationship between intestinal iron (Fe3+) absorption, hypoxia and erythropoiesis in the mouse. Br J Haematol 1988;68:373-378.

Ramm GA, Powell LW, Halliday JW. Pathways of intracellular trafficking and release of ferritin by the liver in vivo: the effect of chloroquine and cytochalasin D. Hepatology 1994;19:504-513.

Randell EW, Parkes JG, Olivieri NF, Templeton DM. Uptake of non-transferrin-bound iron by both reductive and nonreductive processes is modulated by intracellular iron. J Biol Chem 1994;269:16046-16053.

Richardson DR, Ponka P. The molecular mechanisms of the metabolism and transport of iron in normal and neoplastic cells. Biochim Biophys Acta 1997;1331:1-40.

Rivard SR, Lanzara C, Grimard D, Carella M, Simard H, Ficarella R, Simard R, D'Adamo AP, De BM, Gasparini P. Autosomal dominant reticuloendothelial iron overload (HFE type 4) due to a new missense mutation in the FERROPORTIN 1 gene (SLC11A3) in a large French-Canadian family. Haematologica 2003a;88:824-826.

Rivard SR, Lanzara C, Grimard D, Carella M, Simard H, Ficarella R, Simard R, D'Adamo AP, Ferec C, Camaschella C, Mura C, Roetto A, De BM, Bechner L, Gasparini P. Juvenile hemochromatosis locus maps to chromosome 1q in a French Canadian population. Eur J Hum Genet 2003b;11:585-589.

Rivard SR, Mura C, Simard H, Simard R, Grimard D, Le GG, Raguenes O, Ferec C, De BM. Clinical and molecular aspects of juvenile hemochromatosis in Saguenay-Lac-Saint-Jean (Quebec, canada). Blood Cells Mol Dis 2000;26:10-14.

Rivera S, Liu L, Nemeth E, Gabayan V, Sorensen OE, Ganz T. Hepcidin excess induces the sequestration of iron and exacerbates tumor-associated anemia. Blood 2005a;105:1797-1802.

Rivera S, Nemeth E, Gabayan V, Lopez MA, Farshidi D, Ganz T. Synthetic hepcidin causes rapid dose-dependent hypoferremia and is concentrated in ferroportin-containing organs. Blood 2005b;106:2196-2199.

Robb A, Wessling-Resnick M. Regulation of transferrin receptor 2 protein levels by transferrin. Blood 2004;104:4294-4299.

Roberts FD, Charalambous P, Fletcher L, Powell LW, Halliday JW. Effect of chronic iron overload on procollagen gene expression. Hepatology 1993;18:590-595.

Robson KJ, Merryweather-Clarke AT, Cadet E, Viprakasit V, Zaahl MG, Pointon JJ, Weatherall DJ, Rochette J. Recent advances in understanding haemochromatosis: a transition state. J Med Genet 2004;41:721-730.

Roetto A, Daraio F, Porporato P, Caruso R, Cox TM, Cazzola M, Gasparini P, Piperno A, Camaschella C. Screening hepcidin for mutations in juvenile hemochromatosis: identification of a new mutation (C70R). Blood 2004;103:2407-2409.

Roetto A, Merryweather-Clarke AT, Daraio F, Livesey K, Pointon JJ, Barbabietola G, Piga A, Mackie PH, Robson KJ, Camaschella C. A valine deletion of ferroportin 1: a common mutation in hemochromastosis type 4. Blood 2002;100:733-734.

Roetto A, Papanikolaou G, Politou M, Alberti F, Girelli D, Christakis J, Loukopoulos D, Camaschella C. Mutant antimicrobial peptide hepcidin is associated with severe juvenile hemochromatosis. Nat Genet 2003;33:21-22.

Roetto A, Totaro A, Cazzola M, Cicilano M, Bosio S, D'Ascola G, Carella M, Zelante L, Kelly AL, Cox TM, Gasparini P, Camaschella C. Juvenile hemochromatosis locus maps to chromosome 1q. Am J Hum Genet 1999;64:1388-1393.

Roetto A, Totaro A, Piperno A, Piga A, Longo F, Garozzo G, Cali A, De GM, Gasparini P, Camaschella C. New mutations inactivating transferrin receptor 2 in hemochromatosis type 3. Blood 2001;97:2555-2560.

Rouault TA. Hereditary hemochromatosis--sometimes having a real complex can be a good thing. Hepatology 1998;28:890-891.

Roy CN, Andrews NC. Anemia of inflammation: the hepcidin link. Curr Opin Hematol 2005;12:107-111.

Roy CN, Blemings KP, Deck KM, Davies PS, Anderson EL, Eisenstein RS, Enns CA. Increased IRP1 and IRP2 RNA binding activity accompanies a reduction of the labile iron pool in HFE-expressing cells. J Cell Physiol 2002;190:218-226.

Roy CN, Custodio AO, de GJ, Schneider S, Akpan I, Montross LK, Sanchez M, Gaudino A, Hentze MW, Andrews NC, Muckenthaler MU. An Hfe-dependent pathway mediates hyposideremia in response to lipopolysaccharide-induced inflammation in mice. Nat Genet 2004;36:481-485.

Roy CN, Enns CA. Iron homeostasis: new tales from the crypt. Blood 2000;96:4020-4027.

Sahlstedt L, von BL, Ebeling F, Ruutu T, Parkkinen J. Effective binding of free iron by a single intravenous dose of human apotransferrin in haematological stem cell transplant patients. Br J Haematol 2002;119:547-553.

Salter-Cid L, Brunmark A, Li Y, Leturcq D, Peterson PA, Jackson MR, Yang Y. Transferrin receptor is negatively modulated by the hemochromatosis protein HFE: implications for cellular iron homeostasis. Proc Natl Acad Sci U S A 1999;96:5434-5439.

Santos M, Clevers H, de SM, Marx JJ. Adaptive response of iron absorption to anemia, increased erythropoiesis, iron deficiency, and iron loading in beta2-microglobulin knockout mice. Blood 1998;91:3059-3065.

Scheiber-Mojdehkar B, Sturm B, Plank L, Kryzer I, Goldenberg H. Influence of parenteral iron preparations on non-transferrin bound iron uptake, the iron regulatory protein and the expression of ferritin and the divalent metal transporter DMT-1 in HepG2 human hepatoma cells. Biochem Pharmacol 2003;65:1973-1978.

Schimanski LM, Drakesmith H, Merryweather-Clarke AT, Viprakasit V, Edwards JP, Sweetland E, Bastin JM, Cowley D, Chinthammitr Y, Robson KJ, Townsend AR. In vitro functional analysis of human ferroportin (FPN) and hemochromatosis-associated FPN mutations. Blood 2005;105:4096-4102.

Sham RL, Phatak PD, West C, Lee P, Andrews C, Beutler E. Autosomal dominant hereditary hemochromatosis associated with a novel ferroportin mutation and unique clinical features. Blood Cells Mol Dis 2005;34:157-161.

Sharma N, Laftah AH, Brookes MJ, Cooper B, Iqbal T, Tselepis C. A role for tumour necrosis factor alpha in human small bowel iron transport. Biochem J 2005;390:437-446.

Sharp P, Tandy S, Yamaji S, Tennant J, Williams M, Singh Srai SK. Rapid regulation of divalent metal transporter (DMT1) protein but not mRNA expression by non-haem iron in human intestinal Caco-2 cells. FEBS Lett 2002;510:71-76.

Shayeghi M, Latunde-Dada GO, Oakhill JS, Laftah AH, Takeuchi K, Halliday N, Khan Y, Warley A, McCann FE, Hider RC, Frazer DM, Anderson GJ, Vulpe CD, Simpson RJ, McKie AT. Identification of an intestinal haem transporter. Cell 2005;122:789-801.

Sheikh N, Dudas J, Ramadori G. Changes of gene expression of iron regulatory proteins during turpentine oil-induced acute-phase response in the rat. Lab Invest 2007.

Sherlock S, Dooley J. Diseases of the Liver and Biliary System. -706. 2002. London, Blackwell.

Sheuer P, Leftowitch J. Liver biopsy interpretation. 2000. W.B. Saunders Company; 6th edition.

Simon M, Bourel M, Alexandre JL, Brissot P, Hita de NY, Scordia C. [Letter: Heridity of hemochromatosis: its relation with HL-A system]. Nouv Presse Med 1976;5:1762.

Simpson RJ, Debnam ES, Laftah AH, Solanky N, Beaumont N, Bahram S, Schumann K, Srai SK. Duodenal nonhaem iron content correlates with iron stores in mice, but the relationship is altered by Hfe gene knock-out. Blood 2003;101:3316-3318.

Sproule TJ, Jazwinska EC, Britton RS, Bacon BR, Fleming RE, Sly WS, Roopenian DC. Naturally variant autosomal and sex-linked loci determine the severity of iron overload in beta 2-microglobulin-deficient mice. Proc Natl Acad Sci U S A 2001;98:5170-5174.

Stadtman ER, Wittenberger ME. Inactivation of Escherichia coli glutamine synthetase by xanthine oxidase, nicotinate hydroxylase, horseradish peroxidase, or glucose oxidase: effects of ferredoxin, putidaredoxin, and menadione. Arch Biochem Biophys 1985;239:379-387.

Stal P, Hultcrantz R. Iron increases ethanol toxicity in rat liver. J Hepatol 1993;17:108-115.

Syed BA, Beaumont NJ, Patel A, Naylor CE, Bayele HK, Joannou CL, Rowe PS, Evans RW, Srai SK. Analysis of the human hephaestin gene and protein: comparative modelling of the N-terminus ecto-domain based upon ceruloplasmin. Protein Eng 2002;15:205-214.

Szewczenko-Pawlikowski M, Dziak E, McLaren MJ, Michalak M, Opas M. Heat shock-regulated expression of calreticulin in retinal pigment epithelium. Mol Cell Biochem 1997;177:145-152.

Tan CC, Ratcliffe PJ. Rapid oxygen-dependent changes in erythropoietin mRNA in perfused rat kidneys: evidence against mediation by cAMP. Kidney Int 1992;41:1581-1587.

Tavill AS, Sharma BK, Bacon BR. Iron and the liver: genetic hemochromatosis and other hepatic iron overload disorders. Prog Liver Dis 1990;9:281-305.

Tchernitchko D, Bourgeois M, Martin ME, Beaumont C. Expression of the two mRNA isoforms of the iron transporter Nramp2/DMTI in mice and function of the iron responsive element. Biochem J 2002;363:449-455.

Tector AJ, Olynyk JK, Britton RS, Janney CG, O'Neill R, Bacon BR. Hepatic mitochondrial oxidative metabolism and lipid peroxidation in iron-loaded rats fed ethanol. J Lab Clin Med 1995;126:597-602.

Theil EC. Ferritin: structure, function, and regulation. Adv Inorg Biochem 1983;5:1-38.

Theil EC. The ferritin family of iron storage proteins. Adv Enzymol Relat Areas Mol Biol 1990;63:421-449.

Theil EC. Ferritin: at the crossroads of iron and oxygen metabolism. J Nutr 2003;133:1549S-1553S.

Thomas C, Oates PS. Ferroportin/IREG-1/MTP-1/SLC40A1 modulates the uptake of iron at the apical membrane of enterocytes. Gut 2004;53:44-49.

Thomson AM, Rogers JT and Leedman PJ. Iron-regulatory proteins, iron-responsive elements and ferritin mRNA translation. The Intern. J. Biochem. & Cell Bio. 1999; 31 (10): 1139-1152.

Thorstensen K. Hepatocytes and reticulocytes have different mechanisms for the uptake of iron from transferrin. J Biol Chem 1988;263:16837-16841.

Thorstensen K, Romslo I. Uptake of iron from transferrin by isolated rat hepatocytes. A redox-mediated plasma membrane process? J Biol Chem 1988;263:8844-8850.

Tolosano E, Altruda F. Hemopexin: structure, function, and regulation. DNA Cell Biol 2002;21:297-306.

Tomatsu S, Orii KO, Fleming RE, Holden CC, Waheed A, Britton RS, Gutierrez MA, Velez-Castrillon S, Bacon BR, Sly WS. Contribution of the H63D mutation in HFE to murine hereditary hemochromatosis. Proc Natl Acad Sci U S A 2003;100:15788-15793.

Torrance JD, Bothwell TH. Tissue iron stores. Methods in hematology (Iron). (Cook, JD eds.), 90-115. 1980. New York, Churchill Livingstone.

Torti SV, Kwak EL, Miller SC, Miller LL, Ringold GM, Myambo KB, Young AP, Torti FM. The molecular cloning and characterization of murine ferritin heavy chain, a tumor necrosis factor-inducible gene. J Biol Chem 1988;263:12638-12644.

Townsend A, Drakesmith H. Role of HFE in iron metabolism, hereditary haemochromatosis, anaemia of chronic disease, and secondary iron overload. Lancet 2002;359:786-790.

Trenor CC, III, Campagna DR, Sellers VM, Andrews NC, Fleming MD. The molecular defect in hypotransferrinemic mice. Blood 2000;96:1113-1118.

Trinder D, Fox C, Vautier G, Olynyk JK. Molecular pathogenesis of iron overload. Gut 2002a;51:290-295.

Trinder D, Macey DJ, Olynyk JK. The new iron age. Int J Mol Med 2000a;6:607-612.

Trinder D, Morgan E. Inhibition of uptake of transferrin-bound iron by human hepatoma cells by nontransferrin-bound iron. Hepatology 1997;26:691-698.

Trinder D, Oates PS, Thomas C, Sadleir J, Morgan EH. Localisation of divalent metal transporter 1 (DMT1) to the microvillus membrane of rat duodenal enterocytes in iron deficiency, but to hepatocytes in iron overload. Gut 2000b;46:270-276.

Trinder D, Olynyk JK, Sly WS, Morgan EH. Iron uptake from plasma transferrin by the duodenum is impaired in the Hfe knockout mouse. Proc Natl Acad Sci U S A 2002b;99:5622-5626.

Trinder D, Zak O, Aisen P. Transferrin receptor-independent uptake of differic transferrin by human hepatoma cells with antisense inhibition of receptor expression. Hepatology 1996;23:1512-1520.

Trousseau A. Glycosurie, diabete sucre. Clinique Medical de l'Hotel-Dieu de Paris 2, 663-698. 1865.

Truksa J, Peng H, Lee P, Beutler E. Bone morphogenetic proteins 2, 4, and 9 stimulate murine hepcidin 1 expression independently of Hfe, transferrin receptor 2 (Tfr2), and IL-6. Proc Natl Acad Sci U S A 2006;103:10289-10293.

Tsukamoto H. Oxidative stress, antioxidants, and alcoholic liver fibrogenesis. Alcohol 1993;10:465-467.

van Weert AW, Dunn KW, Gueze HJ, Maxfield FR, Stoorvogel W. Transport from late endosomes to lysosomes, but not sorting of integral membrane proteins in endosomes, depends on the vacuolar proton pump. J Cell Biol 1995;130:821-834.

varez-Hernandez X, Liceaga J, McKay IC, Brock JH. Induction of hypoferremia and modulation of macrophage iron metabolism by tumor necrosis factor. Lab Invest 1989;61:319-322.

Varga AC, Wrana JL. The disparate role of BMP in stem cell biology. Oncogene 2005;24:5713-5721.

Viatte L, Lesbordes-Brion JC, Lou DQ, Bennoun M, Nicolas G, Kahn A, Canonne-Hergaux F, Vaulont S. Deregulation of proteins involved in iron metabolism in hepcidin-deficient mice. Blood 2005;105:4861-4864.

Vokurka M, Krijt J, Sulc K, Necas E. Hepcidin mRNA levels in mouse liver respond to inhibition of erythropoiesis. Physiol Res 2006;55:667-674.

von Recklinhausen D. "Hamochromatose" Tageblatt der naturforscheden Versammlung. Heidelberg 1890, 324. 1889.

Vulpe CD, Kuo YM, Murphy TL, Cowley L, Askwith C, Libina N, Gitschier J, Anderson GJ. Hephaestin, a ceruloplasmin homologue implicated in intestinal iron transport, is defective in the sla mouse. Nat Genet 1999;21:195-199.

Waheed A, Parkkila S, Saarnio J, Fleming RE, Zhou XY, Tomatsu S, Britton RS, Bacon BR, Sly WS. Association of HFE protein with transferrin receptor in crypt enterocytes of human duodenum. Proc Natl Acad Sci U S A 1999;96:1579-1584.

Wallace DF, Clark RM, Harley HA, Subramaniam VN. Autosomal dominant iron overload due to a novel mutation of ferroportin1 associated with parenchymal iron loading and cirrhosis. J Hepatol 2004;40:710-713.

Wallace DF, Pedersen P, Dixon JL, Stephenson P, Searle JW, Powell LW, Subramaniam VN. Novel mutation in ferroportin1 is associated with autosomal dominant hemochromatosis. Blood 2002;100:692-694.

Wallace DF, Summerville L, Lusby PE, Subramaniam VN. First phenotypic description of transferrin receptor 2 knockout mouse, and the role of hepcidin. Gut 2005;54:980-986.

Wang RH, Li C, Xu X, Zheng Y, Xiao C, Zerfas P, Cooperman S, Eckhaus M, Rouault T, Mishra L, Deng CX. A role of SMAD4 in iron metabolism through the positive regulation of hepcidin expression. Cell Metab 2005;2:399-409.

Wassell J. Haptoglobin: function and polymorphism. Clin Lab 2000;46:547-552.

Weinstein DA, Roy CN, Fleming MD, Loda MF, Wolfsdorf JI, Andrews NC. Inappropriate expression of hepcidin is associated with iron refractory anemia: implications for the anemia of chronic disease. Blood 2002;100:3776-3781.

Weintraub LR, Conrad ME, Crosby WH. Absorption of haemoglobin iron by the rat. Proc Soc Exp Biol Med 1965;120:840-843.

Weiss G, Goodnough LT. Anemia of chronic disease. N Engl J Med 2005;352:1011-1023.

Wessling-Resnick M. Iron imports. III. Transfer of iron from the mucosa into circulation. Am J Physiol Gastrointest Liver Physiol 2006;290:G1-G6.

West AP, Jr., Bennett MJ, Sellers VM, Andrews NC, Enns CA, Bjorkman PJ. Comparison of the interactions of transferrin receptor and transferrin receptor 2 with transferrin and the hereditary hemochromatosis protein HFE. J Biol Chem 2000;275:38135-38138.

Wheby MS. Site of iron absorption in man. Scand J Haematol 1970;7:56-62.

Wheby MS, Jones LG, Crosby WH. Studies on iron absorption. Intestinal regulatory mechanisms. J Clin Invest 1964;43:1433-1442.

Whipple GH, Robscheit-Robbins FS. Favourable influence of liver, heart and skeletal muscle in diet on blood regeneration in anemia. American Journal of Physiology 72, 408-418. 1925a.

Whipple GH, Robscheit-Robbins FS. Iron reaction favourable, arsenic and germanium dioxide almost inert, in severe anemia. American Journal of Physiology 72, 419-430. 1925b.

Whitfield JB, Cullen LM, Jazwinska EC, Powell LW, Heath AC, Zhu G, Duffy DL, Martin NG. Effects of HFE C282Y and H63D polymorphisms and polygenic background on iron stores in a large community sample of twins. Am J Hum Genet 2000;66:1246-1258.

Widdowson EM, McCance RA. The absorption and excretion of iron before, during and after a period of very high intake. Biochem.J. 31, 2029-2034. 1937.

Wittwer CT, Herrmann MG, Moss AA, Rasmussen RP. Continuous fluorescence monitoring of rapid cycle DNA amplification. Biotechniques 1997;22:130-138.

Wright TL, Brissot P, Ma WL, Weisiger RA. Characterization of non-transferrin-bound iron clearance by rat liver. J Biol Chem 1986;261:10909-10914.

Wrighting DM, Andrews NC. Interleukin-6 induces hepcidin expression through STAT3. Blood 2006;108:3204-3209.

Wyllie JC, Kaufman N. An electron microscopic study of haem uptake by rat duodenum. Lab Invest 1982;47:471-476.

Yamaji S, Sharp P, Ramesh B, Srai SK. Inhibition of iron transport across human intestinal epithelial cells by hepcidin. Blood 2004;104:2178-2180.

Yang F, Liu XB, Quinones M, Melby PC, Ghio A, Haile DJ. Regulation of reticuloendothelial iron transporter MTP1 (Slc11a3) by inflammation. J Biol Chem 2002;277:39786-39791.

Yeh KY, Yeh M, Glass J. Hepcidin regulation of ferroportin 1 expression in the liver and intestine of the rat. Am J Physiol Gastrointest Liver Physiol 2004;286:G385-G394.

Zhang AS, Xiong S, Tsukamoto H, Enns CA. Localization of iron metabolism-related mRNAs in rat liver indicate that HFE is expressed predominantly in hepatocytes. Blood 2004;103:1509-1514.

Zhou XY, Tomatsu S, Fleming RE, Parkkila S, Waheed A, Jiang J, Fei Y, Brunt EM, Ruddy DA, Prass CE, Schatzman RC, O'Neill R, Britton RS, Bacon BR, Sly WS. HFE gene knockout produces mouse model of hereditary hemochromatosis. Proc Natl Acad Sci U S A 1998;95:2492-2497.

Zoller H, Pietrangelo A, Vogel W, Weiss G. Duodenal metal-transporter (DMT-1, NRAMP-2) expression in patients with hereditary haemochromatosis. Lancet 1999;353:2120-2123.

Appendix I

Disease or condition	Gene responsible	Human mutation/s	Mouse model	Strains of Mouse Model	References *
Haemochromatosis	HFE	R74X, G93fs (nonsense mutations)	HFE KO	C57BL/6	(Bahram et al. 1999;Bensaid et al. 2004;Chua et al. 2004;Dupic et al. 2002a;Fleming et al. 2001;Knutson et al. 2001;Lebeau et al. 2002;Trinder et al. 2002b)
				DBA	(Bensaid et al. 2004;Dupic et al. 2002a)
				AKR	(Fleming et al. 2001)
				C3H	
		C282Y	C282Y KO	C57BL/6J	(Levy et al. 1999b)
			C294Y		(Tomatsu et al. 2003)
		H63D	H67D		
	HJV	At least 30	HJV KO		(Huang et al. 2005)
					(Niederkofler et al. 2005)
			USF2		(Nicolas et al. 2001)
			C/EBPa	BALB/cJ	(Courselaud et al. 2002)
	TFR2	At least 5	TFR2 KO	C57BL/6J	(Wallace et al. 2005)
		X250Y	$TFR2^{Y245X}$		(Fleming et al. 2002)
Ferroportin Disease	IREG1	At least 12	Fpn (null/null)	N/A	(Donovan et al. 2005)
Acaeruloplasminemia	CP	several	CP KO	black Swiss-Webster	(Harris et al. 1999)
Atransferrinaemia	Transferrin	Only 3 cases to date	$Trf^{hpx/hpx}$	BALB/cj	(Craven et al. 1987;Trenor, III et al. 2000)

Table I Mouse models of primary iron overload diseases

**References are representative publications that refer to the mouse models and not to the human diseases mentioned*

Parameters	Hepcidin mRNA (% of control)	SEM	p
Liver iron >10 mg/g dry weight (n=5)	85	12	
Liver iron>5 <10 mg/g dry weight (n=8)	131	32	0.3
Liver iron <5 mg/g dry weight (n=5)	131	16	0.05*
Ferritin >3000 ng/ml (n=6)	117 δ	34	
Ferritin <1500 ng/ml (n=7)	116	29	NS
AST>80iu/l (n=4)	67.0	11.9	
AST<80iu/l (n=12)	106.9	15.8	NS

Table II **Factors affecting hepcidin expression in all Thalassaemic patients (Thalassaemia Major and Thalassaemia Intermedia).** Aspartate transaminase (AST), * Denotes significant difference in hepcidin expression between subjects with liver iron greater than 10 mg/g dry weight compared to subjects with liver iron below 5 mg/g dry weight; δ Ferritin > 1501 and <2999 ng/ml (n=7), not shown on the table, hepcidin values (mRNA %) similar to those described on the table.

Appendix II

PUBLICATIONS DERIVED FROM THE STUDIES DESCRIBED IN THIS THESIS

Downloaded from gut.bmj.com on 27 May 2007

SMALL INTESTINE

Increased duodenal iron uptake and transfer in a rat model of chronic hypoxia is accompanied by reduced hepcidin expression

P S Leung, S K Srai, M Mascarenhas, L J Churchill, E S Debnam

See end of article for authors' affiliations

Gut 2005;**54**:1391–1395. doi: 10.1136/gut.2004.062083

Downloaded from gut.bmj.com on 27 May 2007

Downloaded from gut.bmj.com on 27 May 2007

Downloaded from gut.bmj.com on 27 May 2007

Downloaded from gut.bmj.com on 27 May 2007

Uptake of Non-Transferrin Iron into Human Hepatoma Cells is DMT1-Independent and Modulated by Selective Inhibitors of T-Type Voltage-Dependent Calcium Channels.

Roozina Rafique[¶], Monica S.D. Mascarenhas[‡], Bala Ramesh[‡], Surjit K.S. Srai[‡], John B. Porter[¶].

[¶] Department of Haematology, University College London Medical School, London WC1E 6HX, United Kingdom, [‡]Department of Biochemistry & Molecular Biology, Royal Free and University College London Medical School, Rowland Hill Street, London NW3 2PF, United Kingdom.

Address all correspondence to Dr. R. Rafique at:

Department of Haematology
University College London Medical School

Abstract.

Clearance of plasma non-transferrin bound iron (NTBI) occurs predominantly by hepatocytes and is enhanced by iron loading, through poorly defined mechanisms. Using iron:citrate and human hepatoma HuH7 cells to model hepatocyte NTBI uptake, we show this occurs through T-type but not L-type voltage dependent calcium channels (VDCC). Uptake saturates at 6μM extracellular iron, is maximal at neutral pH, is enhanced by ascorbate and by extracellular Ca^{2+} and is directly proportional to intracellular iron concentrations. Ferrous and ferric iron uptake is inhibited by a range of divalent cations but metabolic and endocytic inhibitors have minimal effect. DMT1 antibody fails to inhibit uptake, in contrast to CaCo2 cells, and DMT1(±IRE) mRNA is unaffected by iron loading of HuH7 cells. Enhancement of iron uptake by membrane depolarisation with KCl or by iron loading is attenuated by T- but not L-type VDCC inhibitors. Enhanced iron uptake by cellular iron preloading may be post-transcriptional because this failed to up-regulate T-type VDCC mRNA and because inhibitors of mRNA or protein synthesis did not abrogate this enhancement. As the iron uptake mechanism into hepatocyte like cells differs from that reported for cardiac myocytes (L-type VDCC), selective therapeutic inhibition of the latter may be feasible.

word count 197

Introduction

Plasma transferrin becomes saturated in iron overload conditions or when haematopoiesis is interrupted *(Hershko, Graham et al. 1978); (Batey, Lai Chung Fong et al. 1980; Bradley, Gosriwitana et al. 1997),* leading to non-transferrin bound iron species in plasma at concentrations up to 10μM *(Porter, Abeysinghe et al. 1996).* Plasma NTBI is chemically heterogeneous but a significant proportion is bound to plasma citrate *(Grootveld, Bell et al. 1989)* and some is loosely associated with plasma proteins such as albumin *(Lovstad 1993; Loban, Kime et al. 1997).* The distribution of NTBI uptake into tissues differs from transferrin mediated uptake *(Craven, Alexander et al. 1987)* and is responsible for the iron loading of pancreas, anterior pituitary and cardiac myocytes in transfusional iron overload. The liver is the predominant site of iron storage in iron overload and clears 60-80% of NTBI by first pass extraction *(Zimelman, Zimmerman et al. 1977; Brissot, Wright et al. 1985).* The mechanism of NTBI uptake into hepatocytes however is still unclear and is addressed in this paper. A second question that is addressed is how iron loading or iron depletion of cells may modulate NTBI uptake. A number of studies have shown that NTBI uptake into hepatocytes is up-regulated by iron loading *(Randell, Parkes et al. 1994; Parkes, Randell et al. 1995; Scheiber-Mojdehkar, Zimmermann et al. 1999)* whilst others have failed to see any effect *(Wright, Brissot et al. 1986; Baker, Baker et al. 1998).*

Studies on NTBI uptake mechanisms in intact animals *(Craven, Alexander et al. 1987),* liver perfusion models (*Brissot, Wright et al. 1985; Wright, Brissot et al. 1986; Wright, Fitz et al. 1988*), primary cultures of rat hepatocytes *(Thorstensen 1988; Thorstensen and Romslo 1988; Barisani, Berg et al. 1995; Baker, Baker et al. 1998; Graham, Morgan et al. 1998; Graham, Morgan et al. 1998)* or human hepatoma cells *(Randell, Parkes et al. 1994; Parkes, Randell et*

al. 1995; Trinder and Morgan 1998), favour the involvement of a temperature-sensitive, saturable, carrier-mediated process, which has a pre-requisite for ferric iron reduction, is driven by a transmembrane potential difference, is calcium-dependent and is inhibited by other divalent cations. A candidate for hepatocellular NTBI uptake is the divalent metal transporter, DMT1, but there is conflicting evidence regarding its role (*Trinder, Oates et al. 2000; Gunshin, Allerson et al. 2001; Gunshin, Fujiwara et al. 2005).* In this paper we have investigated the possible role of DMT1-mediated iron uptake and have examined the possibility of alternative mechanisms.

A common feature of tissues susceptible to iron overload is the large number and activity of voltage-dependent calcium channels (VDCC) *(Catterall 2000; Muth, Varadi et al. 2001; Peri, Triggle et al. 2001).* Recently, it has been shown that VDCC may provide a major pathway for iron entry into cardiac cells under conditions of iron overload *(Oudit, Sun et al. 2003; Oudit, Trivieri et al. 2006).* However studies with L-type specific calcium channel antagonists in HepG2 cells *(Randell, Parkes et al. 1994)* and neonatal cardiac myocytes *(Parkes, Olivieri et al. 1997)* reported little or no effect on iron uptake. In human liver, five different subtypes of VDCC are known to be expressed; the L-type $Ca_v1.1$, 1.2 and 1.3 and the T-type Ca_v 3.1 and 3.2, although their function is not known *(Williams, Washburn et al. 1999; Okamoto, Jeong et al. 2001).* Currently, pharmacological differentiation is the best means for distinguishing between the different channel types. The L-type channels are blocked by organic calcium channel antagonists, including dihydropyridines (e.g. nifedipine), phenylalkylamines (e.g. verapamil) and benzothiazepines (e.g. diltiazem). The N, P/Q and R-type channels are relatively insensitive to the L-type calcium channel antagonists but are blocked by specific polypeptide toxins, including the conotoxins and agatoxins *(Abernethy and Schwartz 1999; Triggle 1999).* The T-type channels are resistant to both the organic antagonists and to the polypeptide toxins but are

preferentially blocked by the benzimidazole, mibefradil *(Martin, Lee et al. 2000)* and by the diphenylbutylpiperidines, such as pimozide and penfluridol *(Enyeart, Biagi et al. 1992)*.

Here we have used the HuH7 cell line, derived from human hepatoma cells and iron citrate at physiologically-relevant concentrations as a model for NTBI uptake into hepatocytes. HuH7 cells produce liver-specific enzymes, G6Pase and FDPase, in addition to a range of plasma proteins and retain differentiated functions of hepatocytes when grown in fully defined synthetic medium *(Nakabayashi, Taketa et al. 1982)*, unlike primary hepatocyte cultures which may loose differentiated functions. This cell line has also been previously used to characterise hepatic NTBI uptake (*Trinder and Morgan 1998)*. In this study we demonstrate for the first time that hepatic NTBI uptake can be mediated by T-type VDCC.

Intro 761 words

Materials and Methods

Materials- ^{59}Iron(III) chloride (in 0.1 M HCl) was purchased from GE Healthcare (Amersham, Bucks, UK). RPMI 1640 medium containing L-glutamine and 25 mM HEPES buffer, was purchased from Gibco BRL (Invitrogen Life Technologies Inc, Paisley, UK). Foetal calf serum was from PAA Laboratories (Somerset, UK). Pronase was purchased from Roche Diagnostics Ltd (East Sussex, UK). Deferoxamine (Desferal®) was obtained from Novartis (Basel-Switzerland). Iron atomic absorption standard solution and 2,4-dinitrophenol were from Aldrich Chemical Company Inc (Dorset, UK). Manganese(II) chloride, calcium chloride 2-hydrate, copper (II) chloride 2-hydrate, zinc (II) chloride, cadmium (II) chloride 1-hydrate, cobalt (II) chloride 6-hydrate, nickel (II) chloride 6-hydrate, iron (II) sulphate 7-hydrate and citric acid, potassium chloride were purchased from VWR International, Dorset, UK. Dulbecco's modified Eagle's minimal essential medium (DMEM), penicillin, gentamicin, streptomycin, Trypan blue, ferric ammonium citrate (FAC), ascorbic acid, dimethyl sulfoxide (DMSO), Bafilomycin A_1 (from *Streptomyces griseus*), verapamil, nifedipine, mibefradil, NNC 55-0396, pimozide, penfluridol, amiloride, ethosuximide, BayK8644, kurtoxin, cycloheximide, actinomycin D and MOPS (3-[N-Morpholino] propanesulfonic acid) were from Sigma (Dorset, UK). All chemicals were of analytical grade. De-ionized water produced by a Millipore Ultrapure system (Simplicity 185, Millipore, Watford, UK) was used throughout.

Antibodies- DMT1 (Divalent Metal Transporter 1) polyclonal antibody, raised in rabbit against a synthetic peptide corresponding to amino acids 310-330 of the human DMT1 sequence, was prepared as described previously *(Tandy, Williams et al. 2000)*. Non-immunized rabbit serum was purchased from DakoCytomation (Denmark).

Cell Culture- The HuH7 human hepatoma cell line was obtained from Dr Nikolai Naoumov (Institute of Hepatology, UCL, London, UK). HuH7 cells were grown in monolayer culture in RPMI 1640 medium containing L-glutamine and 25 mM HEPES buffer, supplemented with 10% heat-inactivated foetal calf serum, 100 U/ml penicillin and 50 μg/ml gentamicin. Caco-2 TC7 cells were cultured in DMEM supplemented with 10% heat-inactivated foetal calf serum, 100 U/ml penicillin and 0.1 mg/ml streptomycin. Cells were seeded at a density of 1.5-2.0 x 10^5 cells per 80-cm^2 flask (Nunclon, Nunc Brand) and grown at 37°C in a humidified atmosphere of 5% CO_2 in air. Cell viability was determined by Trypan blue dye exclusion.

Non-Transferrin Bound Iron (NTBI) Preparation

Ferric(III) citrate complex- A stock solution of ferric citrate was prepared by mixing 10 μM of labelled ($^{59}FeCl_3$) and unlabeled $FeCl_3$ in 0.1 M HCl (iron atomic absorption standard solution) with 100-fold molar excess of citrate (1 mM). The solution was diluted 1:10 in serum-free RPMI medium to give a final pH of 7.4, before adding to cells. Where a low pH was required, the RPMI medium was adjusted with concentrated HCl to the required pH prior to diluting the ferric citrate complex.

Ascorbate-reduced ferric citrate- In order to measure ferrous (Fe^{2+}) uptake in the Caco-2 cells, ferric citrate was prepared by mixing a 10 μM solution of $^{59}FeCl_3$/ $FeCl_3$ (in 0.1 M HCl) with 100-fold molar excess of citrate (1 mM) and 100-fold molar excess of ascorbate (1 mM). The solution was diluted 1:10 in serum-free DMEM to give a final pH of 7.4, before adding to cells. Where a low pH was required the DMEM was adjusted with concentrated HCl before using to dilute the complex. For HuH7 cells, the ascorbate-reduced ferric citrate complex was prepared

in RPMI medium in place of DMEM. The specific activity of all preparations was in the range of 150-200 cpm/pmol Fe.

NTBI Uptake Measurement - HuH7 cells were plated in 60/15 mm CellStar™ tissue culture dishes (Greiner Bio-One) at a density of 2 x 10^6 cells/dish and grown for 24 h in RPMI medium supplemented with 10% FCS, 100 U/ml penicillin and 50 µg/ml gentamicin, until confluent monolayers were formed. To minimize contamination with transferrin, on the day of the uptake experiment the cells were washed twice in serum-free RPMI medium, incubated for 1 h in serum-free medium to allow recycling of internalized transferrin-receptor complexes, and washed a third time with medium prior to the addition of label. The cells were then incubated with 1 ml of 1-10 µM of the [^{59}Fe]-NTBI label, usually for up to 1 h at 37°C. 0.5 µCi of ^{59}Fe was added per plate which was equivalent to adding ~150 000 cpm per plate. At the end of the incubation period, the label was removed and the cells washed four times in ice-cold serum-free RPMI medium to terminate uptake. Internalized and membrane-associated iron were determined by incubating cells with 1 mg/ml pronase at 4°C for 30 min. This procedure also released the cells from the culture dishes. The resulting cell suspension was then centrifuged at 10 400 rpm for 30 s and the radioactivity in the cell pellet (internalized iron) and supernatant (membrane-bound iron) was counted in a LKB Wallac 1282 Compugamma Universal gamma counter (Perkin-Elmer, Bucks, UK).

For Caco-2 iron uptake, cells were plated at low density (1x10^5 cells/ 60 mm plate) and grown for 20 days in supplemented DMEM (10% heat-inactivated foetal calf serum, 100 U/ml

penicillin and 0.1 mg/ml streptomycin) by which time they became fully differentiated and displayed a small intestine phenotype, as has been described previously *(Chantret, Rodolosse et al. 1994)*. Cells were washed before incubating with ascorbate-reduced ^{59}[Fe]-ferric citrate and processed as described for the HuH7 cells, except that the RPMI medium was replaced with DMEM throughout.

All determinations were made in triplicate within each experiment. Experiments were repeated up to three times, and the data shown is representative of a typical experiment. The results are expressed as mean ± SD. The rate of ^{59}Fe uptake is expressed as pmol/min/2 x 10^6 cells. The rate was not corrected for protein as the pronase added to the cells at the end of uptake experiment was found to give variable protein determinations, causing large variations in the protein corrected rate. Expressing the rate as pmol per min per number of cells plated (2 x 10^6) was shown to be a reliable parameter; changes in the rate of iron uptake were found to be consistent when the rate of iron uptake expressed as pmol/min/number of cells plated was compared to the protein corrected rate, pmol/min/mg protein, obtained when the pronase digest had been omitted.

Modulation of Iron Status- Iron loaded cells were obtained by incubating HuH7 monolayers (in 60 mm cell culture dishes) with supplemented RPMI medium containing various amounts of ferric ammonium citrate (FAC; 17.5% Fe by weight) for 24 h, as described by *(Parkes, Randell et al. 1995)*. Iron depleted cells were obtained by incubating monolayers with supplemented RPMI medium containing various concentrations of the iron chelator, desferoxamine (DFO) for 24 h. At the end of the incubation period, the FAC/DFO media was removed and the cells

washed extensively with serum-free RPMI medium to remove extracellular iron. Control cells were treated in the same way, except that the FAC and DFO were omitted from the medium. The rate of NTBI uptake was determined as described above. For RT-PCR analysis, cells were scraped in 1 ml of RNA*later*® (Ambion, Cambs, UK) to preserve the RNA and the cell suspension spun and the pellet retained for subsequent RNA isolation.

Quantitation of Intracellular Iron Content- The total iron content of control and iron loaded HuH7 cells was measured by the colorimetric ferrozine-based assay as described by *(Riemer, Hoepken et al. 2004)*. Briefly, cells were lysed with 50 mM NaOH overnight in a humidified atmosphere. To release iron complexed to cellular proteins the cell lysate was incubated with an acidic KMnO4 solution for 2 h at 60°C before adding the ferrozine reagent. The samples were transferred to a 96-well plate and the absorbance measured at 595 nm on an Anthos 2001 microplate reader (Anthos Labtec Instruments GmbH, Austria). The iron content of the cell sample was calculated by comparing its absorbance to that of a range of $FeCl_3$ standards prepared in the same way and the results normalized against the protein content of the cell lysate.

Determination of Protein Content- The protein content of the cell lysates was determined with the Coomassie Plus™ (Bradford) Protein Assay Kit (Perbio Science UK Ltd) using bovine serum albumin as the standard.

Modulators of NTBI Uptake

Ascorbate, Calcium, and KCl- Stock solutions of ascorbate, calcium chloride and potassium chloride were prepared in water and subsequently diluted in RPMI medium to the required

concentration. All solutions were sterile-filtered by passing through Minisart 0.2 μm syringe filters (Sartorius Ltd, Surrey, UK) before adding to the cells. For these experiments the specific modulator was added concurrently with the addition of the [^{59}Fe]-NTBI label and the rate of NTBI uptake determined as described.

Divalent Metal Ion Competition- the effect of divalent cations on NTBI uptake was determined by adding 0-100 μM of Cu^{2+}, Zn^{2+}, Cd^{2+}, Co^{2+}, Ni^{2+}, Mn^{2+} or Fe^{2+} to 1μM [^{59}Fe]-ferric citrate (Fe^{3+} uptake) or to 1μM [^{59}Fe]-ferric citrate plus 100 μM ascorbate (Fe^{2+} uptake). All competing metals were used as their chloride salts except Fe^{2+}, which was added as ferrous sulphate.

Metabolic and endocytic inhibitors- Stock solutions of the ATP synthesis inhibitor 2,4-dinitrophenol (2,4-DNP) and of the pinocytosis inhibitor, Bafilomycin A_1 were prepared in DMSO and subsequently diluted in serum-free RPMI medium to achieve the desired concentration. For these studies, the cells were pre-incubated for 1 h at 37°C with the indicated concentration of inhibitor which was removed before adding the [^{59}Fe]-NTBI, to prevent the DMSO precipitating the iron in the label. Control cells received the same concentration of DMSO (0.5-2% v/v).

Protein Synthesis Inhibitors- Stock solutions of the protein synthesis inhibitor cycloheximide and the mRNA synthesis inhibitor actinomycin D were prepared in DMSO and subsequently diluted in serum-free RPMI medium to the required concentration. Cells were pre-incubated for 1 h at 37°C with 350 μM cycloheximide or 3.98 μM actinomycin D and the inhibitors removed before determining the rate of iron uptake with [^{59}Fe]-NTBI. Control cells received the same

concentration of DMSO (0.5% v/v). To determine the involvement of *de novo* protein synthesis on FAC stimulated iron uptake, cells were incubated with medium containing FAC and the protein synthesis inhibitors for 24 h after which the cells were washed extensively before determining the rate of iron uptake. Control cells were incubated with FAC medium only.

Calcium Channel Inhibitors- Stock solutions of the L-type calcium channel modulators verapamil, nifedipine, (*R*)-(+)-Bay K8644, (*S*)-(-)-Bay K8644 and the T-type calcium channel blockers pimozide, penfluridol and amiloride were prepared in DMSO whilst the water-soluble T-type antagonists, mibefradil, NNC 55-0396 and kurtoxin were prepared in water. Ethosuximide was prepared in ethanol. Stock solutions were diluted in serum-free RPMI to the required concentration. Cells were treated with the inhibitors for 1 h at 37°C which were removed before determining the rate of [^{59}Fe]-NTBI uptake. Control cells received the same concentration of DMSO or ethanol (0.5-2% v/v). To determine the involvement of calcium channels in FAC-stimulated iron uptake, cells were incubated with medium containing FAC and the appropriate calcium channel inhibitor for 24 h after which cells were washed extensively before determining the rate of iron uptake. Control cells were incubated with FAC medium only.

Antibody Blocking Studies- Unless stated otherwise, cells were pre-incubated with DMT1 antibody for 30 min at 37°C, at dilutions of 1:20-1:50. The antibody solution was removed prior to measuring the rate of NTBI uptake. Control cells were incubated with the same dilution of pre-immune sera from the same rabbit or with commercially obtained non-immunized sera from clinically healthy normal rabbits.

RNA Isolation- RNA was extracted from HuH7 cells treated with RNA*later*® (Ambion, Cambs, UK), using the RNAqueous™-PCR kit for isolation of DNA-free RNA (Ambion, Cambs, UK), according to the manufacturer's instructions.

RT-PCR Analysis- Primers to the genes of interest in the HuH7 cells were designed using the LightCycler-probe design software (Version 1.0, Daho Technology Inc., 2001). 1 μg of total RNA was used for cDNA synthesis with the Abgene Reverse-iT First Strand Synthesis Kit using the PTC-100 Thermal Cycler (MJ Research, Essex, UK). Real-time quantitative gene analysis was performed using a LightCycler System (Roche Molecular Biochemicals, Mannheim, Germany), and QuantiTect SYBR Green PCR Kit (Qiagen, Crawley, UK). The PCR reaction conditions were as suggested in the manufacturer's protocol. This included an initial hot start at 95°C for 15 min, followed by PCR cycling: denaturation at 94°C for 15 sec, annealing at 60°C for 20 sec, extension at 72°C for 30 sec. The temperature was increased to 2°C below the product melting temperature for 5 sec before fluorescent acquisition at the end of each PCR cycle. Melting curve analysis was performed after each PCR run to determine the specificity of the completed reaction. Each run was performed in duplicate. To quantitate the initial amount of template in each reaction the second derivative maximal method was used. This method determined the cycle number at which there was the maximum acceleration to the log linear phase of PCR, this was termed the threshold cycle (Ct). Standard curves were produced for all primer sets. Purified DNA from PCR amplification using primers were serially diluted 10-fold. Standards were run in duplicate alongside glyceraldehyde phosphate dehydrogenase (GAPDH) standards produced in a similar fashion. RT-PCR was performed and the dilution range of the

starting template was adjusted to give a linear range covering 20-25 cycles. All standard curves covered a dynamic range of at least 5 logarithmic orders.

The relative amounts of the target and the reference genes in the samples were then calculated based on the crossing-point analysis (Relative Quantification Software, version 1.01, Roche); the second derivative maximum method was used to automatically determine the crossing point for individual samples. To correct for differences in both RNA quality and quantity between samples, data were normalized using the ratio of the cDNA of interest to that of the housekeeping gene, GAPDH which were assessed in parallel during each experimental run.

RNA isolation was performed using Qiagen RNAeasy Kit (Qiagen, Sussex, UK), and 1 g of total RNA was used for cDNA synthesis with ABgene Reverse-iT 1st Strand Synthesis Kit (ABgene, Surrey, UK). RNA concentration and purity were determined by spectrophotometry. The resulting cDNA transcripts were used for real time polymerase chain reaction PCR (RT-PCR), amplification using the Roche Lightcycler (Roche Diagnostics, Germany) and QuantiTect SYBR Green PCR kit (Qiagen, Sussex, UK), according to the manufacturers' protocol. Primers to the genes of interest and the to the constitutively expressed gene glyceraldehydes phosphate dehydrogenase (GAPDH) in the Huh7 cells were designed from the human sequences using the Lightcycler-probe design software (Version 1.0, Daho Technology Inc., 2001).

To quantify mRNA expression of the genes of interest, standard curves were generated with known amounts of each gene product. A ratio of relative abundance of the gene of interest to GAPDH was calculated by the Lightcycler Relative Quantification software version 1.0 (Roche

diagnostics, Germany). Melting curve analysis was carried out to ensure primer specificity. PCR product were also analysed by gel eletrophoresis and visualised using a Bio-Rad multiImager (Bio-Rad, Herts, UK).

Statistical Analysis- The Student's *t* test (unpaired) was employed to compare significant differences between two data sets. Differences were considered significant at $p < 0.05$.

(Words 2294)

Results

General Characterisics of NTBI Uptake Mechanism

Effects of Iron and Citrate Concentration. The uptake of internalized iron from increasing concentrations of ferric citrate (1:100) at 37°C saturated at an iron concentration of approximately 6 μM, suggesting an iron-carrier mediated process may be involved. Less than 10% of the total uptake was associated with the membrane under these conditions (Fig. 1A).

The effect of increasing citrate:iron ratio on ferric citrate uptake was determined by incubating cells with iron citrate species prepared with increasing concentrations of citrate (1-10 mM) and a constant iron concentration of 1 μM. Optimal iron uptake was observed at iron:citrate ratios of 1:1 to 1:100 whilst at the higher ratios (>1:500) uptake was reduced by 60-80% (Fig. 1B). Interestingly, polymeric iron uptake (no citrate) was taken up almost as efficiently as oligomeric and dimeric iron citrate species (1:1-1:100 iron: citrate).

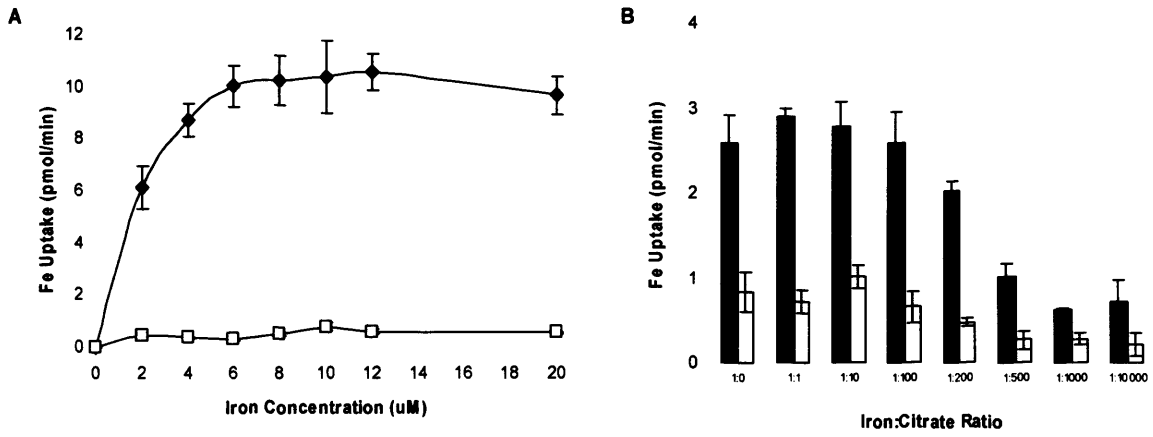

Fig. 1. Effect of iron and citrate concentration on iron uptake in HuH7 cells. **(A)** Effect of increasing iron concentration on iron citrate uptake in human hepatoma cells. HuH7 cells were incubated with increasing concentrations of ^{59}Fe-citrate at a constant iron citrate ratio of 1:100, for 60 min at 37°C. The figure shows intracellular (◆) and membrane-associated (□) uptake. **(B)** Effect of increasing citrate concentration on iron citrate uptake in human hepatoma cells. HuH7 cells were incubated with increasing concentrations of citrate at a constant iron concentration of 1 μM, for 60 min at 37°C. The figure shows intracellular (solid bars) and membrane-associated (open bars) uptake. Results are expressed as mean ± SD of triplicate determinations.

Effect of Ascorbate. To determine what effect the redox state of iron had on the NTBI uptake mechanism, increasing concentrations of ascorbate (0-1000 μM) were used to reduce ferric iron to the ferrous form. Uptake of iron citrate was stimulated by ascorbate in a concentration-dependent manner up to a concentration of 500 μM ascorbate at which maximal stimulation of 260% was observed (Fig. 2). Higher concentrations had no further stimulatory effect. These results suggest uptake of iron is dependent on the reduction of ferric iron to ferrous iron prior to internalization and are consistent with a divalent ion transport mechanism.

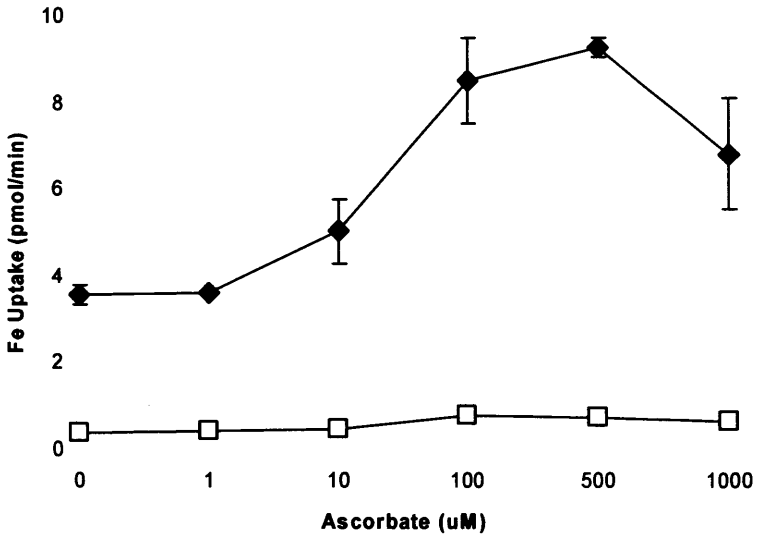

Fig. 2. Effect of ascorbate on NTBI uptake in human hepatoma cells. HuH7 cells were incubated with 1 μM iron citrate (1:100) and increasing concentrations of ascorbate, for 60 min at 37°C. The figure shows intracellular (◆) and membrane-associated (□) uptake. Results are expressed as mean ± SD of triplicate determinations.

Effect of Divalent Cations. To determine whether a shared transport mechanism was involved in the uptake of ferric and ferrous iron, we looked at the pattern of competition by the following divalent metal ions; Cu^{2+}, Zn^{2+}, Cd^{2+}, Co^{2+}, Ni^{2+}, Mn^{2+} and Fe^{2+}. The results are summarized in Fig 3.

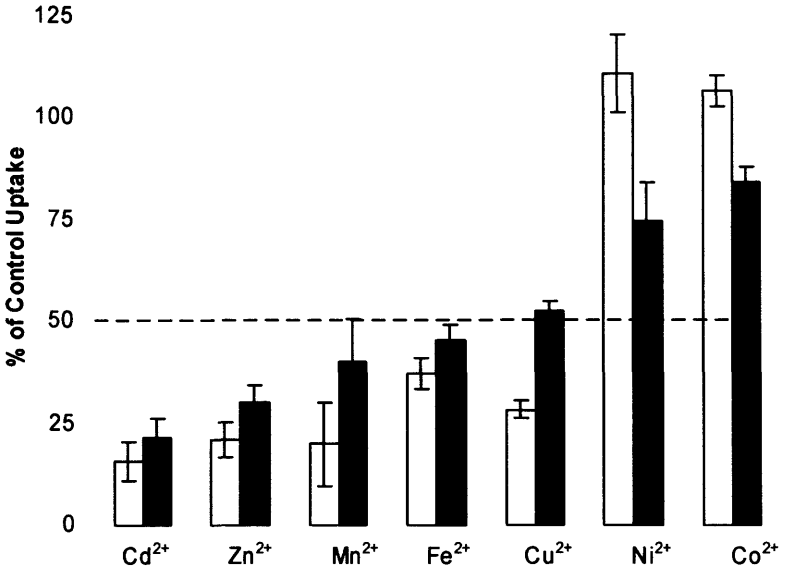

Fig. 3. Divalent metal ion inhibition of NTBI uptake in human hepatoma cells. 0-100 μM of each divalent metal ion was added to 1μM [^{59}Fe]-ferric citrate (Fe^{3+} uptake) [solid bars] or to 1μM [^{59}Fe]-ferric citrate plus 100 μM ascorbate (Fe^{2+} uptake) [open bars], and the rate of iron uptake determined over 30 min at 37°C. The results are calculated as a percentage of control uptake (no competing metal ion) and expressed as mean ± SD of triplicate determinations. Iron uptake was inhibited in a concentration-dependent manner for all divalent ions tested, with the exception of nickel and cobalt. The results shown are for inhibition at a divalent metal ion concentration of 10 μM only.

The pattern of inhibition by the divalent metal ions was generally very similar for both ferrous and ferric uptake in the HuH7 cells, in keeping with a common transport process. Cadmium, manganese, zinc and copper were the strongest inhibitors of iron uptake, inhibiting by 50% or more whilst nickel and cobalt were the least inhibitory, particularly for ferrous uptake. These results are consistent with a shared or non-selective divalent cation transport mechanism.

Role of DMT1 in Transmembrane NTBI Uptake

DMT1 Blocking Antibody. HuH7 cells were incubated with DMT1 antisera (rabbit anti-human, middle antibody raised against 4th extracellular loop of DMT1) at a dilution of 1:20 for 30 min at 37°C. Ferric citrate (1:100) uptake was measured at both physiological pH (7.4) and at low pH (6.5), as DMT1 is a proton-dependent transporter and has optimal function at low pH. Antibody blocking had no effect on ferric citrate (Fe^{3+}) uptake at either low or high pH when compared to unblocked cells and cells blocked with pre-immune serum (data not shown).

As DMT1 is a divalent transporter, the blocking experiment was repeated with Fe^{2+} by using ascorbate-reduced iron citrate, and compared in HuH7 cells and differentiated Caco2 cells. When Caco2 cells are grown for 20 plus days they become fully differentiated and display a small intestine-phenotype with a well defined brush border and positive DMT1 expression *(Fleet, Wang et al. 2003)*. Iron uptake was measured at pH 7.4 and pH 5.5 (Fig. 4A). At pH 7.4 both Caco2 and HuH7 cells pre-incubated with DMT1 antisera (1:20) showed little change in the rate of iron uptake compared to control cells treated with pre-immune sera (1:20). However, at pH 5.5, iron uptake in the Caco2 cells blocked with DMT1 antisera was significantly reduced by 45% (p = 0.0098) when compared to cells treated with pre-immune sera (1:20). In contrast, no blocking of iron uptake was observed in the HuH7 cells at pH 5.5 (Fig. 4A). This data suggests that whilst DMT1 is involved in iron uptake in differentiated Caco2 cells it is unlikely to be involved in the uptake of iron at the membrane surface of HuH7 cells.

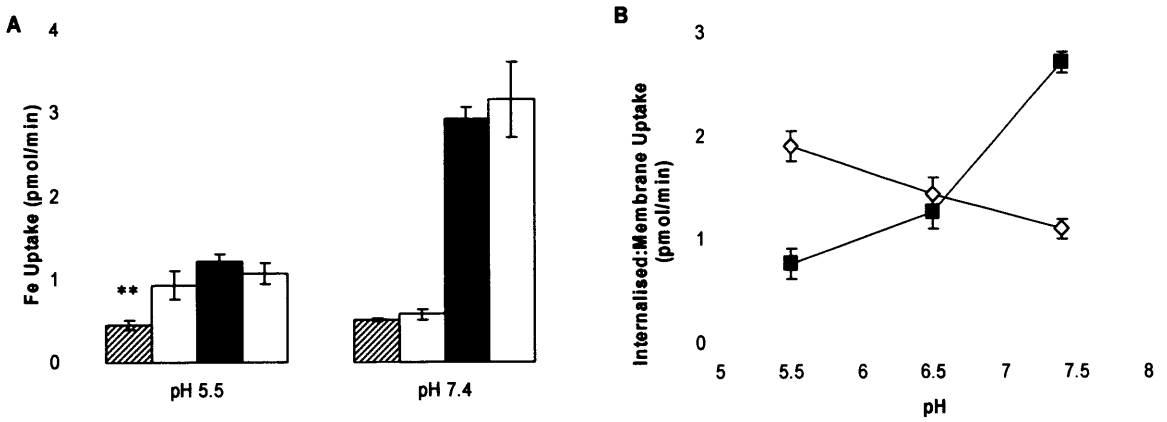

Fig. 4. Role of DMT1 in pH-dependent iron uptake in HuH7 and Caco-2 cells. **(A)** Effect of DMT1 blocking antibody on iron uptake in Caco2 cells and HuH7 cells. Caco2 cells (hatched bars) and HuH7 cells (filled bars) were pre-incubated with a 1:20 dilution of DMT1 antisera or pre-immune sera (open bars), for 30 min at 37°C. The rate of iron uptake was measured at pH 5.5 and pH 7.4 with 1 μM ferric citrate (1:100) in the presence of 100 μM ascorbate, for 30 min at 37°C. **(B)** pH-dependence of iron uptake in HuH7 and Caco-2 cells. HuH7 cells (■) were incubated with 1 μM ferric citrate in pH-adjusted RPMI medium. Caco-2 cells (◇) were incubated with 1 μM ferric citrate plus 100 μM ascorbate, in pH-adjusted DMEM. Iron uptake was determined over 60 min at 37°C. Results are expressed as mean ± SD of triplicate determinations. Student's unpaired *t* test, ** $p < 0.01$.

This data is consistent with the pH-dependence of iron uptake in these two cell lines. Iron internalisation, expressed as a ratio of intracellular: membrane-associated iron uptake, was most efficient at pH 7.4 for HuH7 cells and at pH 5.5 for Caco-2 cells (Fig. 4B), supporting the role of DMT1 in iron uptake in Caco-2 cells and of an alternative iron-transporter in the HuH7 cells. Furthermore, DMT1 expression was not up-regulated by iron loading in the HuH7 cells, as will be discussed later.

Modulation of NTBI Uptake by Iron Loading and Iron Depletion

Effect on NTBI Uptake. Regulation of NTBI uptake in response to modulations in iron status was investigated by iron loading cells with ferric ammonium citrate (FAC) or depleting cells with deferoxamine (DFO). Stimulation of cellular NTBI uptake in response to iron loading occurred in a time- and concentration-dependent manner. The time-course of NTBI uptake stimulation was determined over a 48 h incubation period with FAC. Although an increase in the rate of NTBI uptake was observed after an 1 h incubation with FAC, a 4 h incubation was required for the increase in the NTBI uptake rate to attain significance. At 24 h, the stimulation of NTBI uptake was optimal and by 48 h reached a plateau (data not shown). Hence, a 24 h incubation time with FAC was used for all iron loading experiments. Iron loading with 0-40 μg Fe/ml FAC stimulated the rate of cellular ferric citrate uptake at all concentrations of FAC, with maximal stimulation occurring at a FAC concentration of 10 μg Fe/ml (178 μM) after which the increase in the rate began to fall, as shown in Fig 5A. The decline in the iron uptake rate at higher FAC concentrations may be due to the cytotoxic effects of prolonged exposure to high Fe concentrations.

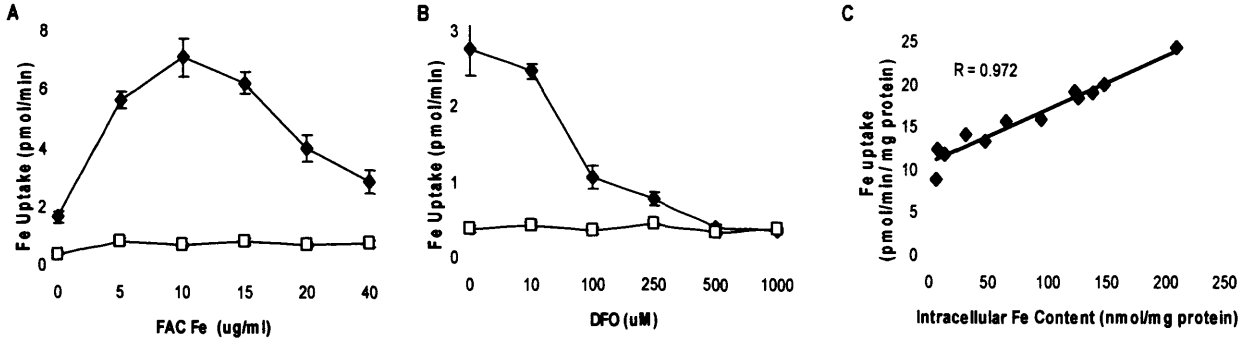

Fig. 5. Effect of iron loading or depletion on NTBI uptake in human hepatoma cells. (A) HuH7 cells were iron loaded by incubating with supplemented RPMI medium containing increasing concentrations of ferric ammonium

citrate for 24 h at 37°C. Cells were washed extensively before determining the rate of NTBI uptake with 1 μM iron citrate (1:100) for 60 min at 37°C. The figure shows intracellular (◆) and membrane-associated (□) uptake. Results are expressed as mean ± SD of triplicate determinations. **(B)** HuH7 cells were iron depleted by incubating with supplemented RPMI medium containing increasing concentrations of deferoxamine for 24 h at 37°C. Cells were washed extensively before determining the rate of NTBI uptake with 1 μM iron citrate (1:100), for 60 min at 37°C. The figure shows intracellular (◆) and membrane-associated (□) uptake. Results are expressed as mean ± SD of triplicate determinations. **(C)** Correlation between the intracellular iron content and the rate of NTBI uptake in human hepatoma cells. The rate of NTBI uptake was determined with 1 μM iron citrate (1:100), after loading cells with various concentrations of ferric ammonium citrate. Total cellular iron content was determined by a ferrozine-based assay, as described under methods. $R = 0.972$, $p < 0.0001$.

Treating normal cells with 100 μM DFO for 24 h resulted in no detectable levels of iron, when measured by the total cellular iron assay. Iron depletion with DFO for 24 h resulted in a dose-dependent decrease in the rate of cellular iron citrate uptake (Fig 5B). Although this may be due to down-regulation of the NTBI uptake mechanism due to depletion of intracellular iron levels, we cannot rule out the toxic effects of DFO on cell function, especially at the higher concentrations. This is supported by the fact that even after a 24 h recovery period from DFO in normal RPMI medium supplemented with FCS, the rate of NTBI uptake remained suppressed (data not shown).

Using FAC concentrations less than 20 μg Fe/ml, a strong linear correlation ($R = 0.972$, $p < 0.0001$) between the rate of NTBI accumulation and total intracellular iron content (measured by ferrozine assay) was observed, suggesting the NTBI uptake rate is modulated by intracellular

iron levels (Fig 5C). This data is consistent with an iron-regulated mechanism of NTBI uptake in the HuH7 cells.

Effect on mRNA for Iron Transport Proteins. The effect of iron loading and depletion on mRNA expression of key iron transport molecules was determined by RT-PCR analysis. RNA was isolated from HuH7 cells which had been pre-incubated with 10 μg Fe/ml FAC or 100 μM DFO for 24 h at 37°C. The results are shown in Table 1. No statistically significant changes were observed in the expression of DMT1(+IRE) or DMT1(-IRE) in response to iron loading and iron depletion, although DMT1(-IRE) was down-regulated by 32% in response to 24 h treatment with 100 μM DFO. These data suggest that DMT1 is not involved in the FAC-stimulated NTBI uptake mechanism as it is not significantly up-regulated in response to iron loading. However, DMT1(-IRE) may be involved in internal iron trafficking as its expression is reduced when the rate of iron uptake is down-regulated by DFO. A highly significant 3-fold increase in TfR1 expression was observed in response to iron depletion whilst iron loading had no effect, suggesting this receptor is not important for mediating the FAC-stimulated NTBI uptake. In contrast, TfR2 which is highly expressed in hepatocytes, was unaffected by changes in iron status and hence does not appear to be regulated by iron.

Table I. Regulation of iron transport molecules in response to iron loading and depletion, in HuH7 cells. RT-PCR analysis (20-25 cycles) of molecules involved in iron transport and homeostasis was performed on RNA isolated from cells iron loaded with FAC or iron depleted with DF0 for 24h and from control cells (no treatment) using gene-

specific primers, as described under Experimental Procedures. Values were normalized to the corresponding GAPDH value and are in arbitrary units (mean ± SD, n=4-9). ***p <0.001; significantly different from control.

	mRNA levels x 10^{-2} (a.u)		
	Control	FAC	DFO
+IRE-DMT1	0.710 ± 0.09	0.840 ± 0.260	0.680 ± 0.100
-IRE-DMT1	0.470 ± 0.160	0.380 ± 0.180	0.320 ± 0.270
TfR1	0.110 ± 0.010	0.104 ± 0.020	0.301 ± 0.05***
TfR2	1.80 ± 0.370	1.70 ± 0.510	1.90 ± 0.380
T-VDCC ($Ca_v3.2$)	15.0 ± 11.0	18.0 ± 10.0	36.0 ± 16.0
L-VDCC ($Ca_v1.3$)	88.0 ± 14.0	51.0 ± 13.0*	96.0 ± 43.0

Role of Voltage Dependent Calcium Channels (VDCC) in NTBI Uptake

Effect of extracellular Calcium on NTBI uptake. The effect of calcium on NTBI uptake was investigated by adding increasing concentrations of calcium chloride (0-5 mM) to the labelling medium (Fig. 6). Although calcium chloride was not added to control cells, they were not in a completely calcium-free medium as the RPMI medium has a calcium concentration of 0.424 mM. The uptake of internalized ferric citrate was stimulated at calcium concentrations > 1 mM and reached maximal values at physiological concentrations (2.5 mM), with a 6-fold increase in the rate of uptake. At higher concentrations (> 3mM) the iron uptake began to fall. Calcium had little effect on the membrane-associated iron uptake. The uptake of ferrous iron (ascorbate-reduced ferric citrate) was stimulated by calcium to a similar extent as ferric iron uptake (data not shown).

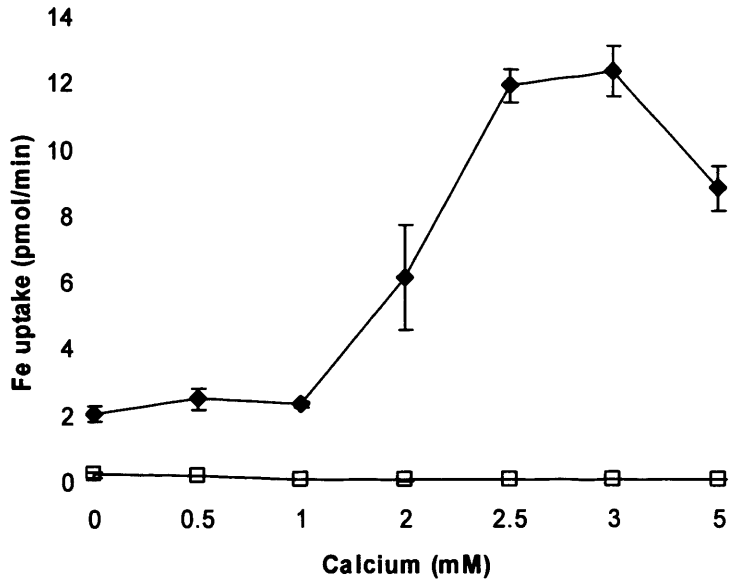

Fig. 6. Effect of calcium on NTBI uptake in human hepatoma cells. HuH7 cells were incubated with 1 μM iron citrate (1:100) label to which had been added increasing concentrations of calcium chloride, and uptake determined at 37°C over 60 min. The figure shows intracellular (◆) and membrane-associated (□) uptake. Results are expressed as mean ± SD of triplicate determinations.

The effect of calcium on the FAC-stimulated NTBI uptake rate was investigated by adding increasing concentrations of calcium chloride (0-3 mM) to the FAC incubation medium. The FAC-stimulated rate was significantly ($p < 0.01$) enhanced further by up to 150% in the presence of 2 mM calcium at all FAC concentrations used (0 – 20 ug Fe/ml). Stimulation of the basal and FAC-loaded NTBI uptake rate by calcium suggests a calcium-dependent iron transporter may be involved.

VDCC Modulators. To explore the possibility of alternative iron transport mechanisms, the involvement of calcium channels in iron uptake was investigated with selective modulators of L- and T-type VDCC (Fig. 7).

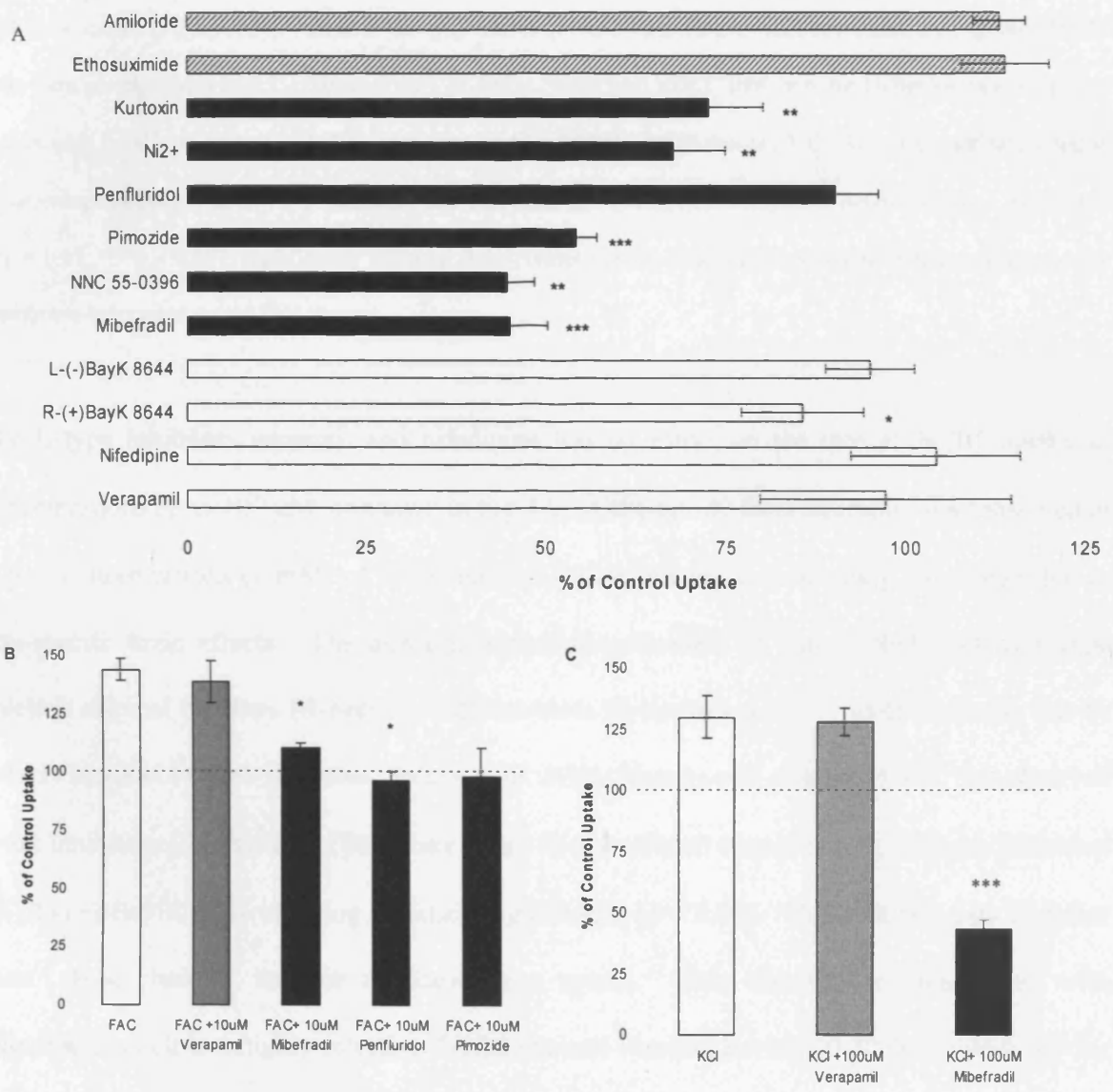

Fig. 7. Effect of selective VDCC modulators on iron uptake in human hepatoma cells. (**A**) HuH7 cells were pre-incubated for 1 h with selective high affinity L-type (open bars), selective high affinity T-type (filled bars) or low-affinity, non-selective T-type (hatched bars) VDCC modulators, before measuring NTBI uptake with 1 μM iron

citrate (1:100) at 37°C over 30 min. The graph shows results at a modulator concentration of 100 μM, with the exception of Kurtoxin which was added at a concentration of 0.1 μM. **(B)** Effect of VDCC blockers on FAC-enhanced iron uptake. HuH7 cells were iron loaded with supplemented RPMI medium containing 10 μg Fe/ml ferric ammonium citrate (FAC) in the absence (open bar) or presence of L-type (grey bar) and T-type (black bars) VDCC inhibitors for 24 h at 37°C. Cells were washed extensively before determining the rate of NTBI uptake with 1 μM iron citrate (1:100) for 60 min at 37°C. **(C)** Effect of VDCC blockers on KCl-stimulated iron uptake. HuH7 cells were pre-incubated with L-type (grey bar) or T-type (black bar) VDCC inhibitors for 1h before measuring iron uptake with 1 μM iron citrate (1:100) in the presence of 5 mM KCl, for 60 min at 37°C. All results are calculated as a percentage of control uptake (no inhibitor) and expressed as mean ± SD of triplicate determinations. *$p < 0.05$, **$p < 0.01$, ***$p < 0.001$; significantly different from control uptake. The VDCC modulators had no effect on the membrane-associated uptake (not shown).

The L-type inhibitors verpamil and nifedipine had no effect on the rate of NTBI uptake at concentrations up to 100 μM, as shown in Fig 7A. Although 20-50% inhibition was observed at higher concentrations (1 mM) of these inhibitors (data not shown), this may have been due to non-specifc toxic effects. The dihydropyridine stereoisomers of Bay K 8644 act as L-type calcium channel blockers (R-isomer) and activators (S-isomer), whilst T-type channels can be weakly blocked by both *(Lievano, Bolden et al. 1994; Vassort and Alvarez 1994)*. We observed weak inhibition (5-15%) of NTBI uptake with 100 μM of both stereoisomers, with the inhibition by (R)-(+)-Bay K 8644 attaining statistical significance ($p = 0.03$). This data suggests T- rather than L-type channels may be mediating iron uptake. This was further investigated with mibefradil which is a highly selective T-type channel blocker, having 10-30 fold selectivity for T- over L-type VDCC *(Martin, Lee et al. 2000)*. We observed a significant reduction of 55 ± 5.2 % in the iron uptake rate with 100 μM mibefradil ($p = 0.00013$) as shown in Fig 7A. Significant levels of inhibition (30-50 %, $p < 0.01$) were also observed with lower concentrations (50 – 75

μM) of mibefradil (not shown). The block of high-voltage-activated L-type channels by mibefradil occurs through the production of an active metabolite by intracellular hydrolysis. NNC 55-0396 is a non-hydrolyzable analog of mibefradil that exerts a selective inhibitory effect on the T-type channels *(Huang, Keyser et al. 2004)*. Treating cells with 100 μM of this analog caused similar levels of inhibition in the iron uptake rate (55 ± 3.8 %, p= 0.00160) as mibefradil, confirming uptake occurs predominately through the low-voltage calcium channel route. The neuroleptic agents pimozide and penfluridol are preferential inhibitors of T-type channels *(Santi, Cayabyab et al. 2002)*. Pre-incubating cells with 100 μM pimozide for 1 h significantly inhibited iron uptake by 45 ± 2.9 % (p = 0.00009) whilst penfluridol had little effect under these conditions (Fig 7A). However, pre-incubating cells with lower concentrations of penfluridol (10 μM) for a longer duration (24 h) resulted in a 55 ± 13.1 % reduction in the iron uptake rate (p= 0.00307), which may reflect the 10 times slower blocking rate of T-type channels by penfluridol compared to pimozide reported by *(Santi, Cayabyab et al. 2002)*. A number of earlier studies indicated that nickel sensitivity was a characteristic feature of low-voltage activated (T-type) calcium channels. However, more detailed analysis has shown that this apparent high sensitivity actually consists of high ($Ca_v3.2$ or α_{1H}) and low ($Ca_v3.1$ and $Ca_v3.3$ or α_{1G} and α_{1I}) affinity sites *(Lee, Gomora et al. 1999; Lacinova, Klugbauer et al. 2000)*. Hence, sensitivity to nickel may help differentiate between different T-channel subtypes. Our data showed that iron uptake was sensitive to inhibition by nickel with a 32 ± 7.4 % reduction (p = 0.00193) in the uptake rate at a nickel concentration of 100 μM, as shown in Fig. 7. Even at lower nickel concentrations (10 μM) we observed a 25 ± 9.5 % inhibition (p = 0.0064) of the iron uptake rate. This data would indicate that iron uptake is predominately mediated via the $Ca_v3.2$ (α_{1H}) T-channel subtype. The scorpion toxin, kurtoxin, is a high affinity blocker of both $Ca_v3.1$ and

$Ca_v3.2$ channels (*Chuang, Jaffe et al. 1998*). We found iron uptake was significantly inhibited by 27 ± 7.5 % ($p = 0.0034$) with 100 nM kurtoxin. Surprisingly, higher concentrations of the toxin appeared to facilitate iron uptake (data not shown). Although ethosuximide and amiloride are thought to be weak non-selective T-type channel inhibitors, lack of sensitivity of T-type channels to these inhibitors has been reported by many authors *(Yunker 2003)*. We also observed relative resistance to these inhibitors, as micromolar concentrations did not inhibit iron uptake (Fig. 7A), whilst milimolar concentrations (1-5 mM) only weakly inhibited (~15%). uptake (not shown).

The effect of the VDCC modulators on the iron loaded enhancement of the iron uptake rate was investigated by loading cells with FAC (10 μg Fe/ml) in the presence of 10 μM of selective T- and L-type channel inhibitors (Fig 7B). The FAC-stimulated rate was significantly attenuated by 77% with mibefradil ($p = 0.0238$) and completely abolished by penfluridol ($p = 0.0149$). Although, the FAC-enhanced rate was also abrogated by pimozide, this did not attain statistical significance. In contrast, the L-type inhibitor verapamil had no effect on the FAC-stimulated rate (Fig 7B).

Previously, it had been shown that NTBI uptake can be stimulated by extracellular potassium, via cell membrane depolarization *(Musilkova and Kovar 2001)*. We found adding 5 mM KCl to the labelling medium significantly enhanced the basal and FAC-loaded iron uptake rates by 115-130 % ($p \leq 0.05$), as shown in Fig 7C. To investigate whether this increase in iron uptake was due to activation of VDCC by KCl-induced membrane depolarisation, we pre-incubated HuH7 cells with 100 μM of L- and T-type channel inhibitors for 1 h, before measuring iron uptake in

the presence of 5 mM KCl. Mibefradil completely abolished the KCl-stimulated rate of iron uptake whilst verapamil had no effect (Fig 7C). These results suggest that membrane depolarization enhances iron uptake by activation of T- but not L-type channels in HuH7 cells.

Collectively, the data with the VDCC modulators is consistent with a component of hepatic NTBI uptake being mediated selectively by T- rather than L-type VDCC and this pathway becomes more significant under conditions of iron overload.

Regulation of VDCC Expression by Iron Status. The effect of iron loading and depletion on expression of L-type ($Ca_v1.3$ or α_{1D}) and T-type ($Ca_v3.2$ or α_{1H}) VDCC was determined by RT-PCR analysis. RNA was isolated from HuH7 cells which had been pre-incubated with 10 μg Fe/ml FAC or 100 μM DFO for 24 h at 37°C. RT-PCR analysis showed T-type channel expression was unaffected by iron loading and was up-regulated ~2.5 fold by iron chelation with DFO, whilst the L-type channel was significantly down-regulated (~ 2-fold) by iron loading ($p = 0.0145$), as shown in Table 1. Thus, stimulation of hepatocyte NTBI uptake by FAC loading is unlikely to involve transcriptional effects on T- or L-type channels and modulation may occur at a post-transcriptional level possibly involving activation of the T-type VDCC.

Effect of Metabolic/ Endocytic and Protein Synthesis Inhibitors on NTBI Uptake

Metabolic Inhibitors. The mitochondrial uncoupler 2,4-dinitrophenol (2,4-DNP), an inhibitor of ATP synthesis, significantly inhibited ($p = 0.042$) the uptake of ferric citrate by 32 ± 2.9 % at a concentration of 0.5 mM. Higher concentrations of 2,4-DNP had no further inhibitory effect on

the uptake rate. This data suggests that the uptake mechanism is partially energy-dependent but occurs predominately by passive, rather than active, transport.

Endocytic Inhibitors. Bafilomycin A_1, is a specific inhibitor of endosomal acidification and inhibits both receptor-mediated and fluid-phase endocytosis. Incubating cells with Bafilomycin A_1 had no effect on the uptake rate of ferric citrate even at concentrations up to 4 μM. Thus the NTBI uptake mechanism does not involve the trafficking of iron through acidic endosomes and supports an endocytosis-independent mechanism such as facilitated or carrier-mediated diffusion which could include permeation through an ion channel.

Protein Synthesis Inhibitors. The mRNA synthesis inhibitor, actinomycin D (3.98 μM), and the protein synthesis inhibitor, cycloheximide (350 μM), had no effect on ferrous or ferric uptake when pre-incubated with HuH7 cells for 1 h, suggesting sufficient endogenous transporters are available after 1 h to mediate iron uptake (data not shown). However, pre-incubating cells with these inhibitors for 24 h caused a significant reduction (64 ± 5.5%, p= 0.00015) in the basal iron uptake rate but had no effect on the FAC-stimulated rate, suggesting *de novo* protein synthesis is not required for the enhanced uptake observed in the iron-loaded cells but rather the mechanism involves the recruitment or activation of an existing transporter(s).

(words incl legends 3978)

Discussion

This paper has addressed two key questions: how is NTBI taken up into hepatocytes and how is this process is regulated. HuH7 hepatoma cells and iron citrate were chosen for these studies for the reasons explained in the introduction. This study shows for the first time that at least half of this uptake is likely to be through T-type calcium cannels but that L-type VDCC are unlikely to be involved.

DMT1.

Before investigating the putative role of VDCCs, an obvious candidate for NTBI uptake was the proton-dependent transporter, DMT1, which has optimal iron transport activity at acid pH of 5.5 *(Gunshin, Mackenzie et al. 1997)*. Indeed this has been proposed as a possible mechanism for NTBI uptake into hepatocytes *(Trinder, Oates et al. 2000) (Chua et al, 2000).* However several lines of evidence do not support DMT1 as an uptake mechanism into HuH7 cells. Firstly our studies with DMT1 antibody showed that ferrous iron uptake was significantly blocked in differentiated Caco2 cells expressing DMT1, but not in HuH7 cells at low pH i.e. when transport by proton-dependent DMT1 is optimal (Figure 4A). These findings reflect the pH-dependence of iron uptake in the two cell lines; iron internalization was most efficient at pH 7.4 for HuH7 cells and at pH 5.5 for Caco-2 cells (Figure 4B), supporting a role for DMT1 in iron uptake in Caco-2 cells and of an alternative iron-transporter in the HuH7 cells. Secondly we failed to observe a significant increase in the expression of DMT1(+IRE) or DMT1(-IRE) in response to iron loading, suggesting that up-regulation of this transporter is not responsible for the FAC-stimulated NTBI uptake rate (Table 1). These findings are consistent with those of *Gunshin, Allerson et al. (2001)* who observed no change in mRNA DMT1 levels in liver Hep3B

cells in response to iron loading with FAC and Trinder *et al*, who found no differences in the expression of DMT1 (± IRE) with varying iron status in rat liver *(Trinder, Oates et al. 2000)*. However, Trinder *et al* (2000) did observe that DMT1 protein staining on hepatocytes plasma membranes was highest in iron loaded rats and absent in iron deficient rats, suggesting post-transcriptional regulation of DMT1 by iron. Although we did not look at the regulation of DMT1 protein expression in response to iron in our HuH7 cells, it is difficult to reconcile a role for this proton-dependant iron transporter in the trans-membrane uptake of NTBI as it would require a low pH environment at the hepatocyte membrane surface to function optimally *(Gunshin, Mackenzie et al. 1997)*. Thirdly the finding that zinc was highly inhibitory (up to 80%, Figure 3) of iron uptake in our HuH7 cells favors a DMT1 independent mechanism of iron uptake. Despite early reports demonstrating Zn^{2+}-dependent conductances in oocytes expressing DMT1 *(Gunshin, Mackenzie et al. 1997)*, several lines of evidence suggest that zinc is not significantly taken up by DMT1. For example, zinc is the weakest metal inhibitor of DMT1-dependent iron uptake in enterocyte-like Caco2 cells (25% inhibition) *(Tandy, Williams et al. 2000)* and uptake in Caco2 cells is unaffected by decreasing DMT1 expression unlike the that of iron (*Tandy, Williams et al. 2000*) *(Tallkvist, Bowlus et al. 2000; Yamaji, Tennant et al. 2001)*. Furthermore lack of Zn^{2+} transport was also demonstrated in K562 and HEK-T cells transfected with DMT1 DNA *(Conrad, Umbreit et al. 2000)*. A limited role for DMT-1 in iron loading of the liver is also supported by the observation that global inactivation of the DMT1 gene in animal models *(Gunshin, Fujiwara et al. 2005)* or functional mutations of this gene in humans *(Mims, Guan et al. 2005; Beaumont, Delaunay et al. 2006; Iolascon, d'Apolito et al. 2006)*, whilst leading to severe microcytic anemia, fail to prevent excess hepatic iron deposition.

Hence, the possibility of alternative mechanisms of NTBI uptake into liver need to be considered.

Other dismissed mechanisms

Several other putative uptake mechanisms for NTBI uptake into HuH7 cells were investigated but were not supported by our observations. An endocytosis driven mechanism is unlikely because Bafilomyicn A_1, a specific inhibitor of endosomal acidification that inhibits both receptor-mediated and fluid-phase endocytosis and blocks cellular acquisition of iron from transferrin *(Yang, Goetz et al. 2002)*, failed to have any impact on NTBI uptake. In our model, iron citrate at a ratio of 1:100 was used which represents physiologically relevant concentrations and at this ratio iron is predominantly monomeric (**Evans et al, 2007?).** Iron uptake from citrate was saturable (Figure 1), in agreement with previously reported data in HuH7 cells *(Trinder and Morgan 1998)* and suggests the involvement of an iron carrier. Inhibition of cellular energy metabolism with the mitochondrial uncoupler 2,4-dinitrophenol (2,4-DNP), partially inhibited the uptake of iron from citrate in our HuH7 cells, suggesting the uptake mechanism is energy-dependent to some extent but occurs predominately by passive, rather than active, transport such as facilitated diffusion. This relative insensitivity of NTBI uptake to inhibitors of cellular energy metabolism and endocytosis in hepatic cells is consistent with earlier studies *(Wright, Brissot et al. 1986; Baker, Baker et al. 1998; Graham, Morgan et al. 1998)*. Iron uptake via transferrin is very unlikely because experiments were done in serum free medium. Furthermore iron depletion of HuH7 cells with deferoxamine caused a 3-fold increase in TfR1 mRNA expression (Table 1) but this was accompanied by down-regulation of the iron uptake rate (Fig 5B), whilst iron loading caused an increase in the iron uptake rate (Fig 5A) but had no effect on TfR1 expression. TfR2 expression in our HuH7 cells was unaffected by changes in iron status and hence does not

appear to mediate FAC-induced NTBI uptake or be regulated by iron (Table 1) as reported previously in mouse liver *(Fleming, Migas et al. 2000)*.

T-type channels.

The significant pharmacological inhibition of iron uptake with a range of T-type VDCC inhibitors such as mibefradil, NNC 55-0396, pimozide, penfluridol, nickel and kurtoxin ($p < 0.05$) at micromolar concentrations provides strong evidence that T-type channels are key transporters in HuH7 cells. L-type channels do not seem to be involved, in contrast to the reported uptake into cardiac myoctyes *(Oudit, Sun et al. 2003)*. Thus the L-type inhibitors, verapamil, nifedipine and Bay K8644 had little or no effect on NTBI uptake at comparable concentrations (Fig. 7A). Voltage-gated ion channels such as VDCC are usually closed at the resting potential of the cell. Upon activation, the membrane depolarizes resulting in opening of the pore and ion entry into the cell. This is followed by a refractory period during which the channel becomes inactivated and is no longer able to conduct ions. Distinguishing features of T-type VDCC are that they require only small depolarizations of the plasma membrane (- 50 mV) to open (low-voltage activated), they close slowly upon repolarization of the membrane (slowly deactivating) and inactivate quickly (transient). The activation and steady-state inactivation curves of T-type channels have a significant overlap, occuring over a similar voltage range, which means channels can open but do not inactivate completely. In fact, T-type channels are known to display a window current in the range of the cell membrane resting potential, providing a latent pathway for constant Ca^{2+} *(Talavera and Nilius 2006)*, and possibly Fe^{2+} influx . Low concentrations of ferrous iron have been shown to depolarize hepatocyte plasma membranes

(Wright, Fitz et al. 1988). Thus exposure of cells to iron could provide a direct mechanism for activation of VDCC and subsequent iron entry. Cell membrane depolarization by extracellular potassium has been shown to stimulate the uptake of NTBI in HeLa and K562 cells, *(Musilkova and Kovar 2001)*. We observed enhancement of both the basal and FAC-loaded iron uptake rates by extracellular potassium in our HuH7 cells (Figure 7C). We also found that mibefradil completely abolished the KCl-stimulated rate of iron uptake whilst verapamil had no effect, suggesting that membrane depolarization enhances iron uptake by activation of T- but not L-type channels in HuH7 cells.

Calcium stimulation

The stimulation of the basal and FAC-loaded NTBI uptake by calcium in HuH7 cells (Figure 6) is consistent with observations in hepatocytes *(Wright, Brissot et al. 1986; Barisani, Berg et al. 1995; Baker, Baker et al. 1998)* and with the involvement of a calcium-dependent iron transporter. The mechanism of calcium enhancement of uptake is not known but is unlikely to result from simple displacement of Fe^{3+} from citrate as suggested by *Mwanjewe, Martinez et al, (2000)* because we found pre-incubation of our HuH7 cells with calcium, followed by its removal prior to adding iron citrate label, still resulted in enhanced iron uptake. It is also unlikely that the calcium functions intracellularly since increasing cytosolic Ca^{2+} levels in fibroblasts with epidermal growth factor had no effect on the iron transport rate, whilst treating cells with the permeable ester of EGTA did not inhibit the iron uptake *(Kaplan, Jordan et al. 1991)*. Interestingly calcium added to HuH7 cells in the presence of calcium channel inhibitors stimulated iron uptake despite being unable to enter the cells (unpublished observation), suggesting the calcium acts extracellularly to enhance iron uptake. Calcium can decrease

plasma membrane fluidity of rat hepatocytes both directly, taking 10-15 min, and indirectly taking about 75 min, through modulation of membrane-bound enzymes that alter the lipid composition *(Livingstone and Schachter 1980; Storch and Schachter 1985)*. Changes in membrane lipid composition and fluidity can influence membrane functions, such as receptor binding, enzyme activity and transmembrane transport including ion permeability *(Benga and Holmes 1984; Mills, Meier et al. 1987; Wang and Zhang 2005)*. Calcium may also activate iron uptake by acting directly on the VDCC. Evidence suggests that the T-type Ca_v 3.2 channel may be uniquely modulated by calcium, which slows the activation and inactivation kinetics of this channel but not of Ca_v 3.1 or Ca_v 3.3 *(Klockner, Lee et al. 1999)*. For example, increasing concentrations of extracellular calcium have been shown to potentiate T-type currents in adrenal glomerulosa cells *(Lu, Fern et al. 1994)*.

Metal inhibition.

The inhibition of uptake by a range of divalent cations (Figure 3) also support the involvement of VDCC in the uptake process. Although calcium channels are primarily employed for transporting Ca^{2+}, both high- (L-type) and low- (T-type) voltage dependent calcium channels (VDCC) transport a range of other divalent cations including Sr^{2+} *(Hess, Lansman et al. 1986; Kaku, Lee et al. 2003)*, Ba^{2+} *(Hess, Lansman et al. 1986; Kaku, Lee et al. 2003)*, Cd^{2+} *(Lansman, Hess et al. 1986; Shaikh, Blazka et al. 1995; Todorovic and Lingle 1998)*, Zn^{2+} *(Busselberg, Michael et al. 1992; Atar, Backx et al. 1995; Shaikh, Blazka et al. 1995; Todorovic and Lingle 1998; Jeong, Park et al. 2003)*, Mn^{2+} *(Castelli, Tanzi et al. 2003; Kaku, Lee et al. 2003)*, Cu^{2+} *(Shaikh, Blazka et al. 1995; Castelli, Tanzi et al. 2003; Jeong, Park et al. 2003)*, Ni^{2+} *(Winegar, Kelly et al. 1991; Funakoshi, Inoue et al. 1997; Todorovic and*

Lingle 1998; Lee, Gomora et al. 1999), Co^{2+} *(Winegar, Kelly et al. 1991; Castelli, Tanzi et al. 2003)* and Fe^{2+} *(Winegar, Kelly et al. 1991; Tsushima, Wickenden et al. 1999)*. The sensitivity of hepatic transferrin-independent iron uptake to transition metals is well documented in the literature where zinc, manganese and cadmium show most inhibition whilst cobalt, copper and nickel show the least *(Wright, Brissot et al. 1986; Randell, Parkes et al. 1994; Baker, Baker et al. 1998; Graham, Morgan et al. 1998; Chua, Olynyk et al. 2004)*. In HuH7 cells, cadmium, manganese, zinc and copper were the strongest inhibitors of iron uptake, inhibiting by 50% or more, whilst nickel and cobalt were the least inhibitory. Cadmium, the strongest inhibitor of iron uptake, is known to be taken up by calcium channels in hepatocytes *(Blazka and Shaikh 1991)* and human hepatic cell lines *(Souza, Bucio et al. 1997)*. Inhibition of iron uptake showed no obvious relationship to ironic radius: Ni^{2+} and Co^{2+} which have smaller or similar ionic radii to Fe^{2+} were the least inhibitory whilst larger competing ions such as Cd^{2+} and Zn^{2+} were potent inhibitors (Fig. 3). The effectiveness of the transition metals to compete with iron transport is more likely to reflect the affinity of the transporter for the various metals.

Iron stimulation of uptake.

An important objective of this study was to determine if and how modulation of cellular iron content affects NTBI uptake. Key findings are that NTBI uptake is directly proportional to intracellular iron content (Figure 5C) and that up-regulation of NTBI uptake is abrogated in HuH7 cells by blocking with known inhibitors in T-type but not L-type channels (Figure 7B). Enhancement of transferrin-independent iron uptake by iron loading has been previously reported in a variety of cell types *(Kaplan, Jordan et al. 1991)* (Oshiro, Nakajima et al. 1993),

(Parkes, Hussain et al. 1993) (Randell, Parkes et al. 1994; Parkes, Randell et al. 1995; Scheiber-Mojdehkar, Zimmermann et al. 1999). However an abrogation of enhancement of iron uptake by VDCC inhibitors has not been previously reported. The mechanism by which iron loading of cells might stimulate calcium channel mediated iron uptake requires further consideration. Because maximal enhancement in iron uptake was seen after a 24 h incubation period with FAC, we initially considered that this would require up-regulation of synthesis of the iron transporter, in this case T-type VDCC. However, T-type VDCC mRNA expression was unaffected by iron loading with FAC, whilst L-type VDCC expression was down-regulated by iron loading. Furthermore in our HuH7 cells, treatment with protein synthesis inhibitors (actinomycin D and cycloheximide) had no effect on the FAC-stimulated rate, suggesting *de novo* protein synthesis is not required for activation of FAC-induced iron uptake. Hence, post-translational effects are likely to be responsible, consistent with the recruitment or activation of existing transporter(s) *(Kaplan, Jordan et al. 1991).* A possible mechanism of enhanced NTBI uptake would be that iron can permeate VDCC channels and effect the kinetics of these channels. Ferrous iron slows the inactivation of L-type VDCC currents in myocytes resulting in increased iron entry *(Tsushima, Wickenden et al. 1999).* The slowing of Ca^{2+} current inactivation by Fe^{2+} can arise from competition between Fe^{2+} and Ca^{2+} for the C-terminal cytoplasmic Ca^{2+} binding site involved in Ca^{2+}-mediated inactivation of L-type VDCC *(de Leon, Wang et al. 1995).* Thus Fe^{2+}-induced slowing of Ca^{2+} current inactivation may prolong the duration of the channel's active open state, allowing an increase in iron flux into the cells.

Conclusion

In conclusion our findings provide persuasive evidence for DMT1-independent T-type VDCC-dependent uptake of non-transferrin bound iron, in the form of iron citrate, in HuH7 cells. This human cell line has many features of mature hepatocytes and many aspects of NTBI uptake that we observed in HuH7 are similar to those previously reported in primary hepatocytes *(Barisani, Berg et al. 1995; Baker, Baker et al. 1998; Graham, Morgan et al. 1998)* or whole organ perfusion systems (*Brissot, Wright et al. 1985; Wright, Brissot et al. 1986*). Our finding of a maximum of 55 % uptake inhibition with mibefradil suggests that additional NTBI uptake mechanisms may exist in hepatocytes. Candidates could include Zip14, a member of the SLC39A zinc transporter family, found to mediate NTBI uptake into cells *(Liuzzi, Aydemir et al. 2006)*. Our finding that, in contrast to observations in murine cardiac cells *(Oudit, Trivieri et al. 2006)*, L-type inhibitors have no effect on basal or iron induced NTBI uptake provides a possible therapeutic avenue where iron loading of the heart might be prevented in transfusional iron overload by specific inhibitors of L-type mediated iron uptake, without compromising the main site of NTBI clearance, namely the liver.

Discussion 2574 (with refs)

Acknowledgements

This work was supported by grants from the Medical Research Council (UK) and the Cooley's Anaemia Foundation (USA).

References

Abernethy, D. R. and J. B. Schwartz (1999). "Calcium-antagonist drugs." N Engl J Med **341**(19): 1447-57.

Atar, D., P. H. Backx, et al. (1995). "Excitation-transcription coupling mediated by zinc influx through voltage-dependent calcium channels." J Biol Chem **270**(6): 2473-7.

Baker, E., S. M. Baker, et al. (1998). "Characterisation of non-transferrin-bound iron (ferric citrate) uptake by rat hepatocytes in culture." Biochim Biophys Acta **1380**(1): 21-30.

Barisani, D., C. L. Berg, et al. (1995). "Evidence for a Low K-M Transporter for Non-Transferrin-Bound Iron in Isolated Rat Hepatocytes." American Journal of Physiology-Gastrointestinal and Liver Physiology **32**(4): G570-G576.

Batey, R. G., P. Lai Chung Fong, et al. (1980). "A non-transferrin-bound serum iron in idiopathic hemochromatosis." Dig Dis Sci **25**(5): 340-6.

Beaumont, C., J. Delaunay, et al. (2006). "Two new human DMT1 gene mutations in a patient with microcytic anemia, low ferritinemia, and liver iron overload." Blood **107**(10): 4168-70.

Benga, G. and R. P. Holmes (1984). "Interactions between components in biological membranes and their implications for membrane function." Prog Biophys Mol Biol **43**(3): 195-257.

Blazka, M. E. and Z. A. Shaikh (1991). "Differences in cadmium and mercury uptakes by hepatocytes: role of calcium channels." Toxicol Appl Pharmacol **110**(2): 355-63.

Bradley, S. J., I. Gosriwitana, et al. (1997). "Non-transferrin-bound iron induced by myeloablative chemotherapy." Br J Haematol **99**(2): 337-43.

Brissot, P., T. L. Wright, et al. (1985). "Efficient clearance of non-transferrin-bound iron by rat liver. Implications for hepatic iron loading in iron overload states." J Clin Invest **76**(4): 1463-70.

Busselberg, D., D. Michael, et al. (1992). "Zinc (Zn2+) blocks voltage gated calcium channels in cultured rat dorsal root ganglion cells." Brain Res **593**(1): 77-81.

Castelli, L., F. Tanzi, et al. (2003). "Cu2+, Co2+, and Mn2+ modify the gating kinetics of high-voltage-activated Ca2+ channels in rat palaeocortical neurons." J Membr Biol **195**(3): 121-36.

Catterall, W. A. (2000). "Structure and regulation of voltage-gated Ca2+ channels." Annu Rev Cell Dev Biol **16**: 521-55.

Chantret, I., A. Rodolosse, et al. (1994). "Differential expression of sucrase-isomaltase in clones isolated from early and late passages of the cell line Caco-2: evidence for glucose-dependent negative regulation." J Cell Sci **107 (Pt 1)**: 213-25.

Chua, A. C. G., J. K. Olynyk, et al. (2004). "Nontransferrin-bound iron uptake by hepatocytes is increased in the Hfe knockout mouse model of hereditary hemochromatosis." Blood **104**(5): 1519-1525.

Chuang, R. S., H. Jaffe, et al. (1998). "Inhibition of T-type voltage-gated calcium channels by a new scorpion toxin." Nat Neurosci **1**(8): 668-74.

Conrad, M. E., J. N. Umbreit, et al. (2000). "Separate pathways for cellular uptake of ferric and ferrous iron." Am J Physiol Gastrointest Liver Physiol **279**(4): G767-74.

Craven, C. M., J. Alexander, et al. (1987). "Tissue distribution and clearance kinetics of non-transferrin-bound iron in the hypotransferrinemic mouse: a rodent model for hemochromatosis." Proc Natl Acad Sci U S A **84**(10): 3457-61.

de Leon, M., Y. Wang, et al. (1995). "Essential Ca(2+)-binding motif for Ca(2+)-sensitive inactivation of L-type Ca2+ channels." Science **270**(5241): 1502-6.

Enyeart, J. J., B. A. Biagi, et al. (1992). "Preferential block of T-type calcium channels by neuroleptics in neural crest-derived rat and human C cell lines." Mol Pharmacol **42**(2): 364-72.

Fleet, J. C., L. Wang, et al. (2003). "Gene expression profiling of Caco-2 BBe cells suggests a role for specific signaling pathways during intestinal differentiation." Physiol Genomics **13**(1): 57-68.

Fleming, R. E., M. C. Migas, et al. (2000). "Transferrin receptor 2: continued expression in mouse liver in the face of iron overload and in hereditary hemochromatosis." Proc Natl Acad Sci U S A **97**(5): 2214-9.

Funakoshi, T., T. Inoue, et al. (1997). "The mechanisms of nickel uptake by rat primary hepatocyte cultures: role of calcium channels." Toxicology **124**(1): 21-6.

Graham, R. M., E. H. Morgan, et al. (1998). "Characterisation of citrate and iron citrate uptake by cultured rat hepatocytes." J Hepatol **29**(4): 603-13.

Graham, R. M., E. H. Morgan, et al. (1998). "Ferric citrate uptake by cultured rat hepatocytes is inhibited in the presence of transferrin." Eur J Biochem **253**(1): 139-45.

Grootveld, M., J. D. Bell, et al. (1989). "Non-transferrin-bound iron in plasma or serum from patients with idiopathic hemochromatosis. Characterization by high performance liquid chromatography and nuclear magnetic resonance spectroscopy." J Biol Chem **264**(8): 4417-22.

Gunshin, H., C. R. Allerson, et al. (2001). "Iron-dependent regulation of the divalent metal ion transporter." FEBS Lett **509**(2): 309-16.

Gunshin, H., Y. Fujiwara, et al. (2005). "Slc11a2 is required for intestinal iron absorption and erythropoiesis but dispensable in placenta and liver." J Clin Invest **115**(5): 1258-66.

Gunshin, H., B. Mackenzie, et al. (1997). "Cloning and characterization of a mammalian proton-coupled metal-ion transporter." Nature **388**(6641): 482-8.

Hershko, C., G. Graham, et al. (1978). "Non-specific serum iron in thalassaemia: an abnormal serum iron fraction of potential toxicity." Br J Haematol **40**(2): 255-63.

Hess, P., J. B. Lansman, et al. (1986). "Calcium channel selectivity for divalent and monovalent cations. Voltage and concentration dependence of single channel current in ventricular heart cells." J Gen Physiol **88**(3): 293-319.

Huang, L., B. M. Keyser, et al. (2004). "NNC 55-0396 [(1S,2S)-2-(2-(N-[(3-benzimidazol-2-yl)propyl]-N-methylamino)ethyl)-6-fluo ro-1,2,3,4-tetrahydro-1-isopropyl-2-naphtyl cyclopropanecarboxylate dihydrochloride]: a new selective inhibitor of T-type calcium channels." J Pharmacol Exp Ther **309**(1): 193-9.

Iolascon, A., M. d'Apolito, et al. (2006). "Microcytic anemia and hepatic iron overload in a child with compound heterozygous mutations in DMT1 (SCL11A2)." Blood **107**(1): 349-54.

Jeong, S. W., B. G. Park, et al. (2003). "Divalent metals differentially block cloned T-type calcium channels." Neuroreport **14**(11): 1537-40.

Kaku, T., T. S. Lee, et al. (2003). "The gating and conductance properties of Cav3.2 low-voltage-activated T-type calcium channels." Jpn J Physiol **53**(3): 165-72.

Kaplan, J., I. Jordan, et al. (1991). "Regulation of the transferrin-independent iron transport system in cultured cells." J Biol Chem **266**(5): 2997-3004.

Klockner, U., J. H. Lee, et al. (1999). "Comparison of the Ca2 + currents induced by expression of three cloned alpha1 subunits, alpha1G, alpha1H and alpha1I, of low-voltage-activated T-type Ca2 + channels." Eur J Neurosci **11**(12): 4171-8.

Lacinova, L., N. Klugbauer, et al. (2000). "Low voltage activated calcium channels: from genes to function." Gen Physiol Biophys **19**(2): 121-36.

Lansman, J. B., P. Hess, et al. (1986). "Blockade of current through single calcium channels by Cd2+, Mg2+, and Ca2+. Voltage and concentration dependence of calcium entry into the pore." J Gen Physiol **88**(3): 321-47.

Lee, J. H., J. C. Gomora, et al. (1999). "Nickel block of three cloned T-type calcium channels: low concentrations selectively block alpha1H." Biophys J **77**(6): 3034-42.

Lievano, A., A. Bolden, et al. (1994). "Calcium channels in excitable cells: divergent genotypic and phenotypic expression of alpha 1-subunits." Am J Physiol **267**(2 Pt 1): C411-24.

Liuzzi, J. P., F. Aydemir, et al. (2006). "Zip14 (Slc39a14) mediates non-transferrin-bound iron uptake into cells." Proc Natl Acad Sci U S A **103**(37): 13612-7.

Livingstone, C. J. and D. Schachter (1980). "Calcium modulates the lipid dynamics of rat hepatocyte plasma membranes by direct and indirect mechanisms." Biochemistry **19**(21): 4823-7.

Loban, A., R. Kime, et al. (1997). "Iron-binding antioxidant potential of plasma albumin." Clin Sci (Lond) **93**(5): 445-51.

Lovstad, R. A. (1993). "Interaction of serum albumin with the Fe(III)-citrate complex." Int J Biochem **25**(7): 1015-7.

Lu, H. K., R. J. Fern, et al. (1994). "Ca(2+)-dependent activation of T-type Ca2+ channels by calmodulin-dependent protein kinase II." Am J Physiol **267**(1 Pt 2): F183-9.

Martin, R. L., J. H. Lee, et al. (2000). "Mibefradil block of cloned T-type calcium channels." J Pharmacol Exp Ther **295**(1): 302-8.

McKie, A. T., D. Barrow, et al. (2001). "An iron-regulated ferric reductase associated with the absorption of dietary iron." Science **291**(5509): 1755-9.

McKie, A. T., P. Marciani, et al. (2000). "A novel duodenal iron-regulated transporter, IREG1, implicated in the basolateral transfer of iron to the circulation." Mol Cell **5**(2): 299-309.

Mills, P. R., P. J. Meier, et al. (1987). "The effect of changes in the fluid state of rat liver plasma membrane on the transport of taurocholate." Hepatology **7**(1): 61-6.

Mims, M. P., Y. Guan, et al. (2005). "Identification of a human mutation of DMT1 in a patient with microcytic anemia and iron overload." Blood **105**(3): 1337-42.

Musilkova, J. and J. Kovar (2001). "Additive stimulatory effect of extracellular calcium and potassium on non-transferrin ferric iron uptake by HeLa and K562 cells." Biochim Biophys Acta **1514**(1): 117-26.

Muth, J. N., G. Varadi, et al. (2001). "Use of transgenic mice to study voltage-dependent Ca2+ channels." Trends Pharmacol Sci **22**(10): 526-32.

Mwanjewe, J., R. Martinez, et al. (2000). "On the Ca2+ dependence of non-transferrin-bound iron uptake in PC12 cells." J Biol Chem **275**(43): 33512-5.

Nakabayashi, H., K. Taketa, et al. (1982). "Growth of human hepatoma cells lines with differentiated functions in chemically defined medium." Cancer Res **42**(9): 3858-63.

Okamoto, T., S. Y. Jeong, et al. (2001). "Expression of the alpha1D subunit of the L-type voltage gated calcium channel in human liver." Int J Mol Med **8**(4): 413-6.

Oshiro, S., H. Nakajima, et al. (1993). "Redox, transferrin-independent, and receptor-mediated endocytosis iron uptake systems in cultured human fibroblasts." J Biol Chem **268**(29): 21586-91.

Oudit, G. Y., H. Sun, et al. (2003). "L-type Ca2+ channels provide a major pathway for iron entry into cardiomyocytes in iron-overload cardiomyopathy." Nat Med **9**(9): 1187-94.

Oudit, G. Y., M. G. Trivieri, et al. (2006). "Role of L-type Ca2+ channels in iron transport and iron-overload cardiomyopathy." J Mol Med.

Oudit, G. Y., M. G. Trivieri, et al. (2006). "Role of L-type Ca2+ channels in iron transport and iron-overload cardiomyopathy." J Mol Med **84**(5): 349-64.

Parkes, J. G., R. A. Hussain, et al. (1993). "Effects of iron loading on uptake, speciation, and chelation of iron in cultured myocardial cells." J Lab Clin Med **122**(1): 36-47.

Parkes, J. G., N. F. Olivieri, et al. (1997). "Characterization of Fe2+ and Fe3+ transport by iron-loaded cardiac myocytes." Toxicology **117**(2-3): 141-51.

Parkes, J. G., E. W. Randell, et al. (1995). "Modulation by iron loading and chelation of the uptake of non-transferrin-bound iron by human liver cells." Biochim Biophys Acta **1243**(3): 373-80.

Peri, R., D. J. Triggle, et al. (2001). "Regulation of L-type calcium channels in pituitary GH(4)C(1) cells by depolarization." J Biol Chem **276**(34): 31667-73.

Porter, J. B., R. D. Abeysinghe, et al. (1996). "Kinetics of removal and reappearance of non-transferrin-bound plasma iron with deferoxamine therapy." Blood **88**(2): 705-13.

Randell, E. W., J. G. Parkes, et al. (1994). "Uptake of non-transferrin-bound iron by both reductive and nonreductive processes is modulated by intracellular iron." J Biol Chem **269**(23): 16046-53.

Riemer, J., H. H. Hoepken, et al. (2004). "Colorimetric ferrozine-based assay for the quantitation of iron in cultured cells." Anal Biochem **331**(2): 370-5.

Santi, C. M., F. S. Cayabyab, et al. (2002). "Differential inhibition of T-type calcium channels by neuroleptics." J Neurosci **22**(2): 396-403.

Scheiber-Mojdehkar, B., I. Zimmermann, et al. (1999). "Differential response of non-transferrin bound iron uptake in rat liver cells on long-term and short-term treatment with iron." J Hepatol **31**(1): 61-70.

Shaikh, Z. A., M. E. Blazka, et al. (1995). "Metal transport in cells: cadmium uptake by rat hepatocytes and renal cortical epithelial cells." Environ Health Perspect **103 Suppl 1**: 73-5.

Souza, V., L. Bucio, et al. (1997). "Cadmium uptake by a human hepatic cell line (WRL-68 cells)." Toxicology **120**(3): 215-20.

Storch, J. and D. Schachter (1985). "Calcium alters the acyl chain composition and lipid fluidity of rat hepatocyte plasma membranes in vitro." Biochim Biophys Acta **812**(2): 473-84.

Talavera, K. and B. Nilius (2006). "Evidence for common structural determinants of activation and inactivation in T-type Ca(2+) channels." Pflugers Arch.

Tallkvist, J., C. L. Bowlus, et al. (2000). "Functional and molecular responses of human intestinal Caco-2 cells to iron treatment." Am J Clin Nutr **72**(3): 770-5.

Tandy, S., M. Williams, et al. (2000). "Nramp2 expression is associated with pH-dependent iron uptake across the apical membrane of human intestinal Caco-2 cells." J Biol Chem **275**(2): 1023-9.

Thorstensen, K. (1988). "Hepatocytes and reticulocytes have different mechanisms for the uptake of iron from transferrin." J Biol Chem **263**(32): 16837-41.

Thorstensen, K. and I. Romslo (1988). "Uptake of iron from transferrin by isolated rat hepatocytes. A redox-mediated plasma membrane process?" J Biol Chem **263**(18): 8844-50.

Todorovic, S. M. and C. J. Lingle (1998). "Pharmacological properties of T-type Ca2+ current in adult rat sensory neurons: effects of anticonvulsant and anesthetic agents." J Neurophysiol **79**(1): 240-52.

Triggle, D. J. (1999). "The pharmacology of ion channels: with particular reference to voltage-gated Ca2+ channels." Eur J Pharmacol **375**(1-3): 311-25.

Trinder, D. and E. Morgan (1998). "Mechanisms of ferric citrate uptake by human hepatoma cells." Am J Physiol **275**(2 Pt 1): G279-86.

Trinder, D., P. S. Oates, et al. (2000). "Localisation of divalent metal transporter 1 (DMT1) to the microvillus membrane of rat duodenal enterocytes in iron deficiency, but to hepatocytes in iron overload." Gut **46**(2): 270-6.

Tsushima, R. G., A. D. Wickenden, et al. (1999). "Modulation of iron uptake in heart by L-type Ca2+ channel modifiers: possible implications in iron overload." Circ Res **84**(11): 1302-9.

Vassort, G. and J. Alvarez (1994). "Cardiac T-type calcium current: pharmacology and roles in cardiac tissues." J Cardiovasc Electrophysiol **5**(4): 376-93.

Wang, J. and G. J. Zhang (2005). "Influence of membrane physical state on lysosomal potassium ion permeability." Cell Biol Int **29**(6): 393-401.

Williams, M. E., M. S. Washburn, et al. (1999). "Structure and functional characterization of a novel human low-voltage activated calcium channel." J Neurochem **72**(2): 791-9.

Winegar, B. D., R. Kelly, et al. (1991). "Block of current through single calcium channels by Fe, Co, and Ni. Location of the transition metal binding site in the pore." J Gen Physiol **97**(2): 351-67.

Wright, T. L., P. Brissot, et al. (1986). "Characterization of non-transferrin-bound iron clearance by rat liver." J Biol Chem **261**(23): 10909-14.

Wright, T. L., J. G. Fitz, et al. (1988). "Non-transferrin-bound iron uptake by rat liver. Role of membrane potential difference." J Biol Chem **263**(4): 1842-7.

Yamaji, S., J. Tennant, et al. (2001). "Zinc regulates the function and expression of the iron transporters DMT1 and IREG1 in human intestinal Caco-2 cells." FEBS Lett **507**(2): 137-41.

Yang, J., D. Goetz, et al. (2002). "An iron delivery pathway mediated by a lipocalin." Mol Cell **10**(5): 1045-56.

Yunker, A. M. (2003). "Modulation and pharmacology of low voltage-activated ("T-Type") calcium channels." J Bioenerg Biomembr **35**(6): 577-98.

Zimelman, A. P., H. J. Zimmerman, et al. (1977). "Effect of iron saturation of transferrin on hepatic iron uptake: an in vitro study." Gastroenterology **72**(1): 129-31.

The rapid effects of hepcidin on iron metabolism

[1]Timothy Chaston, [1,2]Monica Mascarenhas, [1]Bomee Chung, [2]Joanne Marks, [2]Bhavini Patel, [2]Surjit Kaila Srai and [1]Paul Sharp.

[1]Nutritional Sciences Division, King's College London, UK. [2]Department of Biochemistry & Molecular Biology, University College London, UK.

Correspondence to: Dr Paul Sharp, Department of Nutrition & Dietetics, King's College London,

or

Professor Kaila Srai, Department of Biochemistry & Molecular Biology, University College London (Hampstead Campus),

Running title: hepcidin and iron metabolism

Heading: Red Cells

Word count: Abstract 167; Paper 3,627

Abstract

Reticuloendothelial macrophages together with duodenal enterocytes co-ordinate body iron homeostasis and are believed to be the main target sites for the regulatory actions of hepcidin. In this study we have investigated the rapid effects of hepcidin on serum iron and duodenal iron transport *in vivo* in mice injected with a synthetic hepcidin peptide. Within 4 h of injecting hepcidin, mice developed hypoferremia, which was associated with a significant decrease in ferroportin protein levels in the macrophage-rich red pulp of the spleen. Despite this dramatic decrease in serum iron levels, there was no effect of hepcidin on duodenal iron transport or duodenal ferroportin protein expression in the same mice. These data suggest the rapid response to a rise in hepcidin is tissue-specific. Upon its release hepcidin initially targets macrophage iron recycling. The duodenum appears to be less sensitive to this initial increase in hepcidin levels. The fact that macrophages respond more acutely to a hepcidin challenge is fully consistent with their central role in maintaining body iron homeostasis.

Introduction

Body iron homeostasis is maintained through the absorption of 1-2 mg/day of iron from the diet by the duodenal enterocytes, to replace endogenous iron losses, together with the recycling of some 20-25 mg of iron from effete erythrocytes via the reticuloendothelial macrophages. In addition, there is normally a physiological reserve of iron in the hepatocytes (approximately 1g) which further protect against imbalances in body iron homeostasis. The co-ordination and regulation of all of these processes has been ascribed to hepcidin, a 25 amino acid peptide hormone which is produced in the liver (1, 2). Hepcidin expression is dramatically regulated by the levels of iron in the hepatic stores – expression is increased when liver iron is high and down regulated when the stores are depleted (3). In addition to modulation by stored iron, hepcidin expression also responds to changes in the erythroid requirement for iron. Phlebotomy (4), hemolysis (4, 5) and elevated erythropoietin levels (4), major stimuli for reticulocytosis, all inhibit hepcidin production, and result in increased iron assimilation from the diet. Furthermore hepcidin expression is increased in a number of chronic diseases and by inflammation (2, 4, 6) indicating that pathological imbalances in hepcidin levels have severe consequences for body iron metabolism.

Once released, hepcidin acts as a negative regulator of intestinal iron absorption (7) and macrophage iron recycling (8). In chronic disease for example, this is thought to lead to the underlying anemia that characterizes many disorders (9). The cellular targets and the mode of action of hepcidin have been the subject of much recent work. *In vitro* studies with transfected cell lines, suggest that hepcidin interacts directly with the ferroportin protein resulting in its internalization and degradation (10-12).

The *in vitro* effects of hepcidin on ferroportin expression are rapid with maximal inhibition achieved 3-4 hours following exposure to peptide (10). In *in vivo* studies the effects of hepcidin on serum iron levels are also rapid. Hypoferremia is evident within 1 hour in mice

injected with hepcidin (13). Interestingly serum iron reaches its nadir 2-4 hours post injection suggesting that the time course for the actions of hepcidin is similar both *in vitro* and *in vivo*. In animals with normal iron status serum iron is regulated largely by two separate pathways, macrophage recycling of iron from erythrocytes and duodenal iron absorption. The purpose of the present study was to determine whether the rapid effects of hepcidin on serum iron noted previously (13) were due to inhibition of one or both of these pathways. To address this issue, we injected hepcidin into male C57BL/6 mice fed a normal iron diet and measured changes in serum iron levels and duodenal iron transport 4 h later. In addition, spleen (an abundant source of reticuloendothelial macrophages) and duodenum from control and hepcidin-treated animals were used to measure ferroportin transporter expression.

Methods

Animals and Treatments

All procedures were approved by the Local Animal Ethics committee and were carried out in accordance with current UK Home Office legislation. Male C57BL/6 mice aged 4 weeks were housed in the Comparative Biology Unit at UCL (Hampstead campus) and placed on an iron replete diet (44mg Fe/Kg diet) for 3 weeks prior to experimentation. During this time, animals were allowed *ab libitum* access to water. On the day of study, mice were given a single intraperitoneal injection of either 10μg hepcidin (Peptides International Inc. Louisville, KY) or an equivalent volume of the diluent (saline) and used for experiments 4 hours later. The commercially hepcidin peptide is air-oxidized and has been used successfully in a number of studies (8, 12, 14).

Since there are no robust methods readily available to measure serum hepcidin levels in mice we based our calculation of circulating hepcidin levels on previously published data (13). Extrapolating from this study we estimated that serum hepcidin in our animals would be approximately 300 – 500 nM, which is close to the *in vitro* IC_{50} (700 nM) for the inhibitory effects of hepcidin on ferroportin expression (10).

Blood was collected by cardiac puncture from all animals of the end of the experimental period to measure serum iron and transferrin saturation using a commercially available assay (Randox Laboratories Ltd, Antrim, UK).

Iron uptake

Animals were anaesthetized with pentobarbitone sodium (60 mg/kg, i.p.) and the duodenum was washed through with warm 0.15M NaCl followed by air. The lower end of the duodenal segment (proximal to the ligament of Treitz) was tied off and uptake buffer (0.15M NaCl, 10mM Hepes, pH 6.5) containing 0.2mM $^{59}Fe^{2+}$ complexed with 4mM ascorbate, was instilled proximally from a tied-in syringe. After 10 min, during which time animal body temperature was maintained at 37°C with a thermostatically controlled heating blanket, blood samples and the duodenal segment were removed. The duodenal lumen was emptied of its contents and was flushed thoroughly with buffer containing 2 mM unlabelled iron, followed by 0.15 M NaCl, and finally dried overnight. The mucosa was weighed and, together with weighed blood samples and the animal carcass, were gamma-counted for determination of ^{59}Fe activity. Mucosal iron retention, mucosal iron transfer and total mucosal iron uptake were calculated as described previously (7).

Cell culture

Caco-2 cells were grown in Dulbecco's modified Eagle's medium (DMEM) containing 10% fetal bovine serum for 21 days on Transwell inserts (Corning-Costar, High Wycombe, UK) to achieve a fully differentiated monolayer (15). THP-1 cells, grown in RPMI 1640 medium containing 10% fetal bovine serum, were seeded at $5x10^5$ cells per well in 6-well plates and treated with phorbol myristate acetate (100 nM) to induce differentiation and plate attachment. The day prior to experimentation, cells were placed in serum-free medium. The next morning the culture medium was replaces with fresh serum-free medium and the cells were exposed to hepcidin (1µM) for up to 24h. In Caco-2 cell experiments hepcidin was added only to the basolateral chamber of the Transwell plate.

Western blotting

Total plasma membranes from tissue samples and from cultured cells were prepared as described previously (16, 17). All procedures were performed at 4°C. Briefly, the duodenal mucosae were separated from their underlying musculature by scraping with a glass slide. Splenic tissue was rinsed with PBS and chopped into fragments prior to homogenization. Cultured cells were removed from Transwell plates (Caco-2) and plastic dishes (THP-1) using cell scrapers. Tissue and cell samples were homogenized in phosphate buffered saline (PBS) containing protease inhibitor cocktail (Sigma-Aldrich, Dorset, UK) with an Ultra Turrax homogenizer (2x30 s pulses on full speed). The ensuing homogenates were subjected to a brief centrifugation step (1500 g for 5 min) to precipitate unbroken cells and nuclei and the resulting supernatant was centrifuged for 30 min at 15,000 g to give a total plasma membrane fraction which was resuspended in PBS containing protease inhibitor cocktail, 10% NP-40 and 1% Triton X-100 .

Membranes (40µg) were solubilized in sample loading buffer and subjected to SDS-PAGE. Following immobilization on nitrocellulose, the proteins were exposed to a commercially available anti-ferroportin antibody (Alpha Diagnostics Inc., San Antonio, TX). Cross-reactivity was observed using an HRP-linked secondary antibody (Dako, Cambridgeshire, UK) and ECL Plus (GE Healthcare, Buckinghamshire UK). Band densities were semi-quantified using Scion Image software (Scion Corporation, Frederick, MD). At the end of the experiment, the nitrocellulose membranes were stripped (Western Stripping Buffer, Perbio Science Ltd, Northumberland, UK) and re-probed with antibodies to actin (Sigma-Aldrich) or, for Caco-2 cell studies, villin (Santa Cruz Biotechnology Inc, Santa Cruz, CA) which acted as loading controls.

Immunofluorescence

Tissues from mice injected with hepcidin or saline were perfusion-fixed *in situ* prior to harvesting. Briefly, the abdominal aorta of anaesthetized animals was cannulated and each mouse was perfused with Hanks balanced salt solution (HBS, Sigma-Aldrich) to remove blood, followed by perfusion with HBS containing 2% paraformaldehyde. The spleen and duodenum from each animal were removed, embedded in OCT compound (Merck, Dorset, UK) and frozen in isopentane, pre-cooled in liquid nitrogen and stored at -80 °C until use.

Cryostat sections (7 µm) of spleen and duodenum were mounted onto poly-L-lysine-coated slides (Sigma-Aldrich) and air-dried for 1 h. Sections were washed for 5 min in 0.1 M PBS (pH 7.4) and then blocked for 30 min with PBS containing 10 % normal goat serum (NGS) (Sigma-Aldrich) and 1 % Triton X-100. Sections were briefly washed with PBS and incubated overnight at 4 °C with ferroportin antibody (1:100 dilution). Following overnight incubation, sections were washed (3 x10 min, 0.1 M PBS) and then incubated with FITC-conjugated swine anti-rabbit IgG (Dako) (1:100 dilution) for 1 h at room temperature. Subsequently, sections were washed (3 x10 min, 0.1 M PBS) and mounted with Vectashield mounting medium containing propidium iodide (Vector Laboratories Ltd, Peterborough, UK). Images were subsequently captured using a Leica TCS laser scanning confocal microscope and the manufacturer's dedicated software.

Statistics

Data are presented as mean ± S.E.M. Statistical differences ($P<0.05$) between groups were determined using Student's unpaired t-test or one-way analysis of variance followed by Tukey's post hoc test, where appropriate, using SPSS statistical package (SPSS UK Ltd, Surrey, UK).

Results

Serum iron levels are decreased in hepcidin-treated mice

A major consequence of hepcidin release is the inhibition of iron recycling from reticuloendothelial macrophages (reviewed in 18). Accordingly, in serum samples taken from mice injected with hepcidin (10μg) we observed a substantial decrease in serum iron content (control 14.7 ± 0.9 μmol/L; hepcidin-treated 5.7 ± 2.4 μmol/L. *P<0.01*). Hypoferremia was accompanied by a 40% decrease in transferrin saturation in the hepcidin-treated mice (control 60.7 ± 9.3 %; hepcidin-treated 34.0 ± 10.2 %. *P<0.1*).

Short-term exposure to hepcidin does not alter intestinal iron transport

As well as controlling the rate of iron release from reticuloendothelial macrophages into the circulation, hepcidin also acts directly on duodenal enterocytes to regulate the rate of dietary iron absorption (7). Therefore, to determine the effects of hepcidin on duodenal iron transport we employed an *in vivo* technique that allowed us to measure both mucosal iron uptake and its subsequent transfer across the intestinal epithelium into the animal carcass. Surprisingly, despite the dramatic hepcidin-mediated decrease in serum iron levels, neither duodenal iron uptake nor the subsequent transfer of iron across the duodenal mucosa was altered in hepcidin-treated mice (Figure 1). Taken together, these data suggest that upon its release into the circulation the initial effects of hepcidin are likely to occur at the level of the recycling macrophage rather than the duodenal enterocyte.

Effect of hepcidin on ferroportin levels in spleen and duodenum

The above functional data imply that the initial actions of hepcidin on serum iron occur as a consequence of inhibiting macrophage iron recycling following down-regulation of the ferroportin transporter, which is believed to act as the hepcidin receptor on target cells (10). Furthermore, our duodenal iron transport data suggest that we should see no change in duodenal ferroportin expression. To investigate these possibilities, we isolated spleen (an abundant source of reticuloendothelial macrophages) and duodenum from control and hepcidin-treated animals and measured the expression of ferroportin protein by both immunofluorescence and semi-quantitative western blotting.

In the spleen, ferroportin immunoreactivity was associated with the macrophage-rich red pulp and was substantially reduced in the hepcidin-treated animals (Figure 2a). Quantitative analysis of ferroportin levels in splenic tissue using western blotting were in agreement with the immunofluorescence data and revealed a 60% ($P<0.001$) reduction in ferroportin expression in hepcidin-treated animals (Figure 2b). These findings support our assertion that the recycling macrophage is a major target for the rapid effects of hepcidin on serum iron levels.

In the duodenum, ferroportin was localized to the basolateral membrane of enterocytes. In addition, a number of strongly stained ferroportin-positive cells (most probably macrophages) were also noted in the lamina propria. Ferroportin immunoreactivity in the enterocyte layer was not altered following hepcidin treatment in duodenal tissue (Figure 3a). Interestingly, the ferroportin-positive cells that were evident in the lamina propria of the control animals were absent from the hepcidin-treated mice. Densitometric analysis of the ferroportin western blots from duodenal tissue revealed a small (25%) and statistically insignificant decrease ($P>0.28$) in ferroportin expression in hepcidin-treated mice (Figure 3b).

Taken together with the immunofluorescence images this decrease may be accounted for in part by the absence of the ferroportin-positive macrophage-like cells in the lamina propria of the hepcidin-treated mice, though we cannot rule out a minor effect of hepcidin on enterocyte ferroportin levels. Importantly, the lack of a significant change in ferroportin expression in the duodenum following hepcidin treatment is completely consistent with the duodenal iron transport data (Figure 1) further supporting the notion that the rapid effects of hepcidin occur at the recycling macrophage and not the duodenal enterocyte.

Effect of hepcidin on ferroportin levels in macrophages and intestinal epithelial cells

Since the spleen and duodenum are formed of heterogeneous cell population we wanted to study further the effects of hepcidin on macrophages and enterocytes in isolation. Unfortunately, while it is feasible to isolate and culture macrophages from a number of body sites it is not possible to sustain isolated enterocytes in culture. Therefore, for these studies we decided to utilize two well characterized human cell lines, the THP-1 monocyte/ macrophage line and the enterocyte-like Caco-2 cell. In these studies, hepcidin (1μM) was added to the cell culture medium for up to 24 h and cell extracts were analyzed by western blotting for changes in ferroportin protein expression.

In differentiated THP-1 cells (which exhibit a macrophage phenotype) there was a rapid decrease in ferroportin protein levels (occurring 1-4 hours following exposure to hepcidin) which remained suppressed in the presence of hepcidin for the duration of the study (Figure 4a). In contrast, ferroportin levels in enterocyte-like Caco-2 cells were not altered at any time point following exposure to hepcidin (Figure 4b). While one must exercise some caution in interpreting data from neoplastic cell lines, the data from THP-1 cells and Caco-2 cells are consistent with the results from the *in vivo* study and further support the hypothesis that macrophages are more sensitive to a hepcidin challenge than enterocytes.

Discussion

Hepcidin is recognized as a major regulator of body iron metabolism. A number of studies have demonstrated that hepcidin regulates cellular iron homeostasis by controlling ferroportin expression (8, 10-12, 14). In this model, hepcidin is believed to bind directly to ferroportin and rapidly (within 1-4 hours) induce its internalization and degradation (10). This in turn impairs the release of iron from its target cells (namely the reticuloendothelial macrophages and the duodenal enterocytes) into the circulation. In support of this hypothesis, a recent study in which radio-labeled hepcidin was injected into mice revealed that the peptide concentrates in tissues with the highest concentrations of ferroportin, namely the spleen, liver and duodenum (13).

A number of studies have reported an association between elevated hepcidin levels *in vivo* and subsequent hypoferremia (5, 6, 13, 20, 21). In an elegant study, in which mice were injected with hepcidin, Rivera and colleagues demonstrated that the initial effects of hepcidin on serum iron levels were rapid and dose-dependent (13). Interestingly, the lowest level of serum iron occurred approximately 2-4 hours post-injection. Taken together with the *in vitro* data for the actions of hepcidin on ferroportin expression (10) these two studies suggest that the time course for the actions of hepcidin are similar both *in vitro* and *in vivo*. In each case the maximal effects of hepcidin are evident approximately 4 hours after exposure to hepcidin and we have therefore used this time-point in our studies.

The major contributing pathways controlling serum iron levels are dietary iron absorption via the duodenum and macrophage recycling of iron from senescent erythrocytes. Our starting hypothesis was that hepcidin would affect both of these pathways to exert its rapid hypoferremic effects. To address this issue we injected mice with hepcidin and measured serum iron and duodenal iron transport 4 hours later. In agreement with previous studies

(13) serum iron was dramatically decreased in our hepcidin-treated mice. However, in the same group of animals duodenal iron transport was not altered following injection of hepcidin. This would imply that initially hepcidin targets the macrophage recycling pathway to exert its hypoferremic effects. This notion is supported by recent data from an *in vitro* erythrophagocytosis model showing that exposure to hepcidin results in decrease ferroportin levels inhibition of iron efflux (8).

To determine whether hypoferremia in our animals could be explained by diminution of ferroportin levels in recycling macrophages we isolated the spleen (a rich source of reticuloendothelial macrophages) from hepcidin-treated mice. Ferroportin expression in the spleen was largely associated with the macrophage-rich red pulp, and transporter protein levels were significantly decreased in the hepcidin-treated mice. Since the spleen is a composite of a number of cell types we wanted to confirm that the macrophage is a major target cell type for the actions of hepcidin. For these studies we utilized THP-1 cells which are a well established monocyte/macrophage line. In agreement with our observations in mouse spleen, THP-1 ferroportin levels were decreased significantly within 4 hours of exposure to hepcidin. Similar findings following hepcidin treatment have also been observed in mouse J774 macrophages (8) and mouse bone marrow derived macrophages (14). All of these studies support the published model for the cellular actions of hepcidin (10) and support a scenario whereby hepcidin binds to ferroportin in macrophages, decreases cell surface expression of the transporter and thereby inhibits iron release into the circulation resulting in hypoferremia.

Along with the spleen, the duodenum is one of the major sites of ferroportin expression (22-24) and as such would be expected to respond appropriately to a hepcidin challenge. We were surprised therefore to observe that despite the presence of hypoferremia in the hepcidin-treated animals there was no significant difference in duodenal iron transport or ferroportin expression following the acute exposure to hepcidin. These data are in contrast

to previous studies by our group (7, 19) and by others (25) which have reported decreased intestinal iron transport following chronic hepcidin treatment. Intriguingly, analysis of the iron transport data from all three studies appears to indicate that the major effect of hepcidin in intestinal epithelial cells is on the uptake route rather than the efflux pathway which may indicate that ferroportin is less sensitive to the actions of hepcidin in intestinal cells than in macrophages.

What is the basis for this apparent differential sensitivity of the macrophage and intestinal epithelial cell to hepcidin? Previous work has shown that the effects of hepcidin of serum iron levels are clearly dose-dependent (13) so does the duodenum simply require a higher concentration of hepcidin to elicit a response? From our previous work this would not appear to be the case since there is no impairment in duodenal iron transport in animals injected with 50μg of hepcidin peptide 4 hours previously (see Table 2 in ref. 7). In addition, in our *in vitro* work with Caco-2 cells presented both here and previously (19), there is no evidence for a dose-dependent effect of hepcidin on ferroportin expression.

A second possibility is that there are tissue-specific differences in the temporal kinetics of the response to hepcidin, i.e. the macrophage responds faster than the enterocyte. Our previous data supports this option. In mice given multiple injections of hepcidin over a 24-72 hour period there is a decrease in duodenal iron transport (7). In addition, Caco-2 cells incubated with hepcidin over a similar time course also display decreased iron transport (19, 25). This possible mechanism is further supported by a recent study with transgenic mice containing an inducible hepcidin vector, which exhibit a significant decrease in duodenal ferroportin expression following chronic hepcidin exposure for 3 weeks (26).

Furthermore, we also believe that the basal level of hepcidin will be important in determining the duodenal response to hepcidin. There is clear evidence that when there is a marked hepcidin deficiency, e.g. in iron deficiency (27), hemolytic anemia (5), hypoxia (28) USF2-

null mice (29), and chronic alcohol loading (30), intestinal iron transport and ferroportin transporter expression is elevated. In hemochromatosis also, there is a clear association between hepcidin levels, which are inappropriately low, and duodenal iron absorption, which is inappropriately high (reviewed in 31). These studies all support the hypothesis that chronic changes in hepcidin expression alter duodenal iron transport. We also believe that it is likely that the duodenum's temporal response to hepcidin might change dramatically in models where baseline hepcidin levels are low or absent and it would be interesting to study this in the recently described hepcidin 1 knockout mouse model (32).

Finally, it is possible that the relative abundance of ferroportin in different tissues may contribute lack of a homogeneous response to hepcidin. Anecdotally we found ferroportin much easier to detect in spleen and THP-1 cells than in duodenum and Caco-2 in our western blotting studies. In addition, different ferroportin proteins species (33) and splice variants (34) have been proposed in various cell-types and it is possible that there may be subtle differences in the way these ferroportin isoforms respond to a hepcidin challenge – though obviously further studies would need to be performed to establish this possibility.

In conclusion, our study has shown for the first time that there is a differential tissue-specific sensitivity in response to a rapid increase in hepcidin levels. Following its release into the circulation the initial rapid effects of hepcidin occur at the level of the recycling macrophage resulting in down-regulation of ferroportin protein levels. These changes are associated with the hepcidin-induced hypoferremia. In contrast there were no commensurate changes in either duodenal iron transport or enterocyte ferroportin levels. However, our previous data (7) suggest that duodenal iron transport does decrease at a later stage (24-72 hours post administration of hepcidin). Since reticuloendothelial macrophages recycle some 20-25 mg Fe/day from senescent red blood cells, compared with the 1-2mg Fe/day assimilated from the diet by the duodenal enterocytes, we believe that the acute effects of hepcidin on macrophages is fully consistent with their central role in body iron homeostasis.

Acknowledgements: This work was funded by grants from the Biotechnology and Biological Sciences Research Council, the Medical Research Council and the University of London Central Research Fund. We would like to thank Linda Churchill and Scott Wildman for their help with immunofluorescence studies.

Author contributions: TM & MM contributed equally to this work. TC, MM, BC, JM & BP performed the studies and analyzed the data. PS & SKS designed the studies, analyzed the data and wrote the manuscript.

References

1. Krause A, Neitz S, Magert HJ, Schulz A, Forssmann WG, Schulz-Knappe P, Adermann K. LEAP-1 a novel highly disulfide-bonded human peptide exhibits antimicrobial activity. FEBS Lett 2000;480:147-150.

2. Park CH, Valore EV, Waring AJ, Ganz T. Hepcidin a urinary antimicrobial peptide synthesized in the liver, J Biol Chem 2001;276:7806-7810.

3. Pigeon C, Ilyin G, Courselaud B, Leroyer P, Turlin B, Brissot P, Loreal O. A new mouse liver-specific gene encoding a protein homologous to human antimicrobial peptide hepcidin is overexpressed during iron overload. J Biol Chem 2001;276:7811-7819.

4. Nicolas G, Chauvet C, Viatte L, Danan J,L, Bigard X, Devaux I, Beaumont C, Kahn A, Vaulont S. The gene encoding the iron regulatory peptide hepcidin is regulated by anemia hypoxia and inflammation, J Clin Invest 2002;110:1037-1044.

5. Frazer DM, Wilkins SJ, Millard KN, McKie AT, Vulpe CD, Anderson GJ. Increased hepcidin expression and hypoferraemia associated with an acute phase response are not affected by inactivation of HFE. Br J Haematol 2004;126:434-436.

6. Weinstein DA, Roy CN, Fleming MD, Loda MF, Wolfsdorf JI, Andrews NC. Inappropriate expression of hepcidin is associated with iron refractory anemia: implications for the anemia of chronic disease, Blood 2002;100:3776-3781.

7. Laftah AH, Ramesh B, Simpson RJ, Solanky N, Bahram S, Schumann K, Debnam ES, Srai SK. Effect of hepcidin on intestinal iron absorption in mice. Blood 2004;103:3940-3944.

8. Knutson MD, Oukka M, Koss LM Aydemir F, Wessling-Resnick M. Iron release from macrophages after erythrophagocytosis is up-regulated by ferroportin 1 overexpression and down-regulated by hepcidin. Proc Natl Acad Sci USA 2005;102:1324-1328.

9. Weiss G, Goodnough LT. Anemia of chronic disease. N Engl J Med. 2005;352:1011-1023.

10. Nemeth E, Tuttle MS, Powelson J, Vaughn MB, Donovan A, Ward DM, Ganz T, Kaplan J. Hepcidin regulates cellular iron efflux by binding to ferroportin and inducing its internalization, Science 2004;306:2090-2093.

11. De Domenico I, Ward D,M, Nemeth E, Vaughn MB, Musci G, Ganz T, Kaplan J. The molecular basis of ferroportin-linked haemochromatosis. Proc Natl Acad Sci USA 2005;102:8955-8960.

12. Drakesmith H, Schimanski L,M, Ormerod E, Merryweather-Clarke AT, Viprakasit V, Edwards JP, Sweetland E, Bastin JM, Cowley D, Chinthammitr Y, Robson KJ, Townsend AR. Resistance to hepcidin is conferred by hemochromatosis-associated mutations of ferroportin. Blood 2005;106:1092-1097.

13. Rivera S, Nemeth E, Gabayan V, Lopez MA, Farshidi D, Ganz T, Synthetic hepcidin causes rapid dose-dependent hypoferremia and is concentrated in ferroportin-containing organs. Blood 2005;106:2196-2199.

14. Delaby C, Pilard N, Goncalves AS, Beaumont C, Canonne-Hergaux F. The presence of the iron exporter ferroportin at the plasma membrane of macrophages is enhanced by iron loading and downregulated by hepcidin. Blood 2005;106:3979-3984.

15. Sharp P, Tandy S, Yamaji S, Tennant J, Williams M, Singh Srai SK. Rapid regulation of divalent metal transporter (DMT1) protein but not mRNA expression by non-haem iron in human intestinal Caco-2 cells. FEBS Lett. 2002;510:71-76.

16. Williams M, Sharp P. Regulation of jejunal glucose transporter expression by forskolin. Biochim Biophys Acta. 2002;1559:179-185.

17. Johnson DM, Yamaji S, Tennant J, Srai SK, Sharp PA. Regulation of divalent metal transporter expression in human intestinal epithelial cells following exposure to non-haem iron. FEBS Lett. 2005;579:1923-1929.

18. Ganz T. Molecular pathogenesis of anemia of chronic disease. Pediatr Blood Cancer 2006; 46:554-557.

19. Yamaji S, Sharp P, Ramesh B, Srai SK. Inhibition of iron transport across human intestinal epithelial cells by hepcidin, Blood 2004;104:2178-2180.

20. Nemeth E, Rivera S, Gabayan V, Keller C, Taudorf S, Pedersen BK, Ganz T. IL-6 mediates hypoferremia of inflammation by inducing the synthesis of the iron regulatory hormone hepcidin. J Clin Invest 2004;113:1271-1276.

21. Rivera S, Liu L, Nemeth E, Gabayan V, Sorensen OE, Ganz T. Hepcidin excess induces the sequestration of iron and exacerbates tumor-associated anemia. Blood 2004;105:1797-1802.

22. Abboud S, Haile DJ. A novel mammalian iron-regulated protein involved in intracellular iron metabolism. J Biol Chem. 2000;275:19906-199012.

23. Donovan A, Brownlie A, Zhou Y, Shepard J, Pratt SJ, Moynihan J, Paw BH, Drejer A, Barut B, Zapata A, Law TC, Brugnara C, Lux SE, Pinkus GS, Pinkus JL, Kingsley PD, Palis J, Fleming MD, Andrews NC, Zon LI. Positional cloning of zebrafish ferroportin1 identifies a conserved vertebrate iron exporter. Nature. 2000;403:776-781.

24. McKie AT, Marciani P, Rolfs A, Brennan K, Wehr K, Barrow D, Miret S, Bomford A, Peters TJ, Farzaneh F, Hediger MA, Hentze MW, Simpson RJ. A novel duodenal iron-regulated transporter, IREG1, implicated in the basolateral transfer of iron to the circulation. Mol Cell. 2000;5:299-309.

25. Mena NP, Esparza AL, Nunez MT. Regulation of transepithelial transport of iron by hepcidin. Biol Res 2006;39:191-193.

26. Viatte L, Nicolas G, Lou DQ, Bennoun M, Lesbordes-Brion JC, Canonne-Hergaux F, Schonig K, Bujard H, Kahn A, Andrews NC, Vaulont S. Chronic hepcidin induction

causes hyposideremia and alters the pattern of cellular iron accumulation in hemochromatotic mice. Blood. 2006;107:2952-2958.

27. Frazer DM, Wilkins SJ, Becker EM, Murphy TL, Vulpe CD, McKie AT, Anderson GJ. A rapid decrease in the expression of DMT1 and Dcytb but not Ireg1 or hephaestin explains the mucosal block phenomenon of iron absorption. Gut. 2003;52:340-346.
28. Leung PS, Srai SK, Mascarenhas M, Churchill LJ, Debnam ES. Increased duodenal iron uptake and transfer in a rat model of chronic hypoxia is accompanied by reduced hepcidin expression. Gut. 2005;54:1391-1395.
29. Viatte L, Lesbordes-Brion JC, Lou DQ, Bennoun M, Nicolas G, Kahn A, Canonne-Hergaux F, Vaulont S. Deregulation of proteins involved in iron metabolism in hepcidin-deficient mice. Blood. 2005;105:4861-4864.
30. Harrison-Findik DD, Schafer D, Klein E, Timchenko NA, Kulaksiz H, Clemens D, Fein E, Andriopoulos B, Pantopoulos K, Gollan J. Alcohol metabolism-mediated oxidative stress down-regulates hepcidin transcription and leads to increased duodenal iron transporter expression. J Biol Chem. 2006;281:22974-22982.
31. Fleming RE, Britton RS. Iron Imports. VI. HFE and regulation of intestinal iron absorption. Am J Physiol. 2006;290:G590-4.
32. Lesbordes-Brion JC, Viatte L, Bennoun M, Lou DQ, Ramey G, Houbron C, Hamard G, Kahn A, Vaulont S. Targeted disruption of the hepcidin 1 gene results in severe hemochromatosis. Blood. 2006;108:1402-1405.
33. Canonne-Hergaux F, Donovan A, Delaby C, Wang HJ, Gros P. Comparative studies of duodenal and macrophage ferroportin proteins. Am J Physiol 2006;290:G156-G163.
34. Cianetti L, Segnalini P, Calzolari A, Morsilli O, Felicetti F, Ramoni C, Gabbianelli M, Testa U, .Sposi NM. Expression of alternative transcripts of ferroportin-1 during human erythroid differentiation. Haematologica 2006;90:1595-1606.

Figure legends

Figure 1. No effect of hepcidin on duodenal iron transport. Mice were injected with 10μg hepcidin and used for studies 4 h later. The duodenal lumen was filled with 200μM $^{59}Fe^{2+}$ for10 min and the subsequent levels of ^{59}Fe in duodenal mucosae and the blood and carcass determined by gamma counting. There was no significant difference in mucosal iron retention (grey bars, *P>0.92*), mucosal iron transfer (black bars, *P>0.52*) or total mucosal uptake (white bars, *P>0.48*) iron uptake between the control and hepcidin-treated animals. Data are mean ± S.E.M. of 6 observations in each group.

Figure 2. Ferroportin level are decreased by hepcidin treatment in mouse spleen. Hepcidin-treated mice showed a marked hypoferremia after 4 h. To determine whether this occurred as a consequence of down-regulation of ferroportin levels in the reticuloendothelial system we analyzed transporter expression in spleen. (a) Representative ferroportin-immunofluorescence images. Ferroportin was associated with the macrophage-rich red pulp (arrow) and was not expressed in the immune-cell rich white pulp (*). In hepcidin-treated mice ferroportin immunofluorescence was diminished compared with the saline injected control animals. (b) Western blotting of splenic tissue from hepcidin-treated mice showed a significant decrease in ferroportin (FPN) levels compared with the control group. Expression of the housekeeper protein actin was not altered by hepcidin treatment. Densitometry data are mean ± S.E.M. from 6 spleens in each group *$P<0.001$.

Figure 3. Ferroportin expression in mouse duodenum is not altered following hepcidin treatment. (a) Ferroportin was localized to the basolateral membrane of duodenal enterocytes. Immunoreactivity was not altered following hepcidin treatment. Ferroportin-positive cells (probably macrophages) were also noted in the lamina propria of the duodenal villi from the control but not the hepcidin-treated mice. Representative images presented

here were obtained using the duodena from the same animals used in figure 2. (b) In support of the immunofluorescence data, there was no significant difference in ferroportin levels in mouse duodenum from control and hepcidin-treated animals (*P>0.28*). Expression of the housekeeper protein actin was not altered by hepcidin treatment. Densitometry data are mean ± S.E.M. from 6 duodena in each group.

Figure 4. Expression of ferroportin in THP-1 macrophages and Caco-2 cells following exposure to hepcidin. THP-1 macrophages and Caco-2 cells were incubated for up to 24 h with hepcidin (1 μM). Cells were harvested, homogenised and subjected to Western blotting. (a) In the macrophages, ferroportin (FPN) protein levels were significantly decreased after 4 h of hepcidin treatment compared with basal levels and remained suppressed for the duration of the study. (b) In contrast, in Caco-2 cells, ferroportin levels of were not significantly different from basal levels at either the 4 h or 24 h time point. Expression levels of the housekeeper proteins actin in THP-1 cells and villin in Caco-2 cells were not altered by hepcidin treatment. Densitometry data are presented as the mean ± S.E.M. of 4 experiments in each group. *$P<0.01$ (one-way ANOVA and Tukey's post hoc test) compared with the basal transporter levels.

Figure 1

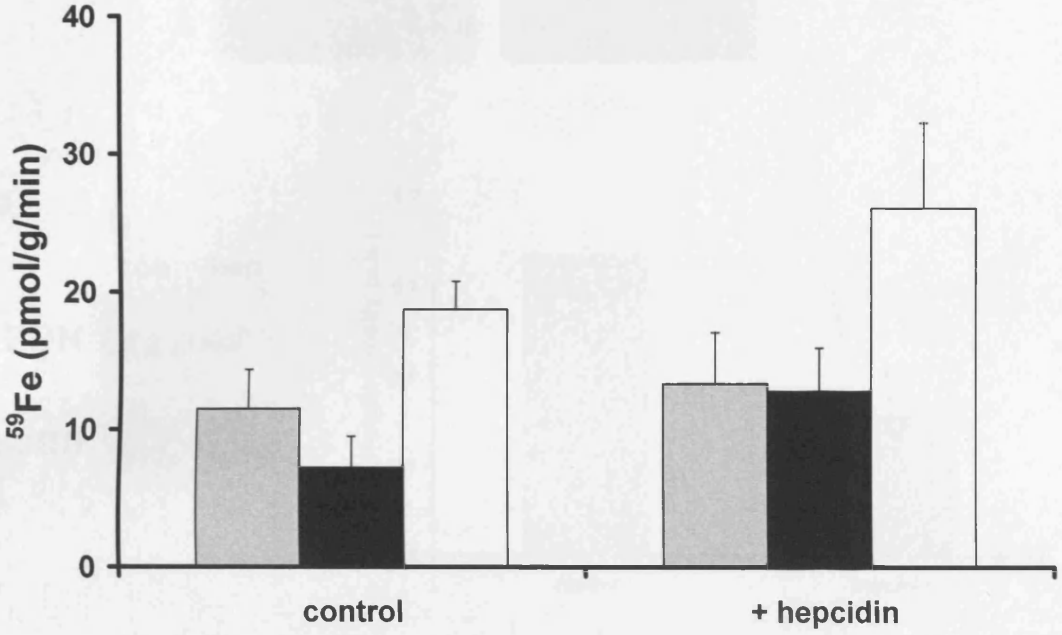

Figure 2

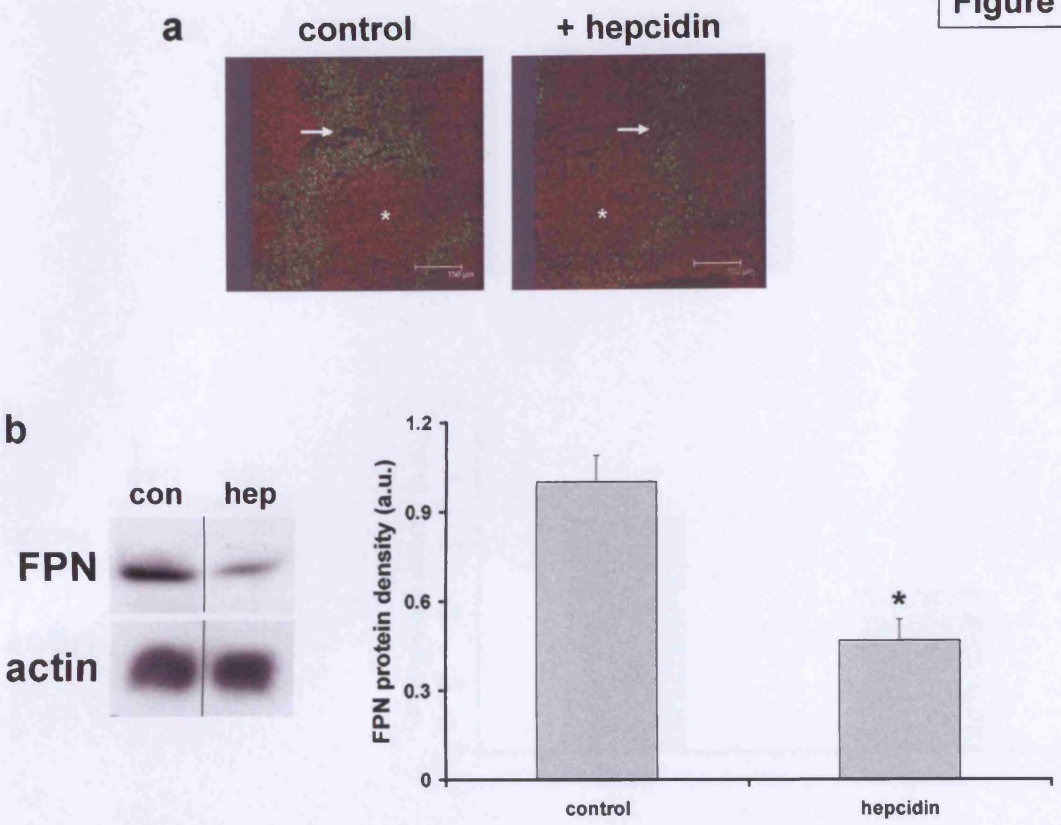
a
control
+ hepcidin
b
con
hep
FPN
actin
FPN protein density (a.u.)
1.2
0.9
0.6
0.3
0
*
control
hepcidin

Figure 3

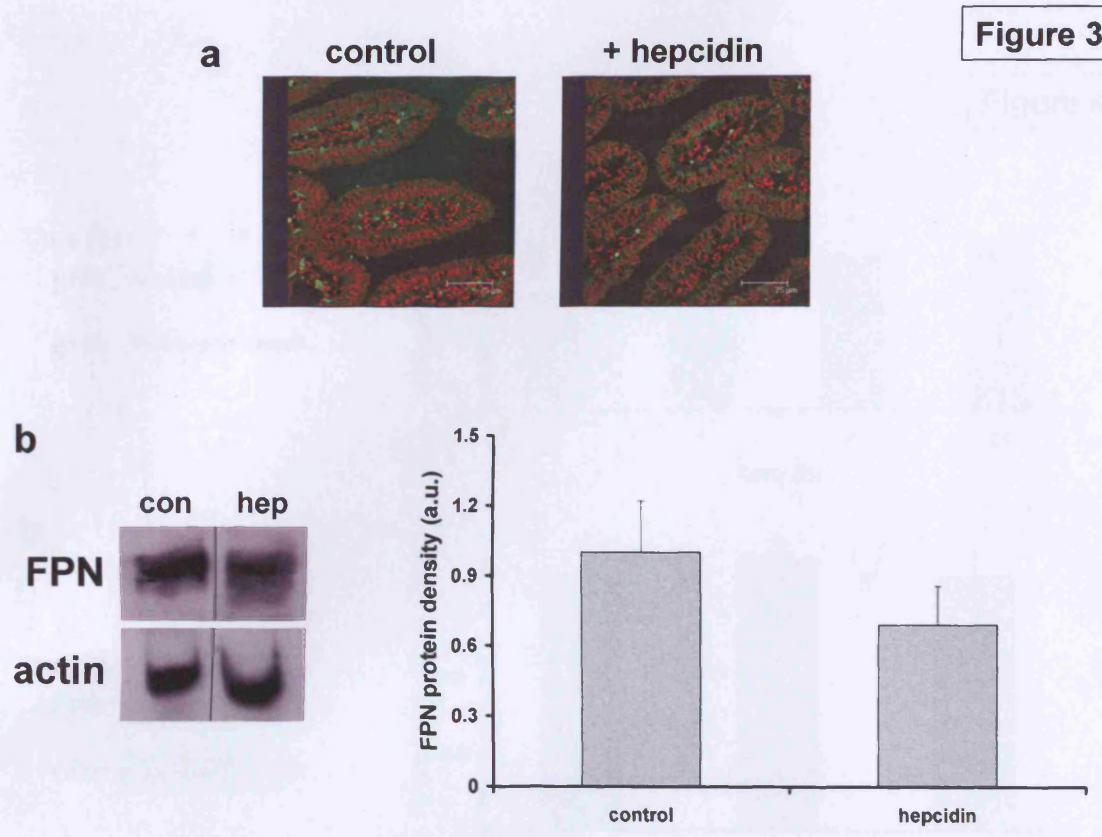
a
control
+ hepcidin
b
con
hep
FPN
actin
FPN protein density (a.u.)
1.5
1.2
0.9
0.6
0.3
0
control
hepcidin

Figure 4

a

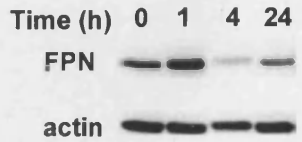
Time (h) 0 1 4 24
FPN
actin

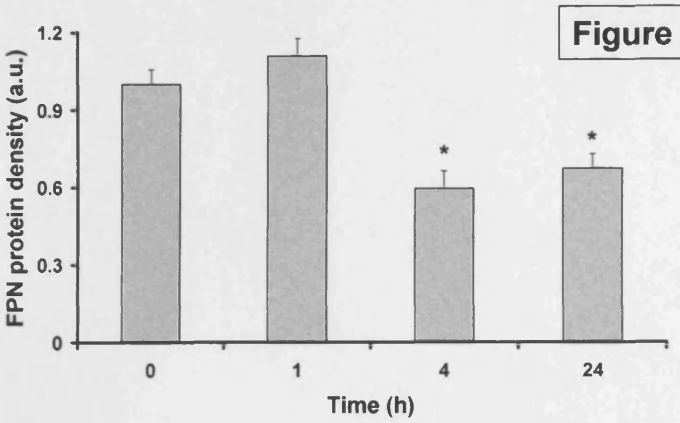
FPN protein density (a.u.)
1.2
0.9
0.6
0.3
0
*
*
0
1
4
24
Time (h)

b

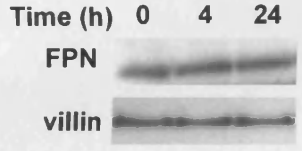
Time (h) 0 4 24
FPN
villin

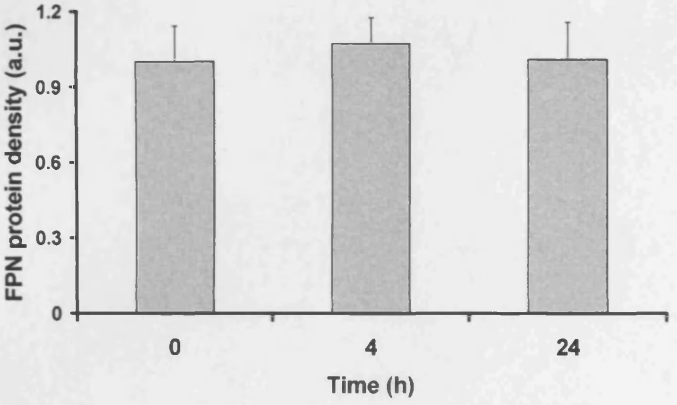
FPN protein density (a.u.)
1.2
0.9
0.6
0.3
0
0
4
24
Time (h)